DATA-DRIVEN BAYESIAN APPROACH TO THE ANALYSIS OF CELL SIGNALLING NETWORKS IN SYNERGISTIC LIGAND-INDUCED NEURITE OUTGROWTH IN PC12 CELLS

SEOW KOK HUEI

NATIONAL UNIVERSITY OF SINGAPORE

2014

DATA-DRIVEN BAYESIAN APPROACH TO THE ANALYSIS OF CELL SIGNALLING NETWORKS IN SYNERGISTIC LIGAND-INDUCED NEURITE OUTGROWTH IN PC12 CELLS

SEOW KOK HUEI

(B.Eng. (Hons.), National University of Singapore)

A THESIS SUBMITTED

FOR THE DEGREE OF DOCTOR OF PHILOSOPHY

IN CHEMCIAL AND PHARMACEUTICAL ENGINEERING

SINGAPORE-MIT ALLIANCE

NATIONAL UNIVERSITY OF SINGAPORE

2014

Declaration

I hereby declare that this thesis is my original work and it has been written by me in its entirety. I have duly acknowledged all the sources of information which have been used in the thesis.

This thesis has also not been submitted for any degree in any university previously.

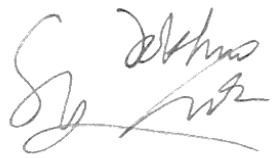

Seow Kok Huei

22nd January 2014

Acknowledgements

"The person who has the most to do with what happens to you is you. It is not the environment, it is not the other people who were there trying to help you or trying to stop you. It is what you decide to do and how much effort you put behind it." ***~ Dr. Benjamin Solomon Carson***

While this Ph.D. journey has been a long and arduous path for me, it is also one that I am extremely grateful for. The testing times have made me realized many shortcomings in myself and forced me to question my outlook and approach to life on many occasions. Without a doubt, this enduring time has in many aspects prepared me better for life ahead and enlightened me in immeasurable ways.

First and foremost, I would like to thank my main supervisor, Professor Too Heng-Phon. It is my blessing and fortune to have him as my advisor. Despite my inadequacies, he did not give up on me. Instead, he has been very supportive and patient in mentoring and guiding me all these years. He has been very inspirational and has devoted an enormous amount of time in helping and advising me both in work and in life. More importantly, he has been pivotal in guiding me how to do good science and in moulding me to be a more matured person.

I would like to thank my co-supervisor Professor Gregory Stephanopoulos, who has given me insightful advices during my candidature, especially during my spell in MIT. I would also like to thank Professors Saif A. Khan, Tong Yen

Wah, Patrick S. Doyle, Raj Rajagopalan, and Rudiyanto Gunawan for having served on my thesis committee and their guidance to my research. I would also like to express my gratitude towards Professor Leong Tze Yun and Dr. Silander Tomi Viljam for their invaluable assistance towards the mathematical modelling aspects of my thesis.

I would also like to thank every lab members for their help and support all these years, especially Dr. Zhou Lihan, Mr Jeremy Lim Qing 'En, Dr. John Wan Guoqiang, and Dr. Zhou Kang. I would like to express my sincere gratitude to my family members for their encouragement during this Ph.D. study. Last but not least, I would also like to express my appreciation to all my close friends, especially Ms. Zhou Yanqing, who had supported me in different ways during the difficult phases of my Ph.D. study.

"Adversity is the true school of the mind." ***~ Katharine Lee Bates***

Table of Contents

Summary

Traditional approaches to cell signalling studies are limited by the use of a single ligand in experiments, and the accompanying single-component analyses. These reductionist frameworks are restricted by their limited physiological relevance as both the intracellular and extracellular environments of cells function as systems of interacting components. In a multi-ligand environment, an important emergent behaviour that is garnering attention is synergism. In particular, synergistic neurite outgrowth, an important process during both neuronal development and treatment of neurodegenerative diseases, is still poorly understood at a systems-level. Furthermore, there is currently a lack of mathematical modeling tools for the analysis of such synergistic systems.

This thesis aimed to further the understanding of the mechanisms underlying synergistic neurite outgrowth through the use of a systems-based mathematical model. This work served as a proof-of-concept study that the developed tool based on Bayesian formalism, for the multi-variant analyses of the perturbation effects of multiple ligands on a small number of known signalling nodes involved in neurite outgrowth, is feasible. Using PC12 cells, an established model used for studying neuronal differentiation, the mechanisms underlying synergistic neurite outgrowth in three systems, NGF-PACAP (NP), FGFb-PACAP (FP), and EGF-PACAP (EP) were investigated.

In the first part of this thesis, the signalling pathways involved in the regulation of synergistic neurite outgrowth in the three systems were investigated. While Erk was required for neurite outgrowth in all three systems, JNK was found to

positively-regulate neurite outgrowth only in the NP and FP systems (Chapter 3). Conversely, PKA was involved in neurite outgrowth only in the FP and EP systems (Chapter 4). This requirement of Erk and differential involvement of JNK and PKA was found to be dependent on the regulation of P90RSK activity. Thus, the JNK-P90RSK and PKA-P90RSK links were identified as *hitherto* unrecognized mechanisms mediating the synergistic effect in neurite outgrowth. Furthermore, the differential regulation of P90RSK in these synergistic systems strongly suggested that these systems can serve as excellent models to decipher the mechanistic regulation of P90RSK by its upstream kinases, Erk, JNK, and PKA.

In a brief follow-up of the study, the potential IEGs and miRNAs that can mediate the effects of these kinases in regulating synergistic neurite outgrowth were identified (Chapter 6). miR-487b-3p, which has not been reported before to be required for neurite outgrowth, was found to be up-regulated during neurite outgrowth. In addition, several IEGs and miRNAs known to be involved in neurite outgrowth were found to be regulated by the same pathways regulating neurite outgrowth in the corresponding system.

Next, the regulation of synergistic neurite outgrowth was further analyzed in terms of its various morphological features. Enhancement of total neurite length was found to be mediated by an increase in the number of neurite extensions, degree of neurite branching, and length of individual neurites. Critically, P38 was found to mediate neurite branching independently of length in the NP and FP systems (Chapter 4). This involvement of distinct signalling pathways in regulating the various morphological features of neurite outgrowth in these systems demonstrated the complexity of this process.

To gain mechanistic insights underlying the synergistic activations of Erk and JNK in the NP system, a modeling framework based on Bayesian formalism, termed TEEBM (Two-phase, Exact structure learning, Expanded-in-time Bayesian Methodology), was developed (Chapter 5). Using this model, a positive feedback between the MEK/Erk and MKK4/JNK pathways was found to mediate the synergistic activations of the two pathways. The model predictions were validated experimentally, suggesting the validity and potential of the developed tool for analyzing signalling networks in any multi-ligand systems, beyond the scope of this study.

List of Tables

List of Figures

List of Abbreviations

Akt/PKB	Protein Kinase B
ANN	Artificial Neural Network
BMA	Bayesian Model Averaging
BN	Bayesian Network
cAMP	Cyclic Adenosine Monophosphate
CREB	cAMP Response Element-Binding Protein
DBN	Dynamic Bayesian Network
DRG	Delayed Response Gene
DS	Degree of Synergism
eDBN	Expanded-In-Time DBN
EGF	Epidermal Growth Factor
EP	EGF-PACAP
Epac	Exchange Protein Activated by cAMP
Erk	Extracellular Signal-Regulated Kinase 1/2
FGFb/FGF2	Basic-Fibroblast Growth Factor
FL	Fuzzy Logic
FP	FGFb-PACAP
GDNF	Glial Cell-Derived Neurotrophic Factor
GPCR	G-Protein-Coupled-Receptor
IEG	Immediate Early Gene
IGF-1	Insulin-like Growth Factor-1
JNK	C-Jun N-Terminal Kinase
MAPK	Mitogen-Activated Protein Kinase
MAPKK	Mitogen-Activated Protein Kinase Kinase
MAPKKK	Mitogen-Activated Protein Kinase Kinase Kinase

MEK	Mitogen-Activated Protein Kinase Kinase 1/2
miRNA	microRNA
MKK4	Mitogen-Activated Protein Kinase Kinase 4
mRNA	Messenger RNA
NGF	Nerve Growth Factor
NP	NGF-PACAP
nsDBN	Non-Stationary DBN
ODE	Ordinary Differential Equation
PACAP	Pituitary Adenylate Cyclase-Activating Peptide
PCA	Principal Component Analysis
PCC	Pearson Correlation Coefficient
PDE	Partial Differential Equation
PI3K	Phosphatidylinositol 3-Kinase
PKA	Protein Kinase A
PKC	Protein Kinase C
PLS	Partial Least Squares
PP	Protein Phosphatase
P38	P38 Mitogen-Activated Protein Kinase
P90RSK	90 kDa Ribosomal S6 kinase
qPCR	Quantitative Polymerase Chain Reaction
RSM	Response Surface Model
RTK	Receptor-Tyrosine-Kinase
TEEBM	Two-phase, Exact structure learning, Expanded-in-time Bayesian Methodology
tvDBN	Time-Varying DBN

List of Manuscripts and Publications

1. **K.H. Seow**, L. Zhou, G. Stephanopoulos, H.P. Too. C-Jun N-Terminal Kinase in Synergistic Neurite Outgrowth in PC12 Cells Mediated through P90RSK. *BMC Neuroscience* **14**:153, 2013. (Chapter 3)
2. **K.H. Seow**, T. Silander, G. Stephanopoulos, T.Y. Leong, H.P. Too. A Novel Bayesian Approach to Network Inference of the Synergistic NGF-PACAP Bi-Ligand System Unveils Positive Feedback during Regulation of Neurite Outgrowth in PC12 Cells. (Manuscript in preparation) (Chapter 5)
3. **K.H. Seow**, G. Stephanopoulos, H.P. Too. Multi-Parameter Morphological Analysis Reveals Complex Regulation of Neurite Features during Synergistic Neurite Outgrowth in PC12 Cells. (Manuscript in preparation) (Chapter 4)
4. Y.K. Ho, **K.H. Seow**, H.P. Too. GDNF Confers Chemoresistance through Specific Isoforms in Human Glioma Cell Line. (Manuscript in preparation)

Chapter 1.

Introduction

1.1. Background

Cell signalling is an important information transmission system which cells utilize to respond to their microenvironments and to carry out their cellular responses such as survival, apoptosis, proliferation, migration, and differentiation. The cell responses are mediated and regulated through the intracellular activities of biomolecules in a dynamical manner. This system of information transmission in cells involves extensive interactions between different classes of proteins, including kinases, phosphatases, transcription factors, and adaptor proteins. These processes are made more complicated by interactions that result in emergent behaviours such as synergism and antagonism.

Defects and abnormalities in signalling mechanisms are often associated with various illnesses such as AIDs, cancer, cardiovascular diseases, diabetes, and neurodegenerative diseases[1-6]. One of the most critical proteins in cell signalling is the protein kinases. They play an important role in regulating and coordinating signalling pathways involved in normal development and operation, and improper functioning of the kinases can lead to various diseases[7]. They are involved in the post-translational phosphorylations of tyrosine, serine, and threonine residues[8] and are implicated in the regulation of many cellular processes[9]. In the human genome, up to 50% of the proteins may be regulated by phosphorylation[10]. Thus, a greater understanding of the defects in such signalling processes can lead to the development of chemotherapeutics, which either inhibit or activate signalling pathways, in treating various diseases. Furthermore, understanding the signalling processes can pave the way for combinatorial drug treatments that give rise

to synergistic therapeutics. Such synergistic behaviours are of utmost importance as the combinatorial effects of the components are greater than the sum of the effects of the constituent parts[1]. These approaches can potentially moderate treatment, achieve higher efficacy, and reduce side effects[11-13] in the treatment of various illnesses.

Cell signalling studies have traditionally been studied solely using reductionist approaches, which try to explain complex phenomena through the functional properties of the individual parts that constitute the multi-component system[14]. However, it is now accepted that reductionism alone cannot lead to a complete understanding of how cells behave as the complex physiological processes cannot be understood simply by knowing how the individual parts work. Given that the activities of cellular components change dynamically and quantitatively, systems-based approaches are necessary for studying the integrated function of the biological systems[15].

The issue of reductionist approaches is present not just in the analysis of interactions between signalling components but also in the use of single ligands in biological studies. This is because cells are exposed to a multitude of ligands in their microenvironments and using a single ligand can result in a mis-represented understanding of cell signalling. It is through the interactions between the signalling responses to the individual ligands that give rise to synergistic behaviours, further highlighting the physiological-relevance of synergism. Thus, there is also a need to shift from a single-ligand to multi-ligand experimental paradigm. This in turn means that developing a systems-based approach in the study of synergistic behaviours is of paramount importance.

To achieve a systems-level analysis of cell signalling networks, mathematical models, which allow multiple components to be analyzed both quantitatively and temporally, are essential tools. However, many of these tools are derived from engineering disciplines and are applied to systems designed by humans. Engineering systems are characterized by well-defined and well-understood processes whereas biological systems are currently defined by vaguely and poorly understood processes. Thus, the main uses of mathematical models differ between engineering and biological systems. These models are used to represent the behaviours of systems in engineering fields but in biological systems, they are used with the aim of gaining insights into the complexity of cells through the analysis of biological data. This reverse-engineering process is further complicated by noisy data, and small number of data-points coupled with high dimensionality. Thus, development of mathematical tools that can be adapted to both the properties of biological systems and biological datasets are of paramount importance towards the advancement of the field.

Moreover, while many tools have been applied to the investigations of biological systems, few have focused on the analyses of multi-ligand biological systems that can give rise to synergistic behaviours. The analyses of multi-ligand systems call for a different framework from those of uni-ligand systems as different information can potentially be extracted from the two different experimental set-ups. Hence, modelling frameworks and parameterizations that can be tailored to extract more information from multi-ligand systems can yield more insights into signalling mechanisms than the mainstream approaches.

While biological processes pertaining to cancer, such as survival, proliferation, migration, and apoptosis, have been relatively well-studied, the process of neuronal differentiation is still poorly understood at the systems-level. During neuronal differentiation, one of the key changes is axonal and dendritic outgrowth from the cell-body. This is of critical importance not just in development, but also in recovery from injuries and neurodegenerative diseases[16]. Upon nerve injury, the speed of nerve regeneration is critical as a full functional recovery can be impeded by delayed regeneration[17]. Thus, acceleration of neurite outgrowth through a synergistic drug-combination approach can provide a valuable treatment strategy. Given the potentials of combinatorial drug therapy in neurodegenerative diseases[3-5], it is imperative to gain a more comprehensive understanding of the mechanisms underlying such synergistic behaviours.

1.2. Scope and Organization of Thesis

Several studies have demonstrated the benefits of the co-administration of neurotrophic factors[18] and the combinatorial treatment of nerve growth factor (NGF) with glial cell-derived neurotrophic factor (GDNF)[19] or insulin-like growth factor (IGF)-1[20] in promoting synergistic axonal or neurite elongation. The aim of this thesis is to further the understanding of synergistic neurite outgrowth, which is still poorly understood at the systems-level. This is facilitated with the aid of mathematical modelling. In this work, a systems-based mathematical modelling approach for the study of synergistic behaviours in multi-ligand systems was developed and applied to the analyses of the mechanisms underlying synergistic neurite outgrowth, a measure of neuronal differentiation. Given that existing methods are still in its

infancy in the analyses of cellular signalling, and methods that can analyse synergistic behaviours in multi-ligand systems are very much lacking, the proposed approach can significantly contribute to the field.

In chapter 2, a literature review of the main modeling methods used in systems biology was presented along with the current knowledge of the regulation of differentiation in PC12 cells. The proposed method for the analysis of synergistic system was also reviewed in view of the challenges involved.

The scope of this project was aimed at the following aspects and is covered from chapters 3 to 6 as follows:

1.2.1. Investigation of a Sub-System Critical for Synergistic Neurite Outgrowth

In Chapter 3, the pathways regulating synergistic neurite outgrowth in three different systems, EGF-PACAP, FGFb-PACAP, and NGF-PACAP, were investigated. Although synergistic neuronal systems have been identified previously, the signalling pathways involved in the regulation of synergistic neurite outgrowth were largely unknown. Using a widely-used cell model for the study of neuronal differentiation, the PC12 cells, these three different synergistic systems were explored in this aspect. Signalling pathways that were synergistically activated were identified and investigated for their involvement in regulating synergistic neurite outgrowth. A differential involvement of these pathways in the three systems was found along with the reason underlying the difference.

1.2.2. Investigation of the Signalling Pathways Regulating the Morphological Structures of Neurite Outgrowth

In chapter 4, emphasis was placed on the analyses of the morphological structures of neurite in the three different synergistic systems, EGF-PACAP, FGFb-PACAP, and NGF-PACAP. The determination of the extent of neurite outgrowth in many studies has primarily been focused on neurite length and the proportion of cells that are differentiated. However, the morphological structures of neurites such as branching and the number of neurites extending from the cell-bodies are equally important parameters. To gain insights into how these morphological features collectively contributed to the synergistic regulation of neurite outgrowth, kinases regulating the process were studied for their involvement in regulating different morphological features of neurites. It was found that morphological features such as neurite length and the degree of branching in the neurites can be regulated independently of one another.

1.2.3. Development of a Modified Bayesian Methodology (TEEBM) for Analyses of Dynamic Signalling Networks

In Chapter 5, the mechanism underlying the synergistic activations of the kinases involved in neurite outgrowth in the NGF-PACAP system was investigated through the use of mathematical modeling. A modified Bayesian approach, termed TEEBM (Two-phase, Exact structure learning, Expanded-in-time Bayesian Methodology) for structure learning was proposed and used to determine if any novel directional influences exist within the pathways. The methodology was proposed to overcome the limitations of existing

approaches in the analysis of multi-ligand cell signalling networks. It addressed issues related to the modeling of the system dynamics, the parameterization of the data, the integration of data from uni- and bi-ligand treatments, and the optimization of the learned network structure. The novel edges that were identified to contribute to synergistic neurite outgrowth by the proposed method were validated experimentally.

1.2.4. Investigation of the Expression of Genes and miRNAs during Synergistic Neurite Outgrowth

In chapter 6, a brief study was performed to determine the expression and regulation of the genes and miRNAs that are potentially involved in neurite outgrowth in the three different synergistic systems, EGF-PACAP, FGFb-PACAP, and NGF-PACAP. While several genes and miRNAs have been implicated in neurite outgrowth, it is unclear if the requirement for different combinations of upstream protein kinases in regulating neurite outgrowth in the three systems can converge onto a common set of genes or miRNAs. The regulation of these genes and miRNAs were found to be different in all three systems, suggesting that yet to be discovered cross-talks between these signalling pathways are likely to be present.

Chapter 2.

Literature Review

2.1. Cell Signalling

Cell signalling is a system of communication utilized by cells to respond to their microenvironments. It involves a complex network of interactions between signalling components present in the cells in a dynamical manner. This leads to cellular actions such as survival, apoptosis, proliferation, migration, and differentiation.

2.1.1. Reductionism versus Systems-Based Approaches

Studies aimed at gaining an understanding into this complex system have traditionally utilized reductionist approaches. Reductionism takes the approach of “divide and conquer” and is based on the belief that the complex system can be solved by breaking it down into smaller and more tractable constituent units[21-23]. Reductionism is extremely useful in identifying the important or involved parts in a system and much of our knowledge today about cell signalling mechanisms are based on an accumulation of such reductionist approaches. However, it is based on the wrong assumption that it is the only solution[24]. The main drawback of reductionism is that breaking down the system into its parts result in loss of critical information about the system as a whole. It is now realized that biological systems are too complex to be explained simply just by an understanding of the constituent parts (Figure 2.1). This is because biological systems exhibit emergent properties, a behaviour that can only be exhibited as a system and not by any isolated constituent part[21,23].

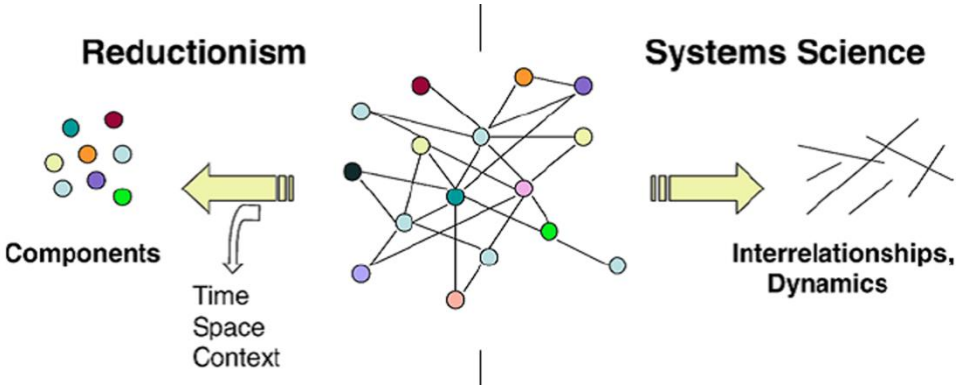

Figure 2.1. Comparison of reductionism and systems science[24].

To circumvent such a drawback, systems-based approaches have been adopted, with a shift from a component to a system-level perspective. The systems standpoint stems from the assumption that the forest cannot be explained by studying the trees individually. It takes into account the holistic and composite characteristics of a problem and analyses the problem with the use of computational and mathematical modelling tools[21]. The main goal is to understand how emergent properties can arise from the non-linear interactions between multiple components. Given that cells respond to their environment in a dynamical manner and are compartmentalized into areas such as the nucleus, cytoplasm, and plasma membrane, a systems-based approach to cell signalling studies should take the space, time, and context of the environment into account.

However, it must be emphasized that this does not mean that reductionist approaches are not useful. Both systems and reductionist approaches are meant to complement each other[21,25] as it is only when the parts of the system have been identified that systems approaches can be used to understand the underlying emergent behaviours.

2.1.2. Single-Ligand versus Multi-Ligand Approaches

The reductionist approach pervades not only in the analysis of interactions between components in a signalling network but also in the use of a single ligand in biological experiments. Again, such an approach is undesirable as cells are exposed to multiple ligands in their microenvironments. When cells are exposed to a single ligand in typical experimental settings, it does not reflect how cells respond to their cellular microenvironments. In the presence of multiple ligands in their microenvironments, extensive interactions between the signalling responses to the individual ligands actually occur. Such interactions can give rise to physiologically-relevant and -pervasive emergent behaviours such as synergism and antagonism. Both phenomenon are important in regulating cellular behaviours and can give rise to greater or less than additive effects, respectively[26,27]. Thus, the main drawback of a single-ligand approach lies in its inability to reflect how signalling responses upon exposure to multiple ligands can result in emergent behaviours.

Again, this does not mean that single-ligand approaches are useless. They have provided a fairly comprehensive understanding of the fundamental signalling responses in cells. Given that the cellular responses to single-ligand treatments have been fairly well studied, it is now imperative that the understanding of cellular responses take on a more informative and physiologically-relevant multi-ligand treatment approach.

2.1.3. Multi-Ligand Synergistic Systems

The analysis of synergistic behaviours in cells has become increasingly important in recent years owing to the potential benefits of understanding

such a phenomenon. After all, cells are constantly exposed to multiple ligands where the responses are integrated resulting in the final phenotype. Furthermore, its importance can already be seen in the increasing number of synergistic drugs in clinical use and studies attempting to find combinatorial drugs for therapeutics purposes[11,12,28]. Understanding the mechanisms underlying synergistic behaviours will be an essential step before the potentials of synergistic therapeutics can be fulfilled. However, mathematical modeling tools that can address this issue at a systems-level are still very much lacking in the field.

The aim of this thesis is to bridge this gap through investigations of the phenomenon of synergistic neurite outgrowth in PC12 cells during neuronal differentiation, a process that is poorly understood but nevertheless, critical during development. In the following sections, a review of mathematical models that are currently applicable to the field of systems biology will first be discussed. This is then followed by a review of the current understanding of pathways involved in neurite outgrowth, including systems that give rise to synergistic neurite outgrowth. Lastly, the gap in the application of existing modeling approaches towards the analysis of synergistic system is presented. This is accompanied by a proposed solution considered in view of the analysis of synergistic neurite outgrowth.

2.2. Mathematical Modeling in Systems Biology

Mathematical models are essential tools for understanding the complexity of cellular systems for several reasons[29-31]. Firstly, it allows the levels of the biological components to be accounted for in a quantitative rather than a qualitative manner. Secondly, temporal variation in the levels of the biological

components can be analyzed through the use of dynamical models. Thirdly, spatial variation in the biological components can be represented using appropriate models. Lastly, mathematical models allow many components to be analyzed concurrently, which can potentially reveal emergent properties that arise as a result of interactions between the components.

2.2.1. Reverse Engineering of Cell Signalling Networks

The process of learning about cell signalling networks from experimental data is known as reverse engineering. It involves the learning of network structure and/or parameters that define the model. There are several forms of network graphs that can be learned, with each form depending on the types of interaction or regulatory relationships defined by the edges in the biological networks. The main types of networks are gene regulatory, metabolic, and signalling. Although different relationships are defined in these networks, the same set of modelling formalisms can be applied to their analyses. There is a wide spectrum of mathematical modeling methods that can be applied for such purposes and they can be classified into mechanistic and data-driven models as shown in Figure 2.2[32-34]. In these network models, the signalling components are called nodes, and the influences that the nodes exert on one another are termed edges. Reverse engineering of these models involve learning of the parameters needed to define the nodes and edges.

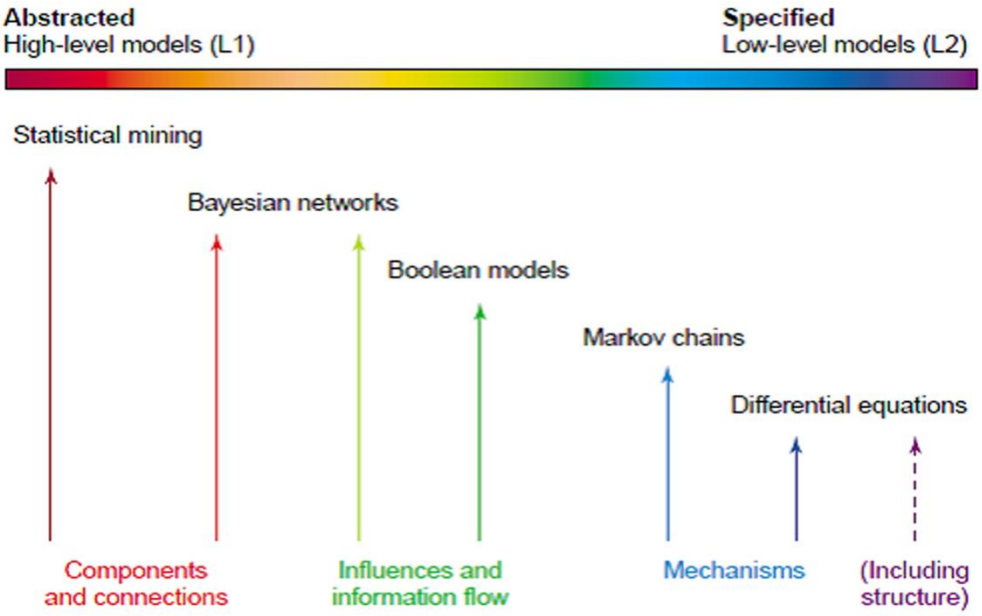

Figure 2.2. A spectrum of high- to low-level computational approaches, ranging from data-driven (abstracted) to mechanistic (specified) models[32].

2.2.2. Mechanistic Modeling

2.2.2.1. Ordinary Differential Equations (ODEs)

The most common form of mechanistic models is ordinary differential equations (ODEs). Such models provide information about the kinetics and dynamics of the different biological processes in the system[35]. In addition to the temporal aspects of the system, additional information such as the spatial distribution of the signalling nodes can also be incorporated into variants of these models known as partial differential equations (PDEs)[36,37]. In an ODE model, the activity of each node, x, is described temporally as a function of that of other nodes as shown in Equation 2.1.

(Equation 2.1) $\frac{dx_i}{dt}(t) = f_i(x_1, x_2, \dots, x_n)$

ODEs are very useful tools for the modeling of biological systems and have been widely applied in the investigation of cellular systems, including cross-talks between pathways[38-40], identification of critical regulators of cellular

behaviours[41], biomarkers discovery[42], and combinatorial drug therapeutics[42]. In such models, the structure of the network is usually known, and learning of the models involves learning the parameters needed to define the set of equations defined in Equation 2.1. Learning of the parameters is typically done using a least-square-error objective function, which serves to minimize the error between experimental data and model output. However, in defining these equations, a large number of parameters are typically needed[43]. This in turn requires a large number of data points before parameter and model identifiability can be achieved. While "-omics" technology can produce a large amount of data, such data is not always useful as the large data size is due to an increase in dimensionality rather than number of measurements of the same components[44]. Sufficient data is necessary to obtain reliable estimates of model parameters and use of parameter-intensive mechanistic models is not appropriate when data is sparse[45]. This demand for data is made worse in the presence of noise, a common characteristic of biological data[46]. However, such problems can be alleviated in systems with strong *a priori* knowledge as such information can be used to reduce the number of unknown parameters in these models.

2.2.3. Data-Driven Modeling

In situations where *a priori* knowledge is sparse, data-driven statistical models are much more appropriate for analysis of the cellular systems[46,47]. This is because the number of parameters needed to define these statistical models is much lower than that required for mechanistic models[43]. The most commonly used data-driven models are the associated networks, Bayesian networks, Boolean networks, neural networks, and regression models.

In this thesis, a modeling framework centralizing on Bayesian networks were used for the analysis of synergistic neurite outgrowth, a cellular behaviour still poorly understood at the systems-level. Among these data-driven models, Bayesian networks are well-suited for the analysis of such multi-ligand systems as they can capture non-linear multivariate dependencies, determine directional influences between signalling nodes, and allow integration of data from different datasets. These different data-driven models and the advantages of Bayesian networks over the other methods are reviewed in the following sections.

2.2.3.1. Artificial Neural Networks (ANNs)

Artificial neural networks (ANNs) were developed based on the idea of the central nervous system, where neurons are highly connected to form a neural network. ANNs typically consist of three or more layers of artificial neurons, or nodes. The first and last layers are termed the input and output layers, respectively whereas the middle layers are called the hidden layers[48]. During the learning process, the relationship between the input and output variables are established through optimization of the weight factors that are associated with the connections of the variables between successive layers. The optimization of the weight factors is based on minimization of the error between the experimental data and the output of the model.

The feasibility of using ANNs in biological systems for prediction of signalling responses to perturbations[49,50], parameter estimations mathematical models[51], identification of disease-causing single nucleotide polymorphisms[52], and classification of disease phenotypes have been demonstrated[53]. This is based on its key advantage of being able to model non-linear

interdependencies between the variables, which in turn allow complex relationships between the layers not to be missed. However, an accompanying problem is that ANNs are "black-box" models, which means that the topologies of neural networks are arbitrary in nature and no meaning should be inferred from them, rendering such models poor choices for gaining mechanistic insights into cell signalling networks[50,54]. Thus, ANNs are not the appropriate choices when the modeling objective is to gain an understanding of how different signalling nodes are inter-connected dynamically during the regulation of synergistic neurite outgrowth.

2.2.3.2. Associated Networks

Association networks are undirected graphs where a measure of statistical dependency or similarity measure is calculated for each edge[33,55]. The most commonly used statistical measures are Pearson correlation coefficient (PCC), R_{ij} (Equation 2.2) and mutual information (MI), I_{ij} (Equation 2.3). Such statistical measures have been used to identify correlations between signalling nodes in a network[56-60], identification of synergy between interacting genes[61], and experimental design to improve estimation of model parameters and prediction capability of the models[62,63].

(Equation 2.2) $$R_{ij} = \frac{cov(X_i, X_j)}{\sqrt{var(X_i)}\sqrt{var(X_j)}},$$

where cov and var mean covariance and variance, respectively.

(Equation 2.3) $$I_{ij} = I(X_i; X_j)$$

$$= \sum_{x_i \in X_i} \sum_{x_j \in X_j} p(x_i, x_j) \log_2 \left(\frac{p(x_i, x_j)}{p(x_i)p(x_j)}\right),$$

where p denotes the probability distribution functions

The PCC measures the linear relationship between the two variables, X_i and X_j, in the data. If the covariance between them is 0, then the variables are not correlated linearly. A value of -1 and 1 indicates perfect negative and positive correlation, respectively. However, it is not a good measure of non-linear correlation. Thus, in situations where the variables exhibit strong non-linear correlation, PCC may not pick up a link between them. In contrast to PCC, MI can measure both linear and non-linear dependencies and it can detect dependencies missed by PCC[56]. MI is always non-negative and will give a positive value for correlated variables[58]. For statistically independent variables, the MI between them is 0. Although these measures are relatively easier to compute and have been successfully applied to biological systems, they face the drawback of giving undirected networks. Thus, in situations where directional influences between the nodes need to be learnt, such correlation methods are not suitable. While such models can provide correlations between different signalling nodes during synergistic neurite outgrowth, its failure to take into account the precedence of the underlying signalling events is a major drawback that renders it a poor modeling option for the aim of this thesis.

2.2.3.3. Bayesian Networks (BNs)

Bayesian networks (BNs) were first introduced by Judea Pearl in the 1980s for the modeling of complex probability models[64]. They are stochastic probabilistic graphical networks, where the edges are all directed[33,65]. These networks are directed acyclic graphs, which prevent the recurrence of information flow in the network. The relationships between the signalling

nodes, as represented by the edges, are defined using conditional probabilities between the child and parent nodes. BNs are defined as functions of G and θ (Equation 2.4). The graph, G, contains the random variables, X_i, and the edges that represent the dependencies between the variables. It encodes independence assumptions where each variable, X_i, is independent of its non-descendants given its parents, π_i, in G. θ denotes the parameters that define G.

(Equation 2.4) $$P(X_1, X_2, \ldots, X_n) = \prod_{i=1}^{n} P(X_i|\pi_i)$$

$$= \prod_{i=1}^{n} \theta_{X_i|\pi_i}$$

Learning BNs involve finding G and θ that can best explain the experimental data. However, a more connected BN can give rise to a better fit to the experimental data, resulting in overfitting of the model. This problem is alleviated by using scoring functions that can penalize the models for complexity. Examples of such scoring functions are minimum description length, Akaike Information Criterion, Bayesian Information Criterion, and normalized maximum likelihood[66].

BNs have the advantage of allowing data from different sources to be integrated in the analyses[67]. They have been widely used for predicting novel regulatory behaviours[68-70], determining cell fate decisions[71], experimental design to improve estimation of model parameters and prediction capability of the models[63,72], parameter learning in mathematical models[73], and model selection to identify the most plausible models among competing hypothesis[74]. Despite the wide applications of BNs, there are several drawbacks associated with it. First, it is possible to have networks with

different edge directions but similar probability distributions[75]. They are known as equivalent networks and cannot be distinguished from the data used for the learning of the BN. In addition, they are also unable to model feedback loops[38]. To overcome this problem, Dynamic BNs (DBNs) were proposed[76]. DBNs model BNs unfolded over discrete time-points, which can capture the dynamics of the system without violating the requirement for a directed acyclic flow of information. Although DBNs models take into account the temporal aspects of the variables, they assume that the relationships between the variables are time-invariant. Such an assumption is not always valid in the analysis of biological systems, especially under non-steady-state conditions[77,78]. Another challenge pertaining to the use of BNs is that inference of BNs is largely dependent on discretized variables and in the process of discretizing data, loss of information can often occur[79,80]. It has been shown that the number of intervals, the width of the intervals, and the minimum number of data-point in each interval can have a significant influence on the resulting model, further emphasizing the importance of minimizing this loss of information[81,82].

The ability of BNs to integrate different information from various data-sources strongly indicates that such models can potentially be applied to the analysis of synergistic neurite outgrowth. This is because an important aspect in this network inference is the integration of data from single-ligand and multi-ligand experiments in the capturing of synergistic information. At the same time, its ability to model multivariate dependencies without any *a priori* information is another advantage that can model important interactions during synergistic neurite outgrowth. While DBNs have its own drawbacks in analyzing cellular systems, they can be overcome through proper parameterizations. These

properties and modifications will be examined further in the later sections when the proposed approach for the analysis of synergistic neurite outgrowth is discussed in greater details.

2.2.3.4. Boolean Networks

Boolean network models were first introduced by Kauffman in 1969 as an abstract model to study the dynamics of gene regulation[83]. In Boolean networks, each node is allowed to take only one of two values as its state (e.g. expressed or not expressed, on or off, phosphorylated or not phosphorylated). The relationships in Boolean networks, are defined by Boolean functions, b_i, such as AND, OR, or NOT. The parameters that define these networks are state transitions that define the state of each child node, X_i, given the state of its parent(s), π_i (Equation 2.5). The optimal Boolean network is found by minimizing the error between the experimental data and model prediction.

(Equation 2.5) $x_i = b_i(\pi_i)$

Such a formalism have been applied for prediction of cellular behaviours[84], identification of regulatory influences during cell signalling[33,85-87], analysis of attractors of the networks such as steady activation states of the components or cellular phenotypes[88-90], prediction of phenotype response[91], and finding a basis set of nodes required for signal transduction[92]. Similar to BNs, Boolean networks also encounter the same difficulties with regards to data discretization[93]. Data discretization in Boolean formalism face an added challenge of minimizing information loss compared to BNs as the variables can only exist in two discretized states[86]. Thus, such a two-state modeling

formalism can miss out on important regulatory mechanisms during network inference. This drawback impedes its application to the analysis of synergistic neurite outgrowth as the interactions between different signalling nodes at multiple quantitative states are likely to have a large bearing in the regulation of synergism.

To overcome the limitation of a two-state model in Boolean networks, a multi-state logic modeling method, fuzzy logic (FL), was developed. Its feasibility in the analysis of cell signalling networks has also been demonstrated in its application to identify interactions between signalling pathways[94]. However, the use of such a multi-state logic framework results in a combinatorial rule explosion problem, where an exhaustive search for all possible rules is not feasible for large networks[95]. Thus, methods that can evaluate multivariate regulatory effects between signalling nodes while not being overwhelmed by this problem are necessary. In the analysis of synergistic neurite outgrowth, this concern is not alleviated by the inability to restrict the possible combinations of the rule due to a lack of *a priori* knowledge about the system.

2.2.3.5. Linear Algebra-Based Analyses

Statistical methods using linear algebra such as principal component analysis (PCA) and partial least squares (PLS) are well known for their applications in multivariate data analysis[47,96]. These methods are extremely useful in dealing with high dimensional data as they can reduce the large number of dimensions to a few new axes called the principal components. Each principal component is a combination of the original signalling axes that exhibit high covariance with each other. While PCA serves to maximize the variance

explained in the variables, PLS extends PCA by maximizing the covariance between the dependent and independent variables.

Despite the advantages of PCA in reducing dimensions and clustering highly correlated variables, PCA do not shed light on how the variables may be related to one another in signalling networks. In biological systems, they have been largely applied to the analyses of microarray data to identify cluster of co-regulated genes[97], determination of cell fate decision[98,99], and model and dimensional reduction[100]. On the other hand, in PLS, each variable can be set as either a dependent or an independent variable, allowing plausible relationships between the two sets of variables to be established. Thus, relationships between the signalling nodes can be obtained, which can be translated to topology in signalling networks. This idea has been used for identification of cross-talks between signalling pathways[101]. It has also been coupled with *a priori* knowledge from the literature to identify a basis set of proteins responsible for regulating cell fate decisions[102,103]. In addition, PLS has been used to identify appropriate drugs for therapeutic purposes[104], and for prediction and classification of disease state[105]. However, the regression component in PLS models is based on the idea of linear multivariate regression[106], which may not capture relationships that are complex and non-linear in signalling networks. Given that the regulation of synergistic behaviours, such as neurite outgrowth, is likely to entail more complex interactions, it is all the more important to realize that such linear models are likely to result in important regulatory mechanisms being overlooked.

2.3. Neuronal Differentiation

Neuronal differentiation is an important process during the development of the nervous systems. During their developmental stages, complex processes involving the growth of neurons, migration of the neurons to their position within the brains, outgrowth of axons and dendrites from the neurons, and the formation of synapses are critical for our normal development. Defects in neuronal differentiation can lead to neurodegenerative diseases such as Alzheimer's, Parkinson's, and Huntington's.

The PC12 cell-line, which is established from a pheochromocytoma of the rat adrenal medulla, is a widely used cell model for the study of neuronal differentiation[107,108]. PC12 cells have provided useful insights into the regulation of various signalling cascades during neuronal differentiation. They respond to several growth factors and neurotrophins by exhibiting distinct morphological changes such as neurite outgrowth, a read-out commonly used as a measure of neuronal differentiation. In respond to stimuli such as the basic-fibroblast growth factor (bFGF), nerve growth factor (NGF), and pituitary adenylate cyclase-activating peptide (PACAP), they differentiate and neurites extend out of the cell-bodies to varying degrees. Binding of these ligands to their respective receptors result in a series of complex and orchestrated events. These include activation of different signalling cascades, modifications of proteins such as phosphorylation and glycosylation, expression of genes such as transcription factors, immediate early genes, and delayed response genes, and regulation of miRNAs, which are master regulators of cellular processes.

Neurite outgrowth occurs by an initial sprouting of neurites and is followed by elongation of axons and dendritic, which are collectively called neurites. The appropriate and ordered manner of growth, guidance, and stabilization of neurites during differentiation involves a complex interplay between extracellular cues and intracellular signalling events. Various signalling pathways, such as cAMP[109], Akt[110], Erk[111], JNK[112], and P38[113] had been reported to be involved in such morphogenesis of neurites.

2.3.1. Regulation of Neurite Outgrowth in PC12 Cells

2.3.1.1. Pituitary Adenylate Cyclase-Activating Peptide (PACAP)

Pituitary adenylate cyclase-activating peptide (PACAP), a member of the secretin superfamily of neuropeptides, was initially isolated from the extracts of ovine hypothalamic on the basis of its ability to stimulate cAMP formation in rat anterior pituitary cells[114]. It is an amidated peptide which exists in either 38-amino acid (PACAP-38) or 27-amino acid (PACAP-27) forms, each derived from the same precursor, prepro-PACAP[115]. Although PACAP can bind to three receptors, PAC1, VPAC1, and VPAC2, only the PAC1 receptor is found in the brain[116].

PACAP and its receptors are widely found in the body, including expression in the pituitary, gonads, placenta, central and peripheral nervous systems, lung, intestinal tract, pancreas, parathyroid gland, and adrenal gland. It can function as a neurotransmitter, neuromodulator, and neurotrophic factor and is known to exert pleiotropic effects in various organs, including modulation of neurotransmitter release, vasodilatation, bronchodilatation, activation of

intestinal motility, augmentation of insulin and histamine secretion, and stimulation of cell multiplication and differentiation[117]. In the nervous system, PACAP is found to regulate differentiation in many regions, including the hypothalamus, cerebral cortex, amygdala, nucleus accumbens, hippocampus and cerebellum of the central nervous system (CNS), and the sensory neurons, sympathetic preganglionic neurons and parasympathetic pre- and postganglionic neurons of the peripheral nervous system[118,119]. Its importance had been demonstrated both in development and adulthood and is involved in the regulation of memory, learning, emotions, and sleep[120]. During the development of the CNS, it decreases the number of mitotic cells and promote neuroblast differentiation[121] whereas in the adult brain, it modulates neurotransmitter release and inhibits apoptosis[122,123]. In the brain tissue, various analyses had shown that PACAP-38 is the predominant form present, with PACAP-27 accounting for less than 10% of the total peptide content[124-128].

In the PC12 cells, PACAP-38 had also been found to be a much stronger neurite-inducing ligand than PACAP-27, further demonstrating the relevance of PACAP-38 in neuronal differentiation[129]. PACAP binds to the PAC1 receptor, a GPCR, and activate a series of signalling pathways. The PAC1 receptor signals through the cyclic AMP (cAMP)[109,111], phospholipase C[130], P38[131], and Erk pathways[132-134]. Among them, the Erk and cAMP pathways have been extensively studied for their involvement in regulating neurite outgrowth.

Binding of PACAP to the PAC1 GPCR causes the stimulation of adenylate cyclase (AC). This leads to the conversion of ATP to cAMP, which in turn

results in activation of its key downstream effectors, protein kinase A (PKA) and exchange proteins activated by cAMP (Epac)[135]. The involvement of cAMP in regulating neurite outgrowth is demonstrated when analogs of both PKA (6-Bnz-cAMP) and Epac (8-pCPT-2'-O-Me-cAMP) were found to induce neurite outgrowth[136]. In the same study, both analogues were found to synergize, and co-treatment of cells with both analogues resulted in neurite outgrowths that were greatly enhanced. Using the same analogues, both Epac and PKA were found to be required for the sustained activation of Erk, an important determinant of neurite outgrowth[137]. Furthermore, CREB, a well-known transcription factor that is a downstream mediator of PKA, has also been found to be critical for regulating brain development, and neurogenesis, including neurite outgrowth, in the adult brain[138]. The PKA inhibitor, H89, was found to inhibit Erk activation by PACAP[139], and inhibition of the GTPase Rap1 was found to block activation of Erk by Epac[137], further demonstrating the involvement of cAMP in regulating PC12 differentiation. In addition, the use of dominant negative MEK inhibited Erk activation by the cAMP analogue 8-CPT, suggesting that activations of Erk by Epac and PKA are both mediated through MEK[140].

The Erk protein belongs to a family of protein kinases known as mitogen-activated protein kinases (MAPK)[141]. These signalling cascades consist of three kinases in series, MAPK kinase kinase (MAPKKK), MAPK kinase (MAPKK), and the MAPK. Erk, a MAPK, is one of the most widely studied kinases for its involvement in neurite outgrowth. The duration of Erk signalling is a well-known critical determining factor of whether differentiation occurs, where sustained but not transient activation of Erk results in differentiation[137]. Treatment of PC12 cells with PACAP had been found to result in sustained

Erk activation[132]. Besides the involvement of cAMP in the activation of Erk as mentioned above, the GTPase Ras and protein kinase C (PKC) had also been reported to regulate the activity of Erk upon PACAP treatment[139]. The involvement of Erk in regulating neurite outgrowth had been found to be mediated through transcription factors that regulate neurite outgrowth such as CREB[142], Elk-1[134], and NF-κB[143]. These transcription factors regulate the expression of many genes that are involved in neuronal differentiation and neurite outgrowth[144,145].

2.3.1.2. Nerve Growth Factor (NGF)

Nerve growth factor (NGF) is the first discovered member of the neurotrophin family[146]. It was isolated from the submandibular gland of adult male mice as a complex consisting of six polypeptides, $\alpha_2\beta_2\gamma_2$[147]. It is the β subunit that exhibits neurotrophic activities[148] and both the α and γ subunits inhibit the actions of the β subunit[149]. The mature and active form of NGF can bind to two neurotrophin receptors, p75NTR and p140TrkA[150].

NGF is important both during development and in adult life[151,152]. It is found mainly in the cortex, hippocampus, pituitary gland, basal ganglia, thalamus, spinal cord, and retina[153] and it is essential for the development and maintenance of neurons both in the peripheral nervous system and the CNS[154]. It has important roles in the survival and functions, such as arousal, attention, consciousness, and memory, of cholinergic neurons of the basal forebrain complex (BFC)[155]. Given that defects in BFC neurons are found in Alzheimer's disease, NGF can potentially be used as a protective or curative factor for such neurodegenerative diseases[156]. NGF regulates phenotypic features in noradrenergic nuclei of hypothalamus and brainstem, and is

involved in the modulation of stress axis activity and in the regulation of autonomic response[157,158]. It is also found in the sensory nervous, autonomic nervous, endocrine, and immune systems[159] and known to play an important role in the functional recovery from brain injury and the prevention of neuronal death[160,161].

Although PC12 cells express both the p75NTR and the p140trkA receptors, it had been shown that the neurite-inducing property of NGF is mediated by the p140TrkA, but not the p75NTR, receptor[150,162]. The induction of neurite outgrowth by NGF in PC12 cells is one of the most widely used systems for the study of signalling pathways involved in the process. Several pathways, such as the Akt[163], Erk[164,165], JNK[112], and P38[113] have been reported to be required for the differentiation of PC12 cells.

NGF activates PI3K, which then subsequently phosphorylates Akt in PC12 cells[163]. The PI3K pathway has been implicated in the cytoskeletal reorganization of the cells during NGF stimulation[166,167], an important process in neuronal differentiation. It has also been found to regulate different aspects of neurotrophin-induced axon morphogenesis, including guidance and elongation[110].

Erk, JNK, and P38 are mitogen-activated protein kinases (MAPKs), which are among the most widely used kinases throughout evolution in many physiological processes[168]. The MEK-Erk signalling cascade is one of the most extensively studied pathways and multiple upstream effectors that are able to activate MEK have been reported[141]. The Ras→C-Raf→MEK and Rap1→B-Raf→MEK pathways have been found to be the main pathways leading to Erk activation upon NGF stimulation[169]. However, the activation

kinetics of the two pathways are different, with the Ras→c-Raf pathway leading to transient Erk activation and the Rap1→B-Raf pathway leading to sustained Erk activation[169]. It is well-known that the sustained and prolonged activation of the MEK-Erk pathway up to an hour is required for neurite outgrowth[165]. Sustained activation of Erk results in its nuclear translocation, activation of transcription factors such as Elk and c-Jun[164], and induction of neural-specific gene expression, leading to neuronal differentiation of PC12 cells[170].

The JNK pathway has also been reported to be required for PC12 cells differentiation[112,164]. Treatment of PC12 cells with NGF was also found to induce sustained JNK activation of up to an hour[171]. The involvement of JNK in regulating neurite outgrowth has been attributed to its ability to phosphorylate c-Jun, an important mediator of neurite outgrowth[172]. Furthermore, the activity of JNK was found to regulated, in part, by MEK, suggesting that the involvement of MEK in regulating neurite outgrowth could be mediated to some extent by JNK[112].

Similarly, studies have also shown that the P38 pathway is required for the differentiation of PC12 cells[113,173]. In addition, MEK was also found to regulate the activity of P38, indicating that the involvement of MEK in regulating neurite outgrowth could also be mediated partly by P38[113].

2.3.1.3. Basic-Fibroblast Growth Factor (FGFb)

The basic-fibroblast growth factor (FGFb), the prototypic member of a family of 22 proteins, was first purified as a heparin-binding polypeptide from bovine pituitary[174]. FGF was recognized as an important neurotrophic factor after

high levels of mitogenic activity were found in the brain[175], and both FGFb and its receptors have also been detected in the brain[176-178]. It was found to be a potent neurotrophic factor with the ability to promote neuronal survival and neurite extension under both *in vitro*[179] and *in vivo* conditions[180,181].

FGFs, including FGFb, are important for the development and maintenance of the nervous system, including the outgrowth and survival of brain cells[182-184]. They are required to sustain and regulate the proliferation and differentiation of stem cells during neurogenesis[185]. FGFs and their receptors are also required for the regulation of the survival and neurite outgrowth of neurons from the cerebral cortex, hippocampus, retina, cerebellum, septa area, ciliary ganglion, sympathetic ganglia, and sensory ganglia[186-189]. In addition, they are known to regulate functions such as memory and learning[190]. There are wide medical applications of FGFb as it can potentially be used for the treatment of diseases such as brain ischemia[191], and stroke[192], treatment of neurodegenerative disorders such as Alzheimer's and Parkinson's disease[190], and survival of grafted neurons in transplantation[193].

Treatment with FGFb is known to promote neurite outgrowth in PC12 cells[194,195]. While activation of Akt by FGFb has been correlated to neurite outgrowth, the direct involvement of Akt in regulating the process has yet to be verified[196]. In addition, the P38 MAPK was found to be not required for neurite outgrowth induced by FGFb[197]. However, similar to treatments with NGF and PACAP, sustained Erk activation has also been found to be essential for FGFb-induced neurite outgrowth[198,199].

2.3.1.4. Epidermal Growth Factor (EGF)

Epidermal growth factor (EGF) is the founding member of the EGF-family of ligands and was first isolated from the submaxillary glands of mouse[200]. High levels of the EGF-family of ligands and their receptors are found in the brain and they are important for the morphogenesis of the brain and the functions of both the developing and adult brains[201,202].

The EGF-family of ligands and their receptors are found in various regions of the brain such as the developing cortical plate, hippocampus, septum, and hypothalamus[202,203]. They are important for the survival, migration, differentiation, and proliferation of neurons in these regions of the brain[202]. In addition, they regulate biological functions such as psychomotor behaviours, learning, memory, object recognition, and synaptic plasticity[204]. Defects in the system has been associated with illness such as Parkinson's disease[205], Alzheimer's disease[206], gliomas[207], and psychiatric disorder[204].

Despite the importance of EGF in the brain, EGF is not known to induce neurite outgrowth. In the PC12 cells, unlike NGF and FGFb, EGF induces only survival and proliferation, but not differentiation[111,208,209].

2.3.2. Regulation of Synergistic Neurite Outgrowth in PC12 Cells

All these three growth factors, NGF[210-213], FGFb[214], and EGF[215,216] are well-known to cooperate with cyclic adenosine monophosphate (cAMP)-elevating agents to result in synergistic neurite outgrowth. Examples of such cAMP-elevating agents include PACAP, forskolin, and cAMP-analogues. However, the pathways and mechanisms involved in regulating such synergistic neurite

outgrowth have not been well-studied. The main finding made in these systems is that sustained Erk activation, an important prerequisite for neurite outgrowth, was observed. In addition, the P38 MAPK pathway has also been found to regulate neurite outgrowth induced by NGF-cAMP[212].

While the Erk and P38 MAPK signalling pathways are required for synergistic neurite outgrowth regulated by these growth factors and cAMP-elevating agent, there is little knowledge of whether other signalling pathways are also involved in the process. More importantly, it is not known if the three systems activate a common set of signalling pathways to mediate the synergistic neurite outgrowth. Besides the Erk, JNK, P38, and Akt pathways, many other signalling components, which can potentially be involved in synergistic neurite outgrowth, are also activated by these ligands. A summary of the signalling pathways activated by these ligands in PC12 cells is shown in Figure 2.3. However, this map is just an addition or superimposition of the individual signalling networks activated by each ligand and cannot explain the resulting multi-ligand emergent behaviours[217,218]. It is consolidated from multiple studies, each under different context and experimental conditions, based on reductionist approaches. Thus, the quantitative and context-dependency nature of the underlying signalling behaviours are unclear. It gives no information with regards to the stoichiometry of the interactions, the dynamics of the protein activities and interactions, and how the activities of the proteins affect the network. Thus, such a map does not illustrate how synergistic behaviours can be achieved through the interactions of the involved pathways.

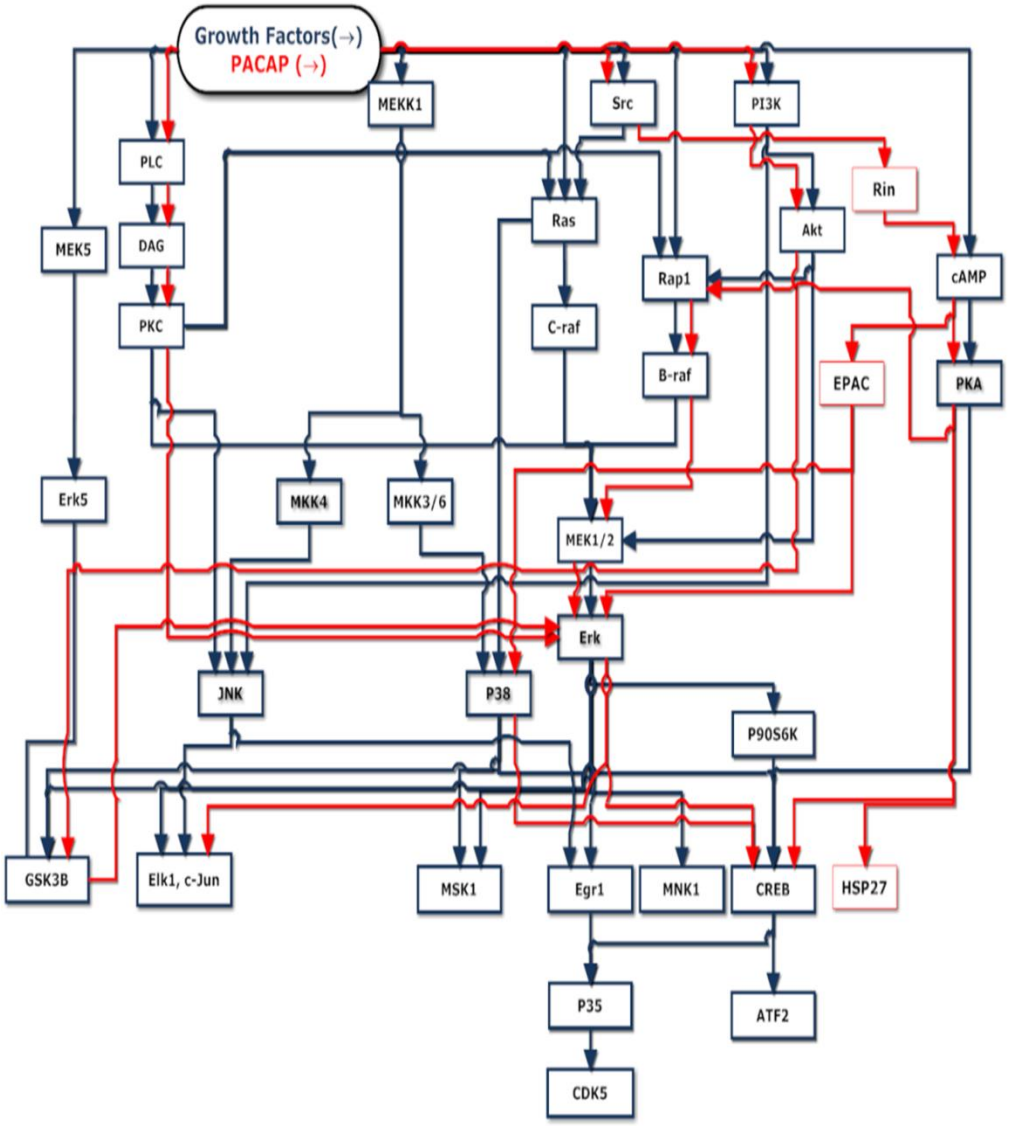

Figure 2.3. Signalling pathways activated by the growth factors (NGF, FGFb, and EGF) and PACAP in PC12 cells during differentiation[111-113,134,135,163,164,169,172,219-226].

2.3.3. Regulation of Morphological Structures of Neurite during Synergistic Neurite Outgrowth in PC12 Cells

With a deeper understanding of the brain today, it is now known that the morphological structures of neurites are linked with higher-order cognitive functions and are important in regulating the functions of the brain[227-229]. As reviewed above, protein kinases such as Erk, JNK, P38, and Akt are important in the regulation of neurite outgrowth during neuronal differentiation. Quantifications of the extent of neurite outgrowth are typically measured

through one or two parameters such as the number of differentiated cells and neurite length[136,164,230]. The number of differentiated cells is based on the number of cells that exhibit neurite outgrowths longer than one or two cell-body diameter. However, the morphological structure of neurites is characterized not just by length alone but also by other features such as the number of neurite extensions from the cell-body and the branching of the neurites[231]. These features collectively dictate the number of neurons that can interact with a particular neuron and guide the spatial boundary within which neurons can form synapses and transmit information between one another.

The importance of gaining insights into the regulation of these features has also resulted in an increasing effort in the development of both manual and automated softwares for the analysis of the morphological structures of neurites[229,232-235]. Such tools are especially important when a large number of cells in any population need to be quantified before any meaningful conclusion can be drawn. Despite the importance of such morphological structures, the mechanisms underlying the regulation of some of these features have not been well-studied.

Although many pathways have been investigated for their roles in regulating neurite length, the mechanisms involved in the regulation of various morphological features is still poorly understood. Enhancement of neurite length during synergism is likely to be due to up-regulation of multiple morphological parameters, such as length of individual neurites, number of neurites, and degree of branching. As mentioned above, pathways such as the Erk and JNK are known to regulate neurite outgrowth during differentiation of PC12 cells. Importantly, these pathways regulate not just the

length of neurites, but also other morphological aspects of neuritogenesis, such as number of neurite extensions and degree of branching[236]. However, these morphological features can also be regulated independently of one another. For instance, P38 had been found to regulate the total neurite length and degree of branching but not number of neurites per cell[237] and Akt had been found to regulate neurite branching but not length[238] in various systems. In addition, studies investigating the branching and elongation of axons have also found that axon branching can be regulated separately from other aspects of neurite outgrowth[239,240]. Thus, regulation of morphological neurite outgrowth involves a complex interplay of different signalling pathways and morphological features. To gain a deeper understanding of synergistic neurite outgrowth, the pathways regulating different morphological features and the impact of these features on global measures of differentiation such as total neurite length need to be addressed.

2.4. Analysis of Synergistic Systems Using PC12 Cells

2.4.1. Lack of Approaches to Analyses of Synergistic Systems

As mentioned in the earlier sections, synergism is a phenomenon that is gaining importance due to its huge benefits in therapeutics. It is an emergent behaviour that can arise as a result of interactions between signalling components in the cells. Thus, the key to understanding such behaviours is to have approaches that can shed light on how specific interactions can give rise to synergism. While synergistic behaviours in various systems have been widely observed[241-244], there have not been many studies that focus on understanding how synergism occurs at a systems-level. While systems-level

modeling have been applied to the analyses of synergism by using regression models[27] or combining ODEs from two systems[245], to identify synergistic drug combinations[246,247], or to develop methods to evaluate the extent of synergy[248], these methods do not give insight into the mechanism underlying synergism in systems with poor *a priori* knowledge. Methods that aim to identify synergistic drug combination or to quantify synergy do not reveal how the drug combinations can lead to synergistic effects. Although the significance of the cross-terms in regression models can suggest the absence or presence of synergy, they give no indication of the mechanism underlying synergy. On the other hand, while ODE models can suggest the kinetic mechanisms underlying synergism, they are not suitable for systems with poor *a priori* knowledge.

2.4.2. Proposed Bayesian Approach to Analysis of Synergistic Neurite Outgrowth

The signalling mechanisms underlying neuronal differentiation, including the PC12 cells model, and neurite outgrowth are still very poorly understood today. Likewise, synergistic neurite outgrowth under multi-ligand condition is also poorly understood mechanistically. To develop modeling frameworks that can effectively analyze such a system, several issues need to be addressed. These issues are outlined in Figure 2.4 and discussed in the following sections.

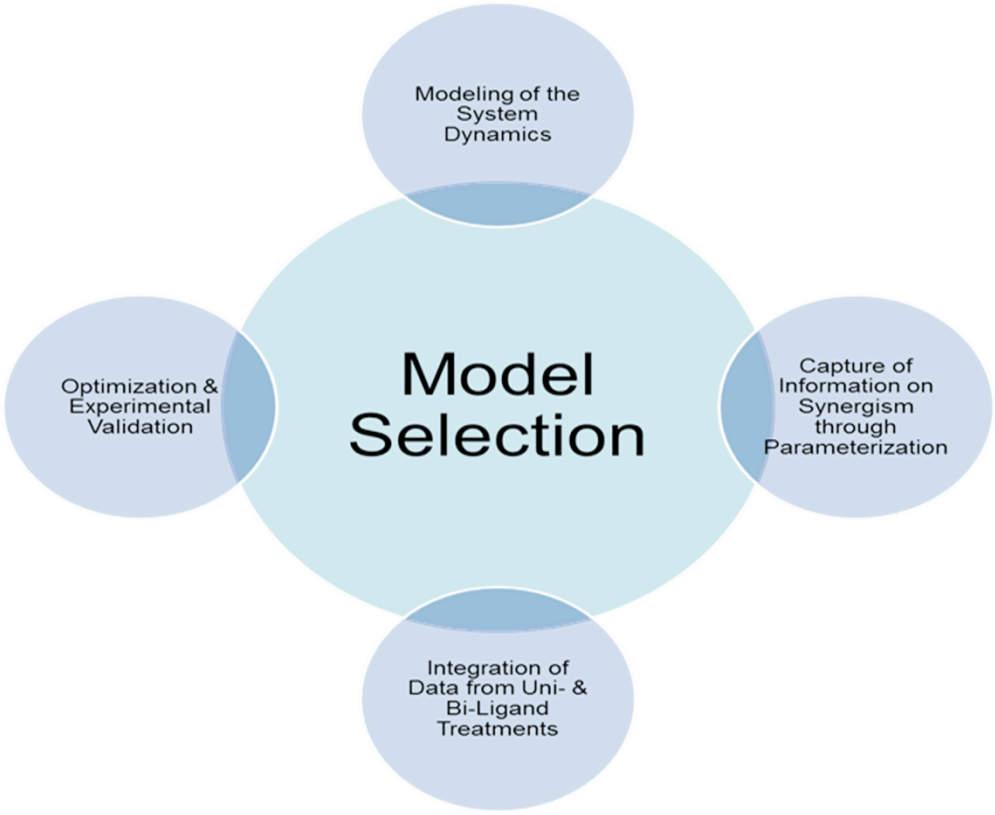

Figure 2.4. Issues to be addressed in the development of an approach for the analysis of synergistic systems.

2.4.2.1. Model Selection

Given this lack of *a priori* understanding, and lack of available modeling tools for such purposes, modeling tools for such network inference must be developed in order to gain insights about the system. An overview of the different modeling methods reviewed earlier is given in Table 2.1 below. BNs are potentially useful for such as purpose as it can be applied even with a lack of *a priori* knowledge. Furthermore, it is not limited by linearity assumptions, or a two-state representation of the variables, like in linear algebra and Boolean network, respectively. While FL models have been proposed as an extension of Boolean models by allowing a multi-state representation of the variables, they are not well suited for the incorporation of *a priori* information about the network topology in cell signalling.

Table 2.1. Properties of different mathematical models[33].

Properties	ODE	ANN	Associated Network	Boolean Network	BN	Linear Algebra
Requires good *a priori* knowledge	√					
Incorporation of *a priori* topology knowledge	√		√		√	
Modeling of dynamics	√	√		√	√	√
Gives directed networks	√			√	√	√
Need for data discretization				√	√	
Allows variables to exist in multiple (>2) states	√	√	√		√	√
Linearity assumption						√

Importantly, in addition to the properties of BNs reviewed above, BNs allow multivariate directional dependencies to be captured. They can also capture both direct molecular interactions as well as indirect influences that occur through components not measured in the experiments. The probabilistic nature of BNs can also accommodate for noise, which is inherent to biological datasets. Thus, BNs can potentially provide insight into poorly understood signalling systems, where mechanistic knowledge is sparingly available, even when noise is present in the datasets.

2.4.2.2. Modeling the Dynamics of the System

Cell signalling is not a static but a temporally-varying process. Consequently, ordinary BNs may not *a priori* be the most natural choice of modelling approach. Thus, DBN were proposed as a variant to BN so that the dynamics in systems can be accounted for. However, DBNs are most suited for the multivariate time-series that form a first order Markov-chain, an assumption that may be plausible when the relationships between the variables are

stationary and do not vary with time, which is unlikely to be true when cells are not at steady-state conditions[77,78]. Moreover, the process, including all the relevant factors in the domain, also needs to be observed in regular intervals. In typical biological experiments where cells are perturbed and the cellular components probed temporally at irregular intervals, the above assumptions are not true.

Recently, non-stationary DBNs (nsDBNs) and time-varying DBNs (tvDBNs) have been developed to relax the restrictive assumption of stationarity[78,249,250]. These approaches work by demarcating time-series data into multiple segments, with each segment spanning different time-frames. The structures are assumed to be piecewise-stationary in time, and non-stationary networks are built as a series of stationary models. These segmented points are also termed Bayesian changepoints. Thus, the inference process involves learning of the location and number of changepoints as well as the network structure. Although these approaches greatly enhance the expressivity of the DBN framework, they are plausible only for observation sequences that are sufficiently long, where the regularities in the change of the independence structure can be captured.

Thus, a different approach is still needed in order to effectively model systems with short-time series data obtained at irregular intervals. To tackle this issue, a DBN expanded-in-time (eDBN), where protein activation levels at different time-points were considered as separate variables, was proposed. This idea is analogous to modeling variables at different time points as separate variables in the ordinary BN. An eDBN is a better approach as it can reduce information loss as compared to traditional BN or DBN approaches. In the BN

approach, for each variable, data across all time-points are grouped into one variable independent of the temporal effects. This can cause different relationships between the proteins at different time-points to offset each other, resulting in a misrepresented network. Likewise, for DBNs, data across all time-points are grouped into two variables, at time t and t+1, which inevitably results in the same drawback as BNs. Although the idea of eDBN had previously been employed[65], the validity of the approach was not validated as the model predictions were not validated experimentally. This problem is not encountered in the work presented in this thesis as the proposed methodology presented here will require the model findings to be validated experimentally.

2.4.2.3. Capture of Information on Synergism through Parameterization

In BN modeling, discretization of data is necessary. While it is important to minimize loss of data during this procedure, it would be beneficial to be able to discretize data in a way such that information regarding to synergism can be captured. In this work, the degree of synergism (DS) is quantified using Equation 2.6, where values > 1 represents synergism.

(Equation 2.6) $$DS = \frac{Effect\ of\ bi{-}ligand\ stimulation}{Effect\ of\ ligand\ A\ stimulation + Effect\ of\ ligand\ B\ stimulation}$$

Discretization of data serves to group the activation levels of each variable obtained under different treatment conditions into different bins, where each bin represents a different discretized degree of activity. However, such discretization does not contain information about the absence/presence or different degrees of synergism. This is because similar activity levels can be

obtained under both uni- or bi-ligand treatments, depending on the ligand concentrations used. A hypothetical example is given in Table 2.2 below, where conditions 4, 5, and 6 result in the same activation levels of protein C. Although all three data-points are grouped into Bin 3, the information that condition 5 but not conditions 4 and 6 resulted in synergism is not reflected in the discretized data.

Table 2.2. Hypothetical example of how traditional methods of data discretization (binning) fail to capture information about synergism.

Condition	Ligand A (μM)	Ligand B (μM)	Activation level of Protein C (Fold change)	Presence of Synergism	Bin
1	0	0	0	-	1
2	0	10	4	-	2
3	10	0	5	-	2
4	100	0	20	-	3
5	10	10	20	Yes	3
6	100	10	20	No	3

To circumvent this limitation, it is proposed that separate bins are used for data obtained under uni- and bi-ligand treatments. An example is illustrated in Table 2.3, where Bins 4, 5, and 6 reflect activity levels under uni-ligand condition, presence of synergism under bi-ligand condition, and absence of synergism under bi-ligand condition. While the use of more bins may add noise to the data, such parameterizations can potentially add more information when used appropriately. Such a parameterization approach essentially means that different information with regards to activation levels and degree of synergism is obtained from uni- and bi-ligand experiments, respectively.

Table 2.3. Hypothetical example of how a modified data discretization (binning) technique can incorporate information about synergism.

Condition	Ligand A (μM)	Ligand B (μM)	Activation level of Protein C (Fold change)	Presence of Synergism	Bin
1	0	0	0	-	1
2	0	10	4	-	2
3	10	0	5	-	2
4	100	0	20	-	3
5	10	10	20	Yes	4
6	100	10	20	No	5

2.4.2.4. Integration of Data from Uni- and Bi-Ligand Treatments

Given that different information is obtained under uni- and bi-ligand treatments, techniques that can integrate the two types of data together are required during the modeling process. If they cannot be integrated, the idea of parameterizing data from uni- and bi-ligand experiments differently would not serve its purpose.

Existing data integration techniques are primarily focused on integration of similar data from different sources or integration of complementary data-types[251,252]. Some examples of such approaches are ordering of datasets[253], correlated clustering[254], weighted contribution of each dataset[255,256], use of mean and mode values of occurrences of each edge in the individual networks[257], and multi-objectives optimization to account for the nature of different experiments[258]. In essence, many of these methods conduct separate statistical analyses on each dataset and integrate the results of each analysis, by analyzing individual links between pairs of nodes independently without considering the context of the whole system[259,260]. Moreover, these

approaches do not account for how ligand-specific treatments can complement one another. In the analysis of synergism, experiments from uni-ligand treatment can complement those of bi-ligand as synergism must be assessed with reference to uni-ligand treatments. Thus, there is a need for systems biology to go beyond connecting different pieces of data to an integrated analysis.

In this methodology, a two-phase learning approach is proposed as a strategy for this integrated analysis. Such an approach is also well-suited for BNs as Bayesian theory offers a principled way to integrate different sources of information by using the results from one information source as a prior knowledge for analyzing another information source. In the first phase, the probabilities of all the possible parent sets for all variables were first estimated using the data from the uni-ligand treatment. In the second phase, these probabilities were then used as a decomposable structure prior for the bi-ligand system. In addition to an approach for data integration, it also serves a way to alleviate the lack of *a priori* knowledge of the signalling network underlying bi-ligand treatment. This is justifiable as long as the same signalling pathways are activated following both uni- and bi-ligand treatments.

2.4.2.5. Optimization and Experimental Validation

Learning of BNs requires search algorithms to find the optimal BN. It is a widely established fact that this process is a non-deterministic polynomial-time hard problem[261,262], meaning that no polynomial time algorithms for finding the most probable BN are likely to exist. Since the number of possible BN structures, given by f(n) in Equation 2.7[263,264], increases super-

exponentially with the number of nodes (n)[265], evaluating all the possible structures is not computationally feasible when n exceeds 6.

(Equation 2.7) $f(n) = \sum_{i=1}^{n}(-1)^{i+1}\binom{n}{i}2^{i(n-i)}f(n-i)$

Thus, most methods for finding the optimal network structure are based on either local or global approximation methods that cannot guarantee the optimal or most probable network. Finding the most optimal network is then performed using a process known as Bayesian model averaging (BMA)[266], which involves finding a network that is an average over all the high scoring networks found during the learning process. There is usually no way of determining, via computational methods, which of the competing high scoring models gives the correct representation of the system. Thus, BMA reduces the uncertainty in the model selection process by taking an average of the high scoring networks and finding a consensus network.

However, advances in the field of dynamic programming have offered a different perspective to this problem. It is a technique that is well-suited for solving global optimization problems and works by breaking down a problem to smaller sub-problems[267,268]. Recently, a dynamic programming algorithm that utilizes the specific structure of the common BN evaluation criteria was proposed for guaranteed inference of the most probable Bayesian network. This exact structure learning algorithm[269] can be applied to systems of 30 variables or less. In addition, this algorithm can overcome another computational challenge in using Bayesian data integration for BN inference. Given the large number of possible BN network structures (Equation 2.7), storage of the prior and posterior probabilities for all the possible network structures would be impractical due to space constraints. This is overcome by

the exact structure learning algorithm as the same structure of network evaluation criteria that it utilizes can be used for storing the prior and posterior network structure distributions compactly. However, it can be argued that selecting the highest-scoring and most optimal network is not advisable given that the top scoring networks can be highly similar and that selection of a consensus model will give a more representative depiction of the system. This is especially true in view of the small datasets obtained in typical biological experiments. Another drawback is that the feasibility of the application of an exact structure learning algorithm in the analyses of cellular signalling networks has yet to be demonstrated.

Although the selection of the highest-scoring network has its drawbacks as highlighted above, this problem is less of an issue in this scenario. In the use of approximation optimization methods, where the search space is always non-exhaustive, there is no way of determining how close the top-scoring networks are to the true optimal structure. On the contrary, the optimal network can be found using dynamic programming. Thus, the chances of having false positives and negatives in the resulting model for dynamic programming would be lower as compared to networks obtained under approximation methods. In addition, performing experimental validation of the model findings, a key step in the workflow of systems biology, is taken into consideration. The results obtained will result in validation or invalidation of the model, which will in turn lead to changes in the model, if necessary.

2.5. Concluding Remarks

Despite the importance of synergistic therapeutics, computational modeling tools that can effectively analyze such behaviours at systems levels are still

lacking. To bridge this gap in the field, using synergistic neurite outgrowth in PC12 cells as the system of study, such a tool will be developed. Neurite outgrowth is an important process of neuronal differentiation during development and abnormalities in this process have led to neurodegenerative diseases such as Alzheimer's and Parkinson's. Thus, the main focus of this thesis is to further the understanding of the mechanisms underlying synergistic neurite outgrowth and a general modeling approach that can be used to effectively analyze behaviours such as synergism in multi-ligand systems was used to complement the analysis. This proposed approach was termed TEEBM (Two-phase, Exact structure learning, Expanded-in-time Bayesian Methodology).

Chapter 3.

C-Jun N-Terminal Kinase in Synergistic Neurite Outgrowth in PC12 Cells Mediated through P90RSK

3.1. Introduction

Given the lack of *a priori* understanding of the pathways involved in synergistic neurite outgrowth, it is imperative to first identify a plausible sub-system of signalling mechanism involved in the regulation of the process. It is only when signalling components involved in this process are identified that the underlying emergent synergistic properties can be analyzed. PC12 cells have been widely used a model widely used for the study of neuronal differentiation and it differentiates in response to ligands such as NGF[107], FGFb[195], and PACAP[111]. In these systems, pathways such as the Erk[164,169], P38[270], JNK[112,164], and PI3K[163] have been widely reported to be required for neurite outgrowth.

Although EGF alone does not induce neurite outgrowth in PC12 cells, it has been found to synergize with cyclic adenosine monophosphate (cAMP)-elevating agents such as PACAP and forskolin, thereby enhancing neurite outgrowth[215,216]. Similarly, cAMP-elevating agents have also been found to synergize with FGFb[214] and NGF[211,212] to enhance neurite outgrowth, where both P38 and Erk have been found to regulate neurite outgrowth induced by NGF-cAMP[212,213]. Whereas NGF, FGFb and EGF can all cooperate with cAMP-elevating agents to enhance neurite outgrowth, an unanswered question is whether these three systems activate a common set of signalling pathways to mediate such synergy.

In this study, we investigated the activation and involvement of various signalling pathways in synergistic neurite outgrowth using three combinations of ligands: NGF-PACAP (NP), FGFb-PACAP (FP) and EGF-PACAP (EP). As expected, all three systems showed a synergistic phosphorylation of Erk

concomitant with neurite outgrowth. Interestingly, JNK, but not Akt or P38, was also synergistically activated in all three systems. Unexpectedly, inhibition of JNK blocked neurite outgrowth in the NP and FP, but not EP, systems. This differential involvement of JNK was found to be dependent on the regulation of P90RSK activity. Thus, a JNK-P90RSK link was identified as a hitherto unrecognized mechanism mediating the synergistic effect in neurite outgrowth. Our results therefore demonstrate the involvement of distinct signalling pathways in regulating neurite outgrowth in response to different synergistic growth factor-PACAP stimulation.

3.2. Results

3.2.1. Response Surface Analyses Suggest that Synergistic Neurite Outgrowth is Regulated by Discrete Mechanisms in Different Systems

In this study, the software HCA-Vision was used for the quantification of neurite outgrowth. Before using it for the analysis of the neurite outgrowths induced by different treatments, its reliability was first verified against a more commonly used and widely accepted tool, NeuronJ, a plug-in for ImageJ[271]. In NeuronJ, quantification of the number of cells and the tracing of the neurites are performed manually (Figure 3.1a). On the other hand, in HCA-Vision, both tasks are automated (Figure 3.1b). The quantification results of the number of cells and the neurite length are as shown in Table 3.1. The quantification results by HCA-Vision were very consistent with those of NeuronJ and manual counting, indicating the reliability of HCA-Vision for the analyses of neurite length.

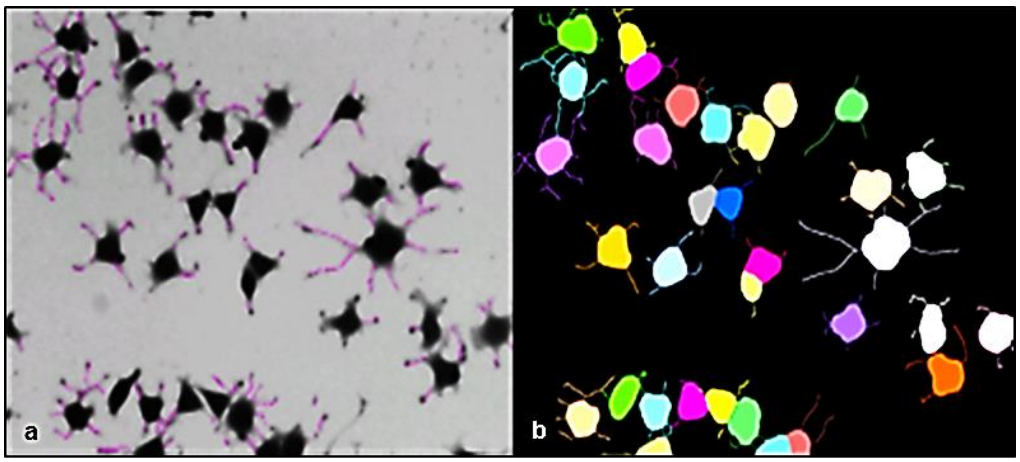

Figure 3.1. Neurite tracing for analyses by NeuronJ and HCA-Vision. (a) Manual neurite tracing using NeuronJ. (b) Automated neurite tracing by HCA-Vision.

Table 3.1. Comparison of neurite length quantification by two softwares, NeuronJ and HCA-Vision.

Read-outs	NeuronJ	HCA-Vision
Number of Cells	33	33
Total Neurite Length (pixels)	5460	5484

NGF[211,212], FGFb[214] and EGF[215,216] are known to synergize with cAMP-elevating agents to enhance neurite outgrowth. NGF or FGFb caused considerably longer neurite outgrowth than EGF or PACAP (Figures 3.2, and 3.3). Representative images of the neurite outgrowth in each system are shown in Figure 3.2a. Following treatment with the growth factors and PACAP, no differences in the expression levels and localization of the neuronal marker, βIII-Tubulin, were observed (Figure 3.2b), which is consistent with the findings of previous studies[272,273].

To better visualize the synergistic action between growth factors and PACAP on neurite length, we used response surface model (RSM)[274] and examined the effect of NGF-PACAP (NP), FGFb-PACAP (FP) and EGF-PACAP (EP) treatments in these cells. The cells were treated with the ligands singly and in combinations. In these plots, the neurite length obtained after 48 hours of combinatorial treatment was compared to that obtained by a summation of

neurite length induced by the individual ligands (additive effect). Surface plots of the three systems—NP (Figure 3.3a(i)), FP (Figure 3.3b(i)), and EP (Figure 3.3c(i))—clearly indicated that combinatorial treatments resulted in longer neurites than the additive effects of single ligand exposure, indicating synergism. These plots also showed that synergism (as indicated by the plateau regions) occurred over a wide range of doses of growth factors and PACAP.

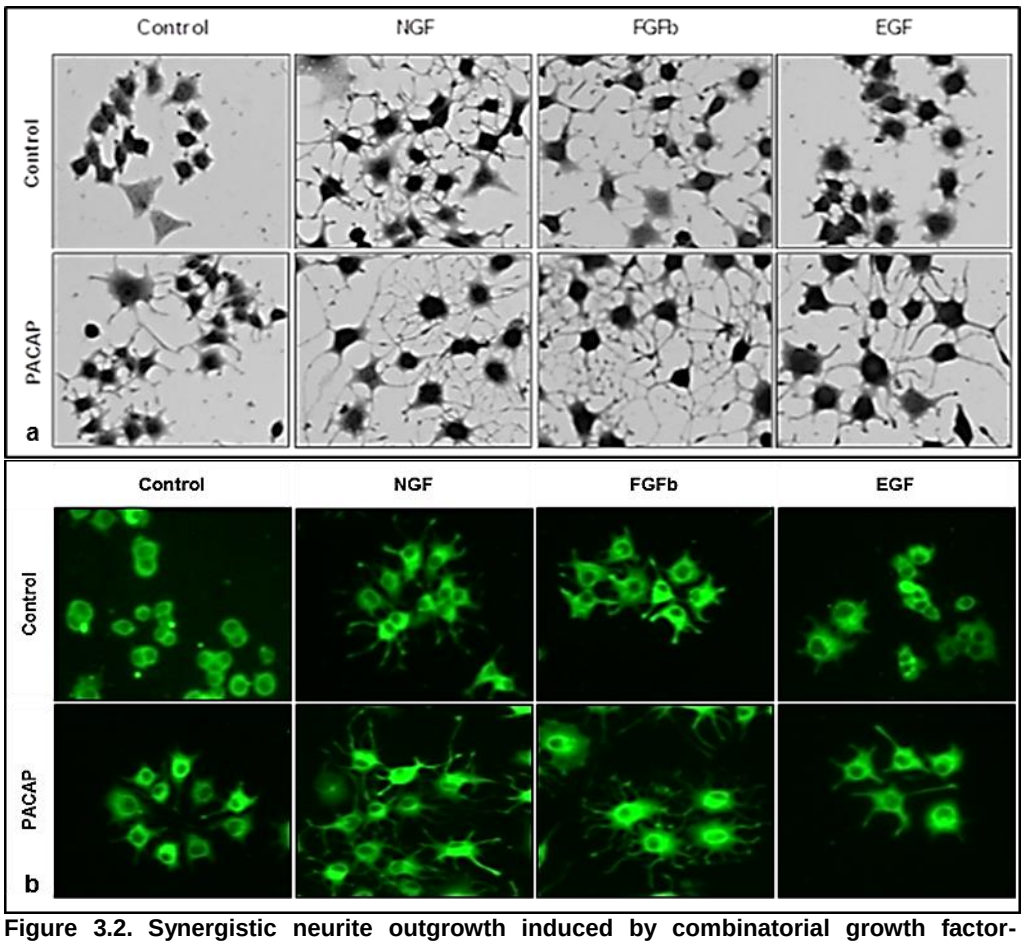

Figure 3.2. Synergistic neurite outgrowth induced by combinatorial growth factor-PACAP treatments. (a) Representative images of cells treated with each growth factor (50 ng/ml) with and without PACAP (100 ng/ml). (b) Representative fluorescent images of cells stained with βIII-Tubulin after being treated with each growth factor (50 ng/ml) with and without PACAP (100 ng/ml).

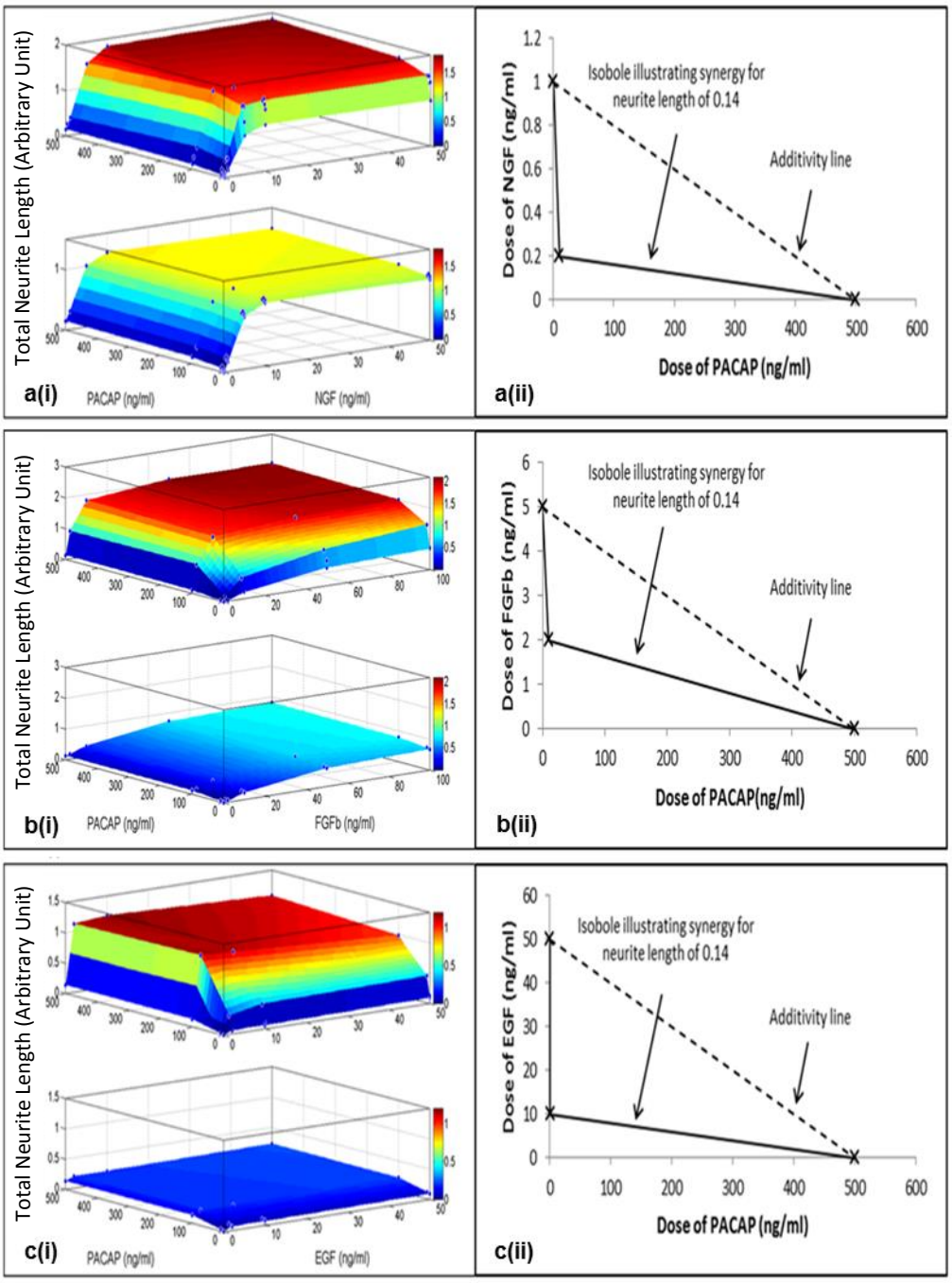

Figure 3.3. Analysis of synergistic neurite outgrowth induced by combinatorial growth factor-PACAP treatments using RSM. (a(i)), (b(i)), (c(i)) Response surface plots for the NGF (0-50 ng/ml)-PACAP (0-500 ng/ml) (NP), FGFb (0-100 ng/ml)-PACAP (0-500 ng/ml) (FP), and EGF (0-50 ng/ml)-PACAP (0-500 ng/ml) (EP) systems, respectively. Top panel: Experimentally obtained results of the growth factor-PACAP combinatorial treatment; Bottom panel: Additive effect calculated through the summation of the individual effects of the growth factors and PACAP. The x, y, and z axes denote concentrations of PACAP (ng/ml), concentrations of growth factors (ng/ml), and neurite length, respectively. (a(ii)), (b(ii)), (c(ii)) Isobologram plots illustrating the concentrations of growth factor and PACAP necessary to obtain a neurite length of 0.14 for the NP, FP, and EP systems, respectively.

To further illustrate that synergistic neurite outgrowth can occur even with low doses of PACAP, an isobologram[275] was plotted for each of the three systems

(Figures 3.3a(ii), 3.3b(ii), and 3.3c(ii)). Significantly higher concentrations of PACAP were required in the absence of any growth factors to obtain similar neurite lengths. In addition, in the NP and FP systems, the saturating neurite length for the combinatorial treatment was about twice that of the additive effect, whereas a difference of about 4-fold was observed for the EP system. This indicates a higher degree of synergism in the EP system, and suggests that synergistic neurite outgrowth in the EP system may differ mechanistically from those of the NP and FP systems.

3.2.2. Synergistic Phosphorylations of Erk and JNK upon Combinatorial Growth Factor-PACAP Treatment

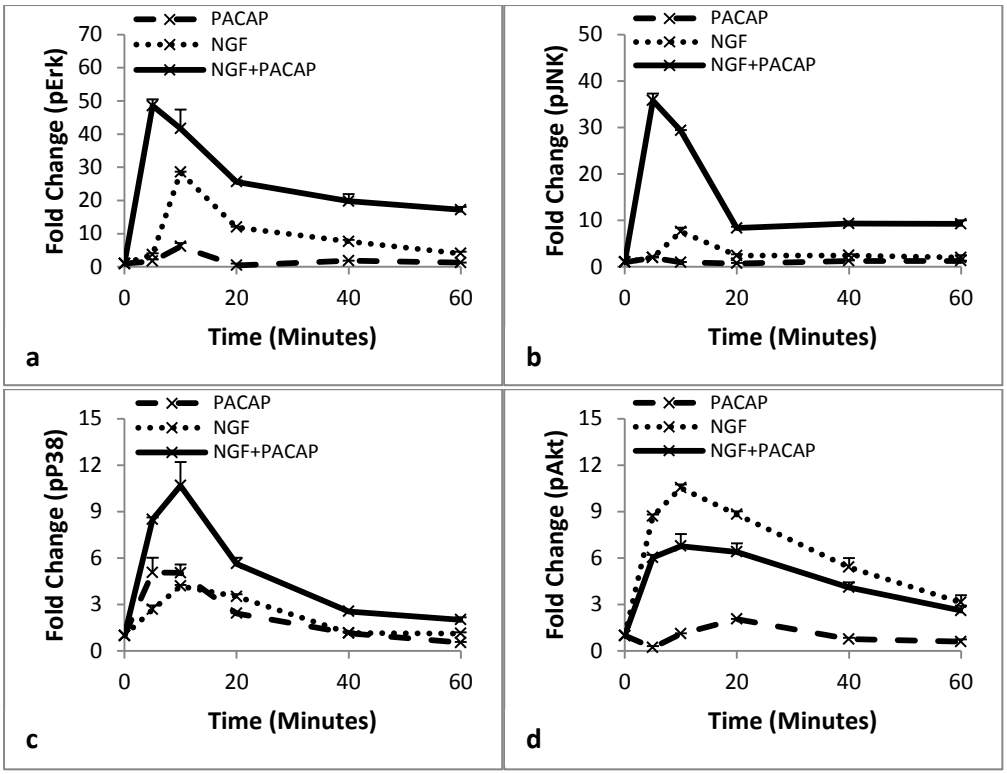

Figure 3.4. Time-course profiles of activations of kinases upon PACAP, NGF, and NP treatments. Fold changes of (a) pErk, (b) pJNK, (c) pP38, and (d) pAkt from 0-1 hour. The concentrations of NGF, and PACAP used were 50 ng/ml, and 100 ng/ml, respectively.

We hypothesized that there was likely to be synergistic activation of the various kinases that regulate synergistic neurite outgrowth. To examine the

pathways involved in regulating synergistic neurite outgrowth in these systems, we conducted a time-course to determine changes in the phosphorylation levels of four kinases—Akt, Erk, JNK, and P38—upon NGF, PACAP, and NP treatments. The kinases were activated throughout the entire 1 hour time-course (Figure 3.4). Thus, for convenience, subsequent analyses were performed only at the 20 and 60 minutes time-points.

After treating the cells with multiple doses of NGF and PACAP, the phosphorylation levels of Erk (Figure 3.5a), JNK (Figure 3.5a), P38 (Figure 3.6a) and Akt (Figure 3.6a) were quantified and analyzed for synergism. Single ligand treatment with NGF but not PACAP induced sustained Erk phosphorylation. To analyze for synergistic activation of Erk, effects upon combinatorial treatments of NP was compared to the additive effect of the individual ligands. In the presence of both ligands, Erk phosphorylation was higher than the additive effects of NGF and PACAP separately (Figure 3.5b). This is in congruence with the finding that NGF and NP treatment but not PACAP induced extensive neurite outgrowth, and is consistent with the idea that sustained Erk phosphorylation is involved in neurite outgrowth[165,170,213].

Similarly, sustained activation of JNK by NGF was observed (Figure 3.5c). In addition, we made the novel discovery that JNK was also synergistically phosphorylated upon combinatorial NP treatment (Figure 3.5c) and it was sustained for up to 1 hour post-stimulation. On the contrary, using the same analyses, synergistic phosphorylations of P38 (Figures 3.6a, and 3.6b) and Akt (Figure 3.6a, and 3.6c) were not observed in the NP system.

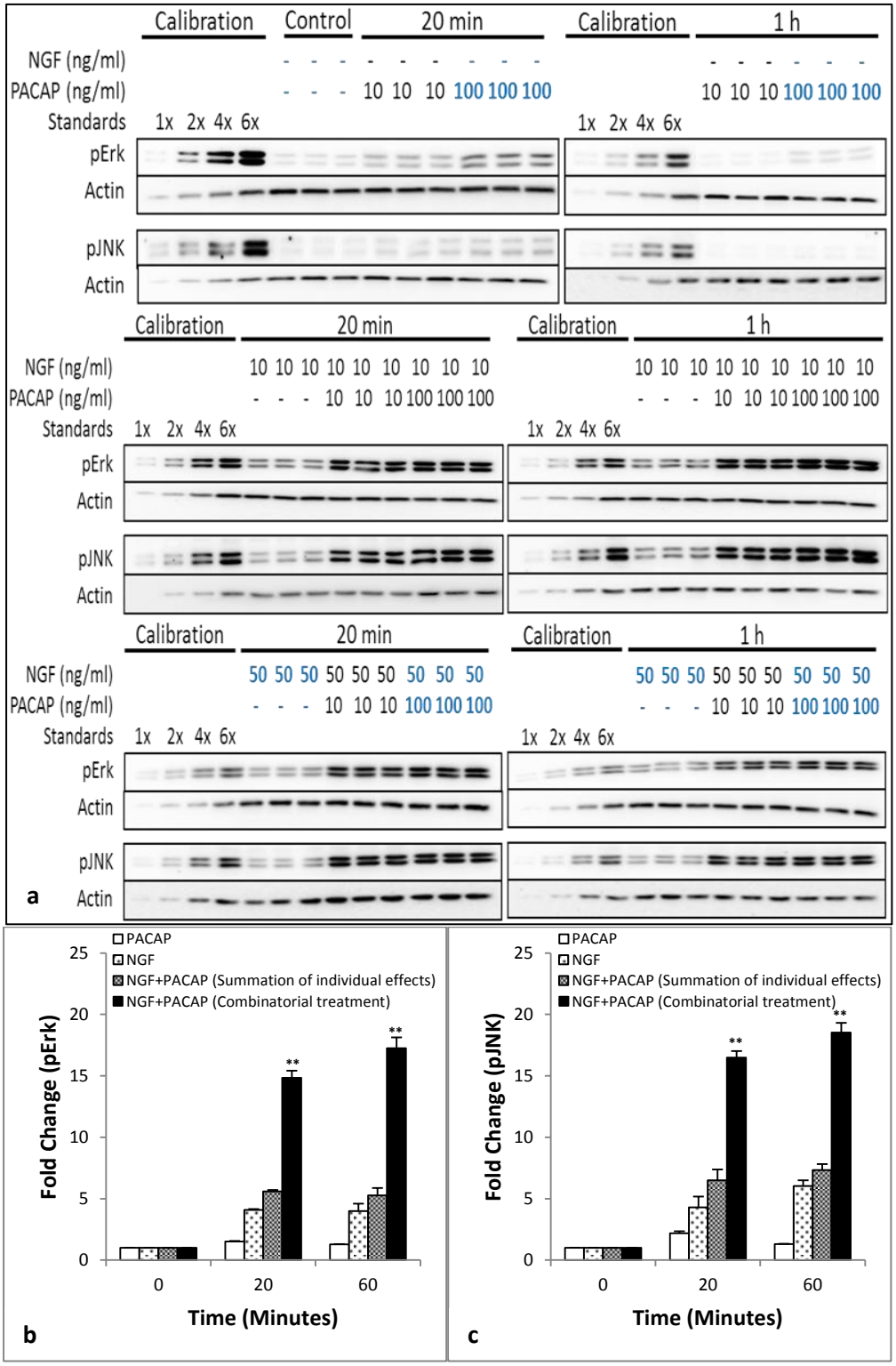

Figure 3.5. Synergistic and sustained phosphorylation of Erk and JNK upon combinatorial NGF and PACAP treatment. (a) Time-course of Erk and JNK phosphorylation at 20 and 60 minutes following NGF (0-50 ng/ml)-PACAP (0-100 ng/ml) (NP) treatment. Phosphorylation levels of the proteins were analyzed by western blotting, and normalized to the levels of actin. Fold-changes in (b) pErk and (c) pJNK were quantified by densitometry. Data for 50 ng/ml NGF and 100 ng/ml PACAP (highlighted in blue) were plotted and analyzed for synergism. Significant differences between combinatorial experimental treatment of NGF-PACAP and summation of their individual effects were calculated using the paired Student's *t*-test. A value of $p<0.05$ was considered significant (**$p<0.01$).

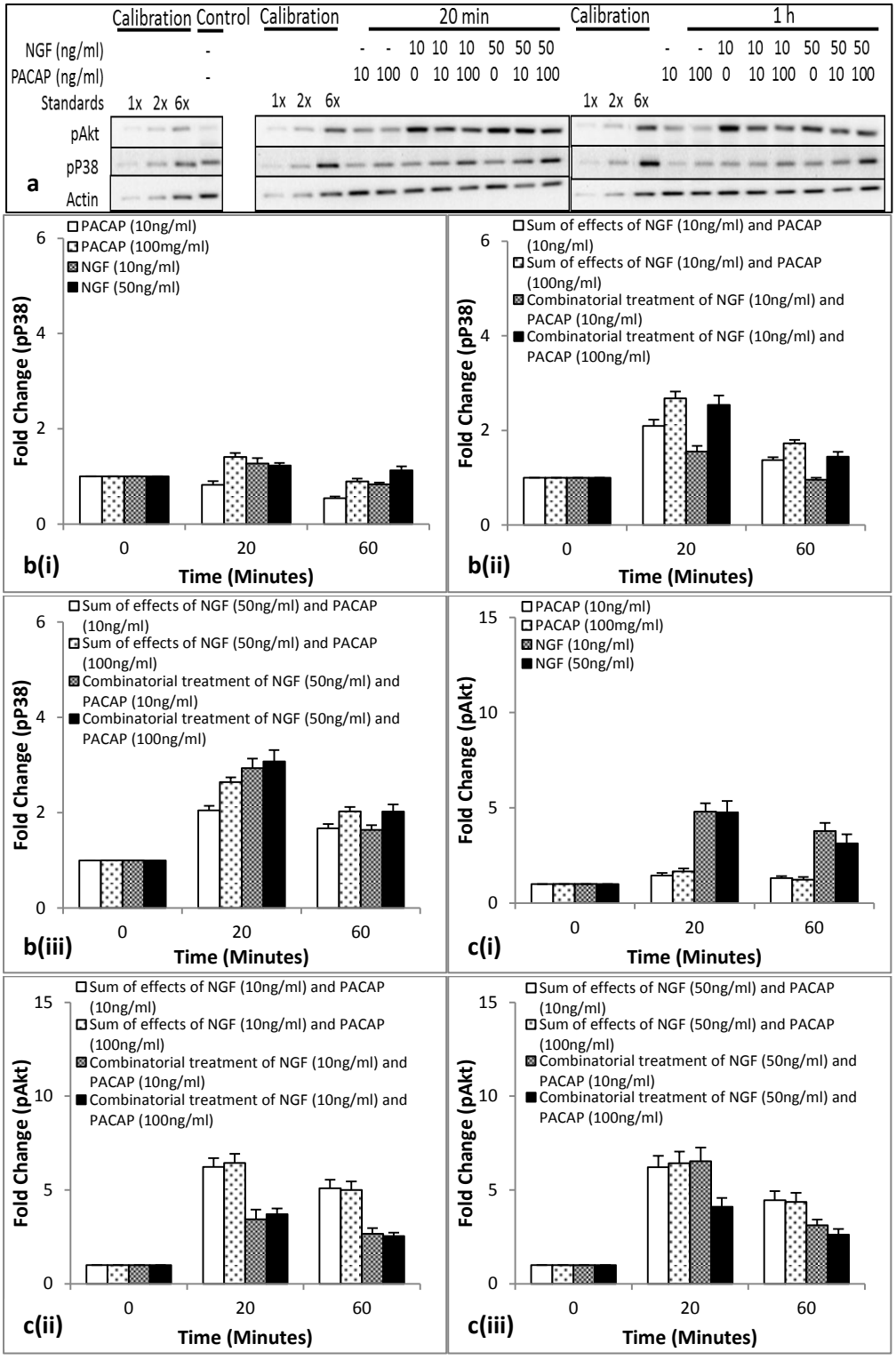

Figure 3.6. Non-synergistic phosphorylation of P38 and Akt upon combinatorial NGF (0-50 ng/ml) and PACAP (0-100 ng/ml) treatments. (a) Time-course of P38 and Akt phosphorylations at 20 and 60 minutes following NGF-PACAP treatments. Phosphorylation levels of the proteins were analyzed by western blotting, and normalized to the levels of actin. Fold changes of (b) pP38, and (c) pAkt under (i) uni-ligand treatments, (ii) bi-ligand treatments at 10 ng/ml of NGF, and (iii) bi-ligand treatments at 50 ng/ml NGF. Significant differences between combinatorial experimental treatment of NGF-PACAP and summation of their individual effects were calculated using the paired Student's *t*-test. A value of $p<0.05$ was considered significant.

Having found that Erk and JNK were synergistically phosphorylated in the NP system, we next investigated if these trends were also common to the FP and EP systems. Similar to the NP system, sustained and synergistic Erk (Figures 3.7a(i), and 3.7b(i)) and JNK (Figures 3.7a(ii), and 3.7b(ii)) phosphorylations were observed for the FP and EP treatments, respectively, within 1 hour of stimulation.

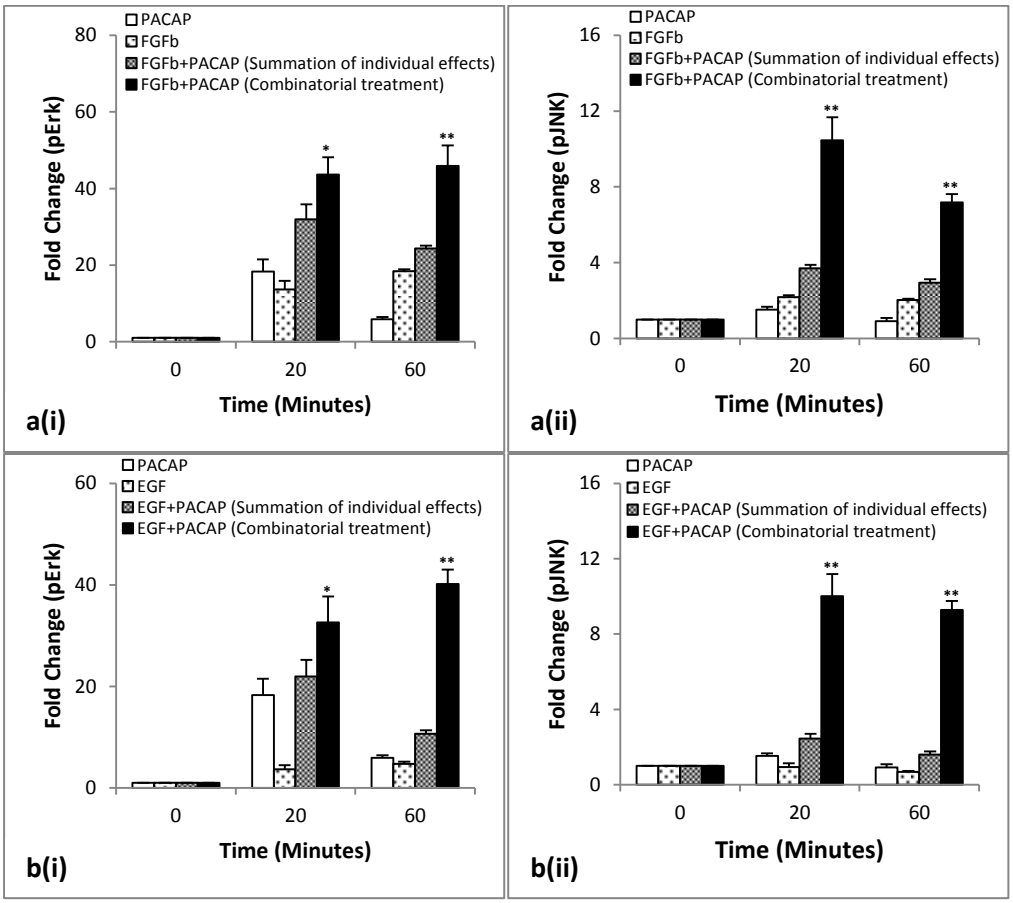

Figure 3.7. Synergistic and sustained phosphorylation of Erk and JNK upon FP and EP treatments. Time-course of quantified Erk and JNK phosphorylation at 20 and 60 minutes upon (a) FGFb (50 ng/ml)-PACAP (100 ng/ml) (FP) or (b) EGF (50 ng/ml)-PACAP (100 ng/ml) (EP) treatment. Fold-change in (i) pErk, and (ii) pJNK were quantified by densitometry and normalized to the levels of actin. Significant differences between combinatorial experimental treatment of growth factor-PACAP and the summation of their individual effects were calculated using the paired Student's *t*-test. A value of $p<0.05$ was considered significant (**$p<0.01$; *$p<0.05$).

Likewise, neither P38 (Figures 3.8a(i), and 3.8b(i)) nor Akt (Figures 3.8a(ii), and 3.8b(ii)) were synergistically phosphorylated in the FP and EP systems. Thus, these results indicate that specific kinases were synergistically

phosphorylated by various combinatorial growth factor-PACAP treatments, suggestive of their roles in mediating synergistic neurite outgrowth.

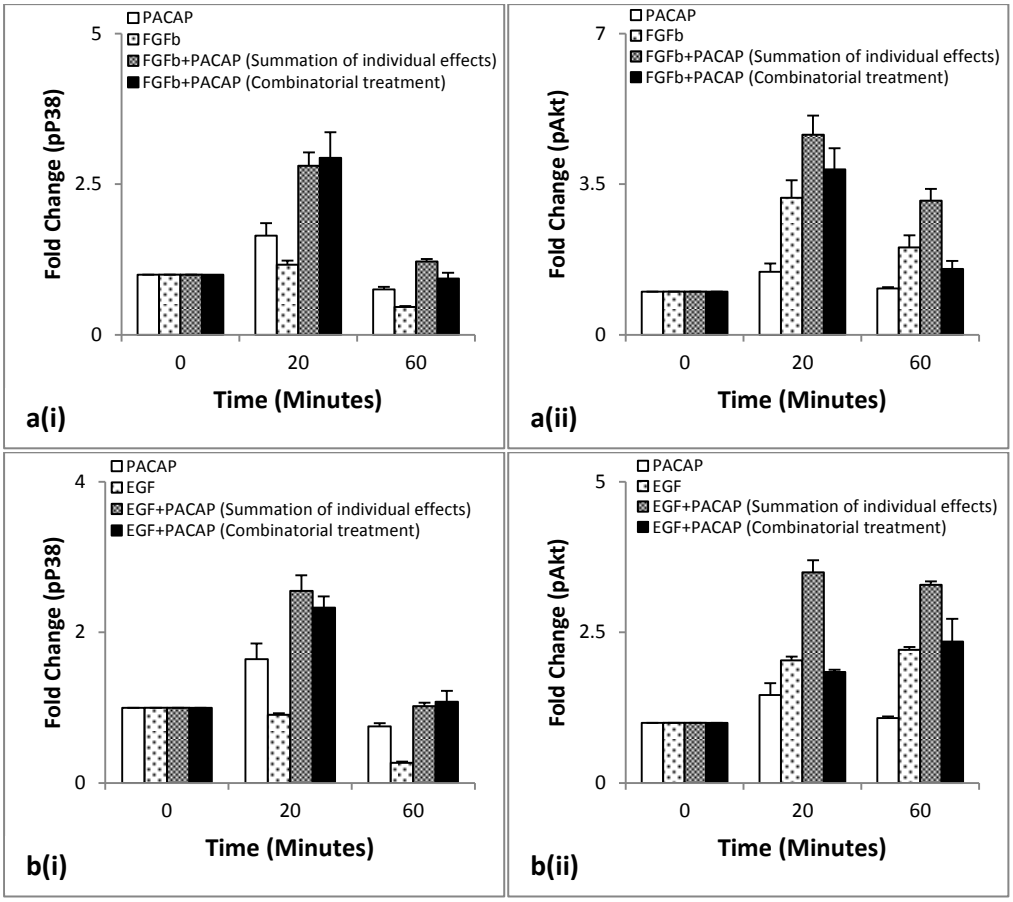

Figure 3.8. Non-Synergistic phosphorylation of P38 and Akt upon FP and EP treatments. Time-course of quantified P38, and Akt phosphorylations at 20 and 60 minutes following (a) FGFb (50 ng/ml)-PACAP (100 ng/ml), and (b) EGF (50 ng/ml)-PACAP (100 ng/ml) treatment. Fold changes of (i) pP38, and (ii) pAkt were quantified by densitometry and normalized to the levels of actin. Significant differences between combinatorial experimental treatment of growth factor-PACAP and summation of their individual effects were calculated using the paired Student's *t*-test. A value of $p<0.05$ was considered significant.

The total protein levels of Erk, JNK, P38 and Akt upon treatment with single ligand or combinations of the growth factors and PACAP were probed across all conditions and time-points (Figure 3.9). Upon quantification of the bands, the standard deviation of the fold changes across all conditions (NGF, EGF, FGFb, NP, EP, and FP at both 20 and 60 minutes) was found to be within 0.2 for all the proteins probed, indicating that the total protein levels were not changed.

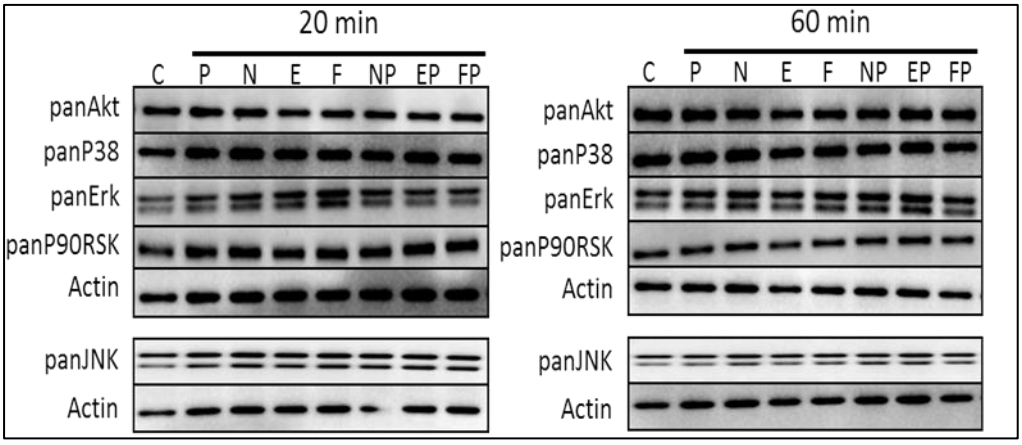

Figure 3.9. Total levels of Erk, JNK, P90RSK, Akt and P38 were not changed following treatments with ligands. The total protein levels were assayed at 20 and 60 minutes post-stimulation. The same control (C, at t=0 minutes) was used for both time-points. The concentrations of growth factors, and PACAP used were 50 ng/ml, and 100 ng/ml, respectively.

3.2.3. Erk Positively Regulates Neurite Outgrowth in All Three Systems Whereas Regulation of the Process by JNK is Positive in the NP and FP Systems but Negative in the EP System

We next examined the role of these synergistically activated kinases in regulating neurite outgrowth using kinase inhibitors. As expected, treatment with the MEK inhibitor, U0126, inhibited neurite outgrowth in the NP system in a dose-dependent manner (Figures 3.10a(i), and 3.10d). Similarly, inhibition of MEK also blocked neurite outgrowth in the FP (Figures 3.10b, and 3.10d) and EP systems (Figures 3.10c, and 3.10d), confirming the involvement of synergistic Erk phosphorylation in neurite outgrowth. Further supporting the involvement of synergistically phosphorylated kinases in regulating synergistic neurite outgrowth, the JNK inhibitor, SP600125, blocked neurite outgrowth in the NP (Figures 3.10a(ii), and 3.10d) and FP systems (Figures 3.10b, and 3.10d). Surprisingly, SP600125 at the same concentration (10 μM) failed to inhibit neurite outgrowth in the EP system, showing instead enhanced neurite outgrowth (Figures 3.10c, and 3.10d). Higher concentrations of SP600125

were deemed to be cytotoxic (data not shown). Positive controls for the effects of U0126 and SP600125 are shown in Figures 3.11a and 3.11b, respectively.

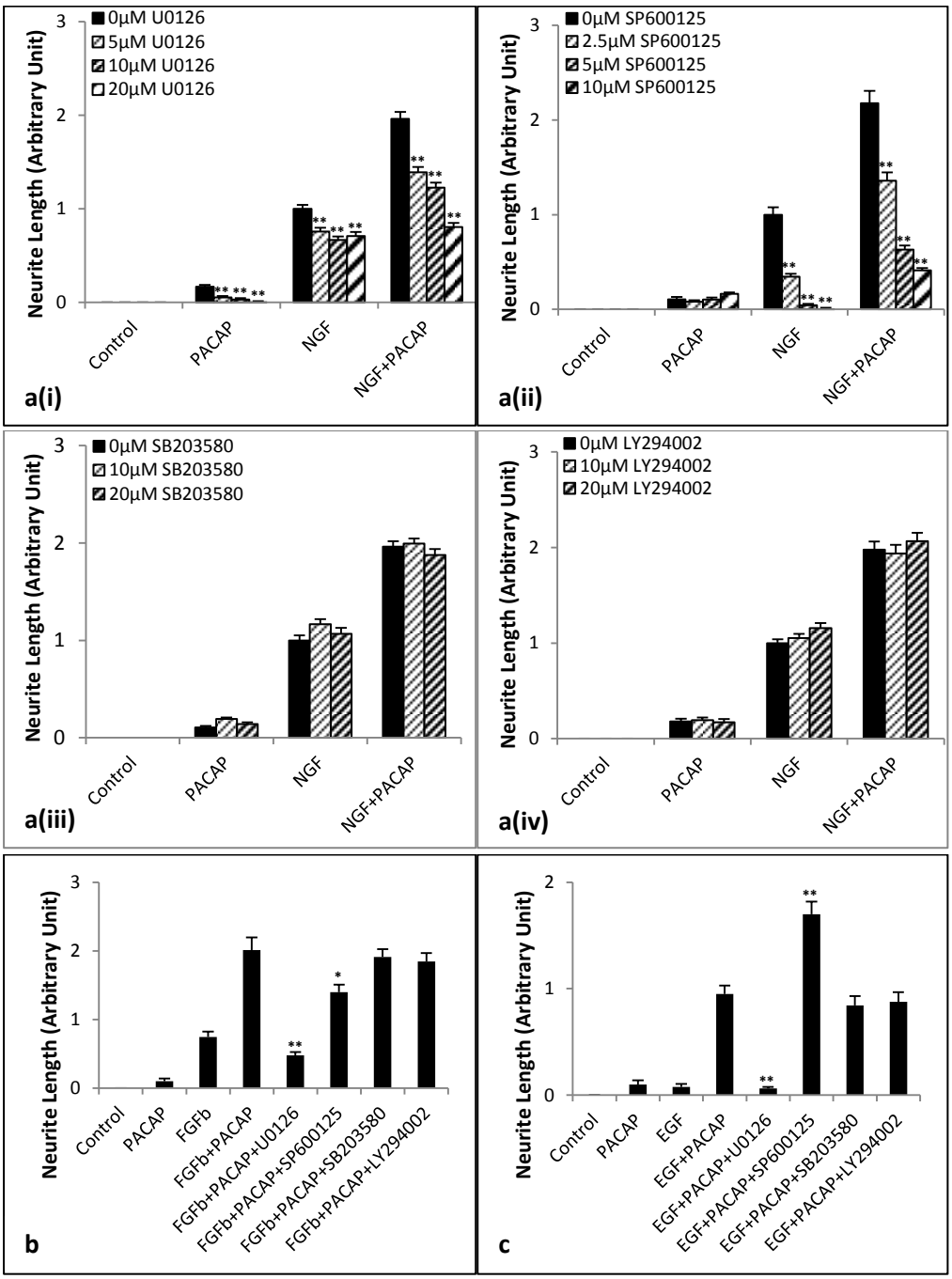

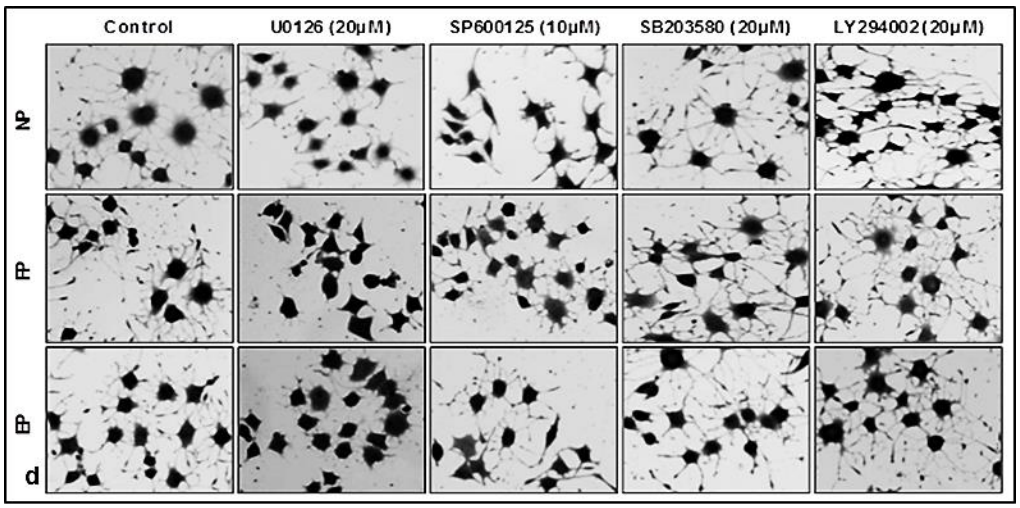

Figure 3.10. Erk is required for neurite outgrowth in all three systems whereas JNK is required only for the NP and FP, but not EP, systems. Concentrations of growth factors and PACAP used were 50 ng/ml and 100 ng/ml, respectively. (a) Dose-response treatment of (i) MEK inhibitor (U0126), (ii) JNK inhibitor (SP600125), (iii) P38 inhibitor (SB203580), and (iv) PI3K inhibitor (LY294002) on neurite outgrowth in the NP system. (b), (c) Effect of U0126 (20 μM), SP600125 (10 μM), SB203580 (20 μM), and LY294002 (20 μM) on neurite outgrowth in the FP, and EP systems, respectively. (d) Representative images of cells treated with growth factors-PACAP in the presence of inhibitors in the three systems, NP, FP and EP. Significant differences between treatments with and without inhibitors were calculated using the paired Student's *t*-test. A value of $p<0.05$ was considered significant (**$p<0.01$; *$p<0.05$).

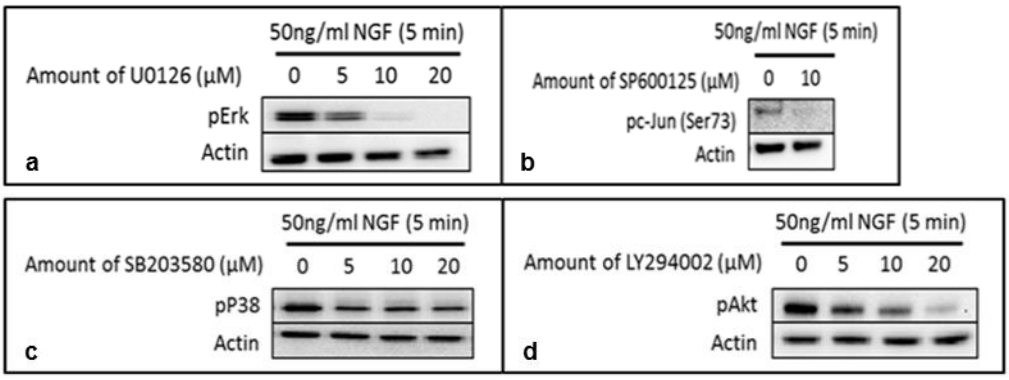

Figure 3.11. Positive controls for the kinase inhibitors following treatment with NGF (50 ng/ml). (a) Inhibition of Erk phosphorylation in the presence of U0126. (b) Inhibition of c-Jun phosphorylation in the presence of SP600125. (c) Inhibition of P38 phosphorylation in the presence of SB203580. (d) Inhibition of Akt phosphorylation in the presence of LY294002.

As expected, inhibition of the non-synergistically activated nodes, P38 and Akt, by SB203580, and LY294002, respectively, did not block neurite outgrowth in all three systems (Figures 3.10a(iii), 3.10a(iv), 3.10b, 3.10c, and 3.10d). Likewise, cells treated with doses of the inhibitors at concentrations higher than 20 μM resulted in high levels of cytotoxicity (data not shown). The positive controls for SB203580 and LY294002 are shown in Figures 3.11c and 3.11d, respectively.

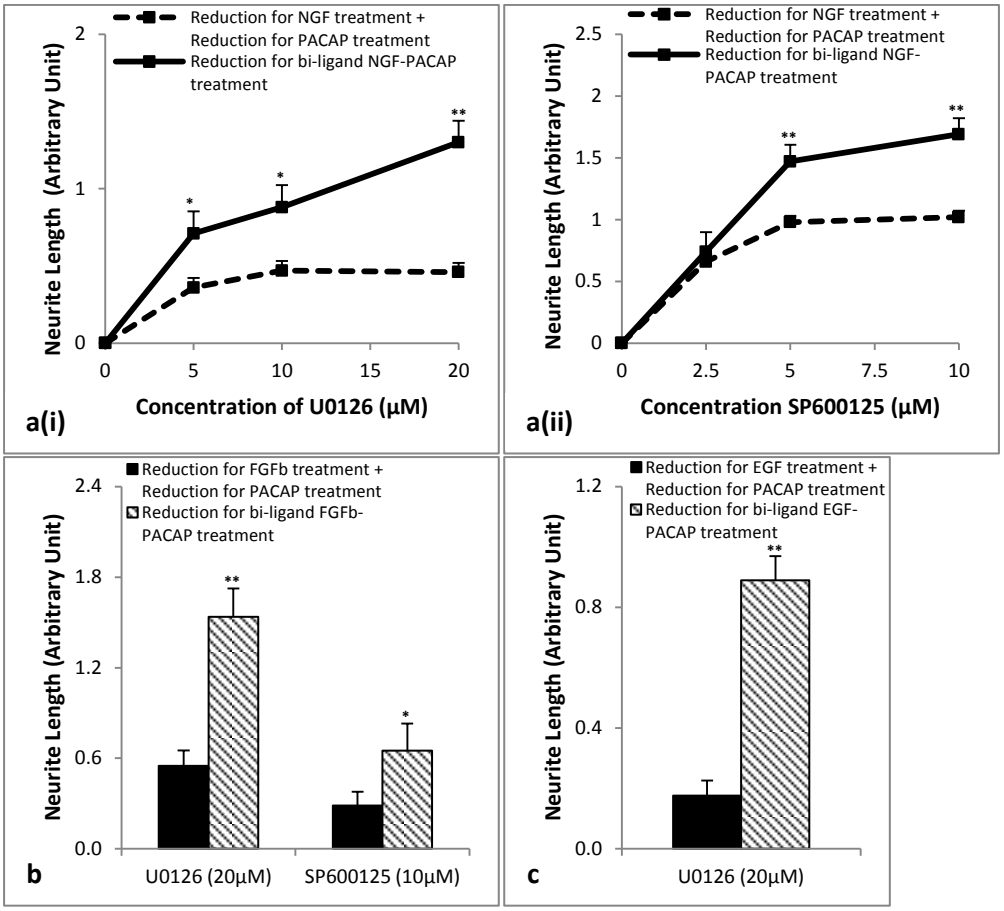

Figure 3.12. Net inhibitor-induced reduction in neurite length is greater in the synergistic systems than in the additive effect of the single ligand treatments. Net reduction in neurite outgrowth in the (a) NP system following treatment with various concentrations of (i) U0126 (MEK inhibitor) and (ii) SP600125 (JNK inhibitor). Reductions in neurite outgrowth in the (b) FP and (c) EP systems in the presence of specific kinase inhibitors. The concentrations of growth factors, and PACAP used were 50 ng/ml, and 100 ng/ml, respectively. Significant differences between the effects of the combinatorial treatment of growth factor-PACAP (bi-ligand) versus the sum of the effects for each single ligand treatment were compared using the paired Student's *t*-test. A value of $p<0.05$ was considered significant (**$p<0.01$; *$p<0.05$).

Next, the reduction in neurite outgrowth, after treatment with inhibitors, for the NP treatment was compared to the sum of reduction of neurite outgrowth in the single ligand treatments. With U0126 (Figure 3.12a(i)) and SP600125 (Figure 3.12a(ii)), the reduction in neurite outgrowth in the NP treatment was greater than the sum of reduction for the single ligand treatments. Similarly, for the FP (Figure 3.12b) and EP (Figure 3.12c) systems, inhibition of the kinases positively regulating neurite outgrowth also resulted in a greater reduction in neurite outgrowth in the combinatorial growth factor-PACAP treatments than the sum of reduction for the respective single ligand

treatments. These results support the involvement of the various kinases in positively regulating synergistic neurite outgrowth in the respective synergistic systems.

Critically, these results also suggest that these systems utilize distinct pathways to regulate neurite outgrowth and that not all synergistically phosphorylated kinases are relevant to the enhancement of neurite outgrowth.

3.2.4. P90RSK is Downstream of both Erk and JNK in the NP and FP Systems but only Downstream of Erk in the EP System

Having found that JNK was positively involved in neurite outgrowth in the NP and FP, but not EP, systems, we sought to identify the downstream targets that may be involved in mediating this differential requirement of JNK. Among the many downstream effectors of JNK, P90RSK has been recently shown to be involved in neurite outgrowth and PC12 cells differentiation[219,276,277]. Thus, we examined if P90RSK was synergistically phosphorylated and if it was involved in JNK-mediated neurite outgrowth.

As expected, P90RSK was synergistically phosphorylated in the NP (Figures 3.13a(i), and 3.13a(ii)), FP (Figure 3.13b(i)) and EP (Figure 3.13c(i)) systems from 20 minutes to 1 hour after stimulation, while the total protein levels of P90RSK across all time-points and conditions were not changed (Figure 3.9). In all three systems, neurite outgrowth was inhibited in the presence of the P90RSK inhibitor, BRD7389[278,279] (Figures 3.13a(iii), 3.13b(ii), 3.13c(ii), and 3.13e). Greater reductions in neurite outgrowth were also achieved in the

combinatorial growth factor-PACAP treatments than for the sum of the reduction in neurite outgrowth in the respective single ligand treatments (Figure 3.13d), supporting the involvement of P90RSK in regulating synergistic neurite outgrowth in all three systems.

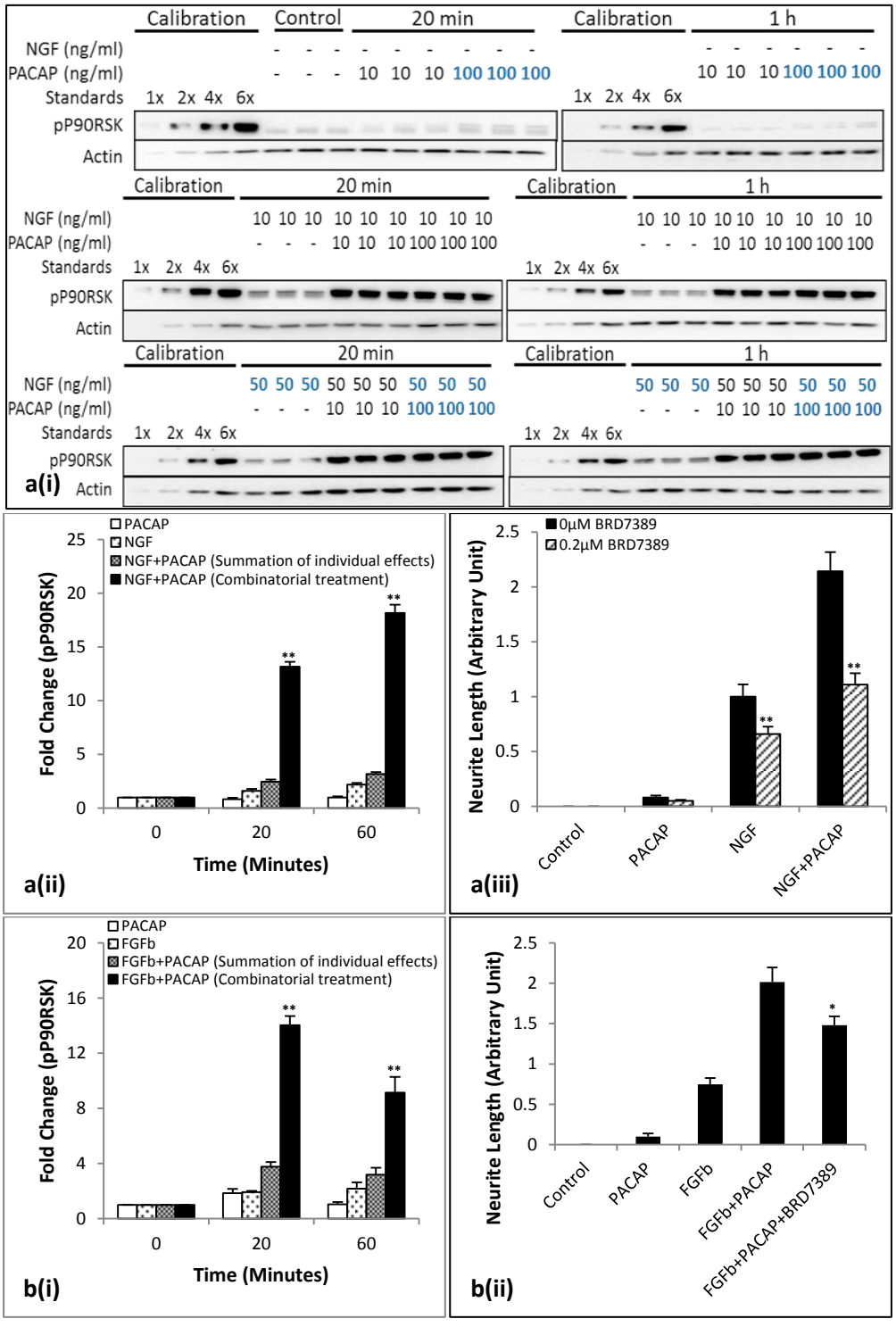

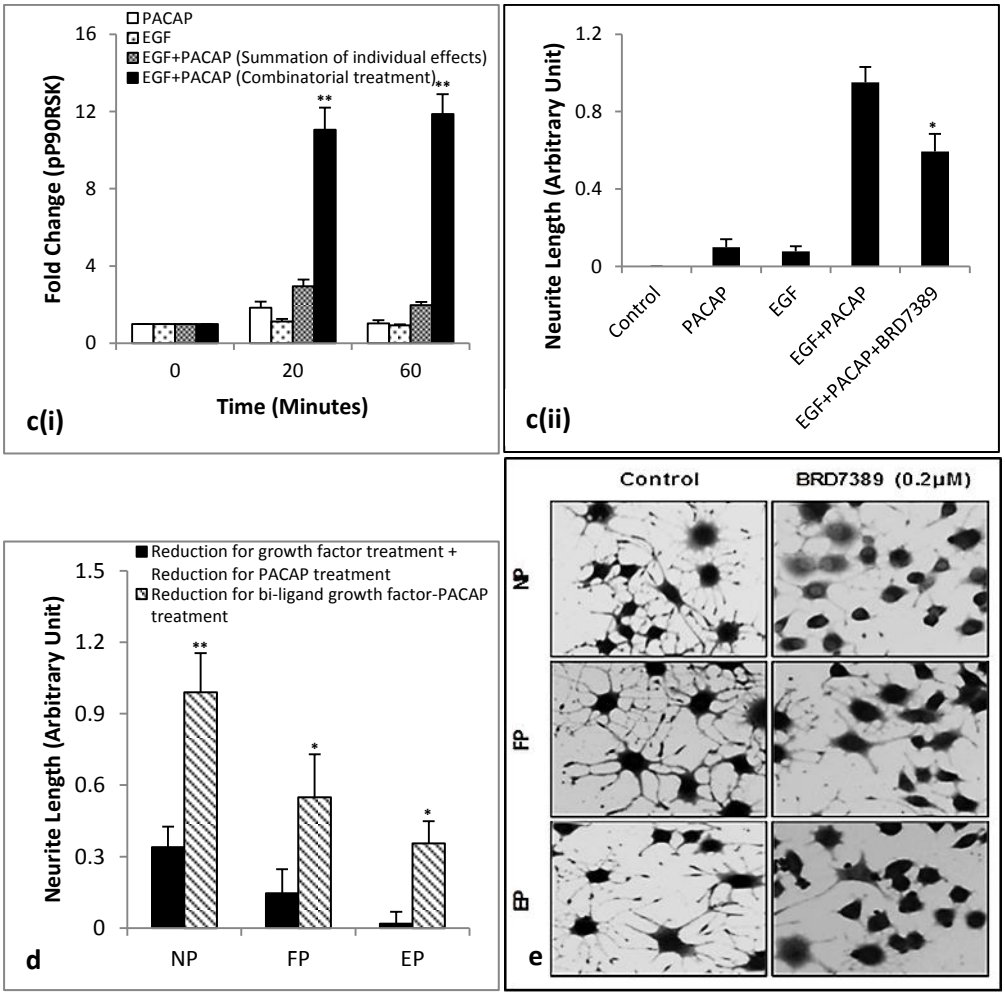

Figure 3.13. P90RSK is synergistically phosphorylated and is involved in neurite outgrowth in all three systems. (a(i)) Time-course of P90RSK phosphorylation at 20 and 60 minutes following NGF (0-50 ng/ml)-PACAP (0-100 ng/ml) treatment. Phosphorylation levels of the proteins were analyzed by Western blotting, and normalized to the levels of Actin. The blots used were the same as those used for pJNK in Figure 3.5a. (a(ii)), (b(i)), (c(i)) Time-course measurements of pP90RSK at 20 and 60 minutes following NGF (50 ng/ml)-PACAP (100 ng/ml) (NP), FGFb (50 ng/ml)-PACAP (100 ng/ml) (FP) or EGF (50 ng/ml)-PACAP (100 ng/ml) (EP) stimulations, respectively. (a(iii)), (b(ii)), (c(ii)) Effect of P90RSK inhibitor, BRD7389 (0.2 μM), on neurite outgrowth in the NP, FP, and EP systems, respectively. (d) Net reduction in neurite outgrowth between combinatorial ligand treatment (bi-ligand) versus the sum of neurite outgrowth reduction from treatment with each ligand separately in the presence of BRD7389 (0.2 μM). (e) Representative images of cells treated with growth factors (50 ng/ml)-PACAP (100 ng/ml) in the presence of BRD7389 in the three systems. Significant differences between the effects of combinatorial experimental treatment of growth factor-PACAP and summation of their individual effects, and that between the effects of treatments with and without inhibitors were calculated using the paired Student's *t*-test. A value of $p<0.05$ was considered significant (**$p<0.01$; *$p<0.05$).

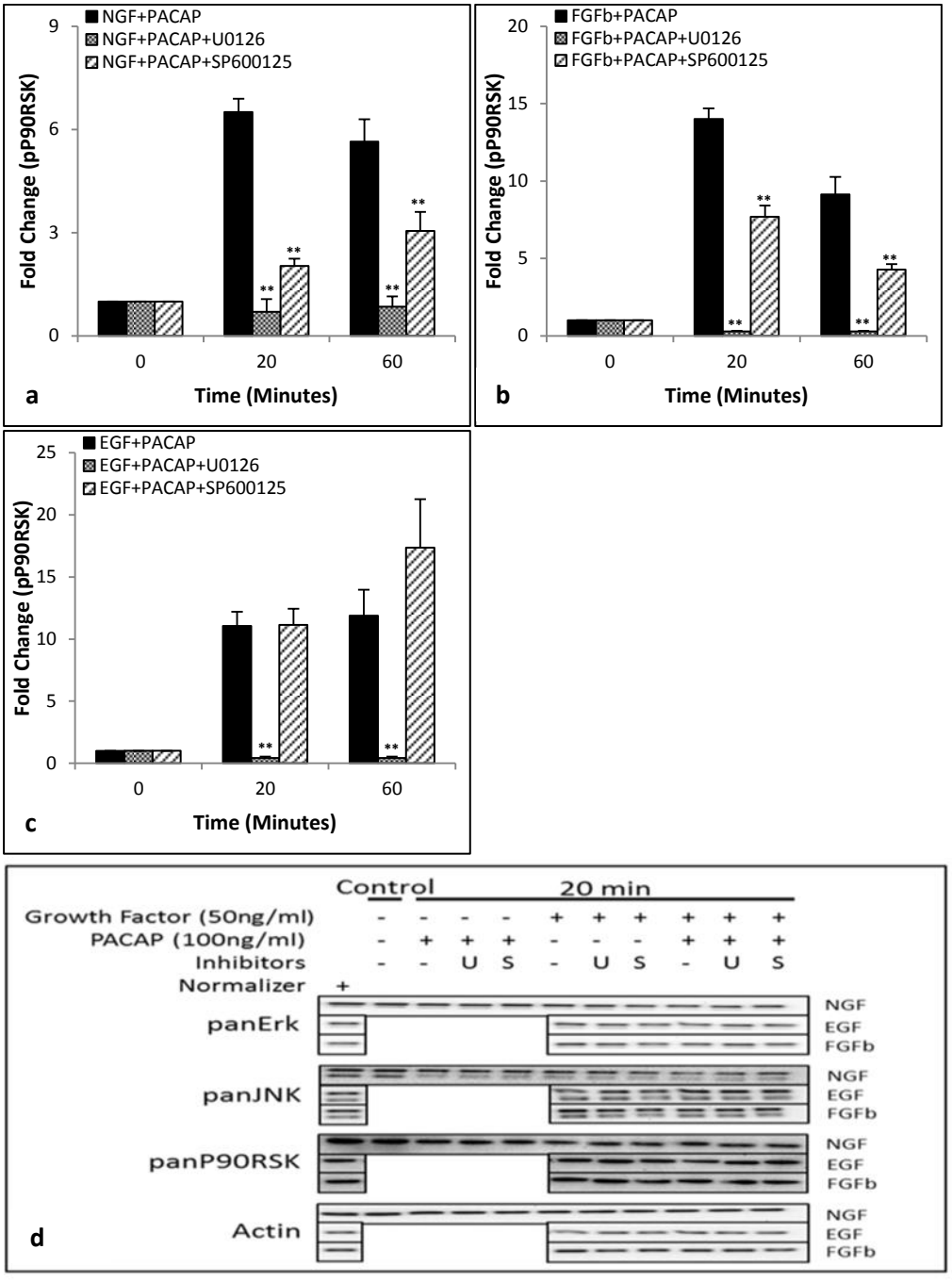

Figure 3.14. P90RSK is regulated by Erk and JNK in the NP and FP systems, but only by Erk in the EP system. (a), (b), (c) Time-course measurement of pP90RSK at 20 and 60 minutes following NGF (50 ng/ml)-PACAP (100 ng/ml), FGFb (50 ng/ml)-PACAP (100 ng/ml), and EGF (50 ng/ml)-PACAP (100 ng/ml) treatment, respectively, in the presence or absence of MEK inhibitor, U0126 (20 μM), or JNK inhibitor, SP600125 (10 μM). (d) The total levels of Erk, JNK, and P90RSK were unchanged during the combinatorial growth factor-PACAP treatments both in the presence and absence of the inhibitors. The total protein levels were assay at 20 minutes post-stimulation. A normalizer (NGF-PACAP co-treated cells) in each blot served as a control to normalize between different blots, where U denotes U0126 (20 μM), and S denotes SP600125 (10 μM). Significant differences between treatments with and without inhibitors were calculated using the paired Student's *t*-test. A value of $p<0.05$ was considered significant (**$p<0.01$).

To validate the role of P90RSK as a downstream effector of synergistically activated JNK in the three systems, the phosphorylation level of P90RSK was examined after inhibition with SP600125. Surprisingly, treatment with SP600125 inhibited P90RSK phosphorylation in the NP (Figure 3.14a) and FP (Figure 3.14b), but not EP (Figure 3.14c), systems. These results strongly suggest that the regulation of P90RSK by the JNK pathway could be a critical determinant of JNK involvement in positively regulating synergistic neurite outgrowth.

In addition to JNK, P90RSK has also been reported to be a downstream target of Erk[280,281]. Unlike the case for JNK inhibition, inhibition of Erk activation with U0126 suppressed P90RSK phosphorylation in all three systems (Figures 3.14a-3.14c), providing further support for the role of P90RSK as an important mediator of neurite outgrowth. In the presence of each of these inhibitors, the total levels of Erk, JNK, and P90RSK were also unchanged (Figure 3.14d).

3.3. Discussions

In this study, we demonstrated the involvement of distinct combinations of signalling pathways in mediating synergistic neurite outgrowth induced by PACAP and different growth factors (Figure 3.15). In these systems, Erk, JNK, and P90RSK were all found to be synergistically phosphorylated. However, synergistic JNK phosphorylation positively regulated neurite outgrowth only in the NP and FP systems. Further investigations led to the crucial finding that the JNK-P90RSK link is critical to the involvement of JNK in positively regulating synergistic neurite outgrowth in some but not all growth factor-PACAP stimulation combinations.

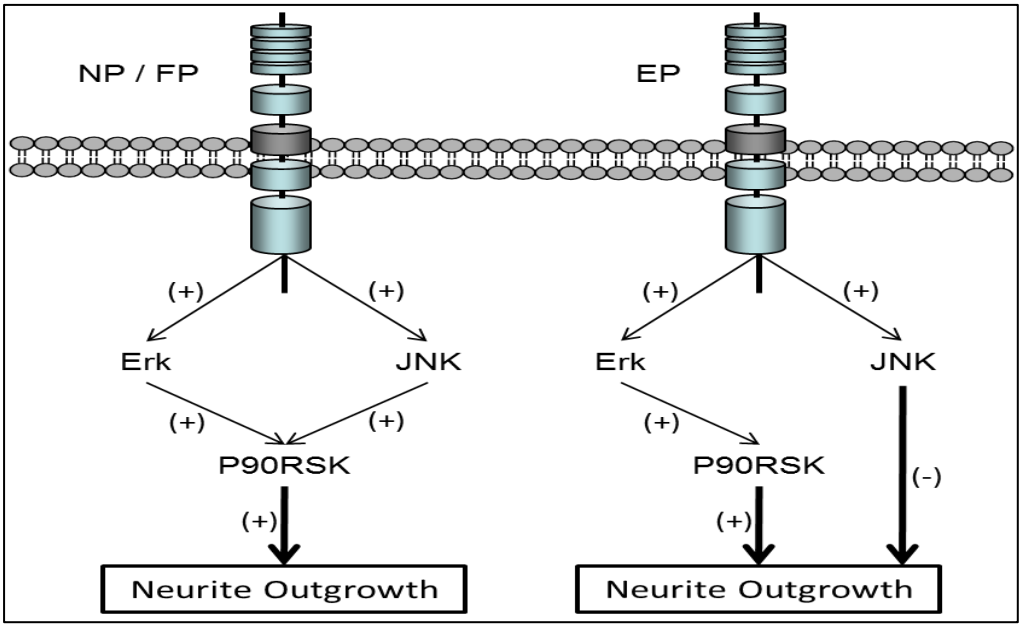

Figure 3.15. A schematic illustration of the different pathways used by the three different synergistic systems, NGF-PACAP (NP), FGFb-PACAP (FP), and EGF-PACAP (EP) in the regulation of neurite outgrowth.

cAMP-elevating agents have long been known to synergize with NGF[211,212], FGFb[214], and EGF[215,216] to enhance neurite outgrowth. Although the pathways used by these individual ligands to regulate neurite outgrowth have been widely studied, little is known about the mechanisms underlying synergistic neurite outgrowth. RSM-based analyses provide a means to quantitatively compare the degree of synergism between different treatments[274]. By such analyses, the degree of synergism in the EP system was found to be higher than those in the NP and FP systems, suggesting that different signalling pathways may regulate neurite outgrowth in these systems.

To determine the pathways involved in synergistic neurite outgrowth, four kinases were examined, each widely reported to be involved in PC12 cells differentiation: Erk[169,282,283], P38[270,282], JNK[112,284], and Akt[163,283,285]. Interestingly, our results showed that Akt and P38 were activated following ligand stimulation but not involved in neurite outgrowth in all three systems. In agreement with this, inhibition of these two kinases also failed to suppress

NGF-induced neurite outgrowth in PC12 cells. These results were consistent with some of the earlier reports exploring neurite outgrowth[286-288] but not others[112,163,164,270,282-285]. A recent systems-based study revealed a two-dimensional Erk-Akt signalling code that was critical in governing PC12 cells proliferation and differentiation[289]. Thus, the controversy surrounding the involvement of P38 and Akt would be more adequately addressed using systems-based approaches in the future.

The sustained activation of Erk has been widely reported to be required for neurite outgrowth during differentiation[165,169,170,213]. Consistent with these reports, synergistic and sustained Erk phosphorylation was found to be involved in neurite outgrowth in all three growth factor-PACAP systems. This was especially evident in the EP system, where transient Erk activation was observed following treatment with EGF or PACAP alone. Similarly, synergistic and sustained JNK phosphorylation was observed in all three systems. Remarkably, inhibition of JNK led to reduced neurite outgrowth in the NP and FP systems, but enhanced outgrowth in the EP system. Although a previous study has found sustained JNK activation to be sufficient to induce PC12 cells differentiation[171], our results showed that sustained JNK activation in the EP system is insufficient to induce neurite outgrowth. These seemingly contradictory findings could imply that the kinetics of JNK activation alone is insufficient to determine if cells undergo differentiation. It is likely that JNK acts in conjunction with other signalling nodes to form a signalling network that regulates neurite outgrowth. Nonetheless, to the best of our knowledge, this is the first report demonstrating the involvement of JNK phosphorylation in synergistic neurite outgrowth.

We have shown that both Erk and JNK were synergistically phosphorylated in all three systems. This may occur through shared common upstream effectors[226] or through independent upstream effectors, such as PKA and Epac[136,290,291]. In preliminary experiments, we observed the involvement of PKA in neurite outgrowth in the EP but not NP system (data not shown); however, a complete understanding of the contribution of PKA and Epac in Erk and JNK activation remains to be determined.

Although synergistic JNK phosphorylation was observed in all three systems, it was not found to positively regulate synergistic neurite outgrowth in the EP system. This suggests a possible difference in downstream signalling. P90RSK, which had previously been found to be required for PC12 cells differentiation[219], was also found to be synergistically activated in all three systems in our study. Interestingly, P90RSK was activated by JNK in the NP and FP, but not EP, systems. Although JNK-mediated activation of P90RSK has not been widely reported, it has been observed following ultraviolet exposure[277], insulin treatment[292], or transforming growth factor alpha treatment[293]. Consistent with previous findings[281], P90RSK was also regulated by Erk in our study. The co-regulation of targets by Erk and JNK is not uncommon, with previous studies showing that these two kinases regulate many common targets, including transcription factors[164,172,294], immediate early genes[295] and differentiation-specific genes[164,295,296]. Despite this, results from several studies have suggested that the binding sites of P90RSK for Erk and JNK are likely to be different[277,297], further indicating that P90RSK may be discretely regulated by the two kinases. Our finding of the differential regulation of P90RSK in the NP and EP systems in this study strongly suggests that these synergistic systems can serve as excellent models to

decipher the mechanistic regulation of P90RSK by its upstream kinases, Erk and JNK. The contributions of Erk, JNK and P90RSK in the mechanism of axonal outgrowths of neurons *in vivo* and *in vitro* will require further clarification in future studies.

3.4. Conclusions

In conclusion, our study has demonstrated that distinct pathways were involved in synergistic neurite outgrowth in different systems. Importantly, our findings of the underlying pathways involved in these systems have two key implications. First, some kinases such as JNK may be synergistically activated by multiple ligands but yet not necessarily involved in the positive regulation of synergistic neurite outgrowth and that its positive involvement in the process is dependent on its interaction with P90RSK. Second, in the EP system, the increased synergy in neurite outgrowth and lack of JNK requirement in the positive regulation of the process suggest that PACAP synergizes differently with different growth factors to enhance neurite outgrowth. These findings reveal that synergistic neurite outgrowths induced by multiple ligands involve the interplay of a network of signals.

Chapter 4.

Multi-Parameter Morphological Analysis Reveals Complex Regulation of Neurite Features during Synergistic Neurite Outgrowth in PC12 Cells

4.1. Introduction

Previously, the involvement of four pathways, Erk[164,169], P38[270], JNK[112,164], and PI3K[163,166], involved in the regulation of total neurite length in three synergistic systems, NP, FP, and EP, were investigated. In addition to these pathways, protein kinase A (PKA)[222] has also been widely reported to be involved in the regulation of various morphological features of neurite outgrowth in PC12 cells.

The morphological properties of neurites represent key aspects of the neuronal phenotype in the nervous system and play critical roles in the processing of information and formation of network connectivity[298,299]. However, neurite outgrowth is a complex process that involves the initiation, elongation and branching of neurites and total length alone gives only a limited depiction of the process[300,301]. The extent and rate of neurite outgrowth dictates the wiring and transmission of information between neurons. Thus, in order to gain a more holistic understanding of neurite outgrowth, other morphological aspects of neurite outgrowth[232,235,302], such as the number of neurites extending from the cell-body, and degree of branching must be investigated as well. These parameters are important as they collectively determine the number of neurons that can interact with each neuron and the spatial boundary within which neurons can transmit information between one another. Moreover, these morphological features can be regulated independently from one another[303] and using only limited morphological features to characterize neurite outgrowth may result in an over-simplified understanding of the mechanisms regulating the process. For instance, P38 had been found to regulate the total neurite length and degree of branching

but not number of neurites per cell[237] and Akt had been found to regulate neurite branching but not length[238] in various systems. To date, many studies addressing neurite outgrowth have largely focused on the analyses of one or two parameters such as neurite length and percentage of differentiated cells. Thus, the mechanisms underlying the morphological complexity of neurite outgrowth is still poorly understood.

While it has been shown previously that the total neurite length in the synergistic systems are regulated by the Erk and JNK pathways, the pathways regulating the other morphological features during this process are still unclear. In this study, we investigated the involvement of various signalling pathways in regulating the morphological structures of neurite in three systems exhibiting synergistic neurite outgrowth, NP, FP, and EP. Building on our previous study, we found that the involvement of PKA in regulating synergistic neurite length in the FP and EP systems was mediated through P90RSK independently of Erk, further suggesting the importance of P90RSK in regulating synergistic neurite outgrowth. As expected, pathways which are involved in the regulation of neurite length in these systems also regulated other morphological parameters such as the number of neurite extensions and branch-points. Surprisingly, in the NP and FP systems, the P38 pathway was found to regulate neurite branching without affecting neurite length. Our study suggests that the different morphological structures of neurites can be regulated by distinct signalling pathways and a more complete understanding of the pathways regulating neurite outgrowth can only be achieved through holistic analyses of the morphology of the neurites.

4.2. Results

4.2.1. Analyses of Neurite Extension

Growth factors such as NGF[211,212], FGFb[214] and EGF[215,216] are known to synergize with cAMP-elevating agents such as PACAP to enhance neurite outgrowth. Previously, in Chapter 3, we have also shown that combinatorial treatments of PACAP with any one of these growth factors resulted in synergistic regulations of total neurite length. In this study, we aimed to determine how this enhancement of total neurite length is achieved morphologically by examining the other features of neurite outgrowths. The number of neurite extensions from the cell-body upon NP (Figure 4.1a), FP (Figure 4.1b), and EP (Figure 4.1c) treatments was first examined. Following treatments with single ligands and with combinations of growth factors and PACAP for 48 hours, the number of neurite extensions was quantified and analyzed using a response surface model (RSM). The number of neurite extensions obtained for the combinatorial growth factor-PACAP treatment was compared to that from a summation of the additive effects of the corresponding individual ligands. In all three systems, the total number of neurite extensions (Figure 4.1) was found to be synergistically regulated. This suggests that the increased number of neurite extensions during combinatorial growth factor-PACAP treatments may contribute to the increase in total neurite length. The reliability of HCA-Vision for the quantification of these morphological parameters was verified through manual quantification.

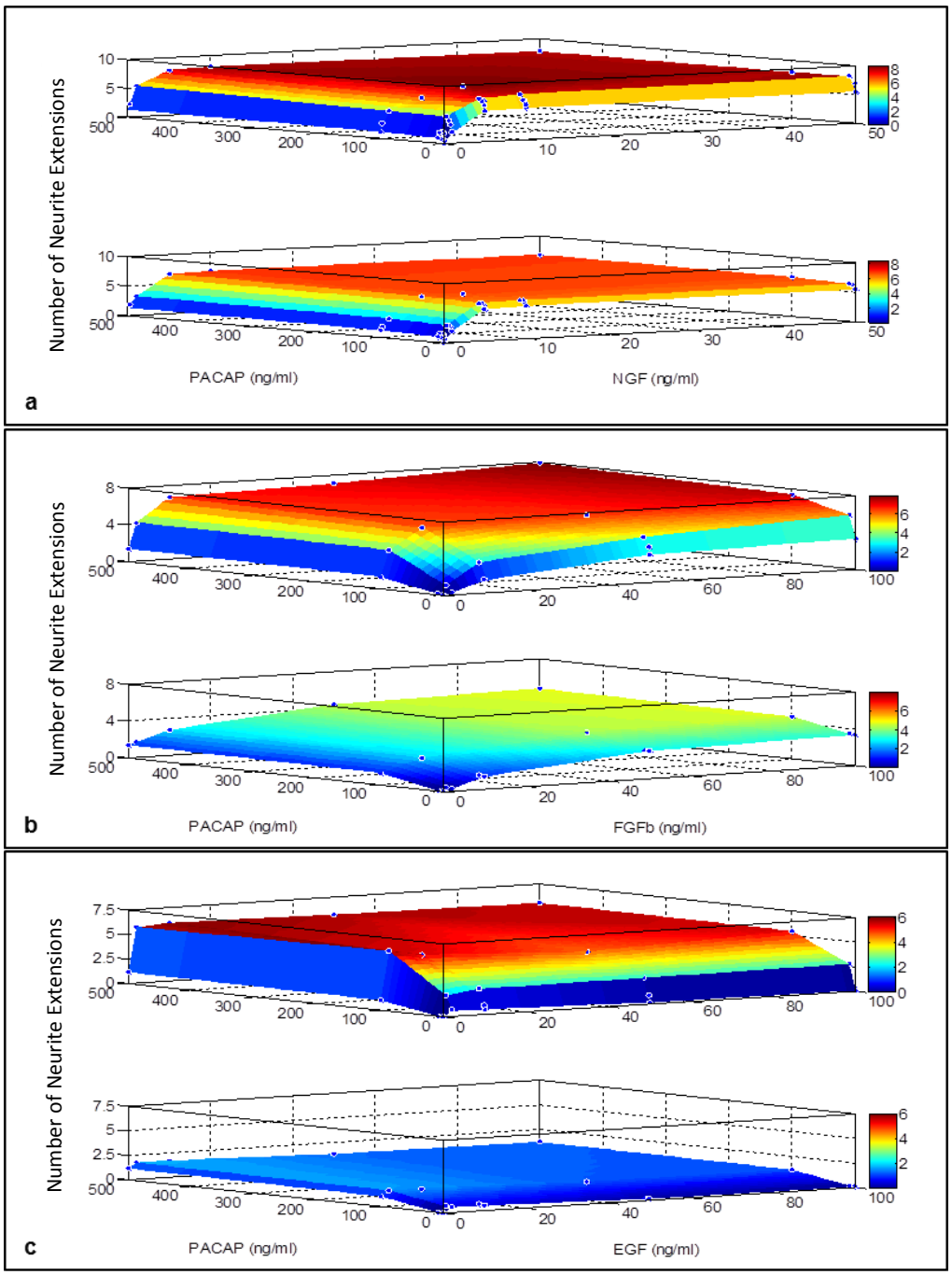

Figure 4.1. Synergistic increase in number of neurite extensions from the cell-body upon combinatorial growth factor-PACAP treatments. (a), (b), (c) Response surface plots of number of neurite extensions after 48 hours of stimulation with NGF (0-50 ng/ml)-PACAP (0-500 ng/ml), FGFb (0-100 ng/ml)-PACAP (0-500 ng/ml), and EGF (0-100 ng/ml)-PACAP (0-500 ng/ml), respectively; Top panel: Experimentally obtained results of the growth factor-PACAP combinatorial treatment; Bottom panel: Additive effect calculated through the summation of the individual effects of the growth factors and PACAP. x, y, and z axes denote concentrations of growth factors (ng/ml), concentration of PACAP (ng/ml), and number of neurite extensions, respectively.

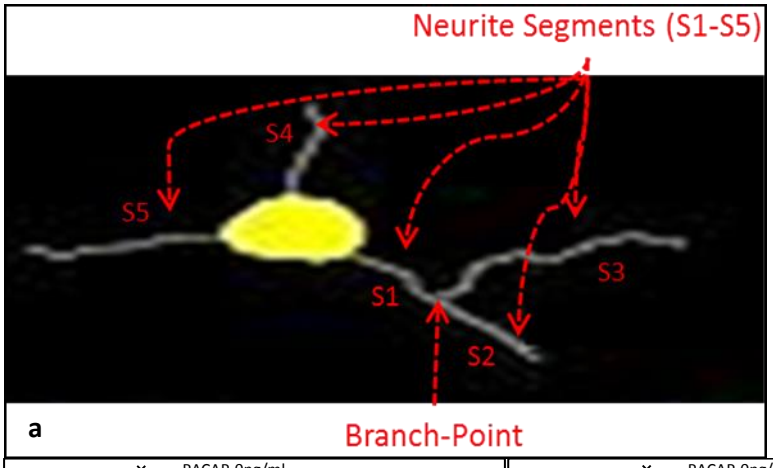

a

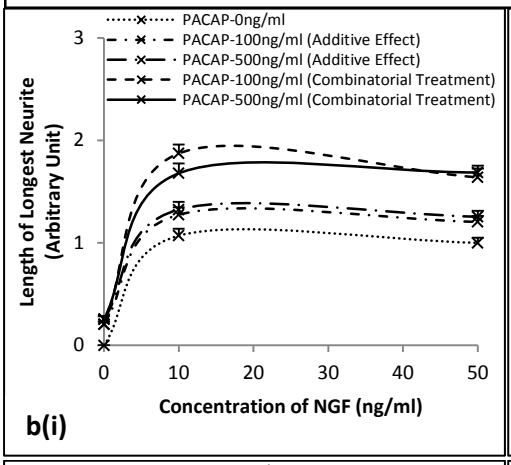

b(i)

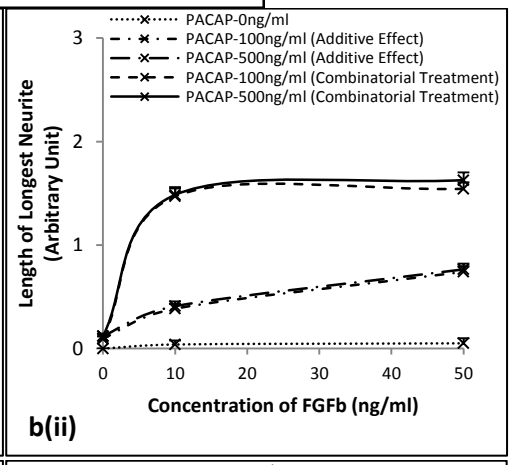

b(ii)

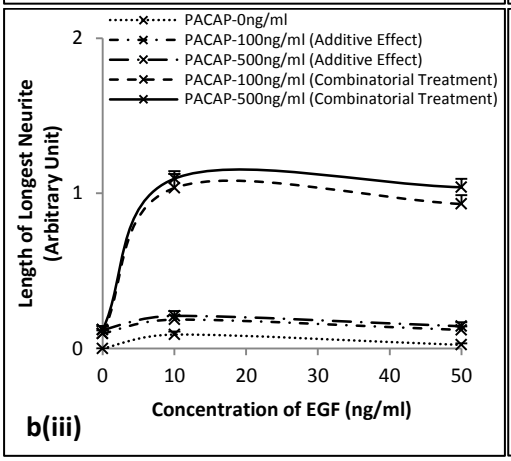

b(iii)

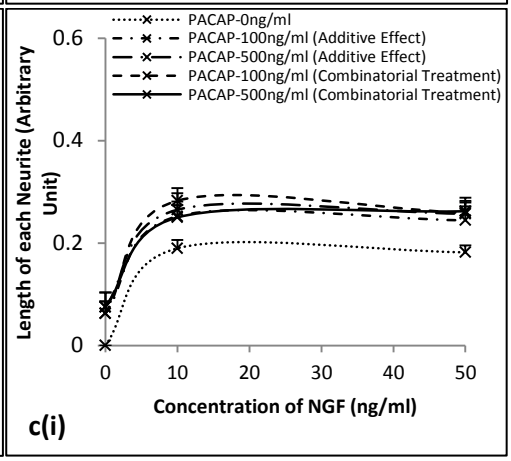

c(i)

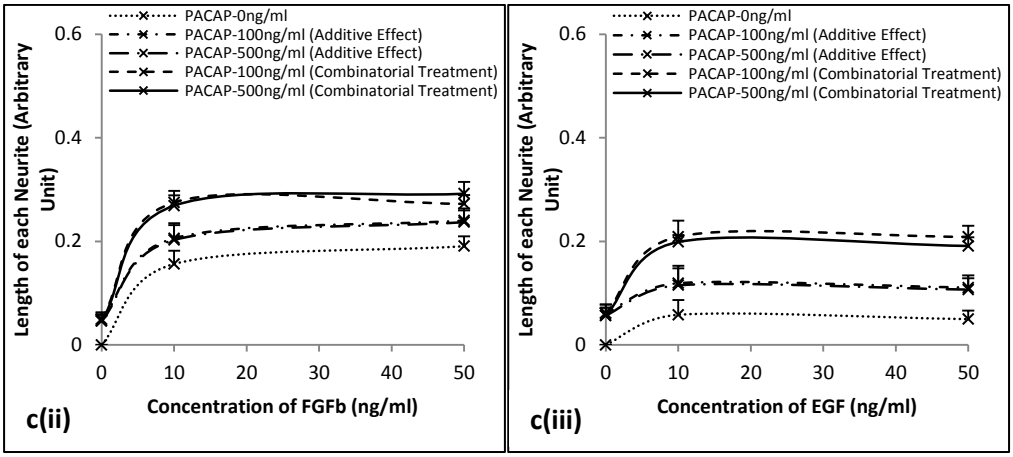

Figure 4.2. Increase in the length of each neurite contributes to the synergistic regulation of total neurite length in all three systems upon combinatorial growth factor-PACAP treatments. (a) Illustration of neurite branching and segments. (b) Length of longest neurite, and (c) average length of each neurite after 48 hours of stimulation with (i) NGF (0-50 ng/ml)-PACAP (0-500 ng/ml), (ii) FGFb (0-50 ng/ml)-PACAP (0-500 ng/ml), and (iii) EGF (0-50 ng/ml)-PACAP (0-500 ng/ml), respectively.

We next examined if the various morphological changes of each neurite was also enhanced. The length of each neurite was examined using two different measures, the length of the longest neurite (S1+S3) and the average length of each neurite (average of S1+S2+S3, S4, and S5) (Figure 4.2a). Investigating the length of the longest neurite (Figure 4.2b), it was also found to be synergistically regulated in all three systems. In addition, the length of each neurite was increased in all three systems (Figure 4.2c). This is especially obvious in the FP (Figure 4.2c(ii)) and EP (Figure 4.2c(iii)) systems, where synergistic behaviours were observed. Thus, our data shows that increases in both the number of neurite protrusions and length of each neurite contribute to the synergistic enhancement of total neurite length.

4.2.2. Analysis of Neurite Branching

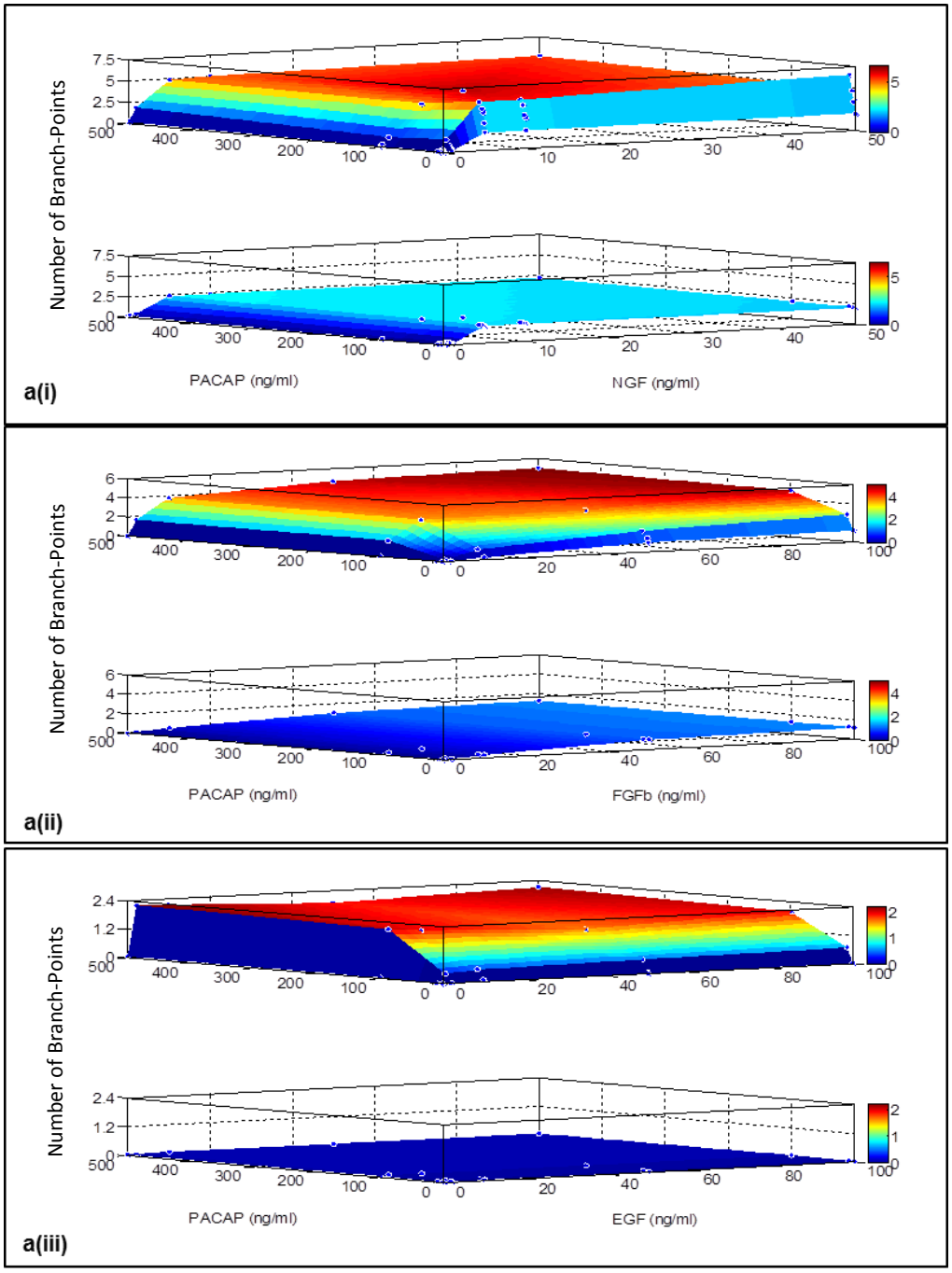

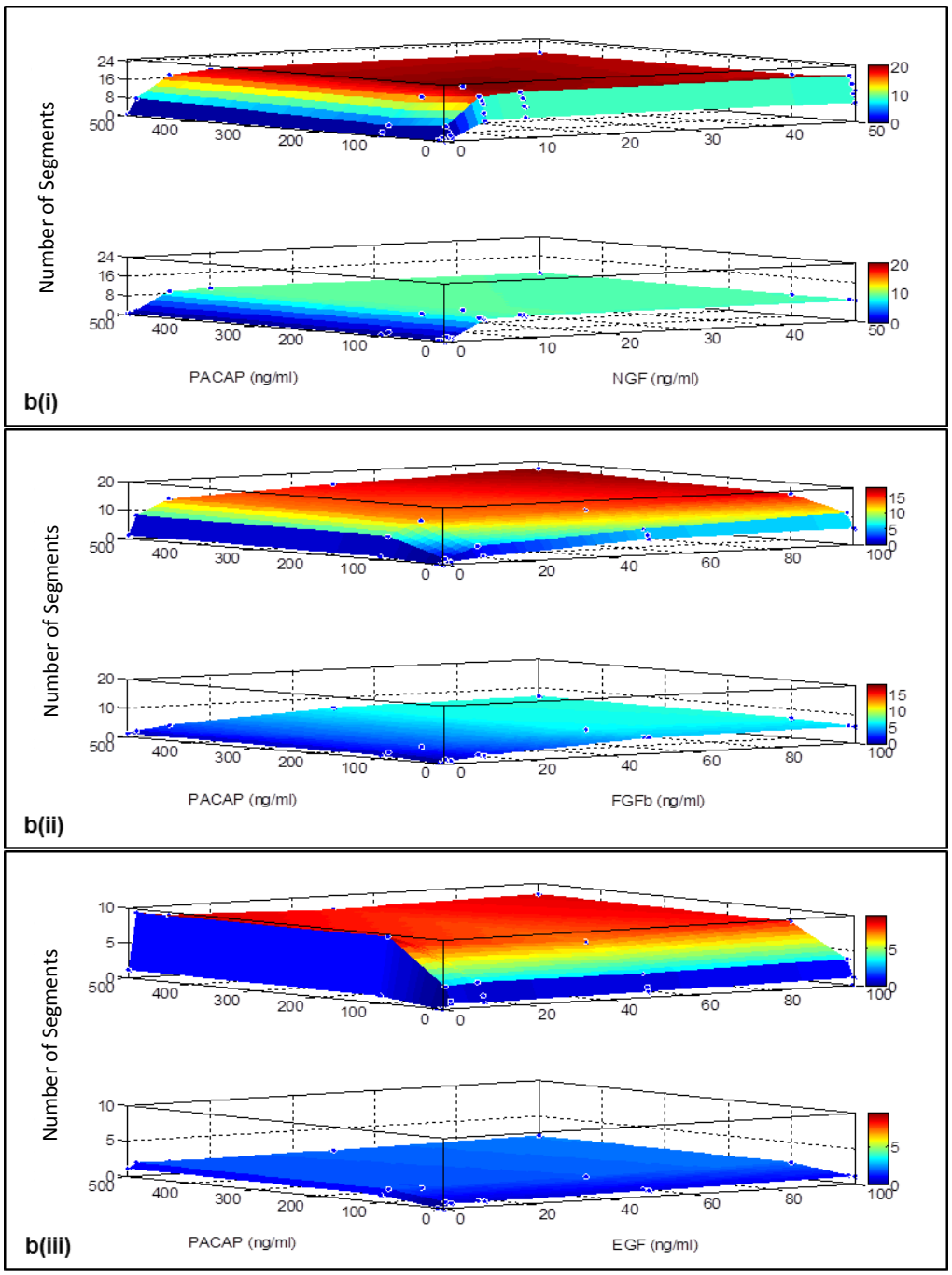

Figure 4.3. Synergistic increase in the number of branch-points in the neurites upon combinatorial growth factor-PACAP treatments. (a) Number of branch-points, and (b) number of segments after 48 hours of stimulation with (i) NGF (0-50 ng/ml)-PACAP (0-500 ng/ml), (ii) FGFb (0-100 ng/ml)-PACAP (0-500 ng/ml), and (iii) EGF (0-100 ng/ml)-PACAP (0-500 ng/ml), respectively. Top panel: Experimentally obtained results of the growth factor-PACAP combinatorial treatment; Bottom panel: Additive effect calculated through the summation of the individual effects of the growth factors and PACAP. x, y, and z axes denote concentrations of growth factors (ng/ml), concentration of PACAP (ng/ml), and number of branch-points or segments, respectively.

Having shown that the length of each neurite is increased, we sought to identify if this increase was due solely to an elongation of the neurites or

accompanied by an increase in the degree branching of neurites. This was measured using two parameters, the number of branch-points and the number of segments, defined as the region of the neurite spanning between a branch-point, cell-body, or the terminal end of the neurite (S1, S2, and S3) (Figure 4.2a). In all three systems, using a RSM analysis, the number of branch-points was also found to be synergistically regulated (Figure 4.3a). Given that a higher degree of branching would result in more neurite segments, the number of neurite segments (Figure 4.3b) was expectedly found to be synergistically regulated as well.

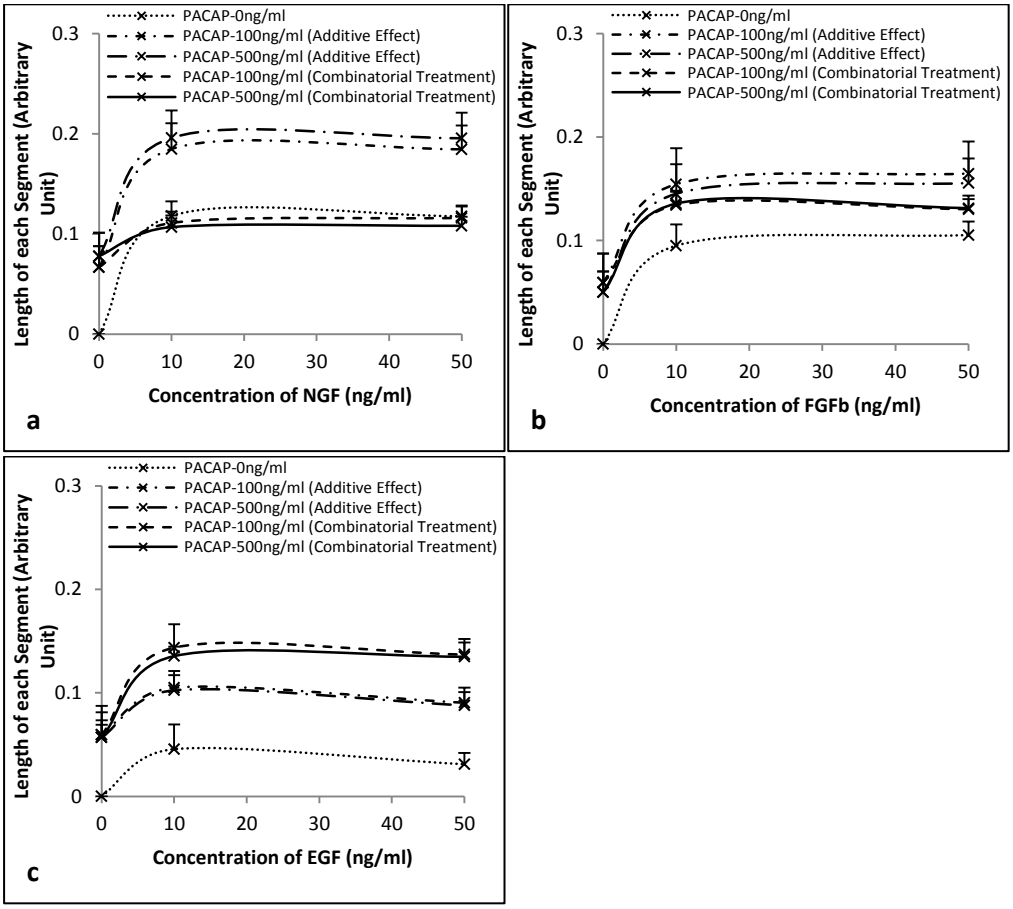

Figure 4.4. Increase in the length of each neurite segments contributes to the synergistic regulation of total neurite length in the EP and FP, but not NP, systems. (a), (b), (c) Length of each neurite segment after 48 hours of stimulation with NGF (0-50 ng/ml)-PACAP (0-500 ng/ml), FGFb (0-50 ng/ml)-PACAP (0-500 ng/ml), and EGF (0-50 ng/ml)-PACAP (0-500 ng/ml), respectively.

To assess if the length of each segment was enhanced during combinatorial growth factor-PACAP treatments, the average length of each segment was quantified. Similar to the average length of each neurite, the average length of each segment was increased in the FP (Figure 4.4b) and EP (Figure 4.4c) systems. This increase is most evident in the EP system as the increase in segment length was synergistic. Surprisingly, the segment length was not enhanced in the NP system (Figure 4.4a), suggesting a differential regulation of synergistic neurite outgrowth in these systems.

4.2.3. PKA Regulates Neurite Length in the FP and EP, but not NP, Systems

In our previously study, we have shown that while Erk was involved in the regulation of total neurite length in all three systems, JNK was positively involved in the process in only the NP and FP systems. Here, we investigated if PKA, which had been reported to be involved in neurite outgrowth in PC12 cells[222,304], was also required for neurite outgrowth in these three systems. Although Erk and JNK were previously reported to be synergistically phosphorylated in all three systems, CREB, a surrogate marker for PKA, was not found to be synergistically phosphorylated in these systems (Figure 4.5). While this suggested that PKA was unlikely to be required for the regulation of neurite length in these systems, inhibition of PKA using H89 surprisingly reduced the total neurite length in the FP and EP (Figure 4.6a) systems. However, inhibition of PKA did not affect the total neurite length in the NP (Figure 4.6a) system.

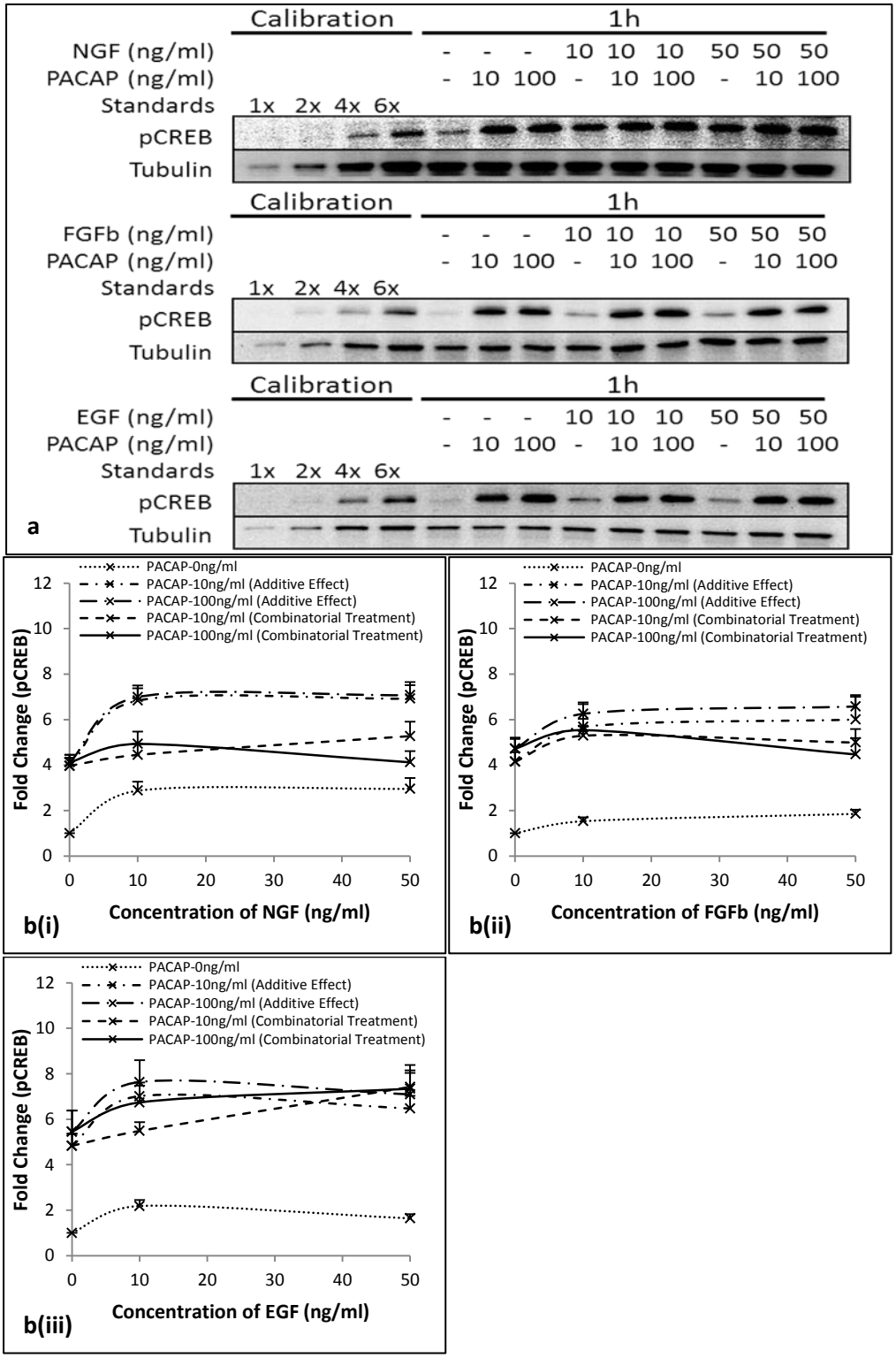

Figure 4.5. CREB is not synergistically phosphorylated upon combinatorial growth factor-PACAP treatments. (a) pCREB levels after stimulation with NGF (0-50 ng/ml)-PACAP (0-100 ng/ml), FGFb (0-50 ng/ml)-PACAP (0-100 ng/ml), or EGF (0-50 ng/ml)-PACAP (0-100 ng/ml) for 60 minutes. pCREB levels were analyzed by Western blotting, and normalized to the levels of Tubulin. (b) Fold changes of pCREB upon (i) NP, (ii) FP, and (iii) EP stimulations were quantified by densitometry and plotted for the analysis of synergism. Significant differences between combinatorial experimental treatment of growth factor-PACAP and summation of their individual effects were calculated using the paired Student's *t*-test. A value of $p<0.05$ was considered significant.

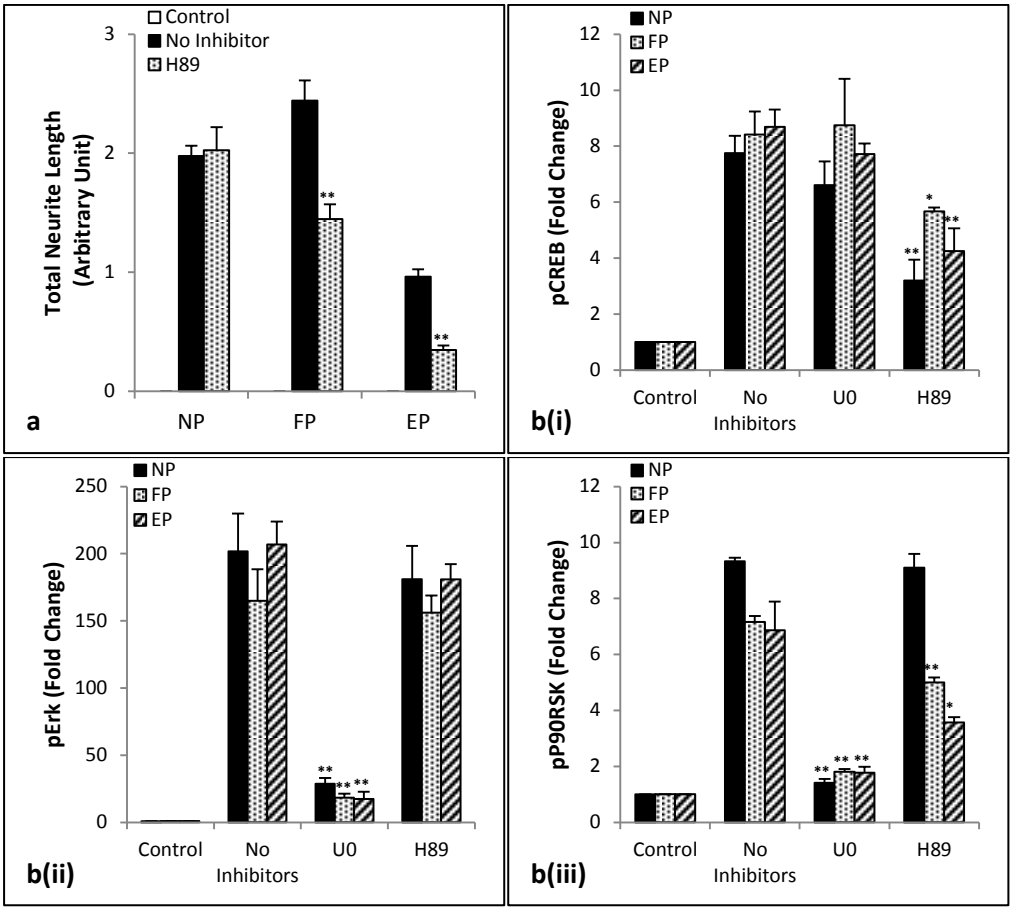

Figure 4.6. Involvement of PKA in regulating total neurite length in the FP and EP, but not NP, systems is mediated by P90RSK independently of Erk. The concentrations of growth factor and PACAP used were 50 ng/ml and 100 ng/ml, respectively. (a) Effect of PKA inhibitor, H89, at 10 μM (H89) on total neurite length after 48 hours of stimulation NP, FP, and EP. (b) Effects of U0126 at 20 μM (U0), and H89 at 10 μM (H89) on levels of (i) pCREB, (ii) pErk, and (iii) pP90RSK after 60 minutes of stimulation with NP, FP, or EP. The phosphorylation levels of these proteins were analyzed by Western blotting, quantified by densitometry, and normalized to the levels of Tubulin. Significant differences between treatments with and without inhibitors were calculated using the paired Student's *t*-test. A value of $p<0.05$ was considered significant (**$p<0.01$; *$p<0.05$).

In PC12 cells, both Erk[164,169] and its downstream target P90RSK[219] had been reported to be required for neurite outgrowth. Previous studies had also suggested that PKA is an upstream effector of Erk in the regulation of neurite outgrowth[216]. To determine if PKA indeed regulated the activity of Erk in the FP and EP systems, the phosphorylation levels of Erk and P90RSK, were probed after stimulation with the ligands in the presence of H89. In the NP system, inhibition of PKA, using pCREB as a control (Figure 4.6b(i)), exhibits no inhibitory effect on Erk (Figure 4.6b(ii)) and P90RSK phosphorylations (Figure 4.6b(iii)), which is consistent with the finding that PKA did not regulate

neurite length in the NP system (Figure 4.6a). In the FP and EP systems, surprisingly, inhibition of PKA resulted in a reduction in the phosphorylation level of P90RSK (Figure 4.6b(iii)) but not Erk (Figure 4.6b(ii)). This suggests that PKA can regulate the activity of P90RSK via an alternative mechanism independently of Erk.

4.2.4. Regulation of Different Morphological Features of Neurite Outgrowth by Distinct Signalling Pathways

As we have seen earlier, enhancement of neurite length in these systems can occur through an increase in the number of neurite extensions, length of each neurite, and degree of branching. However, it is unclear if the pathways regulating neurite length also regulated these morphological features. Inhibition of the kinases involved in the positive regulation of total neurite length was also found to inhibit the number of neurite extensions (Figure 4.7a), length of the longest neurite (Figure 4.7b) and length of each neurite (Figure 4.7c), demonstrating that these pathways regulate synergistic neurite outgrowth through enhancement of these parameters. Representative images of the cells treated with different ligands in both the absence and presence of various inhibitors are as shown in Figure 4.7d.

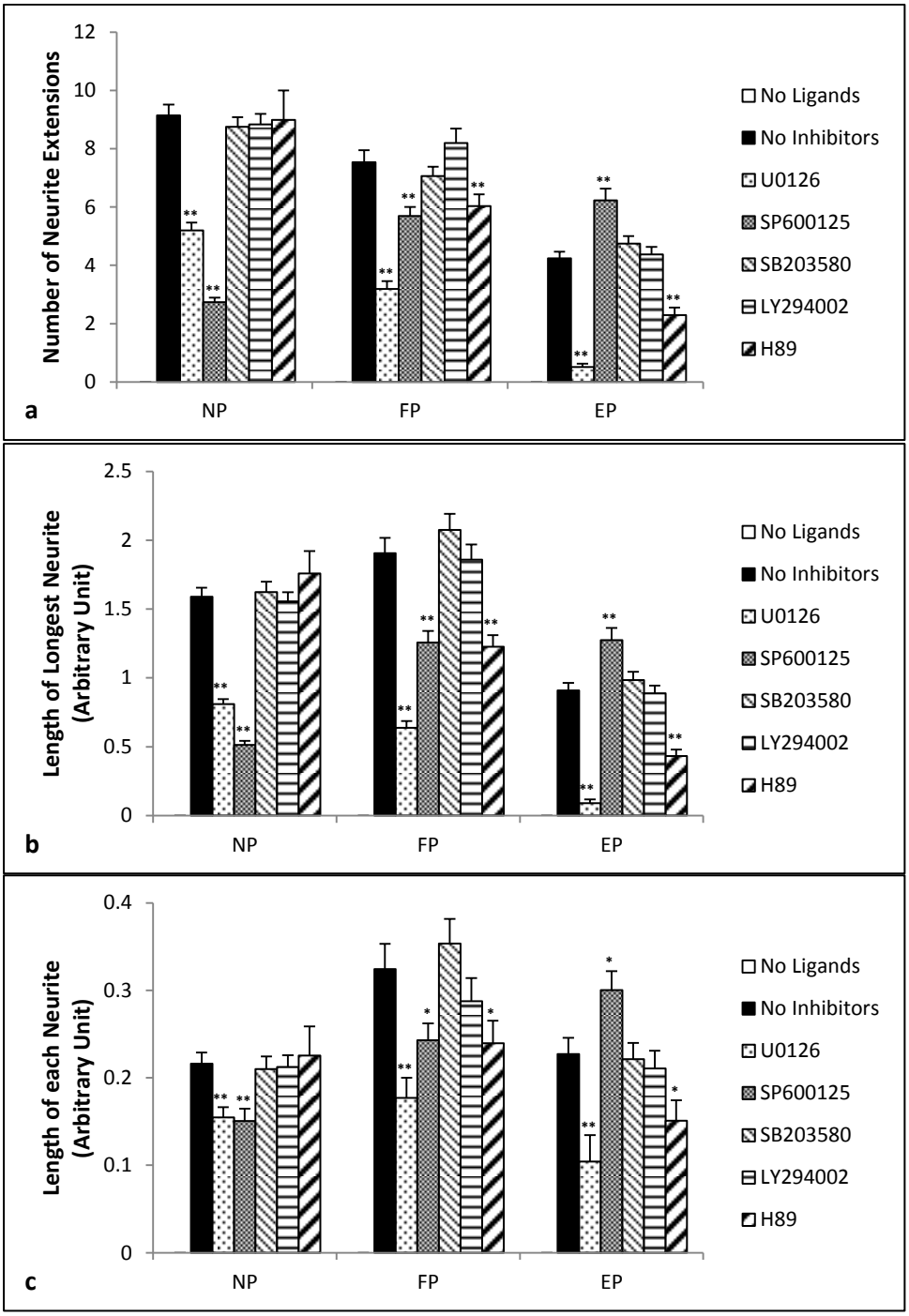
Number of Neurite Extensions
12
10
8
6
4
2
0
NP
FP
EP
a
No Ligands
No Inhibitors
U0126
SP600125
SB203580
LY294002
H89
Length of Longest Neurite (Arbitrary Unit)
2.5
2
1.5
1
0.5
0
b
Length of each Neurite (Arbitrary Unit)
0.4
0.3
0.2
0.1
0
c

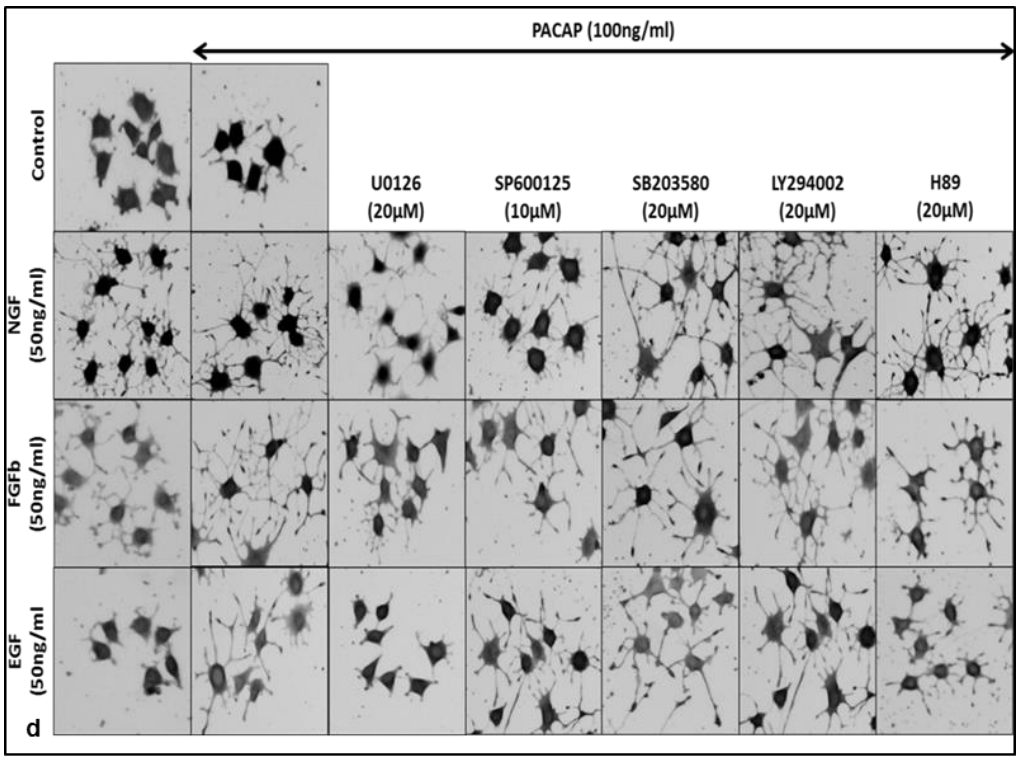

Figure 4.7. Regulation of total neurite length by various signalling pathways is mediated, in part, through number of neurite extensions and length of each neurite. The concentrations of growth factor and PACAP used were 50 ng/ml and 100 ng/ml, respectively. Effects of U0126 (20 μM), SP600125 (10 μM), SB203580 (20 μM), LY294002 (20 μM), and H89 (10 μM) on (a) number of neurite extensions, (b) length of longest neurite, and (c) length of each neurite after 48 hours of stimulation with NGF-PACAP (NP), FGFb-PACAP (FP), and EGF-PACAP (EP). (d) Representative images of cells after different treatments for 48 hours in both the absence and presence of various inhibitors. Significant differences between treatments with and without inhibitors were calculated using the paired Student's *t*-test. A value of $p<0.05$ was considered significant (**$p<0.01$; *$p<0.05$).

We then examined the regulation of the degree of branching by these kinases. As expected, inhibition of the kinases involved in the positive regulation of neurite length also reduced the number of branch-points (Figure 4.8a) and the number of segments (Figure 4.8b). However, the length of each segment was not reduced upon inhibition of these pathways in the NP and FP systems (Figure 4.8c), suggesting that an increase in total neurite length did not occur through an increase in the length of the neurite segments. On the contrary, inhibition of Erk resulted in a decrease in the length of each segment in the EP system (Figure 4.8c), indicating that different mechanisms might regulate synergistic neurite outgrowth in these systems.

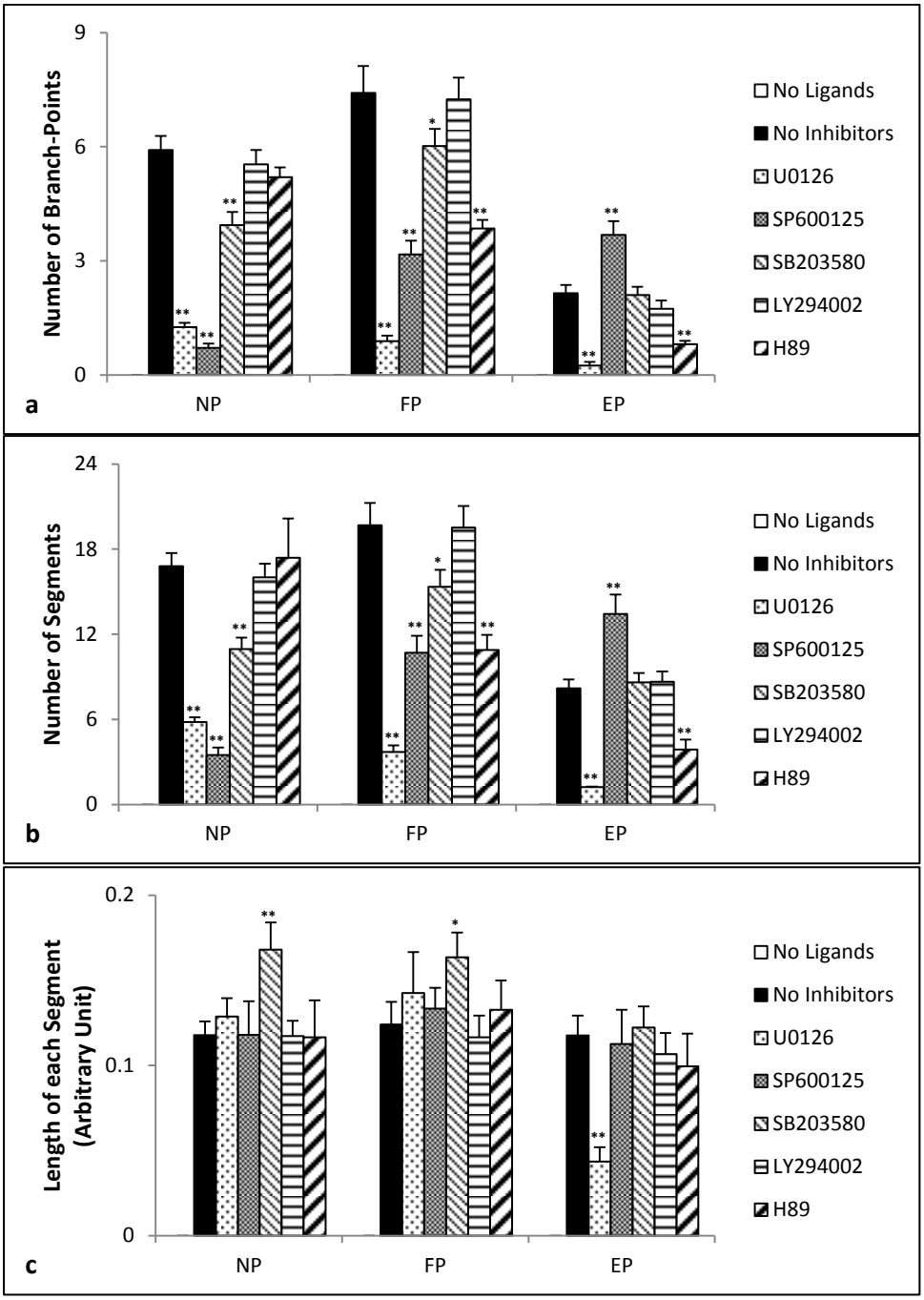

Figure 4.8. P38 regulates the number of branch-points and the number of segments independently of neurite length. The concentrations of growth factor and PACAP used were 50 ng/ml and 100 ng/ml, respectively. Effects of U0126 (20 μM), SP600125 (10 μM), SB203580 (20 μM), LY294002 (20 μM), and H89 (10 μM) on (a) number of branch-points, (b) number of segments, and (c) length of each segment after 48 hours of stimulation with NGF-PACAP (NP), FGFb-PACAP (FP), and EGF-PACAP (EP). Significant differences between treatments with and without inhibitors were calculated using the paired Student's *t*-test. A value of $p<0.05$ was considered significant (**$p<0.01$; *$p<0.05$).

Surprisingly, inhibition of P38 using SB203580 decreased the number of branch-points (Figure 4.8a) and segments (Figure 4.8b) in the NP and FP systems without reduction of the total neurite length (Figure 3.10). This

reduction in the number of branch-points independently of neurite length resulted in an increase in the length of each segment (Figure 4.8c). Thus, our results suggest that different morphological aspects of neurite outgrowth can be regulated independently through distinct signalling pathways.

4.3. Discussions

In this study, we further investigated the regulation of different morphological features underlying synergistic neurite outgrowth. Building on our previous work, we found that the total neurite length was regulated by PKA in the EP and FP, but not NP, systems. Surprisingly, this involvement of PKA in neurite outgrowth was mediated by P90RSK independently of Erk. Investigating the morphological changes during synergistic neurite outgrowth, the synergistic regulation of total neurite length was found to be mediated by an increase in the number of neurite extensions, degree of branching of the neurites, and length of each neurite. These morphological features, which contributed to the enhancement of total neurite length, were all found to be regulated by the same pathways regulating total neurite length. However, P38, which was not involved in the regulation of total neurite length in all three systems, was instead found to regulate the branching of neurites in the NP and FP systems, suggesting that distinct pathways regulate the different morphological features of neurite outgrowth (Table 4.1, and Figure 4.9).

There have been controversies surrounding the role of PKA in regulating neurite outgrowth where both its involvement and non-involvement in regulating neurite outgrowth in PC12 cells had been reported[133,216,222,304,305]. Examining its role in the regulation of synergistic neurite outgrowth, PKA was found to be involved in neurite outgrowth in the FP and EP, but not NP,

systems. Although PKA had previously been reported to regulate the activity of Erk[111,139,306], its involvement in the regulation of neurite outgrowth in the FP and EP systems in this study was found to be mediated through P90RSK, independently of Erk. In addition to the involvement of Erk and JNK in regulating synergistic neurite outgrowth through P90RSK[307] (Chapter 3), this suggests that the regulation of P90RSK by PKA could be yet another mechanism involved in the regulation of the process. P90RSK had previously been shown to be able to interact directly with both the regulatory and catalytic subunits of PKA[308-310]. While it has not been shown that PKA can directly phosphorylate P90RSK, the complex interactions between the catalytic subunits of PKA, regulatory subunits of PKA, PKA anchoring proteins, protein phosphatases (PPs), and P90RSK suggest that the activity of PKA can influence that of P90RSK[309]. Thus, our results indicates that P90RSK could be a convergent point for the three different signalling pathways and further complements the results of previous studies where it was found to be an important mediator of neurite outgrowth[219,276].

Table 4.1. Summary of the kinases involved in the regulation of various morphological features of neurite outgrowth. '+', '-', and '' denote positive, negative, and no regulation, respectively.

Morphological Features	NP				FP				EP			
	Erk	JNK	P38	PKA	Erk	JNK	P38	PKA	Erk	JNK	P38	PKA
Total neurite length	+	+			+	+		+	+	-		+
Number of neurites	+	+			+	+		+	+	-		+
Degree of branching	+	+	+		+	+	+	+	+	-		+
Length of longest neurite	+	+			+	+		+	+	-		+
Average length of each neurite	+	+			+	+		+	+	-		+
Length of each neurite segment			-				-		+			

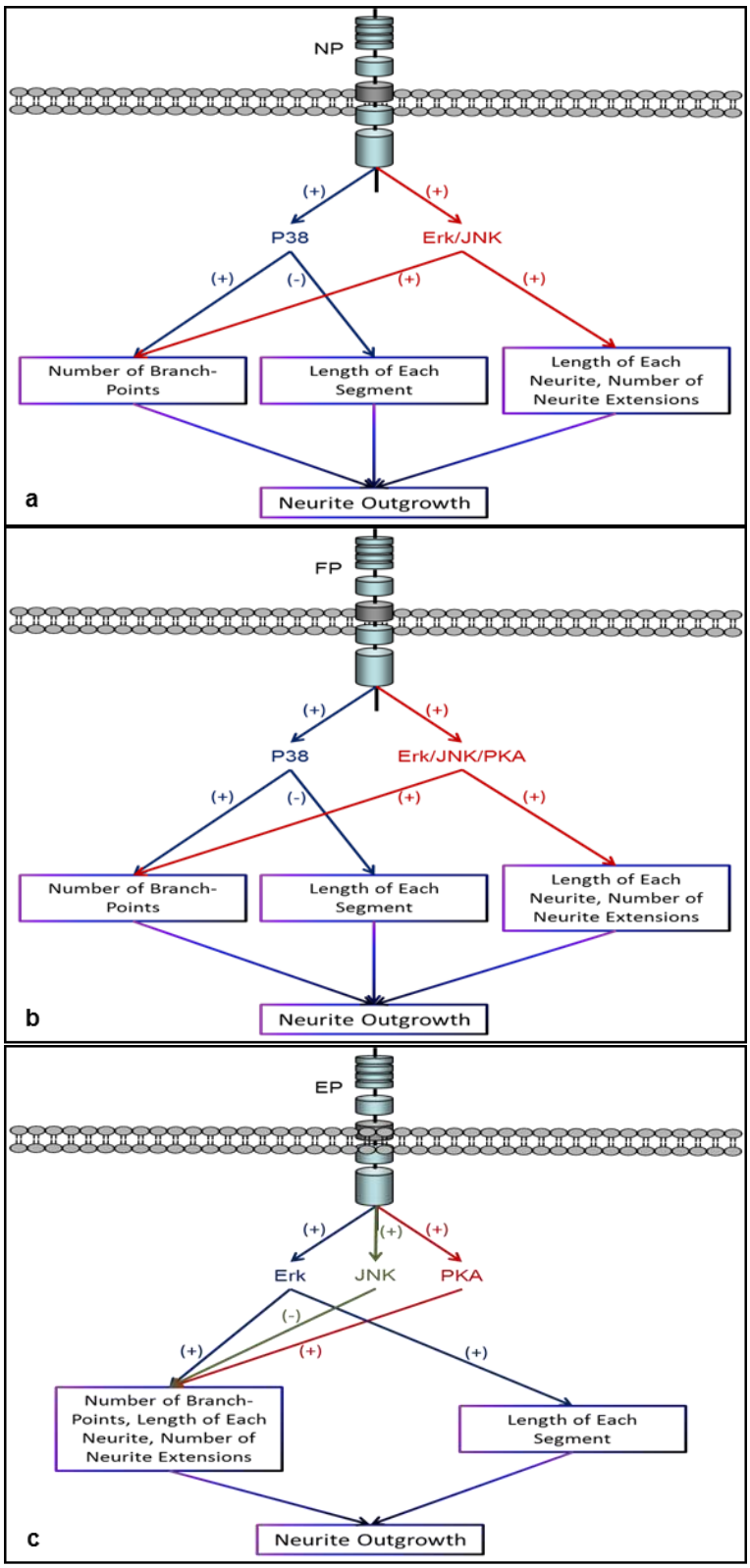

Figure 4.9. A schematic illustration of the different pathways used by the three different synergistic systems, (a) NGF-PACAP (NP), (b) FGFb-PACAP (FP), and (c) EGF-PACAP (EP), in the regulation of various morphological features during neurite outgrowth.

Besides PKA, the other main downstream target of cAMP is Epac[311,312]. Similar to PKA, Epac had also been found to regulate neurite outgrowth in PC12 cells[137,313]. Although our results showed that PKA was not involved in regulating neurite outgrowth in the NP system, it had previously been shown that NGF synergized with Epac to enhance neurite outgrowth[136]. Thus, it is likely that cAMP synergizes with different growth factors via different mechanisms. Interestingly, PKA and Epac had also been found to synergize with one another to enhance neurite outgrowth[290]. Given the controversy surrounding the involvement of Epac and PKA in neurite outgrowth[311], a more holistic systems-based study on these cAMP effectors, and other signalling pathways, such as Erk and JNK, would give a clearer picture of their roles in regulating neurite outgrowth.

To achieve a more comprehensive understanding of neurite outgrowth, its morphologies need to be analyzed to a greater depth[232,314,315] as the neuronal morphology pertaining to the structure and connectivity of neurons are critical for the regulation of neuronal functions[316]. In this study, the enhancement of total neurite length in the three systems was found to occur through an increase in the length of individual neurites, number of neurite protrusions, and branch-points in the neurites. During both neurite elongation and branching, organization of the cytoskeleton occurs. Thus, it is not unexpected that both neurite elongation and branching can be co-regulated by the same pathways[317,318]. This is consistent with previous studies that implicated pathways regulating total neurite length, such as Erk and JNK, in regulating other aspects of neuritogenesis, such as neurite branching and elongation during differentiation of PC12 cells[236]. Both Rac1[319] and map1b[320], which are mediators of the JNK pathway, have also been found to regulate neurite

branching. In addition, *in vivo* studies have also shown that deletion of Erk results in abnormal terminal branching of sensory neurons[321,322].

However, neurite elongation and branching can be seen as two separate phenomena and can be operationally independent as conditions that affect one do not necessary affect the other[239,240]. For instance, the microtubule-severing proteins katanin and spastin regulate primarily axon elongation and branching, respectively[323]. Importantly, branching is a critical process during development as disruption of axon branching can lead to various neurodevelopmental problems including autism spectrum disorders, infantile epilepsy, and mental retardation[324].

Surprisingly, P38, which was not found to regulate neurite length, regulated the branching of neurites in the NP and FP, but not EP, systems. The dynamics of microtubule or actin polymerization are critical processes in the regulation of neurite branching as inhibition of these processes was found to inhibit branching but not elongation[324-326]. One of the main classes of proteins that can regulate actin polymerization and microtubules stabilization is the Rho GTPases RhoA, Cdc42, and Rac1[327]. Among them, Rac1 and Cdc42 had been found to positively regulate neurite outgrowth in PC12 cells[328]. Given that P38 is a downstream signalling effector of Rac and Cdc42 in many systems[141,329], it is plausible that P38 may play a critical role in regulating the morphological branching of neurites. This idea is further supported by a previous work that demonstrated its involvement in regulating the onset of the sprouting of neurites in PC12 cells[164]. In addition, the mixed-lineage kinase (MLK), which lies upstream of P38, has also been found to regulate branching in neurites[330]. To the best of our knowledge, this is the first report indicating that P38 can regulate the branching independently of the elongation of the

neurites. Another interesting finding in our work was that Erk regulated the length of the neurite segments in the EP, but not NP and FP, system. This clearly implies that the same signalling pathways can regulate the morphological structures of neurites in each system differently. Critically, given that these morphological structures are all tightly inter-related to one another, assessment of the mechanisms underlying neurite outgrowth should not just take into account a systems-view of signalling pathways, but also a systems-view of morphological structures.

4.4. Conclusions

This study has demonstrated that different parameters characterizing the morphological features of synergistic neurite outgrowth are regulated by distinct signalling pathways. The involvement of PKA in regulating neurite outgrowth was found to be mediated by P90RSK, independently of the Erk pathway. Together with the findings from our previous work (Chapter 3), P90RSK could be an important convergent point for multiple signalling pathways, such as Erk, JNK, and PKA, rendering it an important mediator of neurite outgrowth. A more elaborated neurite outgrowth under synergistic conditions occurs due to an increase in the length of each neurite, and number of neurite extensions and branch-points. Although inhibition of pathways regulating synergistic neurite length resulted in attenuation of these morphological features, P38 was found to regulate the number of segments and branch-points independently of the length. These results indicate a complex interplay of different signalling pathways in the regulation of the morphological structures of neurite during differentiation.

Chapter 5.

A Novel Bayesian Approach to Network Inference of the Synergistic NGF-PACAP Bi-Ligand System Unveils Positive Feedback during Regulation of Neurite Outgrowth in PC12 Cells

5.1. Introduction

In Chapter 3, we showed that synergistic Erk and JNK activations were required for neurite outgrowth in the NP system[307]. Several studies have also reported synergistic Erk phosphorylation in different models of synergistic neurite outgrowth[216], including the NP system[213]. However, the underlying mechanisms for such synergistic Erk and JNK activations are still poorly understood. Various studies have identified the existence of cross-talks between different signalling cascades[41,112,331,332], which can potentially contribute to synergism in neurite outgrowth. Given the intricacies of the network wiring, the quantitative relationships between different proteins, and the high dimensionality involved, computational modeling offers unique insights into network interactions[218,333]. For instance, a previous study using steady-state-based Modular Response Analysis, had unveiled a positive feedback loop between MEK and Erk in NGF-treated PC12 cells[334], suggesting that such a mechanism may be involved in the synergistic activation of Erk upon NP treatment. However, modeling approaches for the analyses of synergistic behaviours are still lacking. In the analyses of such systems, the main challenges that need to be addressed are the lack of *a priori* knowledge and the ability to parameterize the data from uni-ligand and bi-ligand experiments so that information regarding synergistic behaviours can be extracted.

In view of the wide-ranging implications of synergism, extensive research has been done in this area. However, previous studies have largely focused on the evaluation of multi-component synergy using methods such as Bliss independence model, Loewe additivism model, and the Combinatorial Index

theorem[275,335] without providing much mechanistic insights into how interactions between signalling pathways can lead to the synergistic effects. As discussed previously, the lack of *a priori* knowledge about the mechanisms underlying synergistic neurite outgrowth render data-driven models more appropriate tools than mechanistic models. Among the commonly used data-driven models, such as Bayesian networks (BNs)[69,71], Boolean networks[86], association networks[55], and artificial neural networks (ANNs)[50], for analyzing signalling networks, the advantages of BNs have also been discussed earlier.

Given that current modeling approaches are not well-equipped for the analyses of synergistic systems, we proposed the use of a modified Bayesian methodology to address this issue using the synergistic NP system. The main methodological contribution of this paper was to show that the dynamic programming algorithm for the exact structure learning can be adapted to perform two-phase learning in a computationally feasible manner, an idea that can be exploited for the analyses of multi-ligand systems. Through western blot experiments, we first made a novel observation that MEK and MKK4, upstream effectors of Erk, and JNK[141], respectively, were synergistically activated upon NP treatment. Our developed method, termed TEEBM (Two-phase, Exact structure learning, Expanded-in-time Bayesian Methodology) was then applied to a small set of experimentally-obtained phosphorylation data on these four kinases to infer statistical dependencies between them upon NP stimulation. Our inference results unexpectedly identified a feedback loop involving MEK, Erk, MKK4, and JNK, which contributed to their synergistic activations. These key biological findings were validated experimentally using kinase inhibitors, where inhibition of MEK blocked Erk,

JNK, and MKK4 activations, and inhibition of JNK attenuated MKK4, MEK, and Erk activations, demonstrating the potential of our TEEBM in gaining insights about signalling networks in synergistic systems.

5.2. Mathematical Modeling Procedure

5.2.1. BNs without Intervention Data

BNs were initially used as ordinary statistical models without any specific connection to Bayesian statistics. The name was originally given by the artificial intelligence researcher Judea Pearl, who used these models to represent and manipulate subjective knowledge. However, over the years, the statistical machine learning community has developed Bayesian statistical techniques to infer such models from data. These techniques are adopted in this study and are explained briefly to the extent needed for further developments.

In BNs modelling, the n-variate domain, $V = \{V_1, \dots, V_n\}$, is represented using a directed acyclic graph, G, that encodes the independences between the variables, V_i. In this graphical model, each variable, V_i, is represented by a node, and the arcs of the network, G, can be encoded as a vector containing a subset of the variables of V, i.e. $G = (G_1, \dots, G_n)$, where G_i is a "parent set" of the variable, V_i, that contains the variables from which there is an arc to V_i. The notation, V_i, is used to refer both to the random variable, V_i, and the node, V_i, in the network, G. The statistical meaning of the graph is then defined by the parental Markov condition, which states that the variable, V_i, is conditionally independent of all its non-descendants given its parents, G_i. The

descendants of a node, V_i, refer to all the nodes that can be reached from V_i by following the directed arcs.

Using the parental Markov condition, the joint probability distribution, $P(V)$, can be factorized as $P(V) = \prod_{i=1}^{n} P(V_i|G_i)$.

The specification of the individual terms, $P(V_i|G_i)$, is dependent on the measuring scale of the random variables, V_i and G_i, but in general, this conditional distribution is modelled to be governed by a finite set of parameters θ_{i,G_i}, i.e. $P(V_i|G_i) = P(V_i|G_i, \theta_{i,G_i})$.

5.2.1.1. Bayesian Inference from Data

In the Bayesian learning of any BN structures, G,[336] a dataset, $D = (D_1, \dots, D_N)$, of N exchangeable n-variate data vectors, is used to compute the posterior probability, $P(G|D) = P(D)^{-1}P(D|G)P(G)$. The network prior, $P(G)$, is often assumed to be uniform, or at least decomposable as $P(G) = \prod_{i=1}^{n} P(G_i)$. During the comparisons of the probabilities of different networks, the normalizing denominator, $P(D)$, is cancelled out. Thus, the data-dependent part of the computation is denoted by the marginal likelihood, $P(D|G) = \int P(D|G, \theta)P(\theta)d\theta$.

Although the data vectors, $D_j = (D_{j1}, \dots, D_{jn})$, can be assumed to be conditionally independent given the network and its parameters, i.e. $P(D|G, \theta) = \prod_{j=1}^{N} P(D_j|G, \theta)$, the parameter prior, $P(\theta)$, has to be first defined. To facilitate the elicitation of this prior, it is common to assume that the parameters defining the conditional distributions of different variables are *a*

priori independent, i.e. $P(\theta) = \prod_{i=1}^{n} P(\theta_{i,G_i})$. The posterior probability of the network structure, G, can then be expressed as

(Equation 5.1)
$$\begin{aligned} P(G|D) &\propto P(G)P(D|G) \\ &= P(G)\int \prod_{j=1}^{N} P(D_j|G,\theta)P(\theta)d\theta \\ &= P(G)\int \prod_{j=1}^{N}\prod_{i=1}^{n} P(D_{ji}|D_{jG_i},\theta_{i,G_i})P(\theta_{i,G_i})d\theta \\ &= P(G)\prod_{i=1}^{n}\int \prod_{j=1}^{N} P(D_{ji}|D_{jG_i},\theta_{i,G_i})P(\theta_{i,G_i})d\theta_{i,G_i} \\ &= \prod_{i=1}^{n} P(G_i)P(D_{\cdot i}|D_{\cdot\, G_i}). \end{aligned}$$

Factorization of the posterior distribution as shown above results in a decomposable scoring criterion, which is a requirement for efficient heuristic learning of BNs[336] and for exact structure learning methods. For the latter methods, the most probable BN, for small numbers of variables, can be found in a reasonable time[337-339]. However, reliable estimation of the mode of the marginal likelihood, $P(D|G)$, by integrating out the parameters (as in Equation 5.1), is a non-trivial process as it is very sensitive to the parameter prior, $P(\theta)$, which is difficult to specify in practice. In addition, this sensitivity is exacerbated by datasets with small sample sizes[340]. As suggested in our previous work[341], this sensitivity problem can be circumvented by estimating $P(D|G)$ (Equation 5.2) using another decomposable score called a factorized normalized maximum likelihood (fNML):

(Equation 5.2)
$$\begin{aligned} P(D|G) &= \prod_{i=1}^{n} P(D_{\cdot i}|D_{\cdot_{G_i}}) \\ &= \prod_{i=1}^{n}\prod_{g_i \in dom(G_i)} P\left(D_{\cdot i}\middle|D_{g_i}\right) \\ &= \prod_{i=1}^{n}\prod_{g_i \in dom(G_i)} \frac{P(D_{\cdot i,g_i}|\widehat{\theta}(D_{\cdot i,g_i}))}{\sum_{D'_{\cdot i}} P(D'_{\cdot i}|\widehat{\theta}(D'_{\cdot i}))}, \end{aligned}$$

where $P(D_{\cdot i,g_i})$ denotes the data for the variable, V_i, in cases where its parents have the value configuration, g_i, and $\hat{\theta}(D_{\cdot i,g_i})$ denotes the maximum likelihood parameters for that uni-variate data.

The normalizer is summed over all the uni-variate data sets of the size $|D_{\cdot i,g_i}|$ and it is guaranteed that the fraction defines a proper probability distribution. However, the probabilities defined by the equations above are often extremely small in practice. Thus, for numerical stability, the logarithms of these probabilities are used as scores to be optimized in the actual implementations, and the differences in scores are then logarithms of probability ratios.

5.2.1.2. Expanded-in-Time Parameterization of Protein Variables

Cell signalling is not a static but a temporally-varying process. Consequently, ordinary BNs may not *a priori* be the most natural choice of modelling approach. The most popular graphical model for discrete stationary stochastic process is the dynamic BN (DBN). However, DBNs are most suited for the multivariate time-series that form a first order Markov-chain, an assumption that may be plausible when the process is observed in regular intervals and when all the relevant factors of the domain have been observed. Neither of these two assumptions is true in our case. Recently, non-stationary DBNs (nsDBNs) and time-varying DBNs (tvDBNs) have been developed to relax the restrictive assumption of stationarity[78,249,250]. These models greatly enhance the expressivity of the DBN framework and technically, they could be used in this study. However, these methods are plausible only for observation sequences that are sufficiently long, where the regularities in the change of

the independence structure can be captured. However, in our case, there are only two pairs of time-points in the data, which is insufficient to infer any regularities in the dependency change process. Thus, variables in different time-points were modelled as separate variables in the ordinary BN, where the parameterization of our experimental data was performed as outlined in the next paragraph.

Cells were treated experimentally with a full-factorial combination of NGF (0, 10, and 50 ng/ml) and PACAP (0, 10, and 100 ng/ml) in triplicates. Quantitative western blot using chemiluminescence with standard curve was performed essentially as described previously[342]. Protein phosphorylation levels were measured at three discrete time-points, 5 minutes, 20 minutes, and 60 minutes. The data at 240 minutes were not used for the modeling analysis as the phosphorylation levels of the kinases had dropped close to the basal levels by then. Thus, a total of 27 data-points per protein, per time-point were obtained. The data for each protein was first segregated into 2 groups based on how they were experimentally obtained, uni-ligand or bi-ligand. The data in the uni-ligand group was then binned based on the phosphorylation levels of the proteins across time. For the bi-ligand group, the data was binned based on the degree of synergism, if any, observed. A histogram was plotted for each of the two groups, and the bins were based on the different segmentations observed in the histogram. The data for neurite length was parameterized in the same way. Synergism is defined to be present if the phosphorylation level of the protein under bi-ligand treatment is greater than the sum of the phosphorylation levels of the protein under the two uni-ligand treatments at the same concentrations of ligands. We defined

the degree of synergism as $\frac{Effect\ of\ bi-ligand\ NGF-PACAP\ stimulation}{Effect\ of\ NGF\ stimulation+Effect\ of\ PACAP\ stimulation}$, where values > 1 represents synergism.

5.2.1.3. Two-Phase Learning

Recently, a method to combine differently coded datasets for learning a single BN was proposed[343]. It relied on hypotheses testing, and as such it is only appropriate when the sample sizes are feasible. In cell signalling, obtaining data is labour intensive and it would be convenient to obtain preliminary models to guide the study at the initial stages. As Bayesian learning framework does not theoretically set any lower limit to the sample size, this approach is potentially useful for combining different sources of data. Bayesian reasoning is an online process in which the observations are used to update the prior beliefs into posterior beliefs, which are in turn served as prior beliefs for the subsequent observations. This inherent incrementality makes it convenient to combine different sources of evidence for the inference of a probable model. In BN learning, one batch of data, D^1, can be used to update the $P(G)$ into $P(G|D^1)$, and the next batch, D^2, can then be used to update $P(G|D^1)$ into $P(G|D^1, D^2)$. Using the same argument, this procedure can be generalized to more than two data batches.

In the case that the structure prior is decomposable, i.e. $P(G) = \prod_{i=1}^{n} P(G_i)$, the structure posterior is also decomposable, which also allows efficient learning algorithms for BNs to be used. Under such scenarios, for a small (less than about 30) number of variables, dynamic programming algorithms can be used to find the network structure with the maximal score[337]. In our

work, exact structure learning was used. To the best of our knowledge, such a two-phase exact structure learning approach has not been reported before.

Two phase learning requires the posterior distribution of the first phase, $P(G|D^1)$, to be used as a prior distribution for the second phase. In our experiments, there were 18 variables, which yield about 10^{59} possible networks. Storing the probabilities for each of these would be infeasible because of the space (and even time) constraints. However, due to the decomposability of the posterior probability, it is enough to save the conditional probabilities $P(V_i|\pi)$ of each possible parent set, π, for each variable, V_i. The probabilities of the whole networks are simply products of such local conditional probabilities. For storing the conditional probabilities, only $n2^{n-1}$ real numbers need to be stored. For 18 variables, this evaluates to 2,359,296 real numbers, which, in double precision, requires only 16MB of space. In exact structure learning algorithms, these numbers can be stored on disk. However, with 30 variables, 128GB of space would be needed instead. Thus, this naïve implementation does not scale much further.

5.3. Results

5.3.1. Synergistic MEK, MKK4, Erk, and JNK Activations

We first investigated the involvement and dynamics of the activation of three kinases widely reported to be involved in PC12 differentiation, Erk[164,169], JNK[112,164], and Akt[163], by examining their phosphorylation levels from 0 minutes to 4 hours after stimulation. Synergistic phosphorylations of both Erk (Figures 5.1a, and 5.1b) and JNK (Figures 5.1a, and 5.1c) were observed to peak at 5 minutes and were sustained for up to 1 hour post-stimulation.

However, no synergistic phosphorylation of Akt (Figures 5.1a, and 5.1d) was observed within the time course of the study. The relative neurite lengths at 48 hours following stimulation are plotted as shown in Figure 5.1e. The involvement of Erk, and JNK, but not Akt, in regulating synergistic neurite outgrowth was verified through the use of kinase inhibitors (Figure 5.1f).

MEK and MKK4 are known upstream effectors of Erk[141], and JNK[329], respectively. To gain insight into the possible mechanisms by which Erk, and JNK were synergistically activated, the phosphorylation levels of MEK and MKK4 were examined following NP stimulation. Similarly, both MEK (Figure 5.2a) and MKK4 (Figure 5.2b) were also synergistically activated upon combinatorial NP treatment.

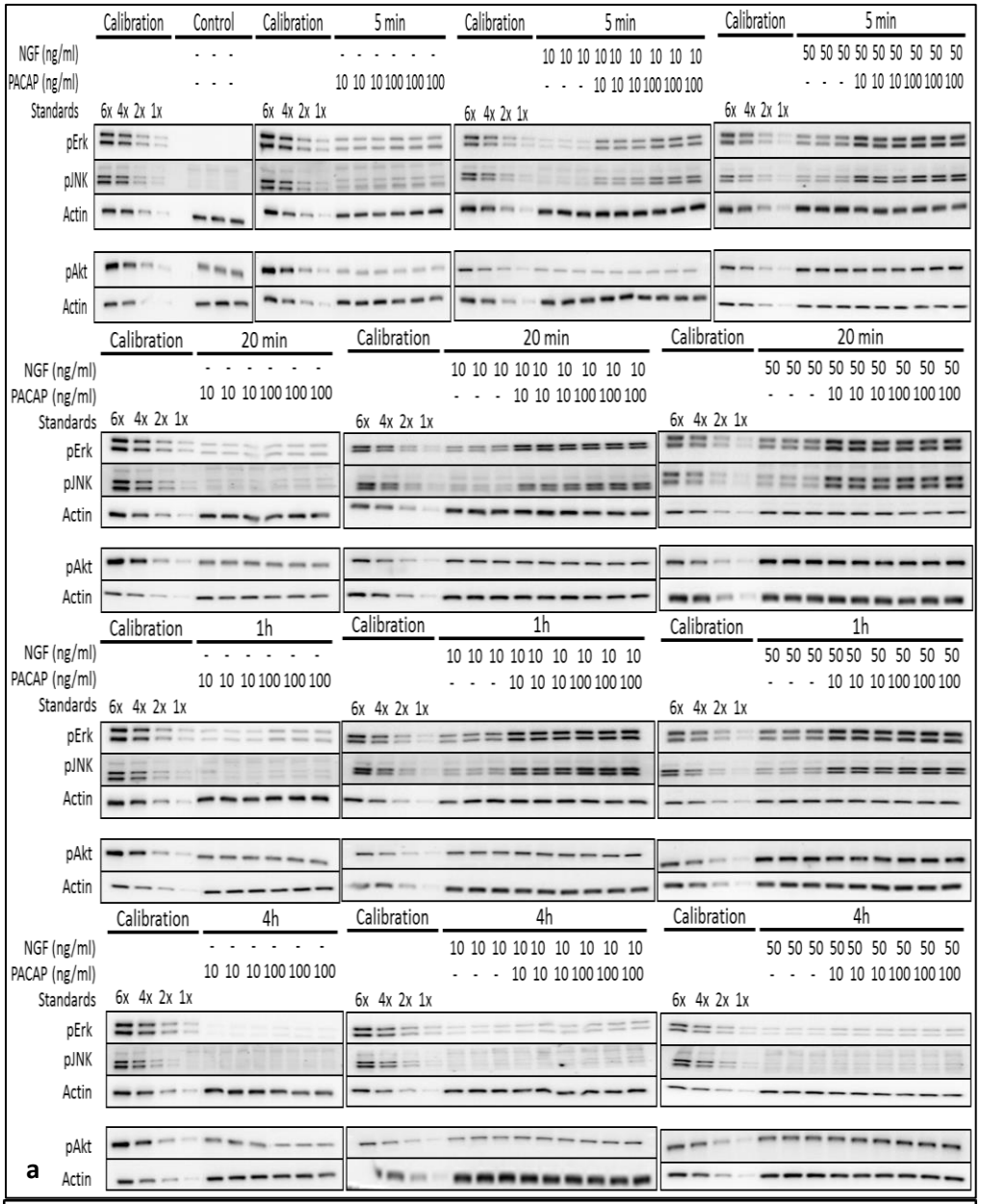
Calibration
Control
5 min
20 min
1h
4h
NGF (ng/ml)
PACAP (ng/ml)
Standards
6x 4x 2x 1x
pErk
pJNK
Actin
pAkt
a

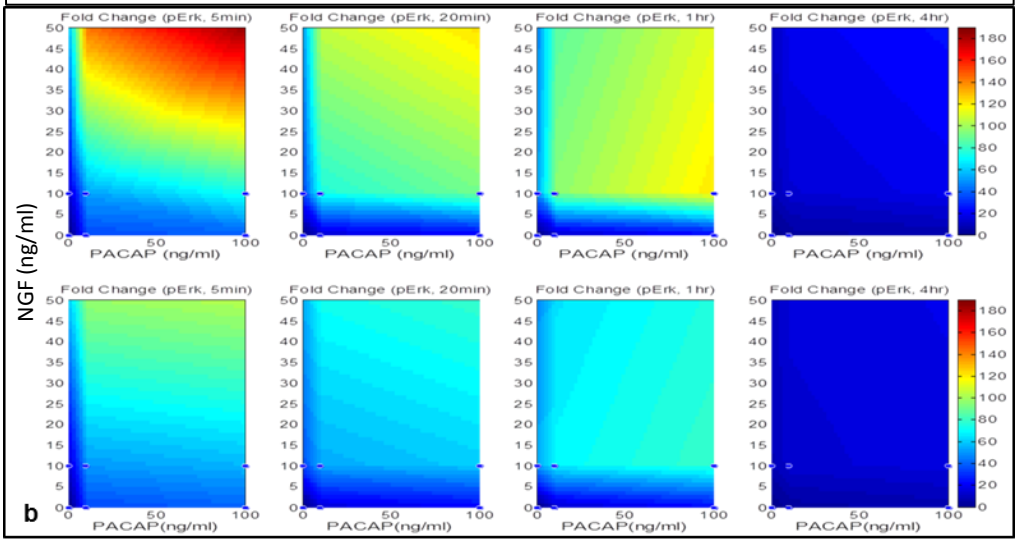
Fold Change (pErk, 5min)
Fold Change (pErk, 20min)
Fold Change (pErk, 1hr)
Fold Change (pErk, 4hr)
NGF (ng/ml)
PACAP (ng/ml)
b

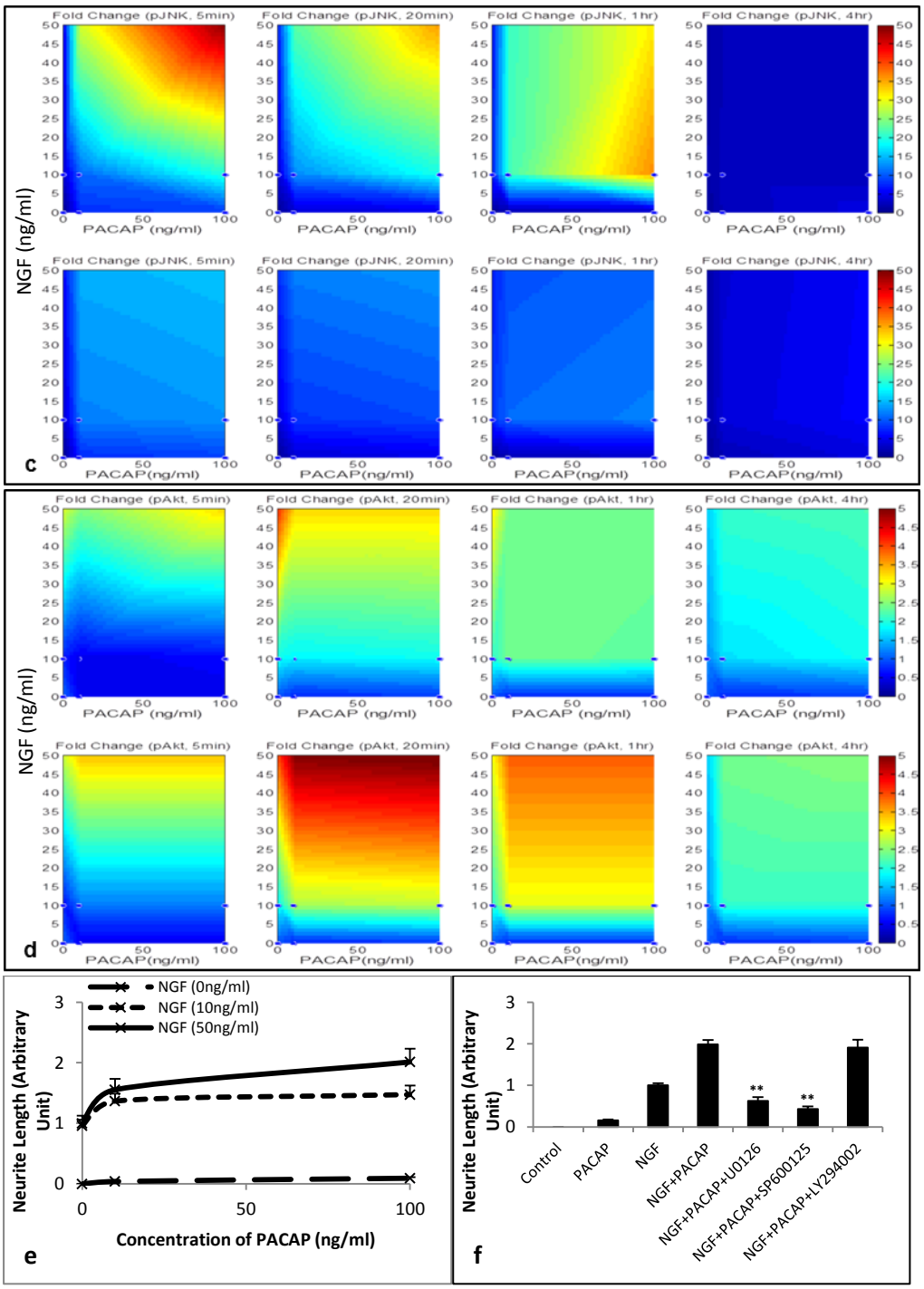

Figure 5.1. Synergistic and sustained phosphorylations of Erk and JNK upon NGF-PACAP treatment. (a) Time-course of Erk, JNK, and Akt phosphorylations from 0-4 hours following NGF (0-50 ng/ml)-PACAP (0-100 ng/ml) treatment. Phosphorylation levels of the proteins were analyzed by Western blotting, and normalized to the levels of Actin. Fold changes of (b) pErk, (c) pJNK, and (d) pAkt were quantified by densitometry and presented as colour plots. Top panel: Experimentally obtained results of the NGF-PACAP combinatorial treatment. Bottom panel: Additive effect calculated through the summation of the individual effects of NGF and PACAP. (e) Quantified neurite outgrowth upon NGF (0-50 ng/ml)-PACAP (0-100 ng/ml) treatment. (f) Effect of the MEK inhibitor, U0126 (20 μM), JNK inhibitor, SP600125 (10 μM), and PI3K inhibitor, LY294002 (20 μM), on neurite outgrowth induced by combinatorial NGF (50 ng/ml)-PACAP (100 ng/ml) stimulation. Significant differences between treatments with and without inhibitors were calculated using the paired Student's *t-test*. A value of $p<0.05$ was considered significant (**$p<0.01$).

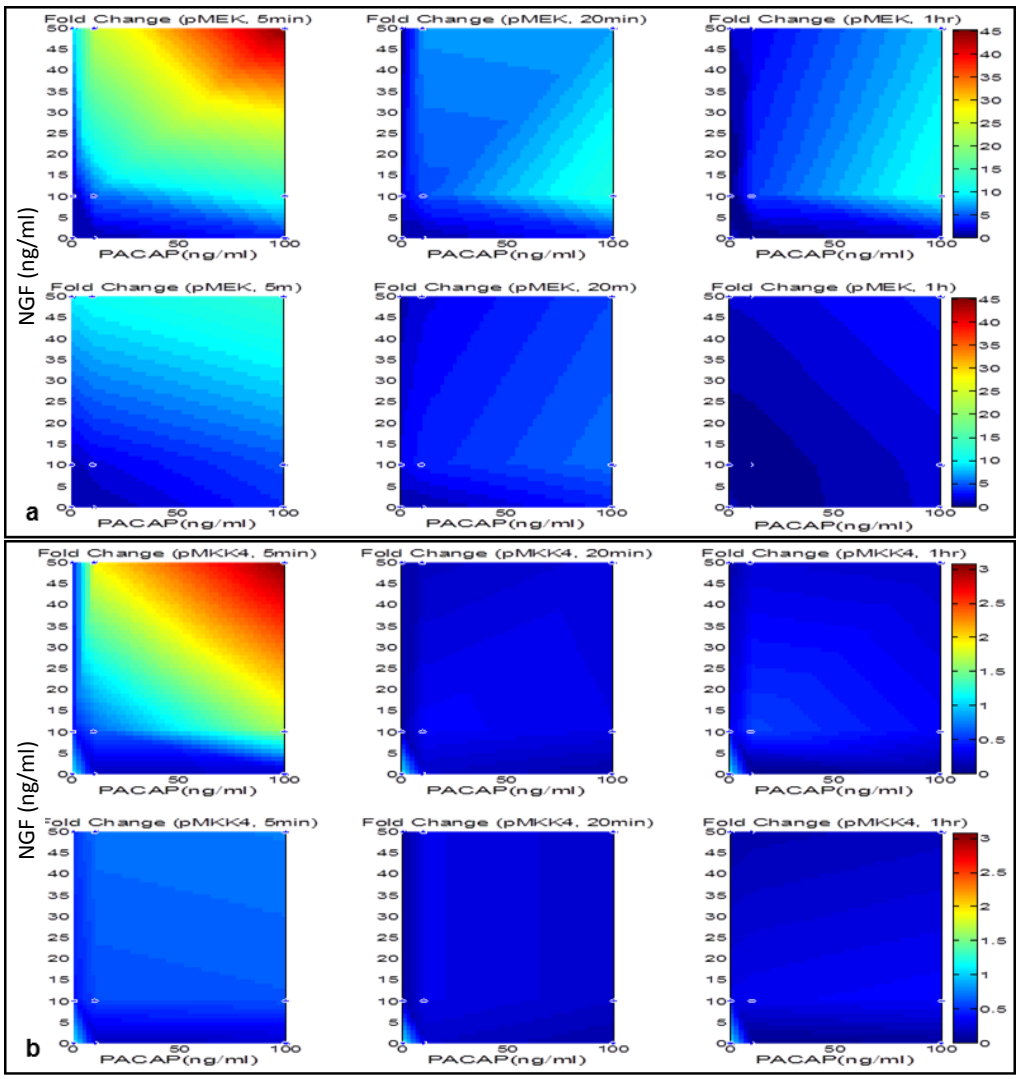

Figure 5.2. Synergistic and sustained phosphorylations of MEK and MKK4 upon NP treatment. Time-course of MEK and MKK4 phosphorylations from 0-1 hour following NGF (0-50 ng/ml)-PACAP (0-100 ng/ml) treatment. Phosphorylation levels of the proteins were analyzed by Western blotting, and normalized to the levels of Actin. Fold changes of (a) pMEK, and (b) pMKK4 were quantified by densitometry and presented as colour plots. Top panel: Experimentally obtained results of the NGF-PACAP combinatorial treatment. Bottom panel: Additive effect calculated through the summation of the individual effects of NGF and PACAP.

5.3.2. Network Inference Using TEEBM

Having identified that MEK, MKK4, and their downstream targets, Erk, and JNK, respectively, were all synergistically activated, we hypothesized that close regulations, such as cross-talks between the two MAPK signalling cascades, or feedbacks between them may be present. To test this hypothesis, Bayesian inference was employed to learn the most probable topological relationships between them.

While tvDBN and nsDBN approaches have been proposed to overcome the limitations of traditional DBN approaches, they were not suitable for our study. In these approaches, the structures are assumed to be piecewise-stationary in time, and non-stationary networks are built as a series of stationary models. These segmentations of points are also termed Bayesian multiple changepoint processes. Thus, the inference process involves learning of the location and number of changepoints as well as the network structure. Such approaches were designed for data with read-outs at an extensive number of time-points and are not feasible for our analysis, where the data available is limited. To tackle this issue, we used a DBN, expanded-in-time (eDBN), where protein activation levels at different time-points were considered as separate variables. This was accompanied by a two-phase learning approach to allow integration of data from uni- and bi-ligand stimulations using an exact learning method. Our two-phase approach allowed data integration to be performed in a way such that the probabilities of all the possible parent sets for all variables were first estimated using the data from the uni-ligand treatment. These probabilities were then used as a decomposable structure prior for the bi-ligand system to overcome the lack of *a priori* knowledge. Given that both the uni-ligand and bi-ligand treatments activated similar pathways, it was justifiable to use data from the uni-ligand treatment to infer a structure prior to facilitate the inference of the network during NP treatment.

The workflow of our learning methodology is as shown in Figure 5.3a. Following discretization of our data, the topological relationships between the different protein variables were learned using our proposed eDBN approach (Figure 5.3b). Network inferences using the same methodology but with the traditional BN (Figure 5.3c) and DBN (Figure 5.3d) approaches, were also

performed. In the literature of NGF- and PACAP-signalling in PC12 cells, it is well-known that neurite outgrowth induced by both ligands requires MEK activation[111,135,230]. Thus, in the inference of these networks, pMEK at the earliest time-point was constrained to be downstream of NGF and PACAP as *a priori* knowledge.

To validate that our inference approach was identifying the most probable network, probabilities of random networks were also evaluated using the eDBN approach. This was done while keeping the properties of the networks, such as the number of edges, and maximum number of parents, similar to our best-scoring network. A total of one billion randomizations were performed. The score distribution following structure randomization indicated that these resulting networks gave a much poorer explanation of our experimental data. The best network obtained using our methodology, with an eDBN approach, had a score of -81.6 whereas the scores obtained with randomized networks were much lower (Figure 5.3e). This provides justification that our learning algorithm had identified the network that can best explain our experimental observations and that randomized networks gave much poorer explanations of our experimental data.

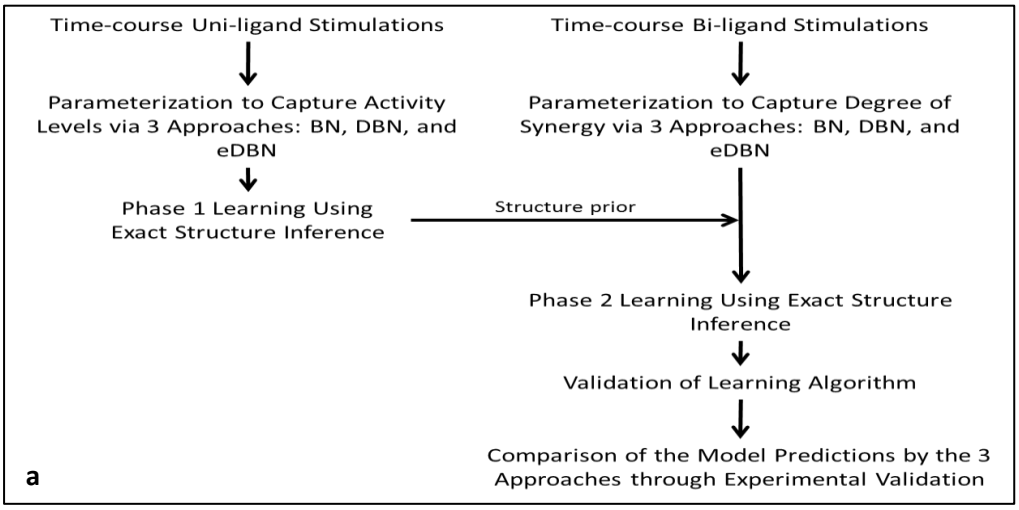

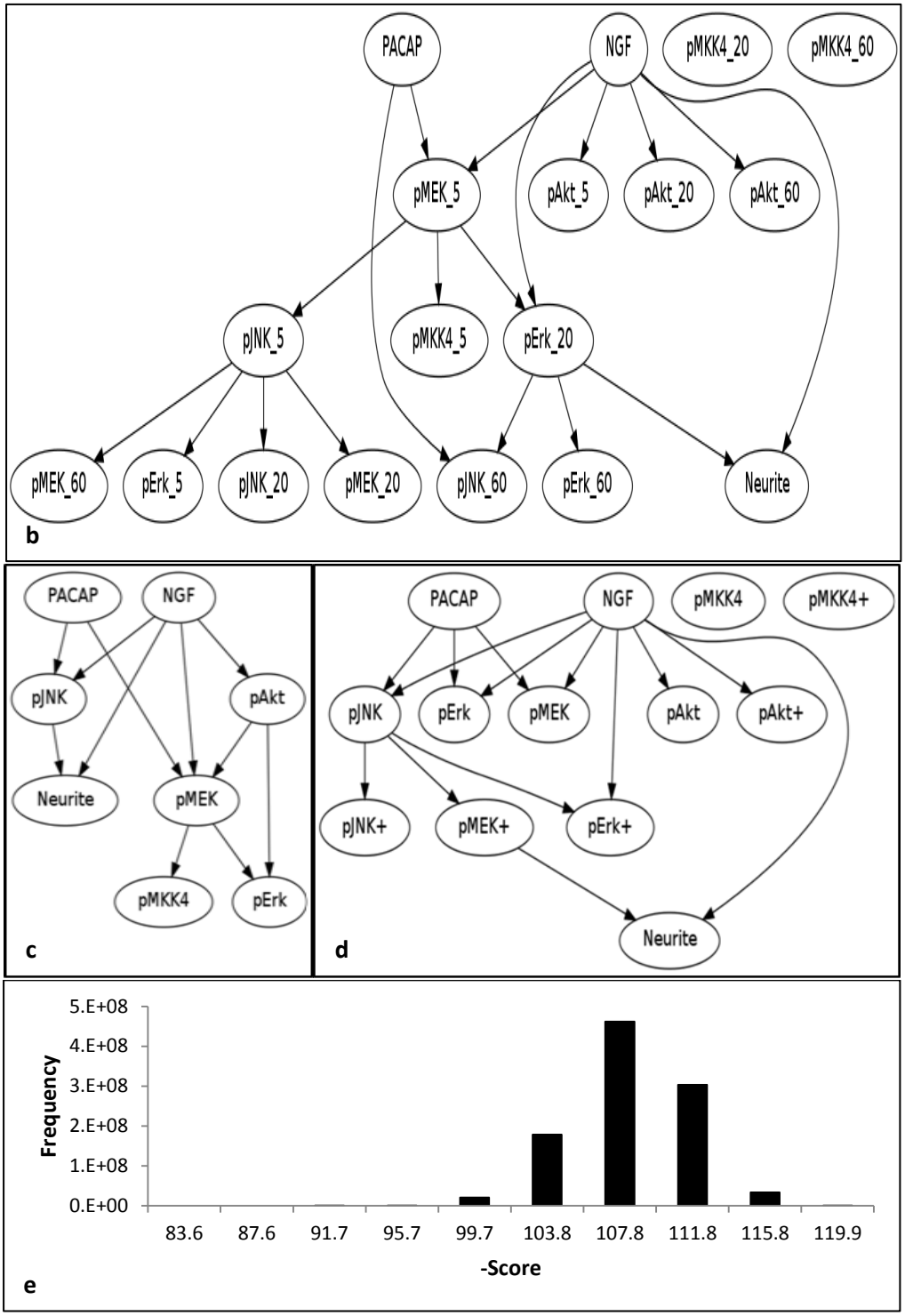

Figure 5.3. Application of proposed methodology for network inference using various Bayesian inference approaches. (a) Workflow of proposed Bayesian methodology. Inferred networks using (b) eDBN, (c) BN, and (d) DBN approaches (Variables with and without "+" are used to denote time t and t+1, respectively). Arrows between the variables represent directional influences between them. (e) Histogram illustrating distribution of network scores following one billion randomizations of the network.

It must be highlighted that our inferences here, without the use of interventional data, only resulted in a network of directional influences based

on statistical dependencies[344]. Using these dependencies between nodes, at the same time-points and across different time-points, we sought to determine the validity of these dependencies experimentally. Thus, our modeling methodology using an eDBN approach did not aim to describe the biological processes in a real-time manner. The dependencies identified using our methodology is summarized in Table 5.1.

Table 5.1. Statistical dependencies learned using our proposed methodology with the three approaches.

Method	eDBN	BN	DBN
Statistical Dependencies	MEK→JNK		
	MEK→MKK4	MEK→MKK4	
	MEK→Erk	MEK→Erk	
	Erk→JNK		
	JNK→MEK		JNK→MEK
	JNK→Erk		JNK→Erk
		Akt→MEK	
		Akt→Erk	

5.3.3. Validation of Predicted Edges Common to BN and eDBN

Comparing the networks inferred using our eDBN (Figure 5.3b) and the traditional BN (Figure 5.3c) approaches, two edges, MEK→Erk and MEK→MKK4, were present in both of them. To validate if these predictions were true, the cells were treated with NP in the presence of the MEK inhibitor, U0126. Consistent with the well-established knowledge that Erk is a downstream target of MEK[141], activation of Erk (Figure 5.4a) was inhibited in the presence of U0126. Similarly, U0126, which had previously been shown not to non-specially inhibit MKK4 and its downstream effector, JNK[345,346], also inhibited the activation of MKK4 (Figure 5.4b), suggesting that it is a downstream target of MEK.

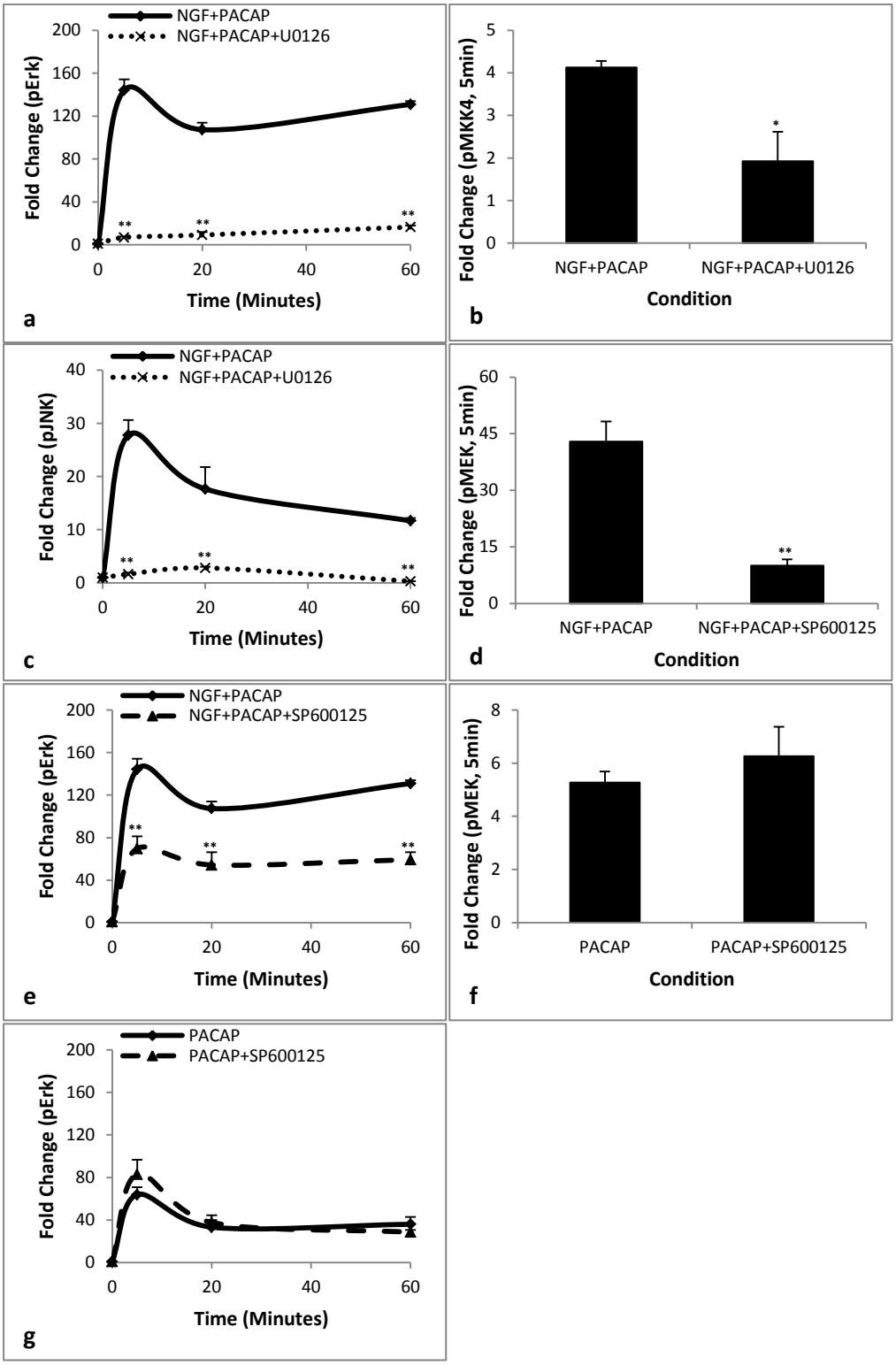

Figure 5.4. Validation of the model predictions made using our proposed methodology. The concentrations of NGF and PACAP used were 50 ng/ml and 100 ng/ml, respectively. Effect of the MEK inhibitor, U0126 (20 μM), on (a) pErk, (b) pMKK4, and (c) pJNK levels following NP stimulation. Effect of the JNK inhibitor, SP600125 (10 μM), on (d) pMEK, and (e) pErk levels following NP stimulation. Effect of the JNK inhibitor, SP600125 (10 μM), on (f) pMEK, and (g) pErk levels following PACAP stimulation. Significant differences between treatments with and without inhibitors were calculated using the paired Student's *t-test*. A value of $p<0.05$ was considered significant (**$p<0.01$; *$p<0.05$).

5.3.4. Validation of Predicted Edges Common to DBN and eDBN

Next, the network inferred using our eDBN (Figure 5.3b) was compared with that obtained using a traditional DBN (Figure 5.3d) approach. Both approaches predicted the edges, JNK→MEK and JNK→Erk, which were validated experimentally. Using the JNK inhibitor, SP600125, the phosphorylation levels of both MEK (Figure 5.4d) and Erk were inhibited (Figure 5.4e). These results were in agreement with previous studies in PC12 cells showing that inhibition of JNK blocks Erk activation[112]. Our results further suggested that this regulation of Erk by JNK occur through the upstream effector of Erk, MEK. The JNK inhibitor, SP600125, was not a non-specific inhibitor of Erk as treatment with SP600125 did not block both MEK (Figure 5.4f) and Erk (Figure 5.4g) activations by PACAP.

5.3.5. Validation of Edges not Predicted by eDBN, and Edges Predicted by eDBN but not by BN or DBN

The MEK→JNK edge was predicted by our eDBN approach but not by the traditional BN or DBN approaches. This was validated experimentally where inhibition of MEK using U0126 led to reduced phosphorylation of JNK (Figure 5.4c). This result further complements our finding that MEK is a regulator of MKK4 (Figure 5.4b).

From the inference results, Akt was found to be upstream of both MEK and Erk in the network learned through BN (Figure 5.3c) but not eDBN (Figure 5.3b). To determine the validity of these edges, cells were treated with NP in the presence of the PI3K inhibitor, LY294002. As expected, LY294002

inhibited the activation of Akt (Figure 5.5a) but not those of both MEK (Figure 5.5b) and Erk (Figure 5.5c). This indicates that the BN approach can result in false positives that were not inferred using the eDBN approach.

In the eDBN-inferred network (Figure 5.3b), both MKK4 and JNK were also not predicted to be downstream targets of Akt. These predictions were validated experimentally (Figures 5.5b, and 5.5d), where LY294002 did not reduce the phosphorylation levels of these proteins.

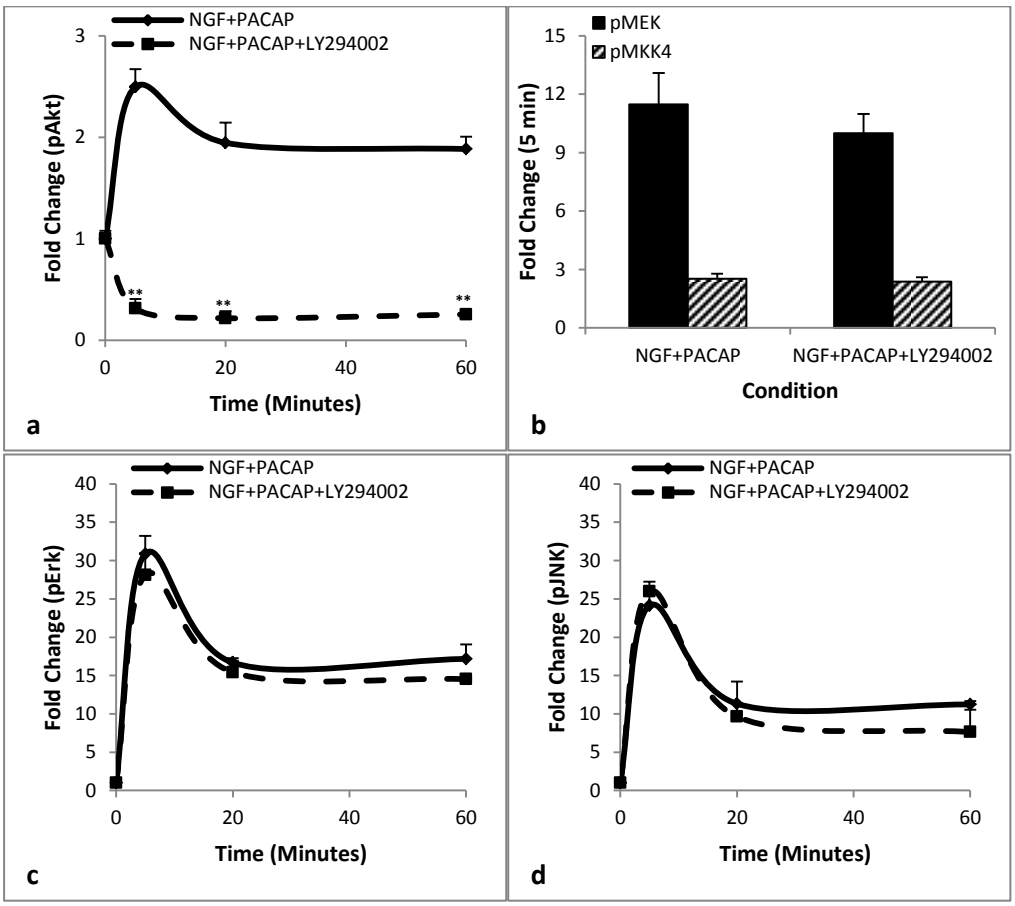

Figure 5.5. Non-involvement of Akt in the regulation of MEK, Erk, MKK4, and JNK. The concentrations of NGF and PACAP used were 50 ng/ml and 100 ng/ml, respectively. Effect of the PI3K inhibitor, LY294002 (20 μM), on (a) MEK and MKK4, (b) pErk, and (c) pJNK levels. Significant differences between treatments with and without inhibitors were calculated using the paired Student's *t-test*. A value of $p<0.05$ was considered significant (**$p<0.01$).

5.3.6. Positive Feedback Involving MEK, MKK4, Erk, and JNK

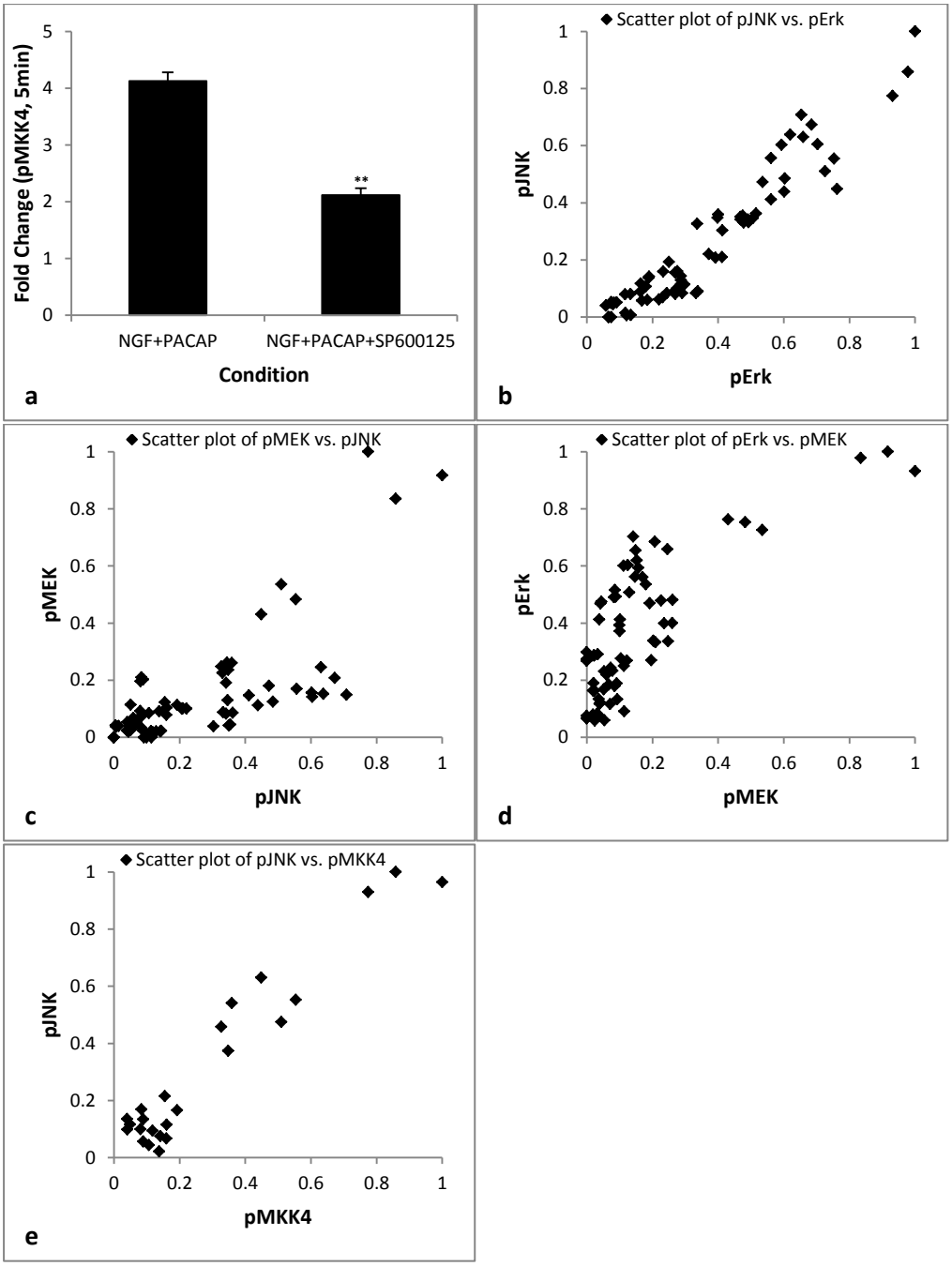

Figure 5.6. Existence of a plausible feedback loop involving MEK, Erk, MKK4, and JNK. The concentrations of NGF and PACAP used were 50 ng/ml and 100 ng/ml, respectively. (a) Effect of the JNK inhibitor, SP600125 (10 μM), on pMKK4 level. Illustration of a positive correlation between the 4 kinases via scatterplots of (b) pJNK vs. pErk, (c) pMEK vs. JNK, (d) pErk vs. pMEK, and (e) pJNK vs. pMKK4. Significant differences between treatments with and without inhibitors were calculated using the paired Student's *t*-test. A value of $p<0.05$ was considered significant (**$p<0.01$).

The edges that were predicted by our eDBN approach were experimentally validated as shown in the previous sections. Given that JNK regulates MEK, and that MEK regulates MKK4 and JNK, our result suggested a plausible positive feedback regulation involving MEK, JNK, and MKK4. If this is true, inhibition of JNK would also block the activity of MKK4. Consistent with our hypothesis, the phosphorylation level of MKK4 was reduced in the presence of SP600125 (Figure 5.6a). This was further complemented by scatterplot analyses (Figures 5.6b-5.6e), which indicated a positive correlation between all the kinases at all time-points. While these scatterplots do not indicate the presence of a loop, the positive correlations between the phosphorylation levels of the kinases are consistent with the findings of the inhibitors assays that the loop is positive in nature. In addition, the conditional probability distributions of the phosphorylation levels of the proteins indicated a positive dependency between the proteins across different time-points.

5.3.7. Arc-Weight Analysis

To further analyze the importance of the predicted edges in regulating the synergistic activation of the kinases, the relative importance of the various edges were determined. If these arcs, which are involved in the feedback loop, are important in explaining the synergistic activations of the four kinases, they should be relatively highly weighted in the network. To assess this weight, we determined the importance of a particular arc by determining the score of the resulting network after removing it. The scores of the networks with and without the arc were then compared. A larger score difference would indicate a higher relative importance of the arc. The relative weights of each arc are as shown in Figure 5.7, with a thicker arc indicating a

relatively higher importance. Investigating the weights of these arcs, edges such as JNK→Erk, MEK→JNK, and MEK→MKK4 were found to be relatively highly weighted, suggesting their importance in explaining our experimental data.

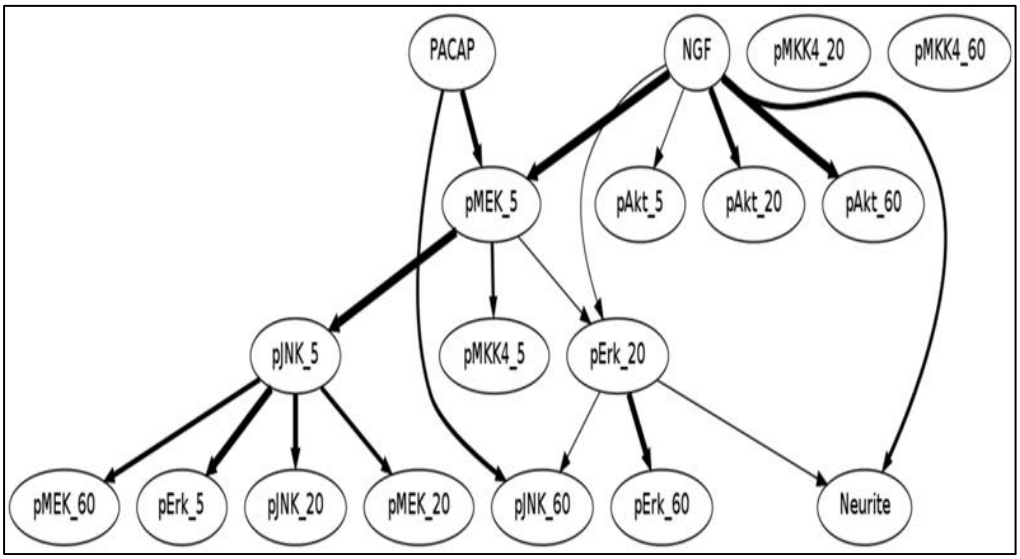

Figure 5.7. Arc-weight analyses of the eDBN network. Relatively strong strengths of the edges involved in feedback as compared to the other edges were obtained.

5.4. Discussions

In this work, we proposed a TEEBM, consisting of a two-phase learning strategy based on an exact structure learning algorithm[337], to infer a network where each protein at each time-point is considered as a separate variable. This Bayesian methodology allows integration of differently-parameterized data from different experimental set-ups, which are critical for the analyses of synergistic systems. In addition, the practicality of using an exact structure learning algorithm and advantages of using an eDBN approach was also demonstrated. In our study, we found that MEK and MKK4 were synergistically activated along with their respective downstream kinases, Erk and JNK, respectively. Applying our TEEBM to analyze the regulation between these kinases, our inference results identified a plausible feedback

loop, involving MEK, Erk, MKK4, and JNK, that contributed to their synergistic activations. This was validated experimentally, suggesting the potential of our TEEBM for network inference.

There are a variety of data-driven modeling techniques, such as Boolean networks, associated networks, neural networks, and BNs, which can be used for network inference[68]. A Boolean's representation of a network using logic gates is restricted as activity levels of the proteins cannot be sufficiently described using two states[86]. Associated networks are often limited as they cannot model dynamics, and are usually unable to capture directional influences[55]. In contrast, the topologies of neural networks are arbitrary in nature and no meaning should be inferred from them[50]. Thus, such models are not suitable for gaining mechanistic knowledge about the system. However, BNs are not impeded by these limitations. In addition, they can capture multivariate statistical dependencies, a dominant feature in biological networks, without having to specify the structure of any equations.

Although complex relationships can be modelled and analysed using BNs, they are not well suited for the analysis of temporal data[347]. DBNs were consequently proposed to overcome this drawback. However, the underlying assumption that the relationships between different nodes are invariant with time[348] is not valid for cellular systems as the complex regulatory mechanisms in biological networks result in neither static nor time-invariant topologies[77,78]. tvDBN and nsDBN, which work by demarcating time-series data into multiple segments, with each segment spanning different time-frames, were recently proposed to circumvent this issue[78,249,250]. However, such approaches are not applicable in situations where the data consist of only a small number of time-

points and an eDBN approach would instead be deemed more appropriate. Although the idea of eDBN had previously been employed[65], no comparison of the approach was made in relation to traditional BN or DBN approaches. As evident in our study, an eDBN approach performed better than traditional DBN and BN methods in the inference of the dependencies between the kinases. In the BN approach, for each variable, data across all time-points were grouped into one variable independent of the temporal effects. This can cause different relationships between the proteins at different time-points to offset each other, resulting in a misrepresented network. Likewise, for DBNs, data across all time-points were grouped into two variables, at time t and t+1. This inevitably results in the same drawback as BNs, which can be overcome with the use of eDBN. Thus, our results clearly demonstrated that the eDBN approach can overcome such a limitation and allow new influences to be learnt.

Data combination from multiple datasets is another area of challenge in systems biology. Various approaches, such as ordering of datasets[253] and multiple dataset integration[254], had been used to identify differentially expressed genes from multiple datasets. In the inferences of regulatory networks, approaches such as a weighted contribution of each dataset[255,256], use of mean and mode values of occurrences of each edge in the individual networks[257], and multi-objectives optimization to account for the nature of different experiments[258] had been employed to learn the optimal network. However, these inferences were all based on simple correlations, which have two main drawbacks. These methods work by identifying links between pairs of nodes without considering the context of the whole system[259] and they are also not effective in distinguishing between direct and indirect interactions[259].

These drawbacks were overcome using our TEEBM encompassing a two-phase learning approach. In addition, the problem of limited *a priori* knowledge of the NP system was alleviated, where data from the uni-ligand treatments was used to learn a structure prior, which was in turn used for inferring the most probable network during bi-ligand stimulation. Thus, our two-phase learning approach is a potential strategy that can be applied to datasets which require different parameterizations to capture different information present in different datasets, just like in the synergistic NP system in this study.

Using our TEEBM for network inference, we found a plausible positive feedback loop involving MEK, Erk, MKK4, and JNK in the regulation of synergistic neurite outgrowth. This is in congruence with previous reports[349,350], including during differentiation of PC12 cells[334,351], of a positive feedback between MEK and Erk. Similar to our model prediction, inhibition of MEK was found to block the activity of JNK[112,226,352]. In addition, synergistic behaviours arising from positive feedback had also been reported in other studies[246,353]. Our experimentally-validated finding of the regulation of MEK by JNK is, to the best of our knowledge, the first report establishing such a feedback across the two pathways during PC12 cells differentiation. This is plausible as both NGF and PACAP activate the MEK pathway. Upon NP treatment, a greater initial MEK activation is achieved, resulting in a more intensive activation of the pathway via feedback than that achieved by either ligand alone. However, our validations of the model predictions were based only on the use of inhibitors, which have drawbacks such as cytotoxicities[354] and non-specificities[346]. Validation of the predictions by the use of other

assays such as RNAi to reduce the contributions of each protein will invariably be useful.

Bayesian inference without interventional data only captures statistical dependencies that do not necessarily correspond to causal influences between variables[355]. Thus, established causalities, such as activation of JNK by MKK4[329], were not identified by our model. This can be explained by the finding that MEK can influence both MKK4 and JNK. As such, it can influence the activity of JNK independently of MKK4. Although our model predicts a feedback involving the four kinases, they were not found to exhibit similar activation profiles. Activations of Erk, JNK, and MEK were sustained whereas that of MKK4 was transient. One key mechanism that reduces the activity of kinases is dephosphorylation by protein phosphatases (PPs). PPs are known to act on MAPKs and MAPKKs[356], with each PP exhibiting different specificity for different kinases[357,358] and is distinctly localized in various cellular compartments[357-359]. Thus, investigating the localizations and activities of the PPs during NP treatment will allow a more detailed network analysis of the regulation of the kinases.

5.5. Conclusions

Our study has demonstrated the use of our proposed TEEBM in uncovering insights into the interactions between different signalling nodes in bi-ligand synergistic systems. Importantly, our approach consists of a two-phase learning strategy using an exact structure learning algorithm to infer a network using an eDBN parameterization. We used a two-phase learning approach to first estimate the BN structure distribution from the uni-ligand experiments, and then used the result as a prior to infer the network for the bi-

ligand case. The practicality of our approach was supported when the predicted feedback loop, with novel cross-talks between the MEK/Erk and MKK4/JNK pathways, was validated experimentally using kinase inhibitors. In performing these validations, our results also showed two other benefits of TEEBM. Firstly, the eDBN strategy performed better than traditional BN and DBN approaches. Secondly, the feasibility of an exact structure learning algorithm, which has not yet been applied to the analysis of cell signalling networks, for learning the optimal topological structure was demonstrated. However, TEEBM is limited to systems with less than 30 variables. Thus, this study has shown that TEEBM can be a potential tool for the analysis of signalling networks in synergistic systems and it can possibly be extended to analyses of other signalling networks in multi-ligand systems.

Chapter 6.

Expressions of IEGs and miRNAs during Synergistic Neurite Outgrowth in PC12 Cells

6.1. Introduction

Kinases are key regulators of cellular behaviours. They are the first signalling events utilized by cells upon stimulation with ligands. The effects of these activated kinases are mediated by their downstream protein, gene, and miRNA targets. In the earlier chapters, we have investigated the involvement of several kinases in the regulation of synergistic neurite outgrowth. Various combinations of the three kinases, Erk, JNK, and PKA were found to be important mediators of neurite outgrowth in the three synergistic systems, NP, FP, and EP. However, the downstream targets of these kinases that can mediate synergistic neurite outgrowth have not been well studied.

Kinases are well-known to regulate the expression of genes. These genetic responses can be broadly classified into two groups, immediate early genes (IEGs) and delayed response genes (DRGs)[360]. IEGs are induced as the first genetic response and are expressed within the first few hours after stimulation without any prior protein synthesis[361,362]. The proteins encoded by these IEGs are mainly transcription factors or regulators of signalling pathways, which are important mediators of cellular events and changes in phenotypes[363]. Many IEGs have been reported to be expressed following treatment with differentiation-inducing agents such as NGF and PACAP. During neuronal differentiation, IEGs such as Egr1[364-366], c-Fos[294], Btg2[367], Fosl[108], and Nr4a1[368] have been found to be involved in the process of neurite outgrowth.

Another important class of cellular components that is essential in the regulation of cellular functions is microRNAs (miRNAs). They are short non-coding hairpin-derived RNAs, which are ~20-24 nucleotides long[369] and they

regulate cellular behaviours by fine-tuning the expression levels of target genes. They post-transcriptionally repress the expression levels of these target messenger RNAs (mRNAs) by binding to their 3' untranslated region (UTR). In addition, complex regulatory relationships exist between miRNAs and mRNAs. It is now known that complex multiple-to-multiple regulatory relationships exist between miRNAs and mRNAs, where each miRNA can regulate multiple genes and each gene is regulated by multiple miRNAs[370]. To date, several miRNAs, such as miR-9[371], miR-21[372], and miR221[373], have been reported to regulate neuronal differentiation.

In this study, the regulation of several mRNAs and miRNAs by pathways involved in synergistic neurite outgrowth in the three synergistic systems, NP, FP, and EP, were investigated. This study revealed that these IEGs and miRNAs were differentially regulated in each system. This is the first report indicating an up-regulation of miR-487b-3p during neurite outgrowth. Moreover, a number of IEGs and miRNAs, which have previously been implicated in neurite outgrowth, were found to be regulated by the same pathways regulating neurite outgrowth in the corresponding system. While functional studies have yet to be performed, this study essentially identified the potential involvement of these genes and miRNAs in regulating synergistic neurite outgrowth.

6.2. Results

6.2.1. Regulation of Expression of IEGs during Synergistic Neurite Outgrowth

Many studies have previously been done to identify genes, including IEGs, expressed upon treatments with differentiation-inducing ligands such as NGF and PACAP[145,295,374-376]. Several IEGs, such as Egr1[364-366], c-Fos[294], Fosl[108], Nr4a1[368], BTG2[367], JunB[108], Arc[377], and Hes1[378,379] have previously been found to be involved in neurite outgrowth and sprouting. Investigating the regulation of these IEGs during synergistic neurite outgrowth, treatment with the growth factors and/or PACAP increased the expression of these genes (Figures 6.1a-6.1g), except for Hes1 (Figure 6.1h). This suggested that these up-regulated IEGs are likely to regulate synergistic neurite outgrowth.

In Chapters 3 and 4, distinct combinations of the kinases, Erk, JNK, and PKA, were found to be required for synergistic neurite outgrowth in different systems. In order to identify the downstream gene targets of these kinases, the expression levels of the up-regulated IEGs were quantified after inhibition of the kinases (Figure 6.2). The expression levels of these genes were normalized to RPL19, which has previously been reported to be stable during differentiation of PC12 cells[380]. Surprisingly, these genes were found to be regulated by different pathways in different systems.

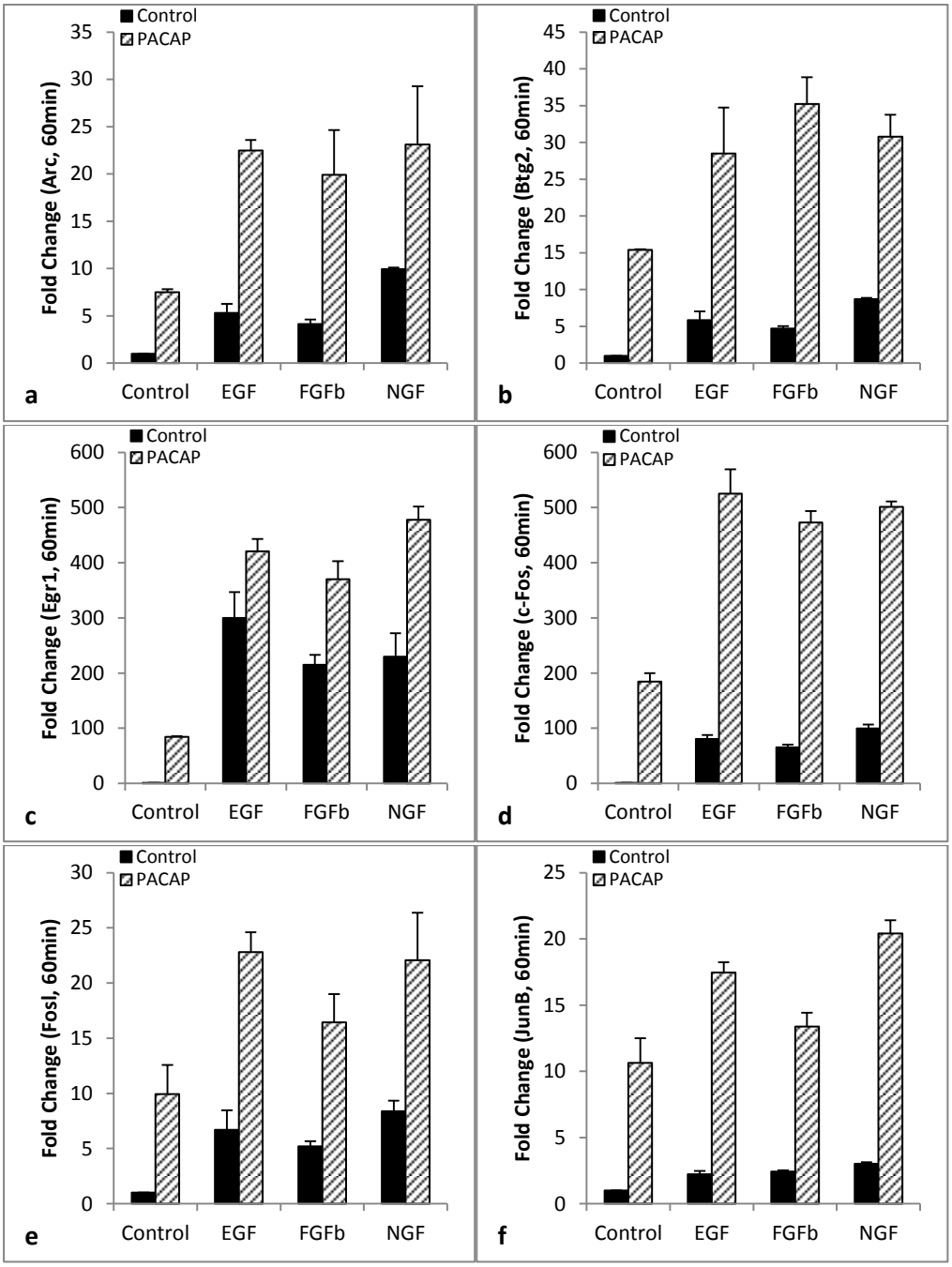
Control
PACAP
Fold Change (Arc, 60min)
Control EGF FGFb NGF
a
Fold Change (Btg2, 60min)
b
Fold Change (Egr1, 60min)
c
Fold Change (c-Fos, 60min)
d
Fold Change (Fosl, 60min)
e
Fold Change (JunB, 60min)
f

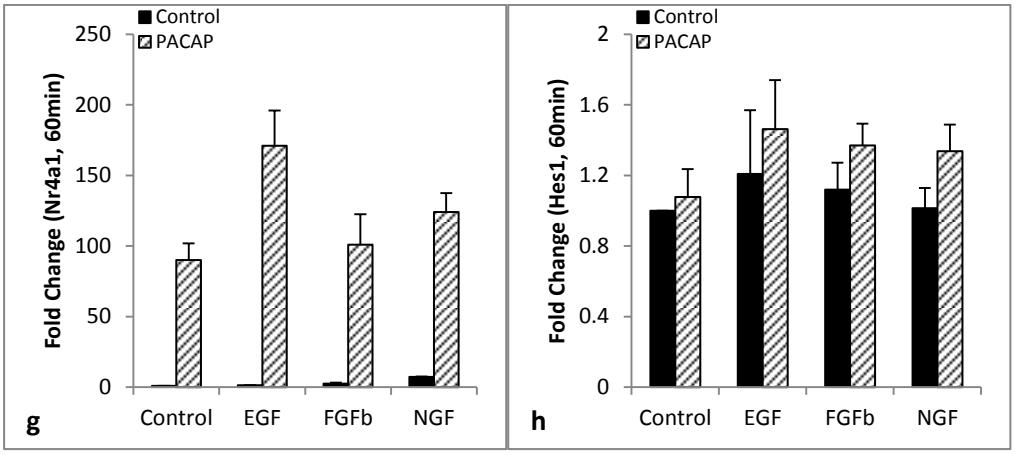

Figure 6.1. Activations of various IEGs following treatments with combinatorial growth factor-PACAP for 60 minutes. Expression levels of (a) Arc, (b) Btg2, (c) Egr1, (d) c-Fos, (e) Fosl, (f) JunB, (g) Nr4a1, and (h) Hes1 following treatments with 50 ng/ml of growth factor (EGF, FGFb, or NGF) and 100 ng/ml of PACAP.

To gain insights into the regulation of neurite outgrowth by these IEGs in different systems, a comparison of the pathways regulating neurite outgrowth and these IEGs was performed as shown in Tables 6.1 to 6.3. In the EP system, IEGs such as Btg2, Egr1, c-Fos, Fosl, and JunB could potentially be involved in the regulation of neurite outgrowth while all the measured IEGs could be involved in the process in the FP system. However, in the NP system, no conclusions of which IEGs were required for neurite outgrowth can be drawn as PKA, which was previously not found to be involved in neurite outgrowth (Chapter 4), regulated the expression all the measured IEGs. This strongly suggested that these IEGs did not function alone in the regulation of neurite outgrowth, and a more in-depth multivariate analysis of the IEGs would be necessary.

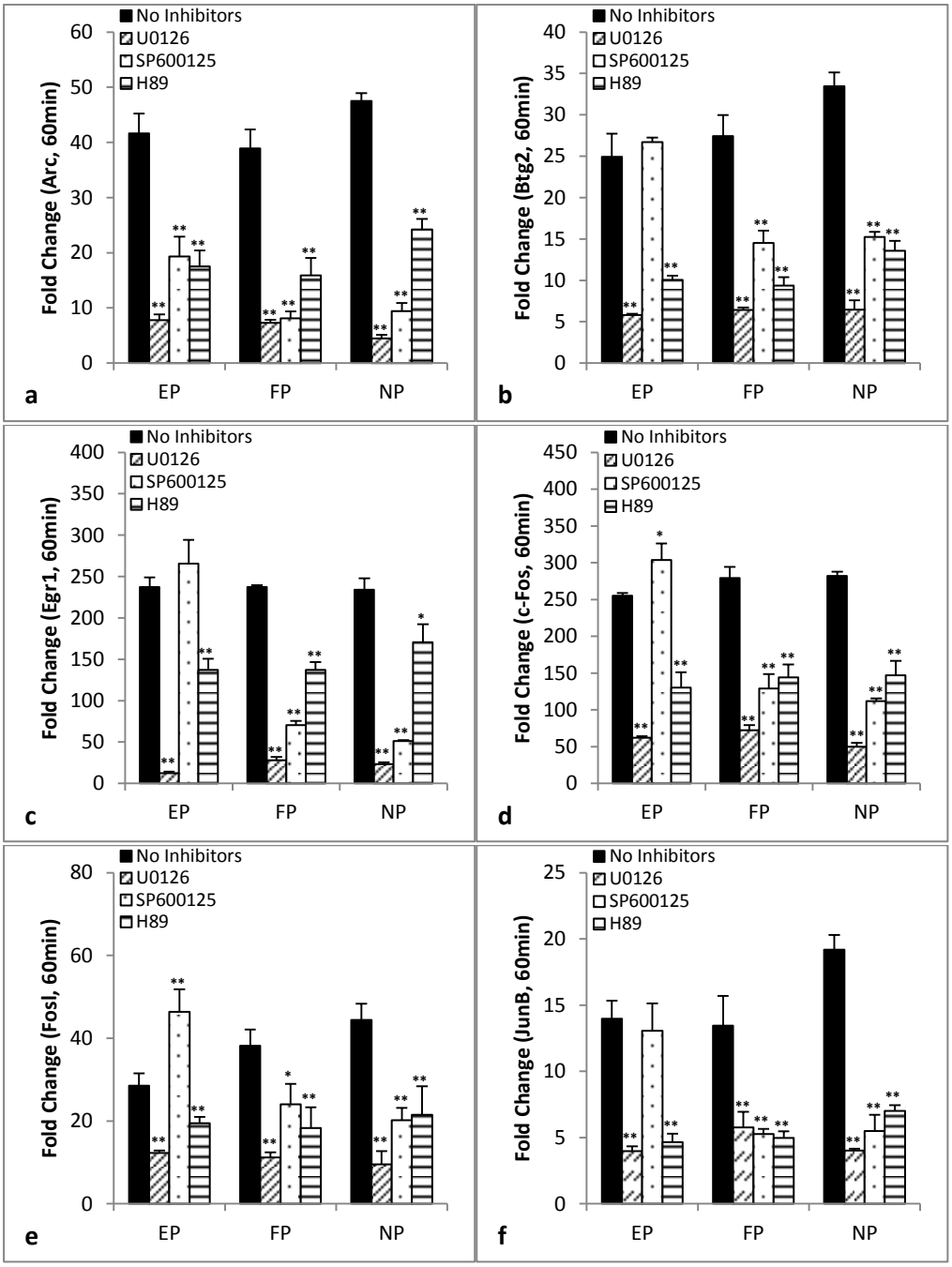
No Inhibitors
U0126
SP600125
H89
Fold Change (Arc, 60min)
Fold Change (Btg2, 60min)
Fold Change (Egr1, 60min)
Fold Change (c-Fos, 60min)
Fold Change (Fosl, 60min)
Fold Change (JunB, 60min)
EP
FP
NP
a
b
c
d
e
f

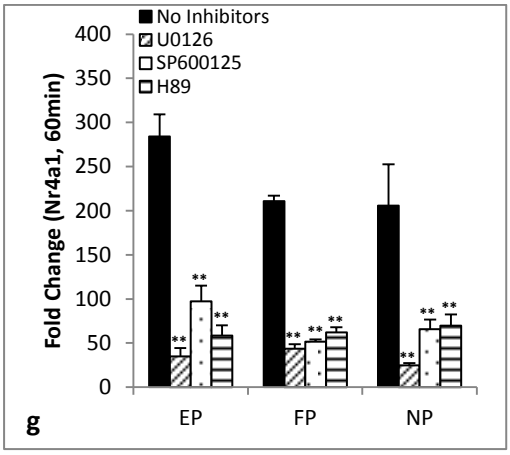

Figure 6.2. IEGs are differentially regulated by upstream kinases in the EP, FP, and NP systems. Expression levels of (a) Arc, (b) Btg2, (c) Egr1, (d) c-Fos, (e) Fosl, (f) JunB, (g) Nr4a1, and (h) Hes1 following treatments with 50 ng/ml of growth factor (EGF, FGFb, or NGF) and 100 ng/ml of PACAP for 60 minutes in the presence of the MEK inhibitor, U0126 (20 μM), JNK inhibitor, SP600125 (10 μM), or PKA inhibitor, H89 (10 μM). Significant differences between treatments with and without inhibitors were calculated using the paired Student's *t*-test. A value of $p<0.05$ was considered significant (**$p<0.01$; *$p<0.05$).

Table 6.1. Summary of the pathways involved in neurite outgrowth and the expression of various IEGs in the EP system. '+', '-', and '' denote positive, negative, and no regulation, respectively.

Kinase	Arc	Btg2	Egr1	C-Fos	Fosl	JunB	Nr4a1	Neurite
Erk	+	+	+	+	+	+	+	+
JNK	+			-	-		+	-
PKA	+	+	+	+	+	+	+	+

Table 6.2. Summary of the pathways involved in neurite outgrowth and the expression of various IEGs in the FP system. '+' denotes positive regulation.

Kinase	Arc	Btg2	Egr1	C-Fos	Fosl	JunB	Nr4a1	Neurite
Erk	+	+	+	+	+	+	+	+
JNK	+	+	+	+	+	+	+	+
PKA	+	+	+	+	+	+	+	+

Table 6.3. Summary of the pathways involved in neurite outgrowth and the expression of various IEGs in the NP system. '+', and '' denote positive, and no regulation, respectively.

Kinase	Arc	Btg2	Egr1	C-Fos	Fosl	JunB	Nr4a1	Neurite
Erk	+	+	+	+	+	+	+	+
JNK	+	+	+	+	+	+	+	+
PKA	+	+	+	+	+	+	+	

6.2.2. Regulation of Expression of miRNAs during Synergistic Neurite Outgrowth

Although many miRNAs have been studied for their roles in regulating various cellular behaviours, their involvements in the regulation of neurite outgrowth have not been well-studied. To date, several miRNAs, such as miR-9[371], miR-21[372], miR-34a[381], miR-128[382], miR-181a[383], and miR-221[373] have been reported to be required for neurite outgrowth. To identify the miRNAs that could be involved in regulating synergistic neurite outgrowth, a panel of fifty-eight miRNAs, including these six miRNAs, with potential functions in the brain[384-417] were profiled after stimulations with NP, EP, and FP. However, the expression levels of most of the profiled miRNAs were not changed (Table 6.4) and only four miRNAs, miR-21-5p, miR-221-3p, miR-382-5p, and miR-487b-3p were up-regulated (Tables 6.5 to 6.7). In all three systems, the expression levels of all four miRNAs were enhanced during combinatorial growth factor-PACAP treatments as compared to treatments with the individual ligands alone. The expression levels of all miRNAs were normalized to the mean expression value of all the profiled miRNAs[418].

Table 6.4. List of rno-miRNAs without changes in their expression levels from 1 hour to 48 hours upon NP, FP, or EP treatments. Concentrations of growth factors and PACAP used were 50 ng/ml and 100 ng/ml, respectively.

miRNAs	NP				FP				EP			
	1h	10h	24h	48h	1h	10h	24h	48h	1h	10h	24h	48h
List of 54 unregulated miRNAs	let-7a-5p, let-7b-5p, let-7d-3p, let-7f-5p, let-7i-5p, 9a-5p, 15b-5p, 16-5p, 17-5p, 19b-3p, 22-3p, 23a-3p, 24-3p, 26b-3p, 26b-5p, 27a-3p, 29b-2-5p, 29c-3p, 30b-5p, 30d-5p, 30e-3p, 30e-5p, 32-5p, 34a-5p, 92b-3p, 93-5p, 96-5p, 103-3p, 106b-5p, 107-3p, 125a-3p, 125a-5p, 126a-5p, 128-3p, 130a-3p, 133a-3p, 136-5p, 141-3p, 142-3p, 142-5p, 150-5p, 151-5p, 181a-5p, 181d-5p, 185-5p, 186-5p, 192-5p, 194-5p,199a-5p, 204-5p, 218a-5p, 340-5p, 378a-3p, 532-3p											

Table 6.5. Regulation of rno-miRNAs from 1 hour to 48 hours upon EP treatment. Concentrations of EGF and PACAP used were 50 ng/ml and 100 ng/ml, respectively.

miRNAs	PACAP				EGF				EP			
	1h	10h	24h	48h	1h	10h	24h	48h	1h	10h	24h	48h
Fold change of miR-21-5p	0.7	1.5	1.5	1.1	0.6	1.2	1.0	1.7	0.6	5.2	3.5	3.5
Fold change of miR-221-3p	0.6	0.1	0.4	0.6	0.1	0.3	0.6	4.2	0.1	0.4	1.4	17.1
Fold change of miR-382-5p	0.8	1.3	1.5	1.3	0.6	1.3	1.2	1.5	0.6	4.7	4.4	3.8
Fold change of miR-487b-3p	0.9	2.3	2.2	1.6	0.7	1.4	1.9	2.0	0.6	6.9	6.4	4.2

Table 6.6. Regulation of rno-miRNAs from 1 hour to 48 hours upon FP treatment. Concentrations of FGFb and PACAP used were 50 ng/ml and 100 ng/ml, respectively.

miRNAs	PACAP				FGFb				FP			
	1h	10h	24h	48h	1h	10h	24h	48h	1h	10h	24h	48h
Fold change of miR-21-5p	0.7	1.5	1.5	1.1	0.9	1.8	1.2	1.6	0.5	6.2	4.7	4.1
Fold change of miR-221-3p	0.6	0.1	0.4	0.6	0.3	0.8	3.3	53.2	0.1	0.8	6.4	67.8
Fold change of miR-382-5p	0.8	1.3	1.5	1.3	0.9	2.2	2.3	1.9	0.6	6.0	5.9	3.6
Fold change of miR-487b-3p	0.9	2.3	2.2	1.6	0.8	3.7	2.7	2.6	0.6	6.6	6.4	4.7

Table 6.7. Regulation of rno-miRNAs from 1 hour to 48 hours upon NP treatment. Concentrations of NGF and PACAP used were 50 ng/ml and 100 ng/ml, respectively.

miRNAs	PACAP				NGF				NP			
	1h	10h	24h	48h	1h	10h	24h	48h	1h	10h	24h	48h
Fold change of miR-21-5p	0.7	1.5	1.5	1.1	0.8	1.4	1.5	1.9	0.7	4.3	5.5	6.2
Fold change of miR-221-3p	0.6	0.1	0.4	0.6	0.3	1.3	4.0	137.6	0.2	0.6	4.5	221.3
Fold change of miR-382-5p	0.8	1.3	1.5	1.3	0.8	1.5	2.9	2.9	0.6	6.2	6.6	6.1
Fold change of miR-487b-3p	0.9	2.3	2.2	1.6	0.9	2.3	3	2.9	0.9	8.1	7.4	7.4

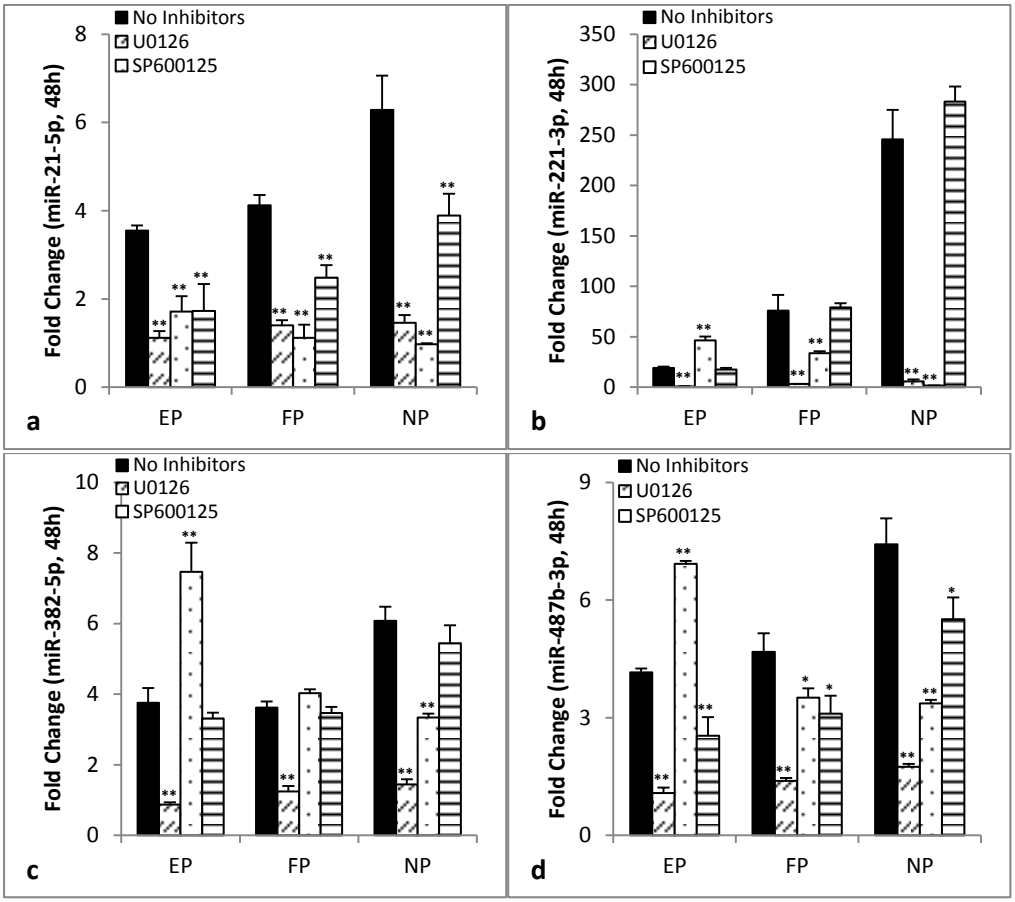

Figure 6.3. miRNAs are differentially regulated by upstream kinases in the EP, FP, and NP systems. Expression levels of (a) miR-21-5p, (b) miR-221-3p, (c) miR-382-5p, and (d) miR-487b-3p following treatments with 50 ng/ml of growth factor (EGF, FGFb, or NGF) and 100 ng/ml of PACAP for 48 hours in the presence of the MEK inhibitor, U0126 (20 μM), JNK inhibitor, SP600125 (10 μM), or PKA inhibitor, H89 (10 μM). Significant differences between treatments with and without inhibitors were calculated using the paired Student's *t*-test. A value of $p<0.05$ was considered significant (**$p<0.01$; *$p<0.05$).

Next, the pathways involved in the regulation of these miRNAs were analyzed similarly to that of the IEGs (Figure 6.3). To gain insights into the regulation of neurite outgrowth by these miRNAs in different systems, the pathways regulating neurite outgrowth and these miRNAs were compared as shown in Tables 6.8 to 6.10. In all three systems, miR-221-3p and miR-382-5p were likely to be involved in the regulation of synergistic neurite outgrowth as the same pathways regulated these miRNAs and neurite outgrowth in the respective system. On the other hand, while miR-487b-3p was possibly involved in neurite outgrowth in the EP and FP systems, miR-21-5p was likely to be required for the regulation of neurite outgrowth only in the FP system.

Again, this strongly suggested that the involvement of specific miRNAs in the regulation of neurite outgrowth was likely to be dependent on multiple factors, and a more in-depth multivariate analysis would be necessary to gain a better understanding of the process.

Table 6.8. Summary of the pathways involved in neurite outgrowth and the expression of various miRNAs in the EP system. '+', '-', and '' denote positive, negative, and no regulation, respectively.

Kinase	miR-21-5p	miR-221-3p	miR-382-5p	miR-487b-3p	Neurite
Erk	+	+	+	+	+
JNK	+	-	-	-	-
PKA	+			+	+

Table 6.9. Summary of the pathways involved in neurite outgrowth and the expression of various miRNAs in the FP system. '+', and '' denote positive, and no regulation, respectively.

Kinase	miR-21-5p	miR-221-3p	miR-382-5p	miR-487b-3p	Neurite
Erk	+	+	+	+	+
JNK	+	+		+	+
PKA	+			+	+

Table 6.10. Summary of the pathways involved in neurite outgrowth and the expression of various miRNAs in the NP system. '+', and '' denote positive, and no regulation, respectively.

Kinase	miR-21-5p	miR-221-3p	miR-382-5p	miR-487b-3p	Neurite
Erk	+	+	+	+	+
JNK	+	+	+	+	+
PKA	+			+	

6.3. Discussions

In this brief investigation, the expression of IEGs and miRNAs were profiled in the NP, FP, and EP systems to identify targets that could potentially be involved in the regulation of synergistic neurite outgrowth. While the profiled IEGs have previously been reported to be required for neurite outgrowth, most of the profiled miRNAs have not been implicated in neurite outgrowth. Surprisingly, only four out of the fifty-eight profiled miRNAs were up-regulated

significantly, and this is the first report indicating an up-regulation of miR-487b-3p during neurite outgrowth. Interestingly, these genes and miRNAs were regulated by distinct signalling pathways in different systems. Although the upstream kinases that regulated these genes and miRNAs may differ for each system, they were found to be regulated by the same pathways regulating neurite outgrowth in the corresponding system.

It is widely-known that expressions of IEGs are often regulated by multiple pathways[164,419]. Although a previous study has found that the functions of upstream kinases can be decoded by its downstream IEGs[420], our results demonstrated otherwise. The PKA pathway, which was required for neurite outgrowth in the FP, but not NP, system (Chapter 4), was found to regulate the same IEGs in both systems. This indicated that different cross-talks between these upstream kinases and other uninvestigated pathways are likely to be present in these systems[421]. This is supported by a previous study where different combinations of activated pathways were found to result in expressions of different subsets of genes in the same cell line[422]. Our results also showed that Erk and JNK co-regulated the expression of the IEGs in both the NP and FP systems. This not only further supports our finding that a feedback cross-talk exists between the Erk and JNK pathways in the NP system (Chapter 5), but also suggests that such a cross-talk could similarly exist in the FP system within the first hour of ligand stimulation.

While gene expression studies in PC12 cells during neuronal differentiation have been widely studied[145,295,371-373], much less are known about the expression of miRNAs levels during the process. miR-221 is currently one of the most well-studied miRNA during neurite outgrowth[373,407], and functional

validation of its role in regulating neurite outgrowth in PC12 cells has also been performed previously in the lab. In addition, it has been reported to be regulated by sustained activation of Erk during neurite outgrowth in PC12 cells[373]. Consistent with these findings, miR-221 was found to be highly expressed and regulated by Erk in all three systems after 48 hours of stimulation. In addition, it was also found to be regulated by JNK but not PKA in all three systems in this study, further indicating its importance in neurite outgrowth. Thus, given that PKA alone, which was activated by PACAP, is a poor inducer of neurite outgrowth[290] (data not shown), our data indicated that PKA interacts with other signalling pathways, rather than Erk or JNK, in enhancing neurite outgrowth in the synergistic systems. Further investigations of the cross-talks between the signalling responses downstream of receptor-tyrosine-kinases (RTK) and G-protein-coupled-receptors (GPCR) is likely to yield insights into the underlying mechanism of such a cross-talk[423,424]. In addition, miR-221 has also been predicted and validated to target PTEN[425], which is a negative regulator of neurite outgrowth in PC12 cells[426,427]. Thus, the possibility that miR-221 enhances neurite outgrowth in the synergistic systems by acting on PTEN needs to be explored further.

In this work, miR-487b-3p was another miRNA found to be up-regulated in all three systems. While it has not been previously reported to be required for neurite outgrowth, it has been shown to be enriched in the neurons in the central nervous systems (CNS) of rats[417]. Thus, it is likely that miR-487b-3p plays a role in neuronal functions and its involvement in neurite outgrowth requires further investigations.

Among the fifty-eight profiled miRNAs, the changes in expression levels for fifty-four of them were relatively small. This could indicate either a lack of regulation or a minute change in their expression levels, which is a characteristic of miRNAs[428-430]. This is because the regulatory relationships between genes and miRNAs are multiple-to-multiple in nature, where each miRNA can regulate multiple genes and each gene is regulated by multiple miRNAs[370]. It has also been increasingly recognized that extracellular miRNAs could be involved in cell-to-cell communication and may have functional relevance in cellular behaviours as they are protected from degradation by extracellular RNases[431]. In addition, extracellular miRNAs have been found to be packaged differently, such as microvesicles, exosomes, or RNA binding proteins such as Ago2, under various conditions, indicating that multiple roles of extracellular miRNAs can exist[432,433]. Thus, investigations of the extracellular miRNAs during synergistic neurite outgrowth may lead to a more in-depth understanding of the importance of miRNAs in this process.

Given that the regulation of synergistic neurite outgrowth is a complex process with a differential regulation of the same genes and miRNAs in different systems, a Bayesian approach such as TEEBM (Chapter 5) can be used to analyze the signalling networks in these systems. The different network structures and conditional probabilistic relationships between the variables will give a depiction of the differences in the signalling mechanisms between different systems in the regulation of neurite outgrowth.

6.4. Conclusions

This study has identified up-regulated IEGs and miRNAs upon combinatorial growth factor-PACAP treatment, which could potentially be involved during synergistic neurite outgrowth. Our data showed that these genes and miRNAs are regulated by different combinations of pathways in each of the three systems, indicating that yet to be discovered cross-talks are likely to be present. While fifty-eight miRNAs were profiled, only four was found to be differentially expressed in the synergistic systems, suggesting that investigation of extracellular miRNAs may yield more insights into the roles of miRNAs in regulating neurite outgrowth. This is also the first study that reports an up-regulation of neuron-enriched miR-487b-3p during neurite outgrowth. Further studies on other signalling pathways and functional validation of the up-regulated IEGs and miRNAs would be required to ascertain their involvement in synergistic neurite outgrowth. This can be complemented by network analyses to shed light on the combinatorial involvement of these kinases, genes, and miRNAs in regulating the process.

Chapter 7.

Conclusions and Future Works

7.1. Conclusions

Although traditional reductionist approaches to the analyses of cell signalling are important in gaining a fundamental understanding of cell signalling, the underlying principle of reductionism poses significant limitations. First, analyses of signalling mechanisms have been carried out through the analyses of individual signalling components, which fail to account for emergent behaviours that can only arise from interactions between these components but not by any constituent parts alone[21,23]. Second, many experiments are performed using only one ligand, which is not physiologically relevant as cells are exposed to multiple stimuli concurrently in their biological microenvironments[26,27]. To better understand cellular behaviours, systems-based approaches that analyze signalling components in a multivariate setting under multi-ligand experimental conditions are needed. In particular, modeling methods that can effectively analyze multi-ligand synergistic systems are very much lacking.

In this thesis, an attempt was made to develop tools for the multi-variant analyses of the effects of multiple sets of ligands on the perturbation of a limited number of known signalling nodes involved in neurite outgrowth. This study is a proof-of-concept that a tractable solution for identifying the dynamics of cell signaling, by analyses of such complex interactions using a modified Bayesian approach, is possible. Hence, the mechanism underlying synergistic neurite outgrowth during PC12 cells differentiation was investigated with the aid of a modified Bayesian network inference approach. The signalling pathways involved in synergistic neurite outgrowth in three different systems, NP, FP, and EP, in PC12 cells were investigated. The

morphological changes upon these treatments include more neurite extensions from the cell-body, more branching of neurites, and an increase in the length of each neurite. Collectively, these changes resulted in synergistic enhancements of total neurite length. An overview of the findings presented in this thesis is illustrated in Figure 7.1.

Five signalling pathways widely reported to be required for neurite outgrowth in PC12 cells, Erk[164,165], JNK[112,164], P38[113,173], Akt[163], and PKA[222], were studied. The synergistic regulation of total neurite length in the three systems was found to be regulated by distinct signalling pathways. In the NP system, only the Erk and JNK pathways were found to positively regulate neurite outgrowth whereas the Erk, JNK, and PKA pathways were required for the process in the FP system. On the contrary, neurite outgrowth in the EP system was positively regulated by Erk and PKA but negatively regulated by JNK. Importantly, the involvement of these pathways in positively regulating synergistic neurite outgrowth was found to be mediated by P90RSK, indicating that P90RSK could be a critical component in the regulation of the process. This is consistent with previous studies where P90RSK was found to mediate differentiation of PC12 cells[219,276,277]. Critically, this is the first study that implicated P90RSK as a downstream effector of both JNK and PKA in the regulation of synergistic neurite outgrowth in PC12 cells. The finding of the differential regulation of P90RSK in the NP, FP, and EP systems in this thesis strongly suggests that these synergistic systems can serve as excellent models to decipher the mechanistic regulation of P90RSK by its upstream kinases, Erk, JNK, and PKA.

In a brief extension of the study, the potential IEGs and miRNAs that can mediate the effects of the upstream kinases in regulating synergistic neurite outgrowth were also investigated. These genes and miRNAs were found to be regulated by different combinations of signalling pathways in each of the three systems, suggesting that yet to be discovered cross-talks between upstream signalling pathways are likely to be present. miR-487b-3p, which has not been previously reported to be involved in neurite outgrowth, was found to be up-regulated during neurite outgrowth. In addition, several IEGs and miRNAs, which have been previously implicated in neurite outgrowth, were found to be regulated by the same pathways regulating neurite outgrowth in the corresponding system. Thus, genes and miRNAs potentially involved in the regulation of synergistic neurite outgrowth were identified.

To gain a deeper understanding of synergistic neurite outgrowth, the morphology of the neurites was investigated more comprehensively in terms of the various morphological changes governing neurite outgrowth. Various studies have demonstrated that the distinct morphological features of neurites can be regulated both independently of different pathways as well as by the same pathways. Both mechanisms were observed in this study. For instance, pathways that positively regulate the total neurite length, such as Erk, JNK, and PKA, also positively regulated the number of neurite extensions, number of branch-points, and the length of the individual neurites. However, P38 was found to positively regulate the branching of neurites without affecting the total neurite length. This is the first study demonstrating that P38 can regulate neurite branching independently of total neurite length during differentiation of PC12 cells in the NP and FP systems. All in all, the current understanding of neurite outgrowth is still very limited, and PC12 cells can serve as an

excellent model to understand the distinct regulation of different morphological features of neurites.

The mechanism underlying the synergistic activations of Erk and JNK in the NP system was further investigated using a systems-based mathematical modeling approach. Given the lack of approaches for the analyses of multi-ligand synergistic systems, a modified Bayesian methodology for network inference was proposed to infer novel regulatory behaviours governing the synergistic activation of the two kinases. This methodology was termed TEEBM (Two-phase, Exact structure learning, Expanded-in-time Bayesian Methodology). It comprises of three distinct elements. First, an expanded-in-time DBN (eDBN) parameterization was used to define the signalling nodes and it overcomes the limitations of traditional DBN approaches where the relationships between different variables are assumed to be time-invariant. Second, a two-phase learning was used to incorporate the different information content obtained from the single- and bi-ligand experiments. This data integration technique was facilitated by the use of a binning procedure that can capture different information from different experimental conditions. Information on activation levels and degree of synergism was extracted from the single- and bi-ligand experiments, respectively. Third, an exact structure learning algorithm[269] was used for structural learning of the network as it can overcome the drawbacks arising from the non-exhaustive nature of widely used approximate search methods. Using this approach, a novel positive feedback between the MEK/Erk and MKK4/JNK signalling pathways was found to mediate the synergistic activations of Erk and JNK. This model prediction was validated experimentally. Thus, this work demonstrates the potential of the proposed TEEBM in the analysis of signalling networks in bi-

ligand synergistic systems, and it can potentially be extended to the analyses of other multi-ligand systems.

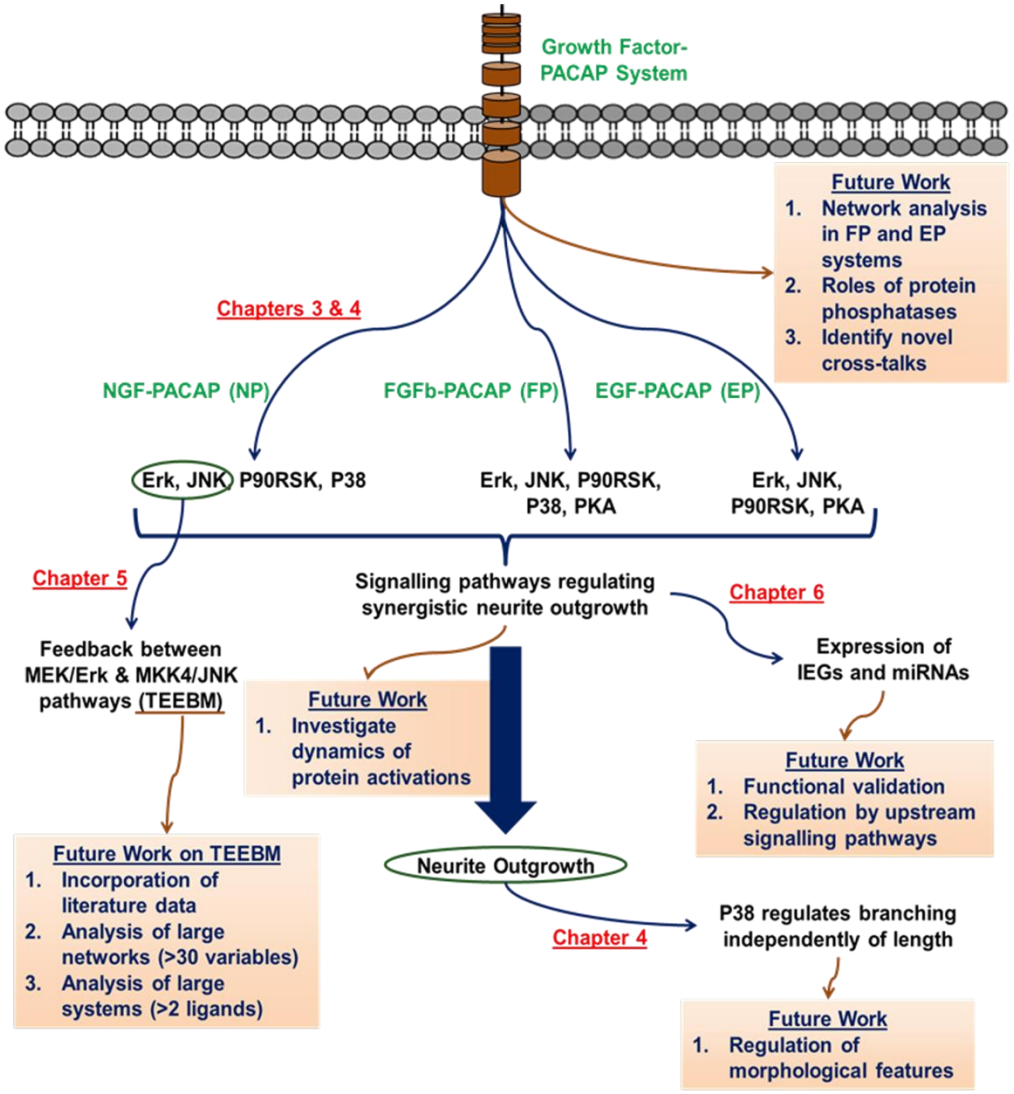

Figure 7.1. Overview of findings in this thesis and recommendations for future works.

7.2. Future Works

Although the work presented here have made some contributions to the field of both neuronal differentiation and systems biology, both areas are still in its infancy with many avenues for further development. This is especially true in light of the analysis of synergism. The study of synergism constitutes a multivariate analysis of the interactions between cellular components, which

requires the use of mathematical models. This essentially constitutes a cyclic loop between the biological issues to be addressed in synergism and the use of appropriate mathematical models to facilitate the process (Figure 7.2). Thus, the availability of suitable mathematical models will be the key to driving the advancements in the understanding of synergism in neuronal differentiation. Although the ideal next step is to further validate the TEEBM presented in this thesis, the lack of *a priori* knowledge about signalling mechanisms underlying synergistic behaviours in bi-ligand systems in the biological literature render such a task impractical. Instead, further validation of this TEEBM can go in conjunction with further employments of the model in understanding neuronal differentiation. As such, the recommendations for future works (Figure 7.1) are centered, where appropriate, on the applications and developments of TEEBM.

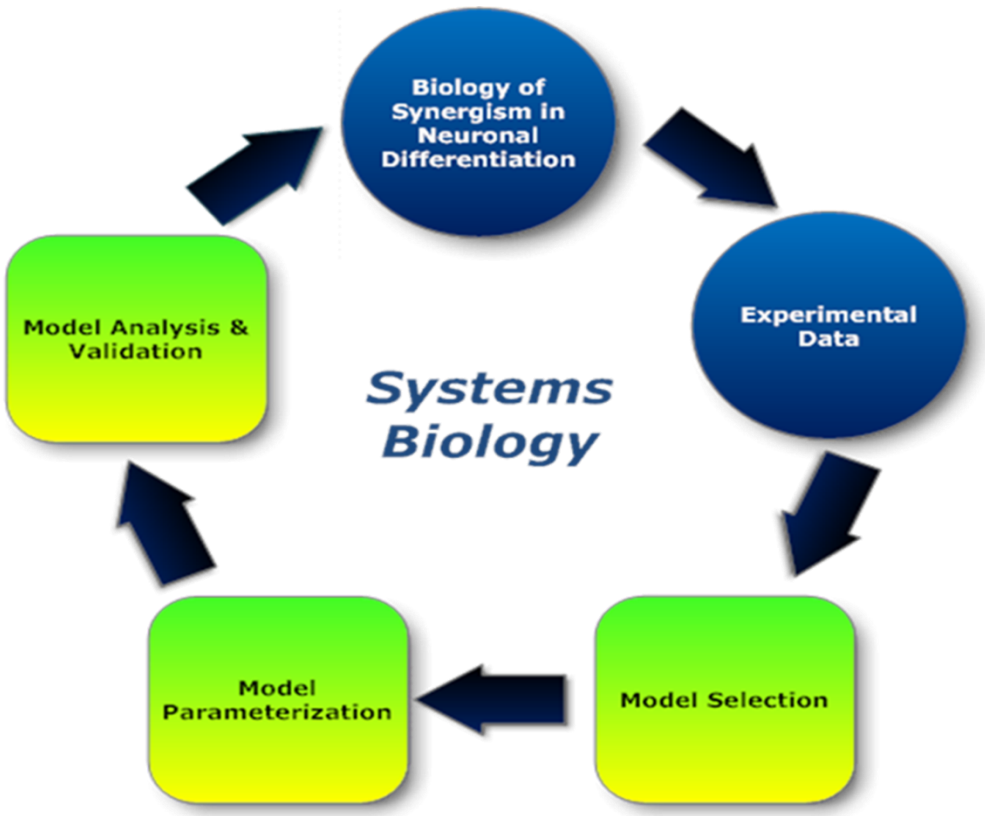

Figure 7.2. Cyclic loop between mathematical modeling and biological advancement in neuronal differentiation.

7.2.1. Application of TEEBM in Understanding Synergistic Neurite Outgrowth

7.2.1.1. Network Analyses of Signalling Pathways Regulating Neurite Outgrowth in the FP and EP Systems

As a subset of signalling pathways involved in the regulation of total neurite length had each been determined for the FP, and EP systems (Chapters 3 and 4), TEEBM can be applied to these systems to gain insights about the underlying signalling networks. In these two systems, the combinations of the pathways regulating neurite outgrowth are both different from that of the NP system. This differential involvement of signalling pathways is likely to result from different activation profiles and interactions between signalling pathways[434]. Thus, these systems serve as valuable platforms that can be used for further validation or refinement of the TEEBM to ensure that pathway cross-talks and signalling responses of different nature can be captured.

7.2.1.2. Investigation of the Differential Involvement of Signalling Pathways in Regulating Neurite Outgrowth in the NP, FP, and EP Systems

In each of these synergistic systems, NP, FP, and EP, different combinations of signalling pathways are involved in the regulation of different aspects of morphological neurite outgrowth (Chapters 3 and 4). Preliminary work has also indicated that different combinations of pathways are involved in the expression and regulation of IEGs and miRNAs potentially required for synergistic neurite outgrowth in these systems (Chapter 6). Furthermore,

these targets were found to be regulated by pathways which are both required and not required for neurite outgrowth. These results strongly suggest that the determinant of the involvement of various signalling pathways in the regulation of synergistic neurite outgrowth is likely to lie in the combinatorial regulation of their downstream effectors, such as IEGs and miRNAs.

Thus, it would be important to first functionally validate the roles of various IEGs and miRNAs in regulating neurite outgrowth. After which, a network analyses should be centered on these signalling components and kinases to understand how they regulate neurite outgrowth in a combinatorial manner. Unraveling such complexities will be critical to the field in two ways. First, downstream components, which are more oriented to the regulation of neurite outgrowth, can be uncovered. This is of great relevance as upstream signalling components are involved in the regulation of a broader range of cellular behaviours. Second, the context under which specific interactions can occur in one system but not another can provide insights into novel signalling mechanisms, which is highly relevant to many different fields of biology.

A BN approach, such as TEEBM, is a practical solution to this problem as a key aspect of BNs is the use of conditional independence in defining the relationships between different variables. This idea of conditional independence can provide the context, such as activation of a particular signalling component, within which a particular interaction is present or relevant and if the interaction is positive or negative in nature.

7.2.1.3. Role of Protein Phosphatases in Regulating the Synergistic Activations of Erk and JNK

It was shown in this thesis that synergistically-activated kinases can potentially regulate the enhancement of neurite outgrowth. The regulation of the synergistic activations of MEK/Erk and MKK4/JNK in the NP system was found to be mediated by a positive feedback loop between these pathways (Chapter 5). Given that there are distinct signalling pathways activated by the two ligands, it would be interesting to investigate if other cross-talks downstream of these two different receptor systems can also play a part in the synergistic regulation of these kinases. For instance, cAMP, a key effector of PACAP, can activate PKA and Epac[135]. Both PKA[435,436] and Epac[437,438] are known to regulate various protein phosphatases (PPs), which are key components in the down-regulation of the activity of protein kinases. PPs are known to act on MAPKs and MAPKKs[356], with each PP exhibiting different specificity for different kinases[357,358] and each distinctly localized in various cellular compartments[357-359]. Thus, down-regulation of these PPs can be another mechanism through which synergistic activations of the Erk and JNK pathways can occur. It would be interesting to further investigate the localizations and activities of the PPs in these systems at a systems-level to gain a more comprehensive understanding of the regulation of these kinases.

The TEEBM presented in this thesis will be useful in predicting the combinatorial effects of different PPs and identifying the points of interactions between these PPs and kinases. This is because MAPK signalling cascades, such as Erk and JNK, are multi-tiered, and there are multiple points along these cascades where different PPs can exert their effects.

7.2.1.4. Identification of Novel Interactions between the Growth Factor and PACAP Signalling Systems

Besides the signalling pathways investigated in this thesis (Chapters 3 and 4), many signalling pathways have also been found to be required for differentiation of PC12 cells. For instance, other pathways activated by the growth factors and PACAP include PLC[439-441], PKC[133,199,442], Src[112,223,225,443], and Erk5[221]. These pathways have been frequently studied in many cellular systems and cross-talks among them[134,444], as well as those that were investigated in this thesis, have been reported. Given that synergistic behaviours occur due to interactions between signalling pathways, it is very plausible that some of these interactions are also critical to the regulation of synergistic neurite outgrowth. As demonstrated in this thesis, the potential points of cross-talks between these signalling pathways can be learned using the TEEBM.

7.2.1.5. Investigation of the Dynamics of Protein Activity in Relation to Neurite Outgrowth

It is now increasingly evident that the dynamical profiles of signalling nodes are critical in governing cellular behaviours. For instance, sustained activation of Erk is critical for neurite outgrowth (Chapter 3), which is consistent with the literature[132,169]. Although any signalling component may be activated over a wide duration of time in these synergistic systems, it is likely that only a specific time-window may be relevant to its regulation of neurite outgrowth. This essentially implies that the relationships between signalling nodes are not time-invariant, a property of cellular systems that has been emphasized in this thesis[77,78]. Thus, while more pathways and signalling mechanisms

regulating synergistic neurite outgrowth are identified, it is just as critical to identify the time-window relevant to the process. In the TEEBM presented in this thesis, an eDBN parameterization was central to the proposed method. It can be used for the analyses of dynamical relationships that are not time-invariant. In addition, its practical usage is not restricted to BNs alone and can be extrapolated to many other types of model formalism.

7.2.1.6. Regulation of Morphological Features during Synergistic Neurite Outgrowth

Synergistic neurite outgrowth is a complex process involving changes in many morphological features. In this thesis, P38 was found to regulate neurite branching independently of total neurite length in the NP and FP systems (Chapter 4), which is consistent with previous studies where different parameters were reported to be regulated independently[303]. Cdc42 and Rac1 are key regulators of actin polymerization and microtubules stabilization, which are important determinants of neurite branching[324-327]. Furthermore, P38 has been found to be a downstream signalling effector of Rac and Cdc42 in many systems[141,329]. Thus, it is plausible that P38 plays a critical role in regulating the branching of neurites and the possibility that this is mediated through Rac1 and Cdc42 should be looked at.

Furthermore, it would be of great interest to investigate the pathways that can regulate other parameters such as segment length, angle of neurite extensions, and angle of neurite branching. In this aspect, the future directions raised above, in general, for synergistic neurite outgrowth can also be applied to the analyses of different morphological parameters. In addition, development of softwares that can simultaneously address more

morphological parameters would be very beneficial. Currently, softwares that can analyze parameters such as branching and length are unable to address the angles of neurite protrusions and branching, and *vice versa*[229,234,235,298,445].

7.2.2. Further Development of TEEBM

The TEEBM used in this thesis comprised of several key features, namely, a two-phase learning strategy, an eDBN parameterization, and an exact structure learning algorithm. It can be further developed in several aspects as outlined in the following sections. Importantly, these proposed developments and applications of TEEBM are not restricted to the analyses of neuronal changes alone and hence, can be extended to other biological systems beyond the scope of this thesis.

7.2.2.1. Maximizing Use of Literature Datasets

The data obtained in typical biological experiments is often continuous in nature. Thus, the discretization of these variables into discrete multinomial variables inevitably results in a loss of information[79,80]. This step is even more critical when the activation profiles of the measured variables are similar. If it is not performed well, a problem analogous to that of multi-collinearity in regression models can occur[446], which results in erroneous model predictions. While many automatic data discretization techniques have been developed to optimize this process, the results have been unsatisfactory and the current opinion is that this process is best carried out by domain experts[447]. In general, it is accepted that more bins will result in the capturing of more dependencies that can more accurately reflect the underlying complexity of a system[447]. However, to ensure that these bins contain information rather than

noise, more experimental data is actually needed. Given that the generation of more data, without increasing the number of dimensions, is seldom feasible, maximizing the use of literature datasets is a potential alternative.

In the literature, a wealth of data is available, with differences in terms of experimental conditions and techniques, and time-course of measurements. To use such data effectively, two potential areas need be addressed. First, the reliability and importance of each dataset need to be ascertained or optimized, so as to establish the contribution of each dataset. Second, proper parameterization of the data in each dataset is needed so that data with different properties can be pooled together in a single analysis. Thus, such approaches can serve as *a priori* knowledge to complement the TEEBM.

7.2.2.2. Analyses of Networks with More than 30 Variables

In this thesis, the proposed TEEBM was used for the analyses of the protein phosphorylation levels measured at discrete time-points (Chapter 5). The drawback of an eDBN parameterization is that the number of variables scales proportionately with the number of time-points, and increasing the number of signalling nodes or time-points will easily result in a network with more than 30 variables.

One possible approach to this problem is to combine TEEBM with the idea behind tvDBNs and nsDBNs, where a series of stationary BNs, each demarcated by a changepoint, are built across time[78,249,250]. In situations with measurements at many time-points, this concept can be extended to TEEBM, where a series of eDBNs are built across the time-course. Another approach

would be to further explore the concept of dynamic programming[267,268], which is the basis of the exact structure algorithm[269], to allow incorporation of more variables. The main strength of dynamic programming lies in its ability to identify recursive independent sub-problems, or sub-networks in the context of BNs, and obtain the optimal solution for each independent sub-problem[268]. This means that each sub-problem needs to be solved only once, which reduce the space and memory requirements for solving the whole problem. Thus, advancements that can allow these sub-problems to be identified and solved more effectively will lead to more efficient algorithms with lower memory requirements, and this in turn allows the inclusion of more variables.

7.2.2.3. Applications of TEEBM to Systems with More than Two Ligands

In the treatment of diseases, one topic of increasing interest is that of synergistic drug therapeutics. Unlike the work on bi-ligand synergistic neurite outgrowth in this thesis, combinatorial drug therapy can go beyond the use of two drugs[244,448,449]. Thus, in the analyses of such systems, the TEEBM must be extended to accommodate for more than two ligands, so that maximal information can be extracted from the experimental data. This can be accomplished by adopting a multi-phase learning procedure in place of that of a two-phase, a concept analogous to that of online-learning in BNs[450]. For instance, in a three-ligand system, phase one, two, and three learning consider the effects of the individual ligand, effects of interactions between different pairs of ligands, and effects of interactions between all three ligands, respectively. Thus, each learning phase is used to account for information, such as the degree of synergism, arising from a different number of ligands.

Chapter 8.

Materials and Methods

8.1. Experimental Materials

Mouse recombinant NGF was purchased from Peprotech (Rocky Hill, NJ). Mouse recombinant EGF was purchased from Shenandoah Biotechnology (Warwick, PA). PACAP was purchased from American Peptide Company (Sunnyvale, CA). MEK inhibitor U0126, JNK inhibitor SP600125, P38 inhibitor SB203580, PI3K inhibitor LY294002, and PKA inhibitor H89 were purchased from LC Laboratories (Woburn, MA). P90RSK inhibitor BRD7389 was purchased from Santa Cruz Biotechnology (Santa Cruz, CA). Primary antibodies against phospho-specific MEK (Ser217/221) (pMEK), phospho-specific Erk1/2 (Thr202/Tyr204) (pErk), pan-Erk1/2, phospho-specific MKK4 (Ser257/Thr261) (pMKK4), phospho-specific JNK (Thr183/Tyr185) (pJNK), pan-JNK, phospho-specific P38 (Thr180/Tyr182) (pP38), pan-P38, phospho-specific Akt (Ser473) (pAkt), pan-Akt, phospho-specific P90RSK (Ser380) (pP90RSK), pan-RSK, and phospho-specific CREB (Ser133) (pCREB) were purchased from Cell Signalling Technologies (Danver, MA). The antibody against phospho-specific c-Jun (Ser73) (pc-Jun) was purchased from Abnova (Taipei, Taiwan). The antibody for the neuronal marker βIII-Tubulin was purchased from R&D Systems (Minneapolis, MN). Human recombinant FGFb and the antibody against actin were purchased from EMD Millipore (Billerica, MA). The TRI-Reagent and antibody against tubulin was purchased from Sigma (Sigma-Aldrich, St. Louis, MO). Horseradish peroxidase-conjugated secondary antibodies, Imperial Protein Stain, Triton X-100, and Hoechst were purchased from Thermo Scientific (Wilmington, DE). Secondary antibodies conjugated with Alexa Fluor 488 were bought from Invitrogen (Carlsbad, CA). ImPromII reverse transcriptase was purchased from Promega (Madison, WI) and KlearTaq DNA polymerase was purchased from KBiosciences (UK).

8.2. Cell Culture

Rat pheochromocytoma PC12 cells (American Type Culture Collection, Manassas, VA) were cultured in Dulbecco's minimum essential medium (DMEM) supplemented with 10% heat inactivated fetal bovine serum (FBS, Sigma-Aldrich) and 5% Horse Serum (HS, Hyclone, Thermo Scientific). Cells were cultured with 100 U/ml penicillin and 100 mg/ml streptomycin, and maintained in a humidified incubator with 5% CO_2 at 37°C.

8.3. Western Blot Analyses

PC12 cells were seeded into the wells of 6-well plates pre-coated with poly-D-lysine at a density of 500,000 cells/well and cultured in growth medium for 48 hours. Following this, cells were incubated in serum-depleted medium (1% FBS, 0.5% HS) for an additional 16 hours. Cells were then simulated with individual or combinations of NGF, FGFb, EGF, and PACAP. For treatments with inhibitors, the cells were pre-incubated for 1 hour with the respective inhibitors prior to stimulations with the ligands. Cells were harvested within 4 hours after ligand stimulation at the stipulated time-points. Treated cells were washed once with PBS and subsequently lysed in 2% sodium dodecyl sulfate (SDS). Protein concentrations in the total cell lysates were quantified using the microBCA assay (Pierce Biotechnology, Rockford, IL). The protein samples were then separated by SDS-polyacrylamide gel electrophoresis (SDS-PAGE), transferred onto nitrocellulose membranes, blocked with 5% milk for an hour before being probed with antibodies against pMEK (phosphorylated MEK) (1:5000 dilution), pErk (1:5000 dilution), pMKK4 (1:1000 dilution), pJNK (1:1000 dilution), pP38 (1:1000 dilution), pAkt (1:1000 dilution), pP90RSK (1:1000 dilution), pCREB (1:1000 dilution), pc-Jun (1:1000

dilution), total Erk (1:5000 dilution), total JNK (1:1000 dilution), total P38 (1:1000 dilution), total Akt (1:1000 dilution), total P90RSK (1:1000 dilution), actin (1:10,000 dilution), and tubulin (1:10,000 dilution). Blots were stripped with Restore Western Stripping Buffer (Pierce Biotechnology) and re-probed for different proteins. The protein bands were developed with Immobilon Western Chemiluminescent HRP Substrate (Millipore) on a ChemiDoc XRS system (Biorad, Hercules, CA). The band intensities were quantified using Quantity One 1-D Analysis software (Biorad). To enable comparisons of signals across different blots, lysates from PC12 cells treated with NGF-PACAP were used to generate a standard curve for each blot[342].

8.4. Measurements of Neurite Outgrowth

PC12 cells were seeded into the wells of 12-well plates at a density of 25,000 cells/well, and cultured as described for western blotting. After treatment with the respective ligands for 48 hours, the cells were fixed with 4% paraformaldehyde for 20 minutes and permeabilized with ice-cold methanol for 15 minutes. The cell bodies were then stained with Imperial Protein Stain for 15 minutes and the nuclei with Hoechst stain for 5 minutes. The images of the cells were then captured using a Zeiss inverted fluorescent microscope (Zeiss Oberkochen, Germany). The length of the neurites was quantified using HCA-Vision software (CSIRO, North Ryde, NSW, Australia). The neurite quantification procedure, which involved neuron body detection, neurite detection, and neurite analysis, was performed as previously described[232]. The neurite length obtained under control conditions (i.e. in the absence of both NGF and PACAP) was subtracted from each treatment condition. Thereafter, the neurite length for each condition was normalized

against that obtained for cells grown under 50 ng/ml of NGF, assigned an arbitrary value of 1. The same procedure was applied to the analysis of the length of the longest neurite. The other morphological parameters analyzed, namely number of neurite extensions, number of branch-points, and number of segments, were not normalized.

8.5. Immunocytochemistry

PC12 cells were seeded into the wells of 12-well plates at a density of 25,000 cells/well, and cultured as described for western blotting. After treatment with the respective ligands for 48 hours, the cells were fixed with 4% paraformaldehyde for 20 minutes and permeabilized with 0.5% Triton-X100/PBS and blocked with normal goat serum (1:10) (Dako, Glostrup, Denmark) in 0.5% Triton X-100/PBS for 60 minutes at 37°C. The cells were incubated with primary antibodies against βIII-Tubulin (1:250) and then further incubated with secondary antibodies conjugated with Alexa Fluor 488 (1:500). The images of the cells were captured using a Zeiss inverted fluorescent microscope (Zeiss Oberkochen).

8.6. Quantitative Polymerase Chain Reaction (qPCR)

PC12 cells were seeded into the wells of 12-well plates at a density of 100,000 cells/well, and cultured as described for western blotting. Total RNA from the cultured cells was isolated using the TRI-Reagent according to the manufacturer's instructions. The integrity of the isolated total RNA was validated by denaturing agarose gel electrophoresis. The concentration of the total RNA isolated was measured using Nanodrop 2000 (Thermo Scientific).

For transcriptomic profiling of mRNAs, 500 ng of total RNA was first reverse transcribed using ImPromII reverse transcriptase and 0.5 µg of random hexamers for 60 minutes at 42°C according to the manufacturer's instructions. The reaction was terminated by heating at 70°C for 5 minutes. For transcriptomic profiling of miRNAs, 100 ng of total RNA was first reverse transcribed using ImPromII reverse transcriptase and 100 nM of multiplex reverse transcription primers for 30 minutes at 42°C. The reaction was terminated by heating at 70°C for 5 minutes.

The primer sequences used for real-time quantitative polymerase chain reaction (qPCR) for the mRNA assays are listed as shown in Table 8.1. The designs for the primers for the rno-miRNA assays are properties of Exploit Technologies Private Limited (Biopolis, Singapore). The research use of these assays is governed by the End User License Agreement.

Table 8.1. Primers used for real-time qPCR for mRNAs in PC12 cells (rno species).

Gene	Forward Primer (5' to 3')	Reverse Primer (5' to 3')
Arc	CCCCAGCAGTGATTCATACCA	GCCGGAAAGACTTCTCAGCAG
Btg2	CAGGACGCACTGACCGATCAT	CTGGCCACCTTGCTGATGATG
Egr1	GCGCTGGTGGAGACAAGTTAT	TGCTCACAAGGCCACTGACTA
c-Fos	GGGGACAGCCTTTCCTACTAC	CTGTCACCGTGGGGATAAAGT
Fosl	CAGGCCCTGTGAGCAGATCAG	CCCGATTTCTCATCCTCCAAC
Hes1	CGACACCGGACAAACCAAAGA	TTGGAATGCCGGGAGCTATCT
JunB	GCTCAACCTGGCAGATCCTTA	TTGCTGTTGGGGACGATCAAG
Nr4a1	AGGGCTGCAAAGGCTTCTTCA	CTTCCTTCACCATGCCCACAG
RPL19	ACCTGGATGCGAAGGATGAG	ACCTTCAGGTACAGGCTGTG

Real-time qPCR using SYBR Green I was performed on the CFX96 (Biorad) in a total volume of 25 µl in 1× XtensaMix-SGTM (BioWORKS, Singapore), containing 2.5 mM $MgCl_2$, 200 nM of primers and 0.5 U of KlearTaq DNA

polymerase. Real-time qPCR for mRNAs were carried out after an initial denaturation for 10 minutes at 95°C followed by 40 cycles of 30 seconds denaturation at 95°C, 30 seconds annealing at 60°C and 30 seconds extension at 72°C. Real-time qPCR for microRNAs were carried out after an initial denaturation for 10 minutes at 95°C followed by 40 cycles of 10 seconds denaturation at 95°C and 30 seconds annealing and extension at 60°C. Melt curve analyses were performed at the end of the reactions to verify the identity of the products.

The threshold cycles (Ct) were calculated using the CFX manager software (Biorad). All real-time PCR quantification was carried out simultaneously with non-template controls (NTCs). The fold changes of the measured mRNAs and miRNAs in the treated samples relative to the control samples were calculated using the equation $2^{-\Delta\Delta Ct}$, where $\Delta\Delta Ct = (Ct_{Target\ Gene} - Ct_{Reference\ Gene})_{Treatment} - (Ct_{Target\ Gene} - Ct_{Reference\ Gene})_{Control}$.

8.7. Statistical Analyses

Statistical significance was determined using the Student's *t*-test and the respective results are displayed as the mean ± standard deviation (S.D.). All experiments and measurements were replicated at least three times.

Bibliography

1. Zimmermann, G.R., Lehar, J. & Keith, C.T. Multi-target therapeutics: when the whole is greater than the sum of the parts. *Drug Discov Today* **12**, 34-42 (2007).
2. Chou, T.C. Drug combination studies and their synergy quantification using the Chou-Talalay method. *Cancer Res* **70**, 440-446 (2010).
3. Marks, W.J., Jr*., et al.* Safety and tolerability of intraputaminal delivery of CERE-120 (adeno-associated virus serotype 2-neurturin) to patients with idiopathic Parkinson's disease: an open-label, phase I trial. *Lancet Neurol* **7**, 400-408 (2008).
4. Marks, W.J., Jr*., et al.* Gene delivery of AAV2-neurturin for Parkinson's disease: a double-blind, randomised, controlled trial. *Lancet Neurol* **9**, 1164-1172 (2010).
5. Wan, G., Zhou, L., Lim, Q., Wong, Y.H. & Too, H.P. Cyclic AMP signalling through PKA but not Epac is essential for neurturin-induced biphasic ERK1/2 activation and neurite outgrowths through GFRalpha2 isoforms. *Cell Signal* **23**, 1727-1737 (2011).
6. Mora-Garcia, P. & Sakamoto, K.M. Cell signaling defects and human disease. *Mol Genet Metab* **66**, 143-171 (1999).
7. Yang, C.Y*., et al.* PhosphoPOINT: a comprehensive human kinase interactome and phospho-protein database. *Bioinformatics* **24**, i14-20 (2008).
8. Manning, G., Plowman, G.D., Hunter, T. & Sudarsanam, S. Evolution of protein kinase signaling from yeast to man. *Trends Biochem Sci* **27**, 514-520 (2002).
9. Johnson, L.N., Noble, M.E. & Owen, D.J. Active and inactive protein kinases: structural basis for regulation. *Cell* **85**, 149-158 (1996).
10. Cohen, P. The origins of protein phosphorylation. *Nat Cell Biol* **4**, E127-130 (2002).
11. Jia, J*., et al.* Mechanisms of drug combinations: interaction and network perspectives. *Nat Rev Drug Discov* **8**, 111-128 (2009).
12. Lehar, J*., et al.* Synergistic drug combinations tend to improve therapeutically relevant selectivity. *Nat Biotechnol* **27**, 659-666 (2009).
13. Kamb, A., Wee, S. & Lengauer, C. Why is cancer drug discovery so difficult? *Nat Rev Drug Discov* **6**, 115-120 (2007).
14. Strange, K. The end of "naive reductionism": rise of systems biology or renaissance of physiology? *Am J Physiol Cell Physiol* **288**, C968-974 (2005).
15. Kitano, H. Systems biology: a brief overview. *Science* **295**, 1662-1664 (2002).
16. Soumyanath, A*., et al.* Centella asiatica accelerates nerve regeneration upon oral administration and contains multiple active fractions increasing neurite elongation in-vitro. *J Pharm Pharmacol* **57**, 1221-1229 (2005).
17. Gordon, T. The role of neurotrophic factors in nerve regeneration. *Neurosurg Focus* **26**, E3 (2009).
18. Logan, A., Ahmed, Z., Baird, A., Gonzalez, A.M. & Berry, M. Neurotrophic factor synergy is required for neuronal survival and disinhibited axon regeneration after CNS injury. *Brain* **129**, 490-502 (2006).
19. Madduri, S., Papaloizos, M. & Gander, B. Synergistic effect of GDNF and NGF on axonal branching and elongation in vitro. *Neurosci Res* **65**, 88-97 (2009).
20. Jones, D.M., Tucker, B.A., Rahimtula, M. & Mearow, K.M. The synergistic effects of NGF and IGF-1 on neurite growth in adult sensory neurons:

convergence on the PI 3-kinase signaling pathway. *J Neurochem* **86**, 1116-1128 (2003).

21. Ahn, A.C., Tewari, M., Poon, C.S. & Phillips, R.S. The limits of reductionism in medicine: could systems biology offer an alternative? *PLoS Med* **3**, e208 (2006).
22. Mazzocchi, F. Complexity and the reductionism-holism debate in systems biology. *Wiley Interdiscip Rev Syst Biol Med* **4**, 413-427 (2012).
23. Van Regenmortel, M.H. Reductionism and complexity in molecular biology. Scientists now have the tools to unravel biological and overcome the limitations of reductionism. *EMBO Rep* **5**, 1016-1020 (2004).
24. Ahn, A.C., Tewari, M., Poon, C.S. & Phillips, R.S. The clinical applications of a systems approach. *PLoS Med* **3**, e209 (2006).
25. Bauchau, V. Emergence and Reductionism: from the Game of Life to Science of Life. in *SELF-ORGANIZATION AND EMERGENCE IN LIFE SCIENCES*, Vol. 331 (eds. Feltz, B., Crommelinck, M. & Goujon, P.) 29-40 (Springer Netherlands, 2006).
26. Doppler, W., Geymayer, S. & Weirich, H.G. Synergistic and antagonistic interactions of transcription factors in the regulation of milk protein gene expression. Mechanisms of cross-talk between signalling pathways. *Adv Exp Med Biol* **480**, 139-146 (2000).
27. Audet, J. Adventures in time and space: Nonlinearity and complexity of cytokine effects on stem cell fate decisions. *Biotechnol Bioeng* **106**, 173-182 (2010).
28. Lehar, J., Krueger, A.S., Zimmermann, G.R. & Borisy, A.A. Therapeutic selectivity and the multi-node drug target. *Discov Med* **8**, 185-190 (2009).
29. Raue, A*., et al.* Lessons Learned from Quantitative Dynamical Modeling in Systems Biology. *PLoS One* **8**, e74335 (2013).
30. Mogilner, A., Wollman, R. & Marshall, W.F. Quantitative modeling in cell biology: what is it good for? *Dev Cell* **11**, 279-287 (2006).
31. Mogilner, A., Allard, J. & Wollman, R. Cell polarity: quantitative modeling as a tool in cell biology. *Science* **336**, 175-179 (2012).
32. Ideker, T. & Lauffenburger, D. Building with a scaffold: emerging strategies for high- to low-level cellular modeling. *Trends Biotechnol* **21**, 255-262 (2003).
33. Daskalaki, A. *Handbook of Research on Systems Biology Applications in Medicine*, (IGI Global, 2009).
34. Hache, H., Lehrach, H. & Herwig, R. Reverse engineering of gene regulatory networks: a comparative study. *EURASIP J Bioinform Syst Biol*, 617281 (2009).
35. Resat, H., Petzold, L. & Pettigrew, M.F. Kinetic modeling of biological systems. *Methods Mol Biol* **541**, 311-335 (2009).
36. Ilea, M., Turnea, M. & Rotariu, M. Ordinary differential equations with applications in molecular biology. *Rev Med Chir Soc Med Nat Iasi* **116**, 347-352 (2012).
37. Vilas, C., Balsa-Canto, E., Garcia, M.S., Banga, J.R. & Alonso, A.A. Dynamic optimization of distributed biological systems using robust and efficient numerical techniques. *BMC Syst Biol* **6**, 79 (2012).
38. Bansal, M., Belcastro, V., Ambesi-Impiombato, A. & di Bernardo, D. How to infer gene networks from expression profiles. *Mol Syst Biol* **3**, 78 (2007).

39. Dalle Pezze, P*., et al.* A dynamic network model of mTOR signaling reveals TSC-independent mTORC2 regulation. *Sci Signal* **5**, ra25 (2012).
40. Sonntag, A.G., Dalle Pezze, P., Shanley, D.P. & Thedieck, K. A modelling-experimental approach reveals insulin receptor substrate (IRS)-dependent regulation of adenosine monosphosphate-dependent kinase (AMPK) by insulin. *FEBS J* **279**, 3314-3328 (2012).
41. von Kriegsheim, A*., et al.* Cell fate decisions are specified by the dynamic ERK interactome. *Nat Cell Biol* **11**, 1458-1464 (2009).
42. Lebedeva, G*., et al.* Model-based global sensitivity analysis as applied to identification of anti-cancer drug targets and biomarkers of drug resistance in the ErbB2/3 network. *Eur J Pharm Sci* **46**, 244-258 (2012).
43. Cho, K.H. & Wolkenhauer, O. Analysis and modelling of signal transduction pathways in systems biology. *Biochem Soc Trans* **31**, 1503-1509 (2003).
44. Tong, W*., et al.* Using decision forest to classify prostate cancer samples on the basis of SELDI-TOF MS data: assessing chance correlation and prediction confidence. *Environ Health Perspect* **112**, 1622-1627 (2004).
45. Kozlov, K., Surkova, S., Myasnikova, E., Reinitz, J. & Samsonova, M. Modeling of gap gene expression in Drosophila Kruppel mutants. *PLoS Comput Biol* **8**, e1002635 (2012).
46. Aldridge, B.B., Burke, J.M., Lauffenburger, D.A. & Sorger, P.K. Physicochemical modelling of cell signalling pathways. *Nat Cell Biol* **8**, 1195-1203 (2006).
47. Janes, K.A. & Yaffe, M.B. Data-driven modelling of signal-transduction networks. *Nature Reviews Molecular Cell Biology* **7**, 820-828 (2006).
48. Linder, R., Richards, T. & Wagner, M. Microarray Data Classified by Artificial Neural Networks. in *Microarrays*, Vol. 382 (ed. Rampal, J.) 345-372 (Humana Press, 2007).
49. Jain, S., Naik, P.K. & Bhooshan, S.V. Non Linear Modeling of Cell Survival/Death Using Artificial Neural Network. in *Computational Intelligence and Communication Networks (CICN), 2011 International Conference on* 565-568 (2011).
50. Chatterjee, M.S., Purvis, J.E., Brass, L.F. & Diamond, S.L. Pairwise agonist scanning predicts cellular signaling responses to combinatorial stimuli. *Nat Biotechnol* **28**, 727-732 (2010).
51. Ling, H., Samarasinghe, S. & Kulasiri, D. Novel recurrent neural network for modelling biological networks: Oscillatory p53 interaction dynamics. *Biosystems* **114**, 191-205 (2013).
52. Johansen, M.B., Izarzugaza, J.M., Brunak, S., Petersen, T.N. & Gupta, R. Prediction of disease causing non-synonymous SNPs by the Artificial Neural Network Predictor NetDiseaseSNP. *PLoS One* **8**, e68370 (2013).
53. Pillai, R.R., Divekar, R., Brasier, A., Bhavnani, S. & Calhoun, W.J. Strategies for molecular classification of asthma using bipartite network analysis of cytokine expression. *Curr Allergy Asthma Rep* **12**, 388-395 (2012).
54. Benitez, J.M., Castro, J.L. & Requena, I. Are artificial neural networks black boxes? *IEEE Trans Neural Netw* **8**, 1156-1164 (1997).
55. Schafer, J. & Strimmer, K. An empirical Bayes approach to inferring large-scale gene association networks. *Bioinformatics* **21**, 754-764 (2005).

56. Numata, J., Ebenhoh, O. & Knapp, E.W. Measuring correlations in metabolomic networks with mutual information. *Genome Inform* **20**, 112-122 (2008).
57. Waltermann, C. & Klipp, E. Information theory based approaches to cellular signaling. *Biochim Biophys Acta* **1810**, 924-932 (2011).
58. Song, L., Langfelder, P. & Horvath, S. Comparison of co-expression measures: mutual information, correlation, and model based indices. *BMC Bioinformatics* **13**, 328 (2012).
59. Margolin, A.A*., et al.* ARACNE: an algorithm for the reconstruction of gene regulatory networks in a mammalian cellular context. *BMC Bioinformatics* **7 Suppl 1**, S7 (2006).
60. Zoppoli, P., Morganella, S. & Ceccarelli, M. TimeDelay-ARACNE: Reverse engineering of gene networks from time-course data by an information theoretic approach. *BMC Bioinformatics* **11**, 154 (2010).
61. Anastassiou, D. Computational analysis of the synergy among multiple interacting genes. *Molecular Systems Biology* **3**(2007).
62. Altay, G. Empirically determining the sample size for large-scale gene network inference algorithms. *IET Syst Biol* **6**, 35-43 (2012).
63. Liepe, J., Filippi, S., Komorowski, M. & Stumpf, M.P. Maximizing the information content of experiments in systems biology. *PLoS Comput Biol* **9**, e1002888 (2013).
64. Pearl, J. *Probabilistic reasoning in intelligent systems: networks of plausible inference*, (Morgan Kaufmann Publishers Inc., 1988).
65. Sachs, K., Gifford, D., Jaakkola, T., Sorger, P. & Lauffenburger, D.A. Bayesian network approach to cell signaling pathway modeling. *Sci STKE* **2002**, pe38 (2002).
66. Liu, Z., Malone, B. & Yuan, C. Empirical evaluation of scoring functions for Bayesian network model selection. *BMC Bioinformatics* **13 Suppl 15**, S14 (2012).
67. Wang, S.Q. & Li, H.X. Bayesian inference based modelling for gene transcriptional dynamics by integrating multiple source of knowledge. *BMC Syst Biol* **6 Suppl 1**, S3 (2012).
68. Hecker, M., Lambeck, S., Toepfer, S., van Someren, E. & Guthke, R. Gene regulatory network inference: data integration in dynamic models-a review. *Biosystems* **96**, 86-103 (2009).
69. Ciaccio, M.F., Wagner, J.P., Chuu, C.P., Lauffenburger, D.A. & Jones, R.B. Systems analysis of EGF receptor signaling dynamics with microwestern arrays. *Nat Methods* **7**, 148-155 (2010).
70. Burger, L. & van Nimwegen, E. Accurate prediction of protein-protein interactions from sequence alignments using a Bayesian method. *Mol Syst Biol* **4**, 165 (2008).
71. Woolf, P.J., Prudhomme, W., Daheron, L., Daley, G.Q. & Lauffenburger, D.A. Bayesian analysis of signaling networks governing embryonic stem cell fate decisions. *Bioinformatics* **21**, 741-753 (2005).
72. Schwartz, S.M., Schwartz, H.T., Horvath, S., Schadt, E. & Lee, S.I. A systematic approach to multifactorial cardiovascular disease: causal analysis. *Arterioscler Thromb Vasc Biol* **32**, 2821-2835 (2012).

73. Golightly, A. & Wilkinson, D.J. Bayesian parameter inference for stochastic biochemical network models using particle Markov chain Monte Carlo. *Interface Focus* **1**, 807-820 (2011).
74. Toni, T., Ozaki, Y., Kirk, P., Kuroda, S. & Stumpf, M.P. Elucidating the in vivo phosphorylation dynamics of the ERK MAP kinase using quantitative proteomics data and Bayesian model selection. *Mol Biosyst* **8**, 1921-1929 (2012).
75. Chickering, D.M. Learning equivalence classes of bayesian-network structures. *J. Mach. Learn. Res.* **2**, 445-498 (2002).
76. Friedman, N., Murphy, K. & Russell, S. Learning the structure of dynamic probabilistic networks. in *Proceedings of the Fourteenth conference on Uncertainty in artificial intelligence* 139-147 (Morgan Kaufmann Publishers Inc., Madison, Wisconsin, 1998).
77. Ahmed, A. & Xing, E.P. Recovering time-varying networks of dependencies in social and biological studies. *Proc Natl Acad Sci U S A* **106**, 11878-11883 (2009).
78. Robinson, J.W. & Hartemink, A.J. Learning Non-Stationary Dynamic Bayesian Networks. *Journal of Machine Learning Research* **11**, 3647-3680 (2010).
79. Cobb, B., Rumí, R. & Salmerón, A. Bayesian Network Models with Discrete and Continuous Variables. in *Advances in Probabilistic Graphical Models*, Vol. 214 (eds. Lucas, P., Gámez, J. & Salmerón, A.) 81-102 (Springer Berlin Heidelberg, 2007).
80. Dimitrova, E.S., Licona, M.P., McGee, J. & Laubenbacher, R. Discretization of time series data. *J Comput Biol* **17**, 853-868 (2010).
81. Gupta, S.K. Use of Bayesian statistics in drug development: Advantages and challenges. *Int J Appl Basic Med Res* **2**, 3-6 (2012).
82. URONEN, P., SILANDER, T., TIRRI, H. & MYLLYMÄKI, P. B-COURSE: A WEB-BASED TOOL FOR BAYESIAN AND CAUSAL DATA ANALYSIS. *International Journal on Artificial Intelligence Tools* **11**, 369-387 (2002).
83. Kauffman, S.A. Metabolic stability and epigenesis in randomly constructed genetic nets. *J Theor Biol* **22**, 437-467 (1969).
84. Paveliev, M.*, et al.* Neurotrophic factors switch between two signaling pathways that trigger axonal growth. *J Cell Sci* **120**, 2507-2516 (2007).
85. Shmulevich, I., Gluhovsky, I., Hashimoto, R.F., Dougherty, E.R. & Zhang, W. Steady-state analysis of genetic regulatory networks modelled by probabilistic boolean networks. *Comp Funct Genomics* **4**, 601-608 (2003).
86. Saez-Rodriguez, J.*, et al.* Discrete logic modelling as a means to link protein signalling networks with functional analysis of mammalian signal transduction. *Mol Syst Biol* **5**, 331 (2009).
87. Saithong, T., Bumee, S., Liamwirat, C. & Meechai, A. Analysis and practical guideline of constraint-based boolean method in genetic network inference. *PLoS One* **7**, e30232 (2012).
88. Lloyd-Price, J., Gupta, A. & Ribeiro, A.S. Robustness and information propagation in attractors of Random Boolean Networks. *PLoS One* **7**, e42018 (2012).
89. Davidich, M.I. & Bornholdt, S. Boolean network model predicts cell cycle sequence of fission yeast. *PLoS One* **3**, e1672 (2008).
90. Wang, R.S., Saadatpour, A. & Albert, R. Boolean modeling in systems biology: an overview of methodology and applications. *Phys Biol* **9**, 055001 (2012).

91. Davidich, M.I. & Bornholdt, S. Boolean network model predicts knockout mutant phenotypes of fission yeast. *PLoS One* **8**, e71786 (2013).
92. Wang, R.S. & Albert, R. Elementary signaling modes predict the essentiality of signal transduction network components. *BMC Syst Biol* **5**, 44 (2011).
93. Berestovsky, N. & Nakhleh, L. An Evaluation of Methods for Inferring Boolean Networks from Time-Series Data. *PLoS One* **8**, e66031 (2013).
94. Aldridge, B.B., Saez-Rodriguez, J., Muhlich, J.L., Sorger, P.K. & Lauffenburger, D.A. Fuzzy logic analysis of kinase pathway crosstalk in TNF/EGF/insulin-induced signaling. *PLoS Comput Biol* **5**, e1000340 (2009).
95. Jin, Y. & Wang, L. *Fuzzy Systems in Bioinformatics and Computational Biology*, (Springer Publishing Company, Incorporated, 2009).
96. Peltier, J. & Schaffer, D.V. Systems biology approaches to understanding stem cell fate choice. *IET Syst Biol* **4**, 1-11 (2010).
97. Butte, A. The use and analysis of microarray data. *Nat Rev Drug Discov* **1**, 951-960 (2002).
98. Sharov, A.A.*, et al.* Transcriptome analysis of mouse stem cells and early embryos. *PLoS Biol* **1**, E74 (2003).
99. Aiba, K.*, et al.* Defining a developmental path to neural fate by global expression profiling of mouse embryonic stem cells and adult neural stem/progenitor cells. *Stem Cells* **24**, 889-895 (2006).
100. Liu, G., Swihart, M.T. & Neelamegham, S. Sensitivity, principal component and flux analysis applied to signal transduction: the case of epidermal growth factor mediated signaling. *Bioinformatics* **21**, 1194-1202 (2005).
101. Gupta, S., Maurya, M.R. & Subramaniam, S. Identification of crosstalk between phosphoprotein signaling pathways in RAW 264.7 macrophage cells. *PLoS Comput Biol* **6**, e1000654 (2010).
102. Janes, K.A. A Systems Model of Signaling Identifies a Molecular Basis Set for Cytokine-Induced Apoptosis. *Science* **310**, 1646-1653 (2005).
103. Platt, M.O., Wilder, C.L., Wells, A., Griffith, L.G. & Lauffenburger, D.A. Multipathway kinase signatures of multipotent stromal cells are predictive for osteogenic differentiation: tissue-specific stem cells. *Stem Cells* **27**, 2804-2814 (2009).
104. Niepel, M.*, et al.* Profiles of Basal and stimulated receptor signaling networks predict drug response in breast cancer lines. *Sci Signal* **6**, ra84 (2013).
105. Zhang, Y.*, et al.* A systems biology-based classifier for hepatocellular carcinoma diagnosis. *PLoS One* **6**, e22426 (2011).
106. Rantalainen, M.*, et al.* Piecewise multivariate modelling of sequential metabolic profiling data. *BMC Bioinformatics* **9**, 105 (2008).
107. Greene, L.A. & Tischler, A.S. Establishment of a noradrenergic clonal line of rat adrenal pheochromocytoma cells which respond to nerve growth factor. *Proc Natl Acad Sci U S A* **73**, 2424-2428 (1976).
108. Watanabe, K.*, et al.* Latent process genes for cell differentiation are common decoders of neurite extension length. *J Cell Sci* **125**, 2198-2211 (2012).
109. Hernandez, A., Kimball, B., Romanchuk, G. & Mulholland, M.W. Pituitary adenylate cyclase-activating peptide stimulates neurite growth in PC12 cells. *Peptides* **16**, 927-932 (1995).

110. Ming, G.*, et al.* Phospholipase C-gamma and phosphoinositide 3-kinase mediate cytoplasmic signaling in nerve growth cone guidance. *Neuron* **23**, 139-148 (1999).
111. Vaudry, D., Stork, P.J., Lazarovici, P. & Eiden, L.E. Signaling pathways for PC12 cell differentiation: making the right connections. *Science* **296**, 1648-1649 (2002).
112. Tso, P.H., Morris, C.J., Yung, L.Y., Ip, N.Y. & Wong, Y.H. Multiple Gi proteins participate in nerve growth factor-induced activation of c-Jun N-terminal kinases in PC12 cells. *Neurochem Res* **34**, 1101-1112 (2009).
113. Yung, L.Y.*, et al.* Nerve growth factor-induced stimulation of p38 mitogen-activated protein kinase in PC12 cells is partially mediated via G(i/o) proteins. *Cell Signal* **20**, 1538-1544 (2008).
114. Miyata, A.*, et al.* Isolation of a novel 38 residue-hypothalamic polypeptide which stimulates adenylate cyclase in pituitary cells. *Biochem Biophys Res Commun* **164**, 567-574 (1989).
115. Arimura, A. Pituitary adenylate cyclase activating polypeptide (PACAP): discovery and current status of research. *Regul Pept* **37**, 287-303 (1992).
116. Vaudry, D.*, et al.* Pituitary adenylate cyclase-activating polypeptide and its receptors: from structure to functions. *Pharmacol Rev* **52**, 269-324 (2000).
117. Thomas, R.L., Crawford, N.M., Grafer, C.M. & Halvorson, L.M. Pituitary Adenylate Cyclase-Activating Polypeptide (PACAP) in the Hypothalamic-Pituitary-Gonadal Axis: A Review of the Literature. *Reprod Sci* **20**, 857-871 (2013).
118. Holighaus, Y., Mustafa, T. & Eiden, L.E. PAC1hop, null and hip receptors mediate differential signaling through cyclic AMP and calcium leading to splice variant-specific gene induction in neural cells. *Peptides* **32**, 1647-1655 (2011).
119. Gonzalez, B.J., Basille, M., Vaudry, D., Fournier, A. & Vaudry, H. [Pituitary adenylate cyclase-activating polypeptide]. *Ann Endocrinol (Paris)* **59**, 364-405 (1998).
120. Vaudry, D.*, et al.* Pituitary adenylate cyclase-activating polypeptide and its receptors: 20 years after the discovery. *Pharmacol Rev* **61**, 283-357 (2009).
121. Lu, N. & DiCicco-Bloom, E. Pituitary adenylate cyclase-activating polypeptide is an autocrine inhibitor of mitosis in cultured cortical precursor cells. *Proc Natl Acad Sci U S A* **94**, 3357-3362 (1997).
122. Uchida, D., Arimura, A., Somogyvari-Vigh, A., Shioda, S. & Banks, W.A. Prevention of ischemia-induced death of hippocampal neurons by pituitary adenylate cyclase activating polypeptide. *Brain Res* **736**, 280-286 (1996).
123. Anderson, S.T. & Curlewis, J.D. PACAP stimulates dopamine neuronal activity in the medial basal hypothalamus and inhibits prolactin. *Brain Res* **790**, 343-346 (1998).
124. Arimura, A.*, et al.* Tissue distribution of PACAP as determined by RIA: highly abundant in the rat brain and testes. *Endocrinology* **129**, 2787-2789 (1991).
125. Ghatei, M.A.*, et al.* Distribution, molecular characterization of pituitary adenylate cyclase-activating polypeptide and its precursor encoding messenger RNA in human and rat tissues. *J Endocrinol* **136**, 159-166 (1993).
126. Masuo, Y.*, et al.* Regional distribution of pituitary adenylate cyclase activating polypeptide (PACAP) in the rat central nervous system as determined by sandwich-enzyme immunoassay. *Brain Res* **602**, 57-63 (1993).

127. Hannibal, J*., et al.* Gene expression of pituitary adenylate cyclase activating polypeptide (PACAP) in the rat hypothalamus. *Regul Pept* **55**, 133-148 (1995).
128. Piggins, H.D., Stamp, J.A., Burns, J., Rusak, B. & Semba, K. Distribution of pituitary adenylate cyclase activating polypeptide (PACAP) immunoreactivity in the hypothalamus and extended amygdala of the rat. *J Comp Neurol* **376**, 278-294 (1996).
129. Deutsch, P.J. & Sun, Y. The 38-amino acid form of pituitary adenylate cyclase-activating polypeptide stimulates dual signaling cascades in PC12 cells and promotes neurite outgrowth. *J Biol Chem* **267**, 5108-5113 (1992).
130. Osipenko, O.N., Barrie, A.P., Allen, J.M. & Gurney, A.M. Pituitary adenylyl cyclase-activating peptide activates multiple intracellular signaling pathways to regulate ion channels in PC12 cells. *J Biol Chem* **275**, 16626-16631 (2000).
131. Sakai, Y. Involvement of p38 MAP Kinase Pathway in the Synergistic Activation of PACAP mRNA Expression by NGF and PACAP in PC12h Cells. *Biochemical and Biophysical Research Communications* **285**, 656-661 (2001).
132. Barrie, A.P., Clohessy, A.M., Buensuceso, C.S., Rogers, M.V. & Allen, J.M. Pituitary adenylyl cyclase-activating peptide stimulates extracellular signal-regulated kinase 1 or 2 (ERK1/2) activity in a Ras-independent, mitogen-activated protein Kinase/ERK kinase 1 or 2-dependent manner in PC12 cells. *J Biol Chem* **272**, 19666-19671 (1997).
133. Lazarovici, P., Jiang, H. & Fink, D., Jr. The 38-amino-acid form of pituitary adenylate cyclase-activating polypeptide induces neurite outgrowth in PC12 cells that is dependent on protein kinase C and extracellular signal-regulated kinase but not on protein kinase A, nerve growth factor receptor tyrosine kinase, p21(ras) G protein, and pp60(c-src) cytoplasmic tyrosine kinase. *Mol Pharmacol* **54**, 547-558 (1998).
134. Ravni, A*., et al.* The neurotrophic effects of PACAP in PC12 cells: control by multiple transduction pathways. *J Neurochem* **98**, 321-329 (2006).
135. Gerdin, M.J. & Eiden, L.E. Regulation of PC12 cell differentiation by cAMP signaling to ERK independent of PKA: do all the connections add up? *Sci STKE* **2007**, pe15 (2007).
136. Christensen, A.E*., et al.* cAMP analog mapping of Epac1 and cAMP kinase. Discriminating analogs demonstrate that Epac and cAMP kinase act synergistically to promote PC-12 cell neurite extension. *J Biol Chem* **278**, 35394-35402 (2003).
137. Kiermayer, S*., et al.* Epac activation converts cAMP from a proliferative into a differentiation signal in PC12 cells. *Mol Biol Cell* **16**, 5639-5648 (2005).
138. Dworkin, S. & Mantamadiotis, T. Targeting CREB signalling in neurogenesis. *Expert Opin Ther Targets* **14**, 869-879 (2010).
139. Bouschet, T*., et al.* Stimulation of the ERK pathway by GTP-loaded Rap1 requires the concomitant activation of Ras, protein kinase C, and protein kinase A in neuronal cells. *J Biol Chem* **278**, 4778-4785 (2003).
140. Vossler, M.R*., et al.* cAMP activates MAP kinase and Elk-1 through a B-Raf- and Rap1-dependent pathway. *Cell* **89**, 73-82 (1997).
141. Cargnello, M. & Roux, P.P. Activation and function of the MAPKs and their substrates, the MAPK-activated protein kinases. *Microbiol Mol Biol Rev* **75**, 50-83 (2011).
142. Yukimasa, N., Isobe, K., Nagai, H., Takuwa, Y. & Nakai, T. Successive occupancy by immediate early transcriptional factors of the tyrosine

hydroxylase gene TRE and CRE sites in PACAP-stimulated PC12 pheochromocytoma cells. *Neuropeptides* **33**, 475-482 (1999).

143. Manecka, D.L., Mahmood, S.F., Grumolato, L., Lihrmann, I. & Anouar, Y. Pituitary adenylate cyclase-activating polypeptide (PACAP) promotes both survival and neuritogenesis in PC12 cells through activation of nuclear factor kappaB (NF-kappaB) pathway: involvement of extracellular signal-regulated kinase (ERK), calcium, and c-REL. *J Biol Chem* **288**, 14936-14948 (2013).
144. Vaudry, D*., et al.* Analysis of the PC12 cell transcriptome after differentiation with pituitary adenylate cyclase-activating polypeptide (PACAP). *J Neurochem* **83**, 1272-1284 (2002).
145. Grumolato, L*., et al.* PACAP and NGF regulate common and distinct traits of the sympathoadrenal lineage: effects on electrical properties, gene markers and transcription factors in differentiating PC12 cells. *European Journal of Neuroscience* **17**, 71-82 (2003).
146. Ebendal, T. Function and evolution in the NGF family and its receptors. *J Neurosci Res* **32**, 461-470 (1992).
147. Varon, S., Normura, J. & Shooter, E.M. Reversible dissociation of the mouse nerve growth factor protein into different subunits. *Biochemistry* **7**, 1296-1303 (1968).
148. Evans, B.A. & Richards, R.I. Genes for the alpha and gamma subunits of mouse nerve growth factor are contiguous. *EMBO J* **4**, 133-138 (1985).
149. Woodruff, N.R. & Neet, K.E. Inhibition of .beta. nerve growth factor binding to PC12 cells by .alpha. nerve growth factor and .gamma. nerve growth factor. *Biochemistry* **25**, 7967-7974 (1986).
150. Niederhauser, O*., et al.* NGF ligand alters NGF signaling via p75(NTR) and trkA. *J Neurosci Res* **61**, 263-272 (2000).
151. Fahnestock, M*., et al.* The nerve growth factor precursor proNGF exhibits neurotrophic activity but is less active than mature nerve growth factor. *J Neurochem* **89**, 581-592 (2004).
152. Fahnestock, M., Yu, G. & Coughlin, M.D. ProNGF: a neurotrophic or an apoptotic molecule? *Prog Brain Res* **146**, 101-110 (2004).
153. McAllister, A.K. Neurotrophins and neuronal differentiation in the central nervous system. *Cell Mol Life Sci* **58**, 1054-1060 (2001).
154. Aloe, L., Bracci-Laudiero, L., Bonini, S. & Manni, L. The expanding role of nerve growth factor: from neurotrophic activity to immunologic diseases. *Allergy* **52**, 883-894 (1997).
155. Dreyfus, C.F. Effects of nerve growth factor on cholinergic brain neurons. *Trends Pharmacol Sci* **10**, 145-149 (1989).
156. Allen, S.J. & Dawbarn, D. Clinical relevance of the neurotrophins and their receptors. *Clin Sci (Lond)* **110**, 175-191 (2006).
157. Spillantini, M.G*., et al.* Nerve growth factor mRNA and protein increase in hypothalamus in a mouse model of aggression. *Proc Natl Acad Sci U S A* **86**, 8555-8559 (1989).
158. Taglialatela, G., Angelucci, L., Scaccianoce, S., Foreman, P.J. & Perez-Polo, J.R. Nerve growth factor modulates the activation of the hypothalamo-pituitary-adrenocortical axis during the stress response. *Endocrinology* **129**, 2212-2218 (1991).
159. Aloe, L., Rocco, M.L., Bianchi, P. & Manni, L. Nerve growth factor: from the early discoveries to the potential clinical use. *J Transl Med* **10**, 239 (2012).

160. Eide, F.F., Lowenstein, D.H. & Reichardt, L.F. Neurotrophins and their receptors--current concepts and implications for neurologic disease. *Exp Neurol* **121**, 200-214 (1993).
161. Segal, R.A. & Greenberg, M.E. Intracellular signaling pathways activated by neurotrophic factors. *Annu Rev Neurosci* **19**, 463-489 (1996).
162. Clary, D.O., Weskamp, G., Austin, L.R. & Reichardt, L.F. TrkA cross-linking mimics neuronal responses to nerve growth factor. *Mol Biol Cell* **5**, 549-563 (1994).
163. Kim, Y., Seger, R., Suresh Babu, C.V., Hwang, S.Y. & Yoo, Y.S. A positive role of the PI3-K/Akt signaling pathway in PC12 cell differentiation. *Mol Cells* **18**, 353-359 (2004).
164. Waetzig, V. & Herdegen, T. The concerted signaling of ERK1/2 and JNKs is essential for PC12 cell neuritogenesis and converges at the level of target proteins. *Mol Cell Neurosci* **24**, 238-249 (2003).
165. Traverse, S., Gomez, N., Paterson, H., Marshall, C. & Cohen, P. Sustained activation of the mitogen-activated protein (MAP) kinase cascade may be required for differentiation of PC12 cells. Comparison of the effects of nerve growth factor and epidermal growth factor. *Biochem J* **288 (Pt 2)**, 351-355 (1992).
166. Kita, Y*., et al.* Microinjection of activated phosphatidylinositol-3 kinase induces process outgrowth in rat PC12 cells through the Rac-JNK signal transduction pathway. *J Cell Sci* **111 (Pt 7)**, 907-915 (1998).
167. Jeon, S., Park, J.K., Bae, C.D. & Park, J. NGF-induced moesin phosphorylation is mediated by the PI3K, Rac1 and Akt and required for neurite formation in PC12 cells. *Neurochem Int* **56**, 810-818 (2010).
168. Widmann, C., Gibson, S., Jarpe, M.B. & Johnson, G.L. Mitogen-activated protein kinase: conservation of a three-kinase module from yeast to human. *Physiol Rev* **79**, 143-180 (1999).
169. Kao, S., Jaiswal, R.K., Kolch, W. & Landreth, G.E. Identification of the mechanisms regulating the differential activation of the mapk cascade by epidermal growth factor and nerve growth factor in PC12 cells. *J Biol Chem* **276**, 18169-18177 (2001).
170. Marshall, C.J. Specificity of receptor tyrosine kinase signaling: transient versus sustained extracellular signal-regulated kinase activation. *Cell* **80**, 179-185 (1995).
171. Heasley, L.E*., et al.* GTPase-deficient G alpha 16 and G alpha q induce PC12 cell differentiation and persistent activation of cJun NH2-terminal kinases. *Mol Cell Biol* **16**, 648-656 (1996).
172. Leppa, S., Saffrich, R., Ansorge, W. & Bohmann, D. Differential regulation of c-Jun by ERK and JNK during PC12 cell differentiation. *EMBO J* **17**, 4404-4413 (1998).
173. Morooka, T. & Nishida, E. Requirement of p38 mitogen-activated protein kinase for neuronal differentiation in PC12 cells. *J Biol Chem* **273**, 24285-24288 (1998).
174. Yu, P.J., Ferrari, G., Galloway, A.C., Mignatti, P. & Pintucci, G. Basic fibroblast growth factor (FGF-2): the high molecular weight forms come of age. *J Cell Biochem* **100**, 1100-1108 (2007).

175. Gomez-Pinilla, F., Lee, J.W. & Cotman, C.W. Basic FGF in adult rat brain: cellular distribution and response to entorhinal lesion and fimbria-fornix transection. *J Neurosci* **12**, 345-355 (1992).
176. Gospodarowicz, D., Cheng, J., Lui, G.M., Baird, A. & Bohlent, P. Isolation of brain fibroblast growth factor by heparin-Sepharose affinity chromatography: identity with pituitary fibroblast growth factor. *Proc Natl Acad Sci U S A* **81**, 6963-6967 (1984).
177. Esch, F*., et al.* Primary structure of bovine pituitary basic fibroblast growth factor (FGF) and comparison with the amino-terminal sequence of bovine brain acidic FGF. *Proc Natl Acad Sci U S A* **82**, 6507-6511 (1985).
178. Imamura, T., Tokita, Y. & Mitsui, Y. Purification of basic FGF receptors from rat brain. *Biochem Biophys Res Commun* **155**, 583-590 (1988).
179. Grothe, C., Otto, D. & Unsicker, K. Basic fibroblast growth factor promotes in vitro survival and cholinergic development of rat septal neurons: comparison with the effects of nerve growth factor. *Neuroscience* **31**, 649-661 (1989).
180. Otto, D., Frotscher, M. & Unsicker, K. Basic fibroblast growth factor and nerve growth factor administered in gel foam rescue medial septal neurons after fimbria fornix transection. *J Neurosci Res* **22**, 83-91 (1989).
181. Dono, R., Texido, G., Dussel, R., Ehmke, H. & Zeller, R. Impaired cerebral cortex development and blood pressure regulation in FGF-2-deficient mice. *EMBO J* **17**, 4213-4225 (1998).
182. Burgess, W.H. & Maciag, T. The heparin-binding (fibroblast) growth factor family of proteins. *Annu Rev Biochem* **58**, 575-606 (1989).
183. Lin, D.A. & Finklestein, S.P. Basic fibroblast growth factor: A treatment for stroke? *Neuroscientist* **3**, 247-250 (1997).
184. Gospodarowicz, D., Ferrara, N., Schweigerer, L. & Neufeld, G. Structural characterization and biological functions of fibroblast growth factor. *Endocr Rev* **8**, 95-114 (1987).
185. Mudo, G*., et al.* The FGF-2/FGFRs neurotrophic system promotes neurogenesis in the adult brain. *J Neural Transm* **116**, 995-1005 (2009).
186. Matsuda, S., Saito, H. & Nishiyama, N. Effect of basic fibroblast growth factor on neurons cultured from various regions of postnatal rat brain. *Brain Res* **520**, 310-316 (1990).
187. Eckenstein, F.P., Shipley, G.D. & Nishi, R. Acidic and basic fibroblast growth factors in the nervous system: distribution and differential alteration of levels after injury of central versus peripheral nerve. *J Neurosci* **11**, 412-419 (1991).
188. Abe, K., Takayanagi, M. & Saito, H. Effects of recombinant human basic fibroblast growth factor and its modified protein CS23 on survival of primary cultured neurons from various regions of fetal rat brain. *Jpn J Pharmacol* **53**, 221-227 (1990).
189. Abe, K., Takayanagi, M. & Saito, H. A comparison of neurotrophic effects of epidermal growth factor and basic fibroblast growth factor in primary cultured neurons from various regions of fetal rat brain. *Jpn J Pharmacol* **54**, 45-51 (1990).
190. Abe, K. & Saito, H. Effects of basic fibroblast growth factor on central nervous system functions. *Pharmacol Res* **43**, 307-312 (2001).

191. Bethel, A., Kirsch, J.R., Koehler, R.C., Finklestein, S.P. & Traystman, R.J. Intravenous basic fibroblast growth factor decreases brain injury resulting from focal ischemia in cats. *Stroke* **28**, 609-615; discussion 615-606 (1997).
192. Ay, H., Ay, I., Koroshetz, W.J. & Finklestein, S.P. Potential usefulness of basic fibroblast growth factor as a treatment for stroke. *Cerebrovasc Dis* **9**, 131-135 (1999).
193. Matsuda, S., Saito, H. & Nishiyama, N. Basic fibroblast growth factor ameliorates rotational behavior of substantia nigral-transplanted rats with lesions of the dopaminergic nigrostriatal neurons. *Jpn J Pharmacol* **59**, 365-370 (1992).
194. Wagner, J.A. & D'Amore, P.A. Neurite outgrowth induced by an endothelial cell mitogen isolated from retina. *J Cell Biol* **103**, 1363-1367 (1986).
195. Rydel, R.E. & Greene, L.A. Acidic and basic fibroblast growth factors promote stable neurite outgrowth and neuronal differentiation in cultures of PC12 cells. *J Neurosci* **7**, 3639-3653 (1987).
196. Hausott, B., Schlick, B., Vallant, N., Dorn, R. & Klimaschewski, L. Promotion of neurite outgrowth by fibroblast growth factor receptor 1 overexpression and lysosomal inhibition of receptor degradation in pheochromocytoma cells and adult sensory neurons. *Neuroscience* **153**, 461-473 (2008).
197. Maher, P. p38 mitogen-activated protein kinase activation is required for fibroblast growth factor-2-stimulated cell proliferation but not differentiation. *J Biol Chem* **274**, 17491-17498 (1999).
198. Hadari, Y.R., Kouhara, H., Lax, I. & Schlessinger, J. Binding of Shp2 tyrosine phosphatase to FRS2 is essential for fibroblast growth factor-induced PC12 cell differentiation. *Mol Cell Biol* **18**, 3966-3973 (1998).
199. Lonic, A.*, et al.* Phosphorylation of serine 779 in fibroblast growth factor receptor 1 and 2 by protein kinase C(epsilon) regulates Ras/mitogen-activated protein kinase signaling and neuronal differentiation. *J Biol Chem* **288**, 14874-14885 (2013).
200. Cohen, S. The stimulation of epidermal proliferation by a specific protein (EGF). *Dev Biol* **12**, 394-407 (1965).
201. Kato, M., Mizuguchi, M. & Takashima, S. Developmental changes of epidermal growth factor-like immunoreactivity in the human fetal brain. *J Neurosci Res* **42**, 486-492 (1995).
202. Estrada, C. & Villalobo, A. Epidermal Growth Factor Receptor in the Adult Brain. in *The Cell Cycle in the Central Nervous System* (ed. Janigro, D.) 265-277 (Humana Press, 2006).
203. Piao, Y.S., Iwakura, Y., Takei, N. & Nawa, H. Differential distributions of peptides in the epidermal growth factor family and phosphorylation of ErbB1 receptor in adult rat brain. *Neuroscience Letters* **390**, 21-24 (2005).
204. Oyagi, A. & Hara, H. Essential roles of heparin-binding epidermal growth factor-like growth factor in the brain. *CNS Neurosci Ther* **18**, 803-810 (2012).
205. Irwin, D.J., Lee, V.M. & Trojanowski, J.Q. Parkinson's disease dementia: convergence of alpha-synuclein, tau and amyloid-beta pathologies. *Nat Rev Neurosci* **14**, 626-636 (2013).
206. Hochstrasser, T., Ehrlich, D., Marksteiner, J., Sperner-Unterweger, B. & Humpel, C. Matrix metalloproteinase-2 and epidermal growth factor are decreased in platelets of Alzheimer patients. *Curr Alzheimer Res* **9**, 982-989 (2012).

207. Nakada, M.*, et al.* Aberrant Signaling Pathways in Glioma. *Cancers* **3**, 3242-3278 (2011).
208. Wu, C.F. & Howard, B.D. K252a-potentiation of EGF-induced neurite outgrowth from PC12 cells is not mimicked or blocked by other protein kinase activators or inhibitors. *Brain Res Dev Brain Res* **86**, 217-226 (1995).
209. Erhardt, J.A. & Pittman, R.N. Ectopic p21(WAF1) expression induces differentiation-specific cell cycle changes in PC12 cells characteristic of nerve growth factor treatment. *J Biol Chem* **273**, 23517-23523 (1998).
210. Gunning, P.W., Landreth, G.E., Bothwell, M.A. & Shooter, E.M. Differential and synergistic actions of nerve growth factor and cyclic AMP in PC12 cells. *J Cell Biol* **89**, 240-245 (1981).
211. Sakai, Y.*, et al.* Involvement of p38 MAP kinase pathway in the synergistic activation of PACAP mRNA expression by NGF and PACAP in PC12h cells. *Biochem Biophys Res Commun* **285**, 656-661 (2001).
212. Hansen, T.O., Rehfeld, J.F. & Nielsen, F.C. Cyclic AMP-induced neuronal differentiation via activation of p38 mitogen-activated protein kinase. *J Neurochem* **75**, 1870-1877 (2000).
213. Sakai, Y.*, et al.* PACAP activates Rac1 and synergizes with NGF to activate ERK1/2, thereby inducing neurite outgrowth in PC12 cells. *Brain Res Mol Brain Res* **123**, 18-26 (2004).
214. Wolff, P.*, et al.* Characterization of myosin V from PC12 cells. *Biochem Biophys Res Commun* **262**, 98-102 (1999).
215. Mark, M.D. & Storm, D.R. Coupling of epidermal growth factor (EGF) with the antiproliferative activity of cAMP induces neuronal differentiation. *J Biol Chem* **272**, 17238-17244 (1997).
216. Yao, H.*, et al.* Cyclic adenosine monophosphate can convert epidermal growth factor into a differentiating factor in neuronal cells. *J Biol Chem* **270**, 20748-20753 (1995).
217. Jordan, J.D., Landau, E.M. & Iyengar, R. Signaling networks: the origins of cellular multitasking. *Cell* **103**, 193-200 (2000).
218. Eungdamrong, N.J. & Iyengar, R. Modeling cell signaling networks. *Biol Cell* **96**, 355-362 (2004).
219. Silverman, E., Frodin, M., Gammeltoft, S. & Maller, J.L. Activation of p90 Rsk1 is sufficient for differentiation of PC12 cells. *Mol Cell Biol* **24**, 10573-10583 (2004).
220. Xing, J., Kornhauser, J.M., Xia, Z., Thiele, E.A. & Greenberg, M.E. Nerve growth factor activates extracellular signal-regulated kinase and p38 mitogen-activated protein kinase pathways to stimulate CREB serine 133 phosphorylation. *Mol Cell Biol* **18**, 1946-1955 (1998).
221. Obara, Y.*, et al.* ERK5 Activity Is Required for Nerve Growth Factor-induced Neurite Outgrowth and Stabilization of Tyrosine Hydroxylase in PC12 Cells. *Journal of Biological Chemistry* **284**, 23564-23573 (2009).
222. Chen, M.C.*, et al.* Involvement of cAMP in nerve growth factor-triggered p35/Cdk5 activation and differentiation in PC12 cells. *Am J Physiol Cell Physiol* **299**, C516-527 (2010).
223. Shi, G.X., Jin, L. & Andres, D.A. Src-dependent TrkA transactivation is required for pituitary adenylate cyclase-activating polypeptide 38-mediated Rit activation and neuronal differentiation. *Mol Biol Cell* **21**, 1597-1608 (2010).

224. Zhang, W*., et al.* GSK3β modulates PACAP-induced neuritogenesis in PC12 cells by acting downstream of Rap1 in a caveolae-dependent manner. *Cellular Signalling* **21**, 237-245 (2009).
225. Kremer, N.E*., et al.* Signal transduction by nerve growth factor and fibroblast growth factor in PC12 cells requires a sequence of src and ras actions. *J Cell Biol* **115**, 809-819 (1991).
226. Waetzig, V. & Herdegen, T. MEKK1 controls neurite regrowth after experimental injury by balancing ERK1/2 and JNK2 signaling. *Mol Cell Neurosci* **30**, 67-78 (2005).
227. Kandel, E.R.S.J.H.J.T.M. *Principles of neural science*, (McGraw-Hill, Health Professions Division, New York, 2000).
228. Nicholls, J.G. *From neuron to brain*, (Sinauer Associates, Sunderland, Mass., 2012).
229. Meijering, E. Neuron tracing in perspective. *Cytometry A* **77**, 693-704 (2010).
230. Das, K.P., Freudenrich, T.M. & Mundy, W.R. Assessment of PC12 cell differentiation and neurite growth: a comparison of morphological and neurochemical measures. *Neurotoxicol Teratol* **26**, 397-406 (2004).
231. Radio, N.M., Breier, J.M., Shafer, T.J. & Mundy, W.R. Assessment of chemical effects on neurite outgrowth in PC12 cells using high content screening. *Toxicol Sci* **105**, 106-118 (2008).
232. Wang, D*., et al.* HCA-Vision: Automated Neurite Outgrowth Analysis. *Journal of Biomolecular Screening* **15**, 1165-1170 (2010).
233. Wu, C., Schulte, J., Sepp, K.J., Littleton, J.T. & Hong, P. Automatic robust neurite detection and morphological analysis of neuronal cell cultures in high-content screening. *Neuroinformatics* **8**, 83-100 (2010).
234. Dehmelt, L., Poplawski, G., Hwang, E. & Halpain, S. NeuriteQuant: an open source toolkit for high content screens of neuronal morphogenesis. *BMC Neurosci* **12**, 100 (2011).
235. Ho, S.Y*., et al.* NeurphologyJ: an automatic neuronal morphology quantification method and its application in pharmacological discovery. *BMC Bioinformatics* **12**, 230 (2011).
236. Xiao, J. & Liu, Y. Differential roles of ERK and JNK in early and late stages of neuritogenesis: a study in a novel PC12 model system. *Journal of Neurochemistry* **86**, 1516-1523 (2003).
237. Shi, G.X. & Andres, D.A. Rit contributes to nerve growth factor-induced neuronal differentiation via activation of B-Raf-extracellular signal-regulated kinase and p38 mitogen-activated protein kinase cascades. *Mol Cell Biol* **25**, 830-846 (2005).
238. Read, D.E. & Gorman, A.M. Involvement of Akt in neurite outgrowth. *Cell Mol Life Sci* **66**, 2975-2984 (2009).
239. Markus, A., Patel, T.D. & Snider, W.D. Neurotrophic factors and axonal growth. *Curr Opin Neurobiol* **12**, 523-531 (2002).
240. Hynds, D.L., Spencer, M.L., Andres, D.A. & Snow, D.M. Rit promotes MEK-independent neurite branching in human neuroblastoma cells. *J Cell Sci* **116**, 1925-1935 (2003).
241. Li, X., Huang, Y., Jiang, J. & Frank, S.J. Synergy in ERK activation by cytokine receptors and tyrosine kinase growth factor receptors. *Cell Signal* **23**, 417-424 (2011).

242. Choung, P.H., Seo, B.M., Chung, C.P., Yamada, K.M. & Jang, J.H. Synergistic activity of fibronectin and fibroblast growth factor receptors on neuronal adhesion and neurite extension through extracellular signal-regulated kinase pathway. *Biochem Biophys Res Commun* **295**, 898-902 (2002).
243. Cardillo, T.M., Trisal, P., Arrojo, R., Goldenberg, D.M. & Chang, C.H. Targeting both IGF-1R and mTOR synergistically inhibits growth of renal cell carcinoma in vitro. *Bmc Cancer* **13**, 170 (2013).
244. Al-Lazikani, B., Banerji, U. & Workman, P. Combinatorial drug therapy for cancer in the post-genomic era. *Nat Biotechnol* **30**, 679-692 (2012).
245. Borisov, N*., et al.* Systems-level interactions between insulin-EGF networks amplify mitogenic signaling. *Mol Syst Biol* **5**, 256 (2009).
246. Jin, G., Zhao, H., Zhou, X. & Wong, S.T. An enhanced Petri-net model to predict synergistic effects of pairwise drug combinations from gene microarray data. *Bioinformatics* **27**, i310-316 (2011).
247. Miller, M.L*., et al.* Drug Synergy Screen and Network Modeling in Dedifferentiated Liposarcoma Identifies CDK4 and IGF1R as Synergistic Drug Targets. *Sci Signal* **6**, ra85 (2013).
248. Yan, H., Zhang, B., Li, S. & Zhao, Q. A formal model for analyzing drug combination effects and its application in TNF-alpha-induced NFkappaB pathway. *BMC Syst Biol* **4**, 50 (2010).
249. Wang, Z.W., Kuruoglu, E.E., Yang, X.K., Xu, Y. & Huang, T.S. Time Varying Dynamic Bayesian Network for Nonstationary Events Modeling and Online Inference. *Ieee T Signal Proces* **59**, 1553-1568 (2011).
250. Grzegorczyk, M. & Husmeier, D. A non-homogeneous dynamic Bayesian network with sequentially coupled interaction parameters for applications in systems and synthetic biology. *Stat Appl Genet Mol Biol* **11**(2012).
251. Villoslada, P. & Baranzini, S. Data integration and systems biology approaches for biomarker discovery: challenges and opportunities for multiple sclerosis. *J Neuroimmunol* **248**, 58-65 (2012).
252. Hwang, D*., et al.* A data integration methodology for systems biology. *Proc Natl Acad Sci U S A* **102**, 17296-17301 (2005).
253. Anvar, S.Y., t Hoen, P.A. & Tucker, A. The identification of informative genes from multiple datasets with increasing complexity. *BMC Bioinformatics* **11**, 32 (2010).
254. Kirk, P., Griffin, J.E., Savage, R.S., Ghahramani, Z. & Wild, D.L. Bayesian correlated clustering to integrate multiple datasets. *Bioinformatics* **28**, 3290-3297 (2012).
255. Wang, Y., Joshi, T., Zhang, X.S., Xu, D. & Chen, L. Inferring gene regulatory networks from multiple microarray datasets. *Bioinformatics* **22**, 2413-2420 (2006).
256. Kato, T., Tsuda, K. & Asai, K. Selective integration of multiple biological data for supervised network inference. *Bioinformatics* **21**, 2488-2495 (2005).
257. Bo-Lin, C., Li-Zhi, L. & Fang-Xiang, W. Inferring gene regulatory networks from multiple time course gene expression datasets. in *Systems Biology (ISB), 2011 IEEE International Conference on* 12-17 (2011).
258. Gupta, R*., et al.* A computational framework for gene regulatory network inference that combines multiple methods and datasets. *BMC Syst Biol* **5**, 52 (2011).

259. Werhli, A.V., Grzegorczyk, M. & Husmeier, D. Comparative evaluation of reverse engineering gene regulatory networks with relevance networks, graphical gaussian models and bayesian networks. *Bioinformatics* **22**, 2523-2531 (2006).
260. Conesa, A., Prats-Montalbán, J.M., Tarazona, S., Nueda, M.J. & Ferrer, A. A multiway approach to data integration in systems biology based on Tucker3 and N-PLS. *Chemometrics and Intelligent Laboratory Systems* **104**, 101-111 (2010).
261. Dagum, P. & Luby, M. Approximating probabilistic inference in Bayesian belief networks is NP-hard. *Artif Intell* **60**, 141-153 (1993).
262. Chickering, D.M., Heckerman, D. & Meek, C. Large-Sample Learning of Bayesian Networks is NP-Hard. *J. Mach. Learn. Res.* **5**, 1287-1330 (2004).
263. Ann Arbor Conference on Graph, T. *New directions in the theory of graphs; proceedings. Edited by Frank Harary*, (Academic Press, New York, 1973).
264. Robinson, R.W. Counting unlabeled acyclic digraphs. in *Combinatorial Mathematics V*, Vol. 622 (ed. Little, C.C.) 28-43 (Springer Berlin Heidelberg, 1977).
265. Hill, S.M.*, et al.* Bayesian inference of signaling network topology in a cancer cell line. *Bioinformatics* **28**, 2804-2810 (2012).
266. Hoeting, J.A., Madigan, D., Raftery, A.E. & Volinsky, C.T. Bayesian Model Averaging: A Tutorial. *Statistical Science* **14**, 382-401 (1999).
267. Bellman, R. On the Theory of Dynamic Programming. *Proc Natl Acad Sci U S A* **38**, 716-719 (1952).
268. Eddy, S.R. What is dynamic programming? *Nat Biotechnol* **22**, 909-910 (2004).
269. Jaakkola, T., Sontag, D., Globerson, A. & Meila, M. Learning Bayesian Network Structure using LP Relaxations. in *13th International Conference on Articial Intelligence and Statistics (AISTATS)*, Vol. 9 (JMLR: W&CP, Chia Laguna Resort, Sardinia, Italy, 2010).
270. Yung, L.Y.*, et al.* Nerve growth factor-induced stimulation of p38 mitogen-activated protein kinase in PC12 cells is partially mediated via Gi/o proteins. *Cellular Signalling* **20**, 1538-1544 (2008).
271. Meijering, E.*, et al.* Design and validation of a tool for neurite tracing and analysis in fluorescence microscopy images. *Cytometry A* **58**, 167-176 (2004).
272. Zhang, Z.*, et al.* Direct Rho-associated kinase inhibition [correction of inhibiton] induces cofilin dephosphorylation and neurite outgrowth in PC-12 cells. *Cell Mol Biol Lett* **11**, 12-29 (2006).
273. Nabiuni, M.*, et al.* In vitro effects of fetal rat cerebrospinal fluid on viability and neuronal differentiation of PC12 cells. *Fluids Barriers CNS* **9**, 8 (2012).
274. Barrera, N.P., Morales, B., Torres, S. & Villalon, M. Principles: mechanisms and modeling of synergism in cellular responses. *Trends Pharmacol Sci* **26**, 526-532 (2005).
275. Chou, T.C. Theoretical basis, experimental design, and computerized simulation of synergism and antagonism in drug combination studies. *Pharmacol Rev* **58**, 621-681 (2006).
276. Nakajima, T.*, et al.* The signal-dependent coactivator CBP is a nuclear target for pp90RSK. *Cell* **86**, 465-474 (1996).
277. Zhang, Y.*, et al.* UVA induces Ser381 phosphorylation of p90RSK/MAPKAP-K1 via ERK and JNK pathways. *J Biol Chem* **276**, 14572-14580 (2001).

278. Fomina-Yadlin, D*., et al.* Small-molecule inducers of insulin expression in pancreatic alpha-cells. *Proc Natl Acad Sci U S A* **107**, 15099-15104 (2010).
279. Park, Y.S. & Cho, N.J. EGFR and PKC are involved in the activation of ERK1/2 and p90 RSK and the subsequent proliferation of SNU-407 colon cancer cells by muscarinic acetylcholine receptors. *Mol Cell Biochem* **370**, 191-198 (2012).
280. Anjum, R. & Blenis, J. The RSK family of kinases: emerging roles in cellular signalling. *Nat Rev Mol Cell Biol* **9**, 747-758 (2008).
281. Romeo, Y., Zhang, X. & Roux, P.P. Regulation and function of the RSK family of protein kinases. *Biochem J* **441**, 553-569 (2012).
282. Kamata, Y., Shiraga, H., Tai, A., Kawamoto, Y. & Gohda, E. Induction of neurite outgrowth in PC12 cells by the medium-chain fatty acid octanoic acid. *Neuroscience* **146**, 1073-1081 (2007).
283. Riese, U., Ziegler, E. & Hamburger, M. Militarinone A induces differentiation in PC12 cells via MAP and Akt kinase signal transduction pathways. *FEBS Lett* **577**, 455-459 (2004).
284. Xu, H., Dhanasekaran, D.N., Lee, C.M. & Reddy, E.P. Regulation of neurite outgrowth by interactions between the scaffolding protein, JNK-associated leucine zipper protein, and neuronal growth-associated protein superior cervical ganglia clone 10. *J Biol Chem* **285**, 3548-3553 (2010).
285. Chen, X., Fu, W., Tung, C.E. & Ward, N.L. Angiopoietin-1 induces neurite outgrowth of PC12 cells in a Tie2-independent, beta1-integrin-dependent manner. *Neurosci Res* **64**, 348-354 (2009).
286. Klesse, L.J., Meyers, K.A., Marshall, C.J. & Parada, L.F. Nerve growth factor induces survival and differentiation through two distinct signaling cascades in PC12 cells. *Oncogene* **18**, 2055-2068 (1999).
287. Yan, C., Liang, Y., Nylander, K.D. & Schor, N.F. TrkA as a life and death receptor: receptor dose as a mediator of function. *Cancer Res* **62**, 4867-4875 (2002).
288. Read, D.E., Reed Herbert, K. & Gorman, A.M. Heat shock enhances NGF-induced neurite elongation which is not mediated by Hsp25 in PC12 cells. *Brain Res* **1221**, 14-23 (2008).
289. Chen, J.Y., Lin, J.R., Cimprich, K.A. & Meyer, T. A two-dimensional ERK-AKT signaling code for an NGF-triggered cell-fate decision. *Mol Cell* **45**, 196-209 (2012).
290. Kopperud, R., Krakstad, C., Selheim, F. & Doskeland, S.O. cAMP effector mechanisms. Novel twists for an 'old' signaling system. *FEBS Lett* **546**, 121-126 (2003).
291. Gerits, N., Kostenko, S., Shiryaev, A., Johannessen, M. & Moens, U. Relations between the mitogen-activated protein kinase and the cAMP-dependent protein kinase pathways: comradeship and hostility. *Cell Signal* **20**, 1592-1607 (2008).
292. Moxham, C.M., Tabrizchi, A., Davis, R.J. & Malbon, C.C. Jun N-terminal kinase mediates activation of skeletal muscle glycogen synthase by insulin in vivo. *J Biol Chem* **271**, 30765-30773 (1996).
293. Samaga, R., Saez-Rodriguez, J., Alexopoulos, L.G., Sorger, P.K. & Klamt, S. The logic of EGFR/ErbB signaling: theoretical properties and analysis of high-throughput data. *PLoS Comput Biol* **5**, e1000438 (2009).
294. Eriksson, M., Taskinen, M. & Leppa, S. Mitogen activated protein kinase-dependent activation of c-Jun and c-Fos is required for neuronal

differentiation but not for growth and stress response in PC12 cells. *J Cell Physiol* **210**, 538-548 (2007).

295. Marek, L*., et al.* Multiple signaling conduits regulate global differentiation-specific gene expression in PC12 cells. *J Cell Physiol* **201**, 459-469 (2004).
296. Zentrich, E., Han, S.Y., Pessoa-Brandao, L., Butterfield, L. & Heasley, L.E. Collaboration of JNKs and ERKs in nerve growth factor regulation of the neurofilament light chain promoter in PC12 cells. *J Biol Chem* **277**, 4110-4118 (2002).
297. Smith, J.A., Poteet-Smith, C.E., Malarkey, K. & Sturgill, T.W. Identification of an extracellular signal-regulated kinase (ERK) docking site in ribosomal S6 kinase, a sequence critical for activation by ERK in vivo. *J Biol Chem* **274**, 2893-2898 (1999).
298. Tapias, V., Greenamyre, J.T. & Watkins, S.C. Automated imaging system for fast quantitation of neurons, cell morphology and neurite morphometry in vivo and in vitro. *Neurobiol Dis* **54**, 158-168 (2013).
299. MacLeod, D*., et al.* The familial Parkinsonism gene LRRK2 regulates neurite process morphology. *Neuron* **52**, 587-593 (2006).
300. Valero, T. & Kintzios, S. Novel aspects of neuronal differentiation in vitro and monitoring with advanced biosensor tools. *Curr Med Chem* **18**, 900-908 (2011).
301. Goldberg, J.L. How does an axon grow? *Genes & Development* **17**, 941-958 (2003).
302. Connolly, G.P. Cell imaging and morphology: application to studies of inherited purine metabolic disorders. *Pharmacol Ther* **90**, 267-281 (2001).
303. Luo, L. & O'Leary, D.D. Axon retraction and degeneration in development and disease. *Annu Rev Neurosci* **28**, 127-156 (2005).
304. Herbst, K.J., Allen, M.D. & Zhang, J. Spatiotemporally regulated protein kinase A activity is a critical regulator of growth factor-stimulated extracellular signal-regulated kinase signaling in PC12 cells. *Mol Cell Biol* **31**, 4063-4075 (2011).
305. Yao, H., York, R.D., Misra-Press, A., Carr, D.W. & Stork, P.J. The cyclic adenosine monophosphate-dependent protein kinase (PKA) is required for the sustained activation of mitogen-activated kinases and gene expression by nerve growth factor. *J Biol Chem* **273**, 8240-8247 (1998).
306. Obara, Y., Labudda, K., Dillon, T.J. & Stork, P.J. PKA phosphorylation of Src mediates Rap1 activation in NGF and cAMP signaling in PC12 cells. *J Cell Sci* **117**, 6085-6094 (2004).
307. Seow, K.H., Zhou, L., Stephanopoulos, G. & Too, H.P. c-Jun N-terminal kinase in synergistic neurite outgrowth in PC12 cells mediated through P90RSK. *BMC Neurosci* **14**, 153 (2013).
308. Chaturvedi, D., Poppleton, H.M., Stringfield, T., Barbier, A. & Patel, T.B. Subcellular localization and biological actions of activated RSK1 are determined by its interactions with subunits of cyclic AMP-dependent protein kinase. *Mol Cell Biol* **26**, 4586-4600 (2006).
309. Chaturvedi, D., Cohen, M.S., Taunton, J. & Patel, T.B. The PKARIalpha subunit of protein kinase A modulates the activation of p90RSK1 and its function. *J Biol Chem* **284**, 23670-23681 (2009).
310. Gao, X., Chaturvedi, D. & Patel, T.B. p90 ribosomal S6 kinase 1 (RSK1) and the catalytic subunit of protein kinase A (PKA) compete for binding the

pseudosubstrate region of PKAR1alpha: role in the regulation of PKA and RSK1 activities. *J Biol Chem* **285**, 6970-6979 (2010).

311. Cheng, X., Ji, Z., Tsalkova, T. & Mei, F. Epac and PKA: a tale of two intracellular cAMP receptors. *Acta Biochim Biophys Sin (Shanghai)* **40**, 651-662 (2008).
312. Grandoch, M., Roscioni, S.S. & Schmidt, M. The role of Epac proteins, novel cAMP mediators, in the regulation of immune, lung and neuronal function. *Br J Pharmacol* **159**, 265-284 (2010).
313. Shi, G.X., Rehmann, H. & Andres, D.A. A novel cyclic AMP-dependent Epac-Rit signaling pathway contributes to PACAP38-mediated neuronal differentiation. *Mol Cell Biol* **26**, 9136-9147 (2006).
314. van Pelt, J., van Ooyen, A. & Uylings, H.B. The need for integrating neuronal morphology databases and computational environments in exploring neuronal structure and function. *Anat Embryol (Berl)* **204**, 255-265 (2001).
315. Van Ooyen, A. Competition in neurite outgrowth and the development of nerve connections. *Prog Brain Res* **147**, 81-99 (2005).
316. Schmitz, S.K.*, et al.* Automated analysis of neuronal morphology, synapse number and synaptic recruitment. *J Neurosci Methods* **195**, 185-193 (2011).
317. Homma, N.*, et al.* Kinesin superfamily protein 2A (KIF2A) functions in suppression of collateral branch extension. *Cell* **114**, 229-239 (2003).
318. Chen, Y., Tian, X., Kim, W.Y. & Snider, W.D. Adenomatous polyposis coli regulates axon arborization and cytoskeleton organization via its N-terminus. *PLoS One* **6**, e24335 (2011).
319. Rosso, S.B., Sussman, D., Wynshaw-Boris, A. & Salinas, P.C. Wnt signaling through Dishevelled, Rac and JNK regulates dendritic development. *Nat Neurosci* **8**, 34-42 (2005).
320. Riederer, B.M. Microtubule-associated protein 1B, a growth-associated and phosphorylated scaffold protein. *Brain Res Bull* **71**, 541-558 (2007).
321. Zhong, J.*, et al.* Raf kinase signaling functions in sensory neuron differentiation and axon growth in vivo. *Nat Neurosci* **10**, 598-607 (2007).
322. Newbern, J.M.*, et al.* Specific functions for ERK/MAPK signaling during PNS development. *Neuron* **69**, 91-105 (2011).
323. Qiang, L., Yu, W., Liu, M., Solowska, J.M. & Baas, P.W. Basic fibroblast growth factor elicits formation of interstitial axonal branches via enhanced severing of microtubules. *Mol Biol Cell* **21**, 334-344 (2010).
324. Lewis, T.L., Jr., Courchet, J. & Polleux, F. Cell biology in neuroscience: Cellular and molecular mechanisms underlying axon formation, growth, and branching. *J Cell Biol* **202**, 837-848 (2013).
325. Williamson, T., Gordon-Weeks, P.R., Schachner, M. & Taylor, J. Microtubule reorganization is obligatory for growth cone turning. *Proc Natl Acad Sci U S A* **93**, 15221-15226 (1996).
326. Challacombe, J.F., Snow, D.M. & Letourneau, P.C. Dynamic microtubule ends are required for growth cone turning to avoid an inhibitory guidance cue. *J Neurosci* **17**, 3085-3095 (1997).
327. Auer, M., Hausott, B. & Klimaschewski, L. Rho GTPases as regulators of morphological neuroplasticity. *Ann Anat* **193**, 259-266 (2011).
328. Govek, E.E., Newey, S.E. & Van Aelst, L. The role of the Rho GTPases in neuronal development. *Genes Dev* **19**, 1-49 (2005).

329. Krishna, M. & Narang, H. The complexity of mitogen-activated protein kinases (MAPKs) made simple. *Cell Mol Life Sci* **65**, 3525-3544 (2008).
330. Tank, E.M., Rodgers, K.E. & Kenyon, C. Spontaneous age-related neurite branching in Caenorhabditis elegans. *J Neurosci* **31**, 9279-9288 (2011).
331. Shen, Y.H.*, et al.* Cross-talk between JNK/SAPK and ERK/MAPK pathways: sustained activation of JNK blocks ERK activation by mitogenic factors. *J Biol Chem* **278**, 26715-26721 (2003).
332. Fey, D., Croucher, D.R., Kolch, W. & Kholodenko, B.N. Crosstalk and signaling switches in mitogen-activated protein kinase cascades. *Front Physiol* **3**, 355 (2012).
333. Papin, J.A., Hunter, T., Palsson, B.O. & Subramaniam, S. Reconstruction of cellular signalling networks and analysis of their properties. *Nat Rev Mol Cell Biol* **6**, 99-111 (2005).
334. Santos, S.D., Verveer, P.J. & Bastiaens, P.I. Growth factor-induced MAPK network topology shapes Erk response determining PC-12 cell fate. *Nat Cell Biol* **9**, 324-330 (2007).
335. Greco, W.R., Bravo, G. & Parsons, J.C. The search for synergy: a critical review from a response surface perspective. *Pharmacol Rev* **47**, 331-385 (1995).
336. Heckerman, D., Geiger, D. & Chickering, D.M. Learning Bayesian Networks - the Combination of Knowledge and Statistical-Data. *Mach Learn* **20**, 197-243 (1995).
337. Silander, T. & Myllymaki, P. A Simple Approach for Finding the Globally Optimal Bayesian Network Structure. in *22nd Annual Conference on Uncertainty in Artificial Intelligence (UAI-06)* (2006).
338. Koivisto, M. & Sood, K. Exact Bayesian structure discovery in Bayesian networks. *Journal of Machine Learning Research* **5**, 549-573 (2004).
339. Parviainen, P. & Koivisto, M. Exact structure discovery in Bayesian networks with less space. in *Proceedings of the Twenty-Fifth Conference on Uncertainty in Artificial Intelligence* 436-443 (AUAI Press, Montreal, Quebec, Canada, 2009).
340. Silander, T., Kontkanen, P. & Myllymaki, P. On sensitivity of the MAP Bayesian network structure to the equivalent sample size parameter. in *Proceedings of the 23rd Conference on Uncertainty in Articial Intelligence (UAI-07)* 360-367 (2007).
341. Silander, T., Roos, T. & Myllymaki, P. Learning locally minimax optimal Bayesian networks. *Int J Approx Reason* **51**, 544-557 (2010).
342. Suzuki, O., Koura, M., Noguchi, Y., Uchio-Yamada, K. & Matsuda, J. Use of sample mixtures for standard curve creation in quantitative western blots. *Exp Anim* **60**, 193-196 (2011).
343. Tsamardinos, I. & Mariglis, A. Multi-Source Causal Analysis: Learning Bayesian Networks from Multiple Datasets. in *Int Fed Info Proc*, Vol. 296 (eds. Iliadis, Maglogiann, Tsoumakasis, Vlahavas & Bramer) 479-490 (Springer US, 2009).
344. Pearl, J. From Bayesian networks to causal networks. *Mathematical Models for Handling Partial Knowledge in Artificial Intelligence*, 157-182 (1995).
345. Davies, S.P., Reddy, H., Caivano, M. & Cohen, P. Specificity and mechanism of action of some commonly used protein kinase inhibitors. *Biochem J* **351**, 95-105 (2000).

346. Bain, J.*, et al.* The selectivity of protein kinase inhibitors: a further update. *Biochem J* **408**, 297-315 (2007).
347. Hernandez-Leal, P., Gonzalez, J.A., Morales, E.F. & Enrique Sucar, L. Learning temporal nodes Bayesian networks. *Int J Approx Reason* **54**, 956-977 (2013).
348. Needham, C.J., Bradford, J.R., Bulpitt, A.J. & Westhead, D.R. A primer on learning in Bayesian networks for computational biology. *PLoS Comput Biol* **3**, e129 (2007).
349. Marchetti, S.*, et al.* Extracellular signal-regulated kinases phosphorylate mitogen-activated protein kinase phosphatase 3/DUSP6 at serines 159 and 197, two sites critical for its proteasomal degradation. *Mol Cell Biol* **25**, 854-864 (2005).
350. Balan, V.*, et al.* Identification of novel in vivo Raf-1 phosphorylation sites mediating positive feedback Raf-1 regulation by extracellular signal-regulated kinase. *Mol Biol Cell* **17**, 1141-1153 (2006).
351. Kholodenko, B.N. Untangling the signalling wires. *Nat Cell Biol* **9**, 247-249 (2007).
352. Mauro, A.*, et al.* PKCalpha-mediated ERK, JNK and p38 activation regulates the myogenic program in human rhabdomyosarcoma cells. *J Cell Sci* **115**, 3587-3599 (2002).
353. Makela, S.M., Osterlund, P. & Julkunen, I. TLR ligands induce synergistic interferon-beta and interferon-lambda1 gene expression in human monocyte-derived dendritic cells. *Mol Immunol* **48**, 505-515 (2011).
354. Zhang, J., Yang, P.L. & Gray, N.S. Targeting cancer with small molecule kinase inhibitors. *Nat Rev Cancer* **9**, 28-39 (2009).
355. Li, G.L. & Leong, T.Y. Active Learning for Causal Bayesian Network Structure with Non-symmetrical Entropy. *Advances in Knowledge Discovery and Data Mining, Proceedings* **5476**, 290-301 (2009).
356. Junttila, M.R., Li, S.P. & Westermarck, J. Phosphatase-mediated crosstalk between MAPK signaling pathways in the regulation of cell survival. *FASEB J* **22**, 954-965 (2008).
357. Owens, D.M. & Keyse, S.M. Differential regulation of MAP kinase signalling by dual-specificity protein phosphatases. *Oncogene* **26**, 3203-3213 (2007).
358. Boutros, T., Chevet, E. & Metrakos, P. Mitogen-activated protein (MAP) kinase/MAP kinase phosphatase regulation: roles in cell growth, death, and cancer. *Pharmacol Rev* **60**, 261-310 (2008).
359. Hunter, T. Protein kinases and phosphatases: the yin and yang of protein phosphorylation and signaling. *Cell* **80**, 225-236 (1995).
360. Yamamoto, K.R. & Alberts, B.M. Steroid receptors: elements for modulation of eukaryotic transcription. *Annu Rev Biochem* **45**, 721-746 (1976).
361. Abraham, W.C., Dragunow, M. & Tate, W.P. The role of immediate early genes in the stabilization of long-term potentiation. *Mol Neurobiol* **5**, 297-314 (1991).
362. Healy, S., Khan, P. & Davie, J.R. Immediate early response genes and cell transformation. *Pharmacol Ther* **137**, 64-77 (2013).
363. O'Donnell, A., Odrowaz, Z. & Sharrocks, A.D. Immediate-early gene activation by the MAPK pathways: what do and don't we know? *Biochem Soc Trans* **40**, 58-66 (2012).

364. Lee, P.G. & Koo, P.H. Rat alpha(2)-macroglobulin inhibits NGF-promoted neurite outgrowth, TrK phosphorylation, and gene expression of pheochromocytoma PC12 cells. *J Neurosci Res* **57**, 872-883 (1999).
365. Levkovitz, Y. & Baraban, J.M. A dominant negative Egr inhibitor blocks nerve growth factor-induced neurite outgrowth by suppressing c-Jun activation: role of an Egr/c-Jun complex. *J Neurosci* **22**, 3845-3854 (2002).
366. Lin, W.F*., et al.* SH2B1beta enhances fibroblast growth factor 1 (FGF1)-induced neurite outgrowth through MEK-ERK1/2-STAT3-Egr1 pathway. *Cell Signal* **21**, 1060-1072 (2009).
367. el-Ghissassi, F*., et al.* BTG2(TIS21/PC3) induces neuronal differentiation and prevents apoptosis of terminally differentiated PC12 cells. *Oncogene* **21**, 6772-6778 (2002).
368. Maruoka, H*., et al.* Dibutyryl-cAMP up-regulates nur77 expression via histone modification during neurite outgrowth in PC12 cells. *J Biochem* **148**, 93-101 (2010).
369. Ebert, M.S. & Sharp, P.A. Roles for microRNAs in conferring robustness to biological processes. *Cell* **149**, 515-524 (2012).
370. Hashimoto, Y., Akiyama, Y. & Yuasa, Y. Multiple-to-multiple relationships between microRNAs and target genes in gastric cancer. *PLoS One* **8**, e62589 (2013).
371. Clovis, Y.M., Enard, W., Marinaro, F., Huttner, W.B. & De Pietri Tonelli, D. Convergent repression of Foxp2 3'UTR by miR-9 and miR-132 in embryonic mouse neocortex: implications for radial migration of neurons. *Development* **139**, 3332-3342 (2012).
372. Strickland, I.T*., et al.* Axotomy-induced miR-21 promotes axon growth in adult dorsal root ganglion neurons. *PLoS One* **6**, e23423 (2011).
373. Terasawa, K., Ichimura, A., Sato, F., Shimizu, K. & Tsujimoto, G. Sustained activation of ERK1/2 by NGF induces microRNA-221 and 222 in PC12 cells. *FEBS J* **276**, 3269-3276 (2009).
374. Lee, K.H., Ryu, C.J., Hong, H.J., Kim, J. & Lee, E.H. CDNA microarray analysis of nerve growth factor-regulated gene expression profile in rat PC12 cells. *Neurochem Res* **30**, 533-540 (2005).
375. Ravni, A*., et al.* A cAMP-dependent, protein kinase A-independent signaling pathway mediating neuritogenesis through Egr1 in PC12 cells. *Mol Pharmacol* **73**, 1688-1708 (2008).
376. Mullenbrock, S., Shah, J. & Cooper, G.M. Global expression analysis identified a preferentially nerve growth factor-induced transcriptional program regulated by sustained mitogen-activated protein kinase/extracellular signal-regulated kinase (ERK) and AP-1 protein activation during PC12 cell differentiation. *J Biol Chem* **286**, 45131-45145 (2011).
377. Lyford, G.L*., et al.* Arc, a growth factor and activity-regulated gene, encodes a novel cytoskeleton-associated protein that is enriched in neuronal dendrites. *Neuron* **14**, 433-445 (1995).
378. Strom, A., Castella, P., Rockwood, J., Wagner, J. & Caudy, M. Mediation of NGF signaling by post-translational inhibition of HES-1, a basic helix-loop-helix repressor of neuronal differentiation. *Genes Dev* **11**, 3168-3181 (1997).

379. Castella, P., Sawai, S., Nakao, K., Wagner, J.A. & Caudy, M. HES-1 repression of differentiation and proliferation in PC12 cells: role for the helix 3-helix 4 domain in transcription repression. *Mol Cell Biol* **20**, 6170-6183 (2000).
380. Zhou, L., Lim, Q.E., Wan, G. & Too, H.P. Normalization with genes encoding ribosomal proteins but not GAPDH provides an accurate quantification of gene expressions in neuronal differentiation of PC12 cells. *BMC Genomics* **11**, 75 (2010).
381. Agostini, M.*, et al.* microRNA-34a regulates neurite outgrowth, spinal morphology, and function. *Proc Natl Acad Sci U S A* **108**, 21099-21104 (2011).
382. Sun, X., Zhou, Z., Fink, D.J. & Mata, M. HspB1 silences translation of PDZ-RhoGEF by enhancing miR-20a and miR-128 expression to promote neurite extension. *Mol Cell Neurosci* **57**, 111-119 (2013).
383. Stappert, L.*, et al.* MicroRNA-based promotion of human neuronal differentiation and subtype specification. *PLoS One* **8**, e59011 (2013).
384. Cimadamore, F., Amador-Arjona, A., Chen, C., Huang, C.T. & Terskikh, A.V. SOX2-LIN28/let-7 pathway regulates proliferation and neurogenesis in neural precursors. *Proc Natl Acad Sci U S A* **110**, E3017-3026 (2013).
385. Favereaux, A.*, et al.* Bidirectional integrative regulation of Cav1.2 calcium channel by microRNA miR-103: role in pain. *EMBO J* **30**, 3830-3841 (2011).
386. Brett, J.O., Renault, V.M., Rafalski, V.A., Webb, A.E. & Brunet, A. The microRNA cluster miR-106b~25 regulates adult neural stem/progenitor cell proliferation and neuronal differentiation. *Aging (Albany NY)* **3**, 108-124 (2011).
387. Wang, W.X.*, et al.* miR-107 regulates granulin/progranulin with implications for traumatic brain injury and neurodegenerative disease. *Am J Pathol* **177**, 334-345 (2010).
388. Muddashetty, R.S.*, et al.* Reversible inhibition of PSD-95 mRNA translation by miR-125a, FMRP phosphorylation, and mGluR signaling. *Mol Cell* **42**, 673-688 (2011).
389. Wei, H.*, et al.* Comparative profiling of microRNA expression between neural stem cells and motor neurons in embryonic spinal cord in rat. *Int J Dev Neurosci* **28**, 545-551 (2010).
390. Greco, S.J. & Rameshwar, P. MicroRNAs regulate synthesis of the neurotransmitter substance P in human mesenchymal stem cell-derived neuronal cells. *Proc Natl Acad Sci U S A* **104**, 15484-15489 (2007).
391. Lee, Y.J., Johnson, K.R. & Hallenbeck, J.M. Global protein conjugation by ubiquitin-like-modifiers during ischemic stress is regulated by microRNAs and confers robust tolerance to ischemia. *PLoS One* **7**, e47787 (2012).
392. Datta Chaudhuri, A., Yelamanchili, S.V. & Fox, H.S. MicroRNA-142 Reduces Monoamine Oxidase A Expression and Activity in Neuronal Cells by Downregulating SIRT1. *PLoS One* **8**, e79579 (2013).
393. Rodriguez-Lebron, E., Liu, G., Keiser, M., Behlke, M.A. & Davidson, B.L. Altered Purkinje cell miRNA expression and SCA1 pathogenesis. *Neurobiol Dis* **54**, 456-463 (2013).
394. Natera-Naranjo, O., Aschrafi, A., Gioio, A.E. & Kaplan, B.B. Identification and quantitative analyses of microRNAs located in the distal axons of sympathetic neurons. *RNA* **16**, 1516-1529 (2010).
395. Hebert, S.S., Sergeant, N. & Buee, L. MicroRNAs and the Regulation of Tau Metabolism. *Int J Alzheimers Dis* **2012**, 406561 (2012).

396. Hebert, S.S*., et al.* MicroRNA regulation of Alzheimer's Amyloid precursor protein expression. *Neurobiol Dis* **33**, 422-428 (2009).
397. Li, J.S. & Yao, Z.X. MicroRNAs: novel regulators of oligodendrocyte differentiation and potential therapeutic targets in demyelination-related diseases. *Mol Neurobiol* **45**, 200-212 (2012).
398. van Spronsen, M*., et al.* Developmental and activity-dependent miRNA expression profiling in primary hippocampal neuron cultures. *PLoS One* **8**, e74907 (2013).
399. Babenko, O., Golubov, A., Ilnytskyy, Y., Kovalchuk, I. & Metz, G.A. Genomic and epigenomic responses to chronic stress involve miRNA-mediated programming. *PLoS One* **7**, e29441 (2012).
400. Xu, W.H., Yao, X.Y., Yu, H.J., Huang, J.W. & Cui, L.Y. Downregulation of miR-199a may play a role in 3-nitropropionic acid induced ischemic tolerance in rat brain. *Brain Res* **1429**, 116-123 (2012).
401. Sempere, L.F*., et al.* Expression profiling of mammalian microRNAs uncovers a subset of brain-expressed microRNAs with possible roles in murine and human neuronal differentiation. *Genome Biol* **5**, R13 (2004).
402. Jovicic, A., Zaldivar Jolissaint, J.F., Moser, R., Silva Santos Mde, F. & Luthi-Carter, R. MicroRNA-22 (miR-22) overexpression is neuroprotective via general anti-apoptotic effects and may also target specific Huntington's disease-related mechanisms. *PLoS One* **8**, e54222 (2013).
403. Baraniskin, A*., et al.* Identification of microRNAs in the cerebrospinal fluid as biomarker for the diagnosis of glioma. *Neuro Oncol* **14**, 29-33 (2012).
404. Hu, K*., et al.* MicroRNA expression profile of the hippocampus in a rat model of temporal lobe epilepsy and miR-34a-targeted neuroprotection against hippocampal neurone cell apoptosis post-status epilepticus. *BMC Neurosci* **13**, 115 (2012).
405. Pandi, G., Nakka, V.P., Dharap, A., Roopra, A. & Vemuganti, R. MicroRNA miR-29c down-regulation leading to de-repression of its target DNA methyltransferase 3a promotes ischemic brain damage. *PLoS One* **8**, e58039 (2013).
406. Ziu, M., Fletcher, L., Rana, S., Jimenez, D.F. & Digicaylioglu, M. Temporal differences in microRNA expression patterns in astrocytes and neurons after ischemic injury. *PLoS One* **6**, e14724 (2011).
407. Hamada, N*., et al.* MicroRNA expression profiling of NGF-treated PC12 cells revealed a critical role for miR-221 in neuronal differentiation. *Neurochem Int* **60**, 743-750 (2012).
408. Kapsimali, M*., et al.* MicroRNAs show a wide diversity of expression profiles in the developing and mature central nervous system. *Genome Biol* **8**, R173 (2007).
409. Das, S*., et al.* Modulation of neuroblastoma disease pathogenesis by an extensive network of epigenetically regulated microRNAs. *Oncogene* **32**, 2927-2936 (2013).
410. Haapa-Paananen, S*., et al.* Functional profiling of precursor MicroRNAs identifies MicroRNAs essential for glioma proliferation. *PLoS One* **8**, e60930 (2013).
411. Li, Z., Gu, X., Fang, Y., Xiang, J. & Chen, Z. microRNA expression profiles in human colorectal cancers with brain metastases. *Oncol Lett* **3**, 346-350 (2012).

412. Kawahara, Y., Zinshteyn, B., Chendrimada, T.P., Shiekhattar, R. & Nishikura, K. RNA editing of the microRNA-151 precursor blocks cleavage by the Dicer-TRBP complex. *EMBO Rep* **8**, 763-769 (2007).
413. Feinberg-Gorenshtein, G.*, et al.* miR-192 Directly Binds and Regulates Dicer1 Expression in Neuroblastoma. *PLoS One* **8**, e78713 (2013).
414. Kole, A.J., Swahari, V., Hammond, S.M. & Deshmukh, M. miR-29b is activated during neuronal maturation and targets BH3-only genes to restrict apoptosis. *Genes Dev* **25**, 125-130 (2011).
415. Yan, H., Fang, M. & Liu, X.Y. Role of microRNAs in Stroke and Poststroke Depression. *ScientificWorldJournal* **2013**, 459692 (2013).
416. Mor, E.*, et al.* MicroRNA-382 expression is elevated in the olfactory neuroepithelium of schizophrenia patients. *Neurobiol Dis* **55**, 1-10 (2013).
417. Jovicic, A.*, et al.* Comprehensive expression analyses of neural cell-type-specific miRNAs identify new determinants of the specification and maintenance of neuronal phenotypes. *J Neurosci* **33**, 5127-5137 (2013).
418. Mestdagh, P.*, et al.* A novel and universal method for microRNA RT-qPCR data normalization. *Genome Biol* **10**, R64 (2009).
419. Dijkmans, T.F.*, et al.* Identification of new Nerve Growth Factor-responsive immediate-early genes. *Brain Res* **1249**, 19-33 (2009).
420. Saito, T.H., Uda, S., Tsuchiya, T., Ozaki, Y. & Kuroda, S. Temporal decoding of MAP kinase and CREB phosphorylation by selective immediate early gene expression. *PLoS One* **8**, e57037 (2013).
421. Barolo, S. & Posakony, J.W. Three habits of highly effective signaling pathways: principles of transcriptional control by developmental cell signaling. *Genes Dev* **16**, 1167-1181 (2002).
422. Sweeney, C.*, et al.* Growth factor-specific signaling pathway stimulation and gene expression mediated by ErbB receptors. *J Biol Chem* **276**, 22685-22698 (2001).
423. Natarajan, K. & Berk, B.C. Crosstalk coregulation mechanisms of G protein-coupled receptors and receptor tyrosine kinases. *Methods Mol Biol* **332**, 51-77 (2006).
424. Pyne, N.J. & Pyne, S. Receptor tyrosine kinase-G-protein-coupled receptor signalling platforms: out of the shadow? *Trends Pharmacol Sci* **32**, 443-450 (2011).
425. Zhao, G.*, et al.* MicroRNA-221 induces cell survival and cisplatin resistance through PI3K/Akt pathway in human osteosarcoma. *PLoS One* **8**, e53906 (2013).
426. Musatov, S.*, et al.* Inhibition of neuronal phenotype by PTEN in PC12 cells. *Proc Natl Acad Sci U S A* **101**, 3627-3631 (2004).
427. Jia, L., Ji, S., Maillet, J.C. & Zhang, X. PTEN suppression promotes neurite development exclusively in differentiating PC12 cells via PI3-kinase and MAP kinase signaling. *J Cell Biochem* **111**, 1390-1400 (2010).
428. Chang, K., Mestdagh, P., Vandesompele, J., Kerin, M. & Miller, N. MicroRNA expression profiling to identify and validate reference genes for relative quantification in colorectal cancer. *Bmc Cancer* **10**, 173 (2010).
429. Gurtan, A.M. & Sharp, P.A. The role of miRNAs in regulating gene expression networks. *J Mol Biol* **425**, 3582-3600 (2013).

430. Lu, T.X. & Rothenberg, M.E. Diagnostic, functional, and therapeutic roles of microRNA in allergic diseases. *J Allergy Clin Immunol* **132**, 3-13; quiz 14 (2013).
431. Hoy, A.M. & Buck, A.H. Extracellular small RNAs: what, where, why? *Biochem Soc Trans* **40**, 886-890 (2012).
432. Wang, K., Zhang, S., Weber, J., Baxter, D. & Galas, D.J. Export of microRNAs and microRNA-protective protein by mammalian cells. *Nucleic Acids Res* **38**, 7248-7259 (2010).
433. Zhu, H. & Fan, G.C. Extracellular/circulating microRNAs and their potential role in cardiovascular disease. *Am J Cardiovasc Dis* **1**, 138-149 (2011).
434. Kholodenko, B.N. Cell-signalling dynamics in time and space. *Nat Rev Mol Cell Biol* **7**, 165-176 (2006).
435. Aggen, J.B., Nairn, A.C. & Chamberlin, R. Regulation of protein phosphatase-1. *Chem Biol* **7**, R13-23 (2000).
436. Pidoux, G. & Tasken, K. Specificity and spatial dynamics of protein kinase A signaling organized by A-kinase-anchoring proteins. *J Mol Endocrinol* **44**, 271-284 (2010).
437. Hong, K., Lou, L., Gupta, S., Ribeiro-Neto, F. & Altschuler, D.L. A novel Epac-Rap-PP2A signaling module controls cAMP-dependent Akt regulation. *J Biol Chem* **283**, 23129-23138 (2008).
438. Purves, G.I., Kamishima, T., Davies, L.M., Quayle, J.M. & Dart, C. Exchange protein activated by cAMP (Epac) mediates cAMP-dependent but protein kinase A-insensitive modulation of vascular ATP-sensitive potassium channels. *J Physiol* **587**, 3639-3650 (2009).
439. Obermeier, A*., et al.* Neuronal differentiation signals are controlled by nerve growth factor receptor/Trk binding sites for SHC and PLC gamma. *EMBO J* **13**, 1585-1590 (1994).
440. Nishimura, T., Ishima, T., Iyo, M. & Hashimoto, K. Potentiation of nerve growth factor-induced neurite outgrowth by fluvoxamine: role of sigma-1 receptors, IP3 receptors and cellular signaling pathways. *PLoS One* **3**, e2558 (2008).
441. Stephens, R.M*., et al.* Trk receptors use redundant signal transduction pathways involving SHC and PLC-gamma 1 to mediate NGF responses. *Neuron* **12**, 691-705 (1994).
442. Sparatore, B*., et al.* Neuronal differentiation of PC12 cells involves changes in protein kinase C-theta distribution and molecular properties. *Biochem Biophys Res Commun* **275**, 149-153 (2000).
443. Shi, G.X., Jin, L. & Andres, D.A. Pituitary adenylate cyclase-activating polypeptide 38-mediated Rin activation requires Src and contributes to the regulation of HSP27 signaling during neuronal differentiation. *Mol Cell Biol* **28**, 4940-4951 (2008).
444. Drew, B.A., Burow, M.E. & Beckman, B.S. MEK5/ERK5 pathway: the first fifteen years. *Biochim Biophys Acta* **1825**, 37-48 (2012).
445. Uylings, H.B. & van Pelt, J. Measures for quantifying dendritic arborizations. *Network* **13**, 397-414 (2002).
446. Allen, M.P. The problem of multicollinearity. in *Understanding Regression Analysis* 176-180 (Springer US, 1997).
447. Uusitalo, L. Advantages and challenges of Bayesian networks in environmental modelling. *Ecological Modelling* **203**, 312-318 (2007).

448. Pritchard, J.R., Lauffenburger, D.A. & Hemann, M.T. Understanding resistance to combination chemotherapy. *Drug Resist Updat* **15**, 249-257 (2012).
449. Zumla, A., Nahid, P. & Cole, S.T. Advances in the development of new tuberculosis drugs and treatment regimens. *Nat Rev Drug Discov* **12**, 388-404 (2013).
450. Daly, R., Shen, Q. & Aitken, S. Learning Bayesian networks: approaches and issues. *The Knowledge Engineering Review* **26**, 99-157 (2011).